NASA-CR-200904

Orbital Injection of the SEDSAT Satellite

Grant NAG8-1046

Tethered Systems Dynamics and Flight Data Analysis

Annual Report

Second Year Research Activity for the period 22 February 1995 through 21 February 1996

Principal Investigators

Enrico C. Lorenzini

Gordon E. Gullahorn

Mario L. Cosmo

Co-Investigators

Manuel Ruiz

Jesus Pelaez

April 1996

TABLE OF CONTENTS

SCOPE

This is the Annual Report prepared by the Smithsonian Astrophysical Observatory for the second year research activity on NASA Marshall Space Flight Center Grant NAG8-1046 with Charles Rupp as Technical Monitor. This report covers the period from 22 February 1995 through 21 February 1996.

SUMMARY

This report deals with the following topics which are all related to the orbital injection of the SEDSAT satellite:

1) Dynamics and Stability of Tether Oscillations after the First Cut

The dynamics of the tether after the first cut (i.e., without the Shuttle attached to it) is investigated. The tether oscillations with the free end are analyzed in order to assess the stability of the rectilinear configuration in between the two tether cuts.

2) Analysis of Unstable Modes

The unstable modes that appear for high libration angles are further investigated in order to determine their occurrences and the possible transition from bound librations to rotations.

3) Orbital Release Strategies for SEDSAT

A parametric analysis of the orbital decay rate of the SEDSAT satellite after the two tether cuts has been carried out as a function of the following free parameters: libration amplitude at the end of deployment, deviation angle from LV at the first cut, and orbital anomaly at the second cut. The values of these parameters that provide a minimum orbital decay rate of the satellite (after the two cuts) have been computed.

4) Dynamics and Control of SEDSAT

The deployment control law has been modified to cope with the new ejection velocity of the satellite from the Shuttle cargo bay. New reference profiles have been derived as well as new control parameters. Timing errors at the satellite release as a function of the variations of the initial conditions and the tension model parameters have been estimated for the modified control law.

INTRODUCTION

Some aspects of the dynamics of SEDSAT orbit injection are studied. After being deployed from the space Shuttle flying in a circular orbit, the SEDSAT satellite and tether will librate zenithwards as a gravity gradient pendulum [1]. At a suitable moment, the tether will be cut at the orbiter end, leaving the tethered system (TS) to enter a higher energy elliptical orbit, safely away from the shuttle. If the TS is straight at cut time, it will continue librating about its center of mass (COM) keeping its rectilinear shape, just as a rigid body. A second cut is done, leaving the satellite and tether to continue separate orbits. The libration can be used to transfer angular momentum from the tether to the satellite, which will reach a higher orbit at the expense of the tether. The mass of the tether is not negligible. The four stages—deployment, libration, TS orbit and satellite orbit— are to be optimized to obtain the longest possible satellite life.

The COM orbit sensitivity to deployment parameters and cut time, studied by Jesus Pelaez in Ref. [2], will be used along this research.

The main topics to be studied are the stability of the rectilinear configuration and the optimization of operational life.

It is known that a straight shape is a solution of the equations of motion of the TS [3, p. 39]. This is precisely the movement desired in order to obtain the maximum transfer of angular momentum from the tether to the satellite. However, we must study whether this movement is stable, since it will not be possible to get the perfect initial conditions at cut time. On the contrary, the tension released at cutting will result in tether shrinking, producing speed and position deviations from the rectilinear shape. We need to know how the perturbations of the rectilinear shape will propagate during the few orbits the injection will take. The main danger comes from the free end. The stability of two-mass tethered satellites has been thoroughly studied: the tension produced by rotation and the two end masses has a stabilizing effect. But in this case one tether end is free [4, 5]. The instability is more likely to appear when the TS swings backwards in the libration, at which time the tension falls to its minimum. Besides, most stability studies have been done for circular orbits, while here the elliptic orbit will induce a forcing term from the inertia forces. The oscillation modes and frequencies will be sought by different methods and the evolution of the libration itself will be investigated.

Another point of concern is selecting the right set of parameters to obtain the maximum satellite useful life. Since the shuttle orbit is fixed, we have only three free parameters: libration amplitude, libration angle at first cut time, and second cut time. The maximum operational life corresponds to maximum orbit energy and minimum eccentricity. This corresponds to minimum orbital decay rate. We will compute the orbital decay rate as a function of the three free parameters.

These two aspects are closely related. It is obvious that the wider the libration amplitude, the greater the speed increase obtained at cut time, and the higher the orbit attained. However, these large librations bring us closer to the instability region. We need to know how far we can go without a catastrophic propagation of perturbations.

3

Stability of Pendular Motion

Elliptic Orbit of the Center of Mass

Within the degree of approximation considered in this study, the center of mass of the TS will follow an unperturbed elliptic orbit. The Deployment, first cut, and second cut will take just a few orbits, so that no perturbations need to be considered: only spherical earth gravitation and inertia forces will be considered. The parameters of the COM orbit are known as a function of the deployment and cut data [2]:

$a=R(1+2(1+u)\epsilon+...)$;

$e=2u\epsilon+...$;

$\omega=\omega_0(1+3(1+u)\epsilon+...)$;

Where $u=3+2\sqrt{3}\sin\theta_M$ and $\epsilon=\xi_f/2R_0$. θ_M is the TS libration amplitude; R_0 is the shuttle's circular orbit radius; ξ_f is the distance from the free end to the center of mass of the TS with the tether straight, while L_f is the final deployed tether length. We will use here the same notation as [2] for u and ϵ, but a different one will be used later on for the study of decay optimization in section 3.

If the TS is straight at cut time, it will keep its straight shape and orbit as a rigid body [3]. The terms coupling COM motion with rotation about the COM are smaller than the approximation considered here, so that the gravidyne effect studied by Beletski is completely negligible for the size of the TS considered [3, pp. 67-68]. We can thus study separately the motion of the COM and the TS motion about its COM.

Pendular Motion Equations
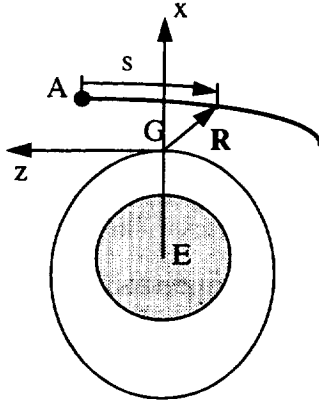
Figure 1 Reference frame for the TS.

The tether is considered as perfectly flexible and inextensible. A reference frame Gxyz is chosen as follows: origin in the tethered system center of mass, Gx aligned with the local vertical towards zenith, Gz aligned with the orbital speed of the center of mass, and Gy completing a right-handed frame. The equations of the TS motion are:

$$\rho\frac{\partial^2 R}{\partial t^2} = \frac{\partial}{\partial s}\left(T\frac{\partial R}{\partial s}\right)+\rho f$$

$$\left|\frac{\partial R}{\partial s}\right| = 1 \qquad\qquad (1)$$

$$\int_0^{L_f} \rho R ds + m_A R_A = 0$$

Where t is time and s the curvilinear abscissa, with origin at the end mass; ρ is the linear density of the tether, L_f its total length, T(s,t) its tension, f the force per unit mass, R(s,t) the position vector, and A the end mass. The second equation corresponds to a perfectly inextensible tether, and the third to taking the COM as origin of the reference frame. We shift to non-dimensional variables using the average orbital rate and tether length:

$$\tau = n(t-t_p), \quad s = L_f\sigma, \quad R = L_f r, \quad T = \rho n^2 L_f^2 F; \quad \text{where } n = \sqrt{\frac{\mu}{a^3}}$$

Obtaining:

$$\ddot{r} = (Fr')' +\frac{1}{L_f n^2}f$$

$$\left|r'\right| = 1 \qquad\qquad (2)$$

$$\int_0^1 r(\sigma,\tau)d\sigma + \frac{\rho L_f}{m_A}r(0,\tau) = 0$$

With boundary conditions:

4

$$\left|_{\sigma=0}\ \begin{cases}\dfrac{\partial F}{\partial \sigma}(0,\tau)=\dfrac{\rho L_f}{m_A}F(0,\tau)\\[2mm] F\dfrac{\partial^2 \mathbf{r}}{\partial \sigma^2}(0,\tau)=\mathbf{0}\end{cases}\right.$$

$$\left|_{\sigma=1}\quad F=0\right.$$

Where $\sigma=0$ is the end mass and $\sigma=1$ the free end. The perturbing force is:

$$\mathbf{f}=-\frac{\omega^2}{\kappa}\begin{Bmatrix}-3x\\ y\\ 0\end{Bmatrix}+\frac{e\omega^2}{\kappa}\begin{Bmatrix}x\cos v-2z\sin v\\ 0\\ z\cos v+2x\sin v\end{Bmatrix}+2\omega\begin{Bmatrix}\dot z\\ 0\\ -\dot x\end{Bmatrix}$$

Where v is the true anomaly of the COM orbit; $\mathbf{r}=(x,y,z)$; $\kappa=1+e\cos v$; $\omega=\dot v$. The $1/L_f$ factor in $\mathbf{f}$ can be dropped if x,y,z are non-dimensional lengths. Only terms of order ε and $e\varepsilon$ are kept; ε^2, $e\varepsilon^2$, and $e^2\varepsilon$ have been dropped.

If, hypothetically, the tether is assumed to keep a rectilinear shape, it will be sufficient to give the position of one of the masses in spherical coordinates [3, p. 378ff]. The equations of motion of a fully deployed massive tether, considered as a rigid body, and without any perturbations nor thrust (dumbbell model), are:

$$\ddot\theta+\dot\omega_y-2\dot\varphi\tan\varphi\left(\dot\theta+\omega_y\right)+\frac{3\mu}{R_G^3}\sin\theta\cos\theta=0$$

$$\ddot\varphi+\left[\left(\dot\theta+\omega_y\right)^2+\frac{3\mu}{R_G^3}\cos^2\theta\right]\sin\varphi\cos\varphi=0$$

$$T=\left[\left(\dot\theta+\omega_y\right)^2-\frac{\mu}{R_G^3}\left(1-3\cos^2\theta\right)\right]P(s)\tag{3}$$

$$P(s)=m_A\left(s_G-s_A\right)+\int_A^s\rho(s)\left(s_G-s\right)ds$$

Where θ and φ are the spherical coordinates of A. Note that the reference frame used here is different from the one in [3]. These expressions are valid only while $T>0$. The tension is a function of t and s, which, for constant ρ and only one mass, is:

$$P(s)=-\rho\frac{s^2}{2}+\rho s_G s+m_A s_C=-\rho\frac{\sigma^2 L_f^2}{2}+\rho bL_f^2\sigma+m_A bL_f$$

Where b is the non-dimensional curvilinear abscissa of the COM: $\quad b=\dfrac{s_G}{L_f}=\dfrac{1}{2\left(1+\dfrac{m_A}{\rho L_f}\right)}$

We shift to the non-dimensional arc length v, which is the same as σ but for taking now G as origin. v is positive towards A and is defined as follows: $v=b-\sigma$. Consequently,

$$P(v)=\frac{\rho L_f^2}{2}\left[(b-1)^2-v^2\right]\tag{4}$$

If we consider in-plane pendular motion only, φ and its derivatives will be zero, and equations (3) reduce only to the θ equations, as follows:

$$\kappa n^2\ddot\theta-2\omega^2e\sin v+3\omega^2\sin\theta\cos\theta=0$$

$$2F=\left[\left(\dot\theta+\frac{\omega}{n}\right)^2-\frac{\omega^2}{\kappa n^2}\left(1-3\cos^2\theta\right)\right]\left[(b-1)^2-v^2\right]\tag{5}$$

Where dots are derivatives with regard to non-dimensional time τ, which is equivalent to the mean anomaly of the COM orbit. ω is the instant angular speed of the orbital frame, which corresponds to the orbit of the COM. Note that, although we are using non-dimensional time, ω is still the derivative of v with regard to real time t. We have:

$$\omega=\frac{dv}{dt}=\sqrt{\frac{\mu}{a^3}}\frac{(1+e\cos v)^2}{\left(1-e^2\right)^{3/2}};\quad \omega^2=\frac{\mu}{R_G^3}(1+e\cos v);\quad \frac{d\omega}{dt}=-2\sqrt{\frac{\mu}{a^3}}\frac{(1+e\cos v)}{\left(1-e^2\right)^{3/2}}e\sin v=-2e\sin v\,\frac{\omega^2}{\kappa}$$

Numerical integration of the equations above requires solving Kepler's equation at every step. It is therefore easier to use the true anomaly as variable:

$$\ddot{\theta} - \frac{2e\sin v}{\kappa}(\dot{\theta}+1) + \frac{3}{\kappa}\sin\theta\cos\theta = 0$$

$$F = \frac{\omega^2}{2n^2}\left[(\dot{\theta}+1)^2 - \frac{1}{\kappa}(1-3\cos^2\theta)\right]\left[(b-1)^2 - v^2\right]$$

(6)

Where $\dot{\theta} = \partial\theta/\partial v$. These equations correspond to the gravity gradient pendulum, plus small damping and forcing terms due to inertia forces in an eccentric orbit. The initial conditions for the integration correspond to the libration in the circular orbit of the shuttle. An adjustment has to be made to the initial deviation and angular speed when the system switches from the circular orbit frame to the new elliptic orbit frame after cutting the tether.

Deviations from the Pendular Motion

In order to study the deviations from a pendular motion, we will erect a reference frame tied to the assumed rigid shape of the TS: origin in the COM, Gξ along the tether towards A, Gη parallel to Gy, and Gζ normal to the tether within the orbital plane. G$\xi\eta\zeta$ moves according to the equations above. The coordinates of the TS points in the new frame will be:

$$\begin{Bmatrix} \xi(\sigma,\tau) \\ \eta(\sigma,\tau) \\ \zeta(\sigma,\tau) \end{Bmatrix} \qquad \begin{Bmatrix} x = \xi\cos\theta - \zeta\sin\theta \\ y = \eta \\ z = \xi\sin\theta + \zeta\cos\theta \end{Bmatrix}$$

(7)

In the new frame, the derivatives to be used in the TS motion equations will be:

$$\ddot{r} = \begin{Bmatrix} \ddot{\xi} \\ \ddot{\eta} \\ \ddot{\zeta} \end{Bmatrix} + 2\dot{\theta}\begin{Bmatrix} -\dot{\zeta} \\ 0 \\ \dot{\xi} \end{Bmatrix} + \ddot{\theta}\begin{Bmatrix} -\zeta \\ 0 \\ \xi \end{Bmatrix} - \dot{\theta}^2\begin{Bmatrix} \xi \\ 0 \\ \zeta \end{Bmatrix}$$

$$(Fr')' = \begin{Bmatrix} F\xi' \\ F\eta' \\ F\zeta' \end{Bmatrix}$$

(8)

$$f\kappa n^2 = \omega^2\begin{Bmatrix} 3(\xi\cos^2\theta - \zeta\sin\theta\cos\theta) \\ -\eta \\ 3(-\xi\cos\theta\sin\theta + \zeta\sin^2\theta) \end{Bmatrix} + e\omega^2\cos v\begin{Bmatrix} \xi \\ 0 \\ \zeta \end{Bmatrix} + 2e\omega^2\sin v\begin{Bmatrix} -\zeta \\ 0 \\ \xi \end{Bmatrix} + 2n\kappa\omega\begin{Bmatrix} \dot{\zeta}+\xi\dot{\theta} \\ 0 \\ -\dot{\xi}+\zeta\dot{\theta} \end{Bmatrix}$$

If we consider the initial conditions of a pendular motion—$\xi(\sigma,0)=\sigma_A-\sigma$, $\eta=0$, $\zeta=0$, and first derivatives zero except $\xi'=-1$—and substitute them into the above equations, we obtain the initial acceleration:

$$\ddot{\xi}(\sigma,0) = -F' + (\sigma_A - \sigma)\left(\frac{3\omega^2}{\kappa n^2}\cos^2\theta + \frac{e\omega^2}{\kappa n^2}\cos v + \frac{2\omega}{n}\dot{\theta} + \dot{\theta}^2\right)$$

$$\ddot{\eta}(\sigma,0) = 0$$

(9)

$$\ddot{\zeta}(\sigma,0) = (\sigma_A - \sigma)\left(-\ddot{\theta} - \frac{3\omega^2}{\kappa n^2}3\cos\theta\sin\theta + \frac{2e\omega^2}{\kappa n^2}\sin v\right)$$

The initial accelerations are linear in $\sigma_A-\sigma$ except for F'. If the tether is initially straight, pendular motion equations apply to the TS-body frame and, therefore:

$$F' = (\sigma_A - \sigma)\left(\frac{3\omega^2}{\kappa n^2}\cos^2\theta + \frac{e\omega^2}{\kappa n^2}\cos v + \frac{2\omega}{n}\dot{\theta} + \dot{\theta}^2\right)$$

$$\ddot{\theta} + \frac{3\omega^2}{\kappa n^2}3\cos\theta\sin\theta - \frac{2e\omega^2}{\kappa n^2}\sin v = 0$$

(10)

F' in (10) is obtained by derivating (6) with regard to v and then switching back to σ. This leads to:

$$\ddot{\xi} = \ddot{\eta} = \ddot{\zeta} = 0 \qquad (11)$$

Pendular motion is thus a solution of the equations of movement for the TS when the initial conditions are rectilinear. What has to be studied now is the stability of this solution, and the speed at which perturbations propagate or die out.

Small Transverse Oscillations

Since the equations of the in-plane and out-of-plane deviations ξ,η,ζ are coupled through the tether continuity equation $|\mathbf{r}'| = 1$ and tension only, they can be studied separately. If they are assumed to be small, they can be decoupled since the coupling terms are of a higher order. Taking into account the equations for pendular motion, we obtain:

$$\ddot{\xi} = \left(F\xi'\right)' + \left(\frac{3\omega^2}{\kappa n^2}\cos^2\theta + \frac{e\omega^2}{\kappa n^2}\cos v + \frac{2\omega\dot{\theta}}{n} + \dot{\theta}^2\right)\xi + 2\left(\frac{\omega}{n} + \dot{\theta}\right)\dot{\zeta}$$

$$\ddot{\eta} = \left(F\eta'\right)' - \frac{\omega^2}{\kappa n^2}\eta \qquad (12)$$

$$\ddot{\zeta} = \left(F\zeta'\right)' + \left(\frac{3\omega^2}{\kappa n^2}\sin^2\theta + \frac{e\omega^2}{\kappa n^2}\cos v + \frac{2\omega\dot{\theta}}{n} + \dot{\theta}^2\right)\zeta - 2\left(\frac{\omega}{n} + \dot{\theta}\right)\dot{\xi}$$

$$\xi'^2 + \eta'^2 + \zeta'^2 = 1$$

Plus the condition that G coincides with the COM:

$$\int_{b-1}^{b} \mathbf{r}\,dv + \frac{m_A}{\rho L_r}\mathbf{r}(b) = 0 \qquad (13)$$

Where $v=b$ is the end mass A and $v=b-1$ (negative, since $b<1$) is the free end. To simplify the notation, the coefficients of ξ and ζ will be called $G(\tau)$ and $H(\tau)$. G is the same function of τ appearing in the non-dimensional tension $F(v,\tau)$. If we consider now the deviations from rectilinear shape and pendular motion to be small, we have:

$$\left.\begin{array}{l} \xi(v,\tau) = v + \varepsilon\xi_1(v,\tau) \\ \eta(v,\tau) = \varepsilon\eta_1(v,\tau) \\ \zeta(v,\tau) = \varepsilon\zeta_1(v,\tau) \end{array}\right\}\varepsilon \ll 1 \qquad (14)$$

Where we have in fact made a change of variable from σ to $v=b-\sigma$. (') refers now to derivation with regard to v, but signs in (12) remain unchanged due to the double derivation. From the continuity equation we deduce that longitudinal perturbations are much smaller than transversal ones:

$$1 + 2\varepsilon\xi_1' + \varepsilon^2\xi_1'^2 + \varepsilon^2\eta_1'^2 + \varepsilon^2\zeta_1'^2 = 1 \quad \Rightarrow \quad -2\xi_1' = \varepsilon\left(\xi_1'^2 + \eta_1'^2 + \zeta_1'^2\right) \qquad (15)$$

Both ξ_1 and ξ_1' are one order of magnitude smaller than the transverse oscillations. Therefore, we should redefine them to show their relative orders of magnitude:

$$\xi(v,\tau) = v + \varepsilon^2\xi_1(v,\tau)$$

$$\eta(v,\tau) = \varepsilon\eta_1(v,\tau)$$

$$\zeta(v,\tau) = \varepsilon\zeta_1(v,\tau) \qquad (16)$$

$$F = F_0 + \varepsilon F_1 = G(\tau)P(v) + \varepsilon F_1(v,\tau)$$

Substituting this into the deviation equations:

$$\varepsilon^2\ddot{\xi}_1 = \left[(F_0 + \varepsilon F_1)(1 + \varepsilon^2\xi_1')\right]' + G(\tau)(v + \varepsilon^2\xi_1) + 2\left(\frac{\omega}{n} + \dot{\theta}\right)\varepsilon\dot{\zeta}_1$$

$$\varepsilon\ddot{\eta}_1 = \left[(F_0 + \varepsilon F_1)(\varepsilon\eta_1')\right]' - \frac{\omega^2}{\kappa n^2}\varepsilon\eta_1 \qquad (17)$$

$$\varepsilon\ddot{\zeta}_1 = \left[(F_0 + \varepsilon F_1)(\varepsilon\zeta_1')\right]' + H(\tau)\varepsilon\zeta_1 - 2\left(\frac{\omega}{n} + \dot{\theta}\right)\varepsilon^2\dot{\xi}_1$$

And keeping only terms of order ε:

$$0 = F_1' + 2\left(\frac{\omega}{n} + \dot{\theta}\right)\dot{\zeta}_1$$

$$\ddot{\eta}_1 = \left(F_o\eta_1'\right)' - \frac{\omega^2}{\kappa n^2}\eta_1 \qquad (18)$$

$$\ddot{\zeta}_1 = \left(F_o\zeta_1'\right)' + H(\tau)\zeta_1$$

While the O(1) term in the first equation is an already known result: $F_0' = -vG(\tau)$

The boundary conditions are:

$$\left|\begin{array}{l}F_1'(b) = -\dfrac{\rho L_f}{m_A}F_1(b) \\ F_1(b-1) = 0\end{array}\right. \quad \left|\begin{array}{l}\eta_1''(b) = 0 \\ \int_{b-1}^{b}\eta_1 dv + \dfrac{m_A}{\rho L_f}\eta_1(b) = 0\end{array}\right. \quad \left|\begin{array}{l}\zeta_1''(b) = 0 \\ \int_{b-1}^{b}\zeta_1 dv + \dfrac{m_A}{\rho L_f}\zeta_1(b) = 0\end{array}\right. \quad (19)$$

No condition can be imposed on the free end except that tension be zero.

As we can see, in the first approximation the transverse in-plane and out-of-plane oscillations are decoupled, and longitudinal oscillations are not present. We will continue developing them in parallel, although they could be treated separately.

The first approach to be tried is separation of variables. We assume solutions of the form:

$$\eta_1(v,\tau) = A(v)Z(\tau); \quad \zeta_1(v,\tau) = B(v)E(\tau); \quad F_0 = G(\tau)P(v) \qquad (20)$$

$$\left\{\begin{array}{l}A\left(\ddot{Z} + \dfrac{\omega^2}{\kappa n^2}Z\right) = GZ(PA')' \quad \Rightarrow \quad \dfrac{\ddot{Z} + \dfrac{\omega^2}{\kappa n^2}Z}{GZ} = \dfrac{(PA')'}{A} = -\lambda_\eta \\[18pt] B\left(\ddot{E} - H(\tau)E\right) = GE(PB')' \quad \Rightarrow \quad \dfrac{\ddot{E} - H(\tau)E}{GE} = \dfrac{(PB')'}{B} = -\lambda_\zeta\end{array}\right. \qquad (21)$$

We obtain a Sturm-Liouville problem. We will try to calculate the eigenvalues and eigenfunctions. They will be the same for in-plane and out-of-plane oscillations, since the spatial problem is the same for both.

Analytical Eigenvalues and Eigenfunctions

The equation to be solved for both transverse oscillations is:

$FA'' + F'A' + \lambda A = 0$; if we substitute $F = \left[(b-1)^2 - v^2\right]/2$, we obtain:

$$\left[(b-1)^2 - v^2\right]A'' - 2vA' + 2\lambda A = 0 \qquad (22)$$

The boundary conditions are:

- $v=b$ $\quad \dfrac{\partial^2 A}{\partial v^2}(b) = 0$ $\qquad\qquad\qquad\qquad (23)$

- $v=b-1$ No condition, since the tip is free. F is already zero there.

- COM $\quad \int_{b-1}^{b}A(v)dv + \dfrac{m_A}{\rho L_f}A(b) = 0$ $\qquad\qquad (24)$

We can substitute $\dfrac{m_A}{\rho L_f} = \dfrac{1-2b}{2b}$. Besides, the two boundary conditions turn out to be the same when the differential equation is used to calculate the integral; this is expected since the eigenfunctions will have one multiplicative constant left free. Besides, since we are studying the movement about the COM, if the initial deviations and speed meet (24), it will be fulfilled for all t. We could use either form of the boundary condition, or a third one obtained from the differential equation:

$$A'(b) = -\frac{\lambda}{b}A(b) \qquad (25)$$

With the change $v=(1-b)x$, and taking $2\lambda=n(n+1)$, we obtain the Legendre Equation:

$$\left[1-x^2\right]A'' - 2xA' + n(n+1)A = 0 \quad \text{With B.C.:} \quad A''\left(\frac{b}{1-b}\right) = 0 \qquad (26)$$

8

Solutions will be Legendre functions $P_n(x)$ and $Q_n(x)$. However, Legendre polynomials of the 2nd kind are not bounded in x=-1, and thus cannot be part of the solution. But $P_n(x)$ cannot be part of the solution either, since they do not meet the boundary conditions: their second derivative becomes zero at the origin, not at x=b/(1-b). But b<<1, so that the odd-order Legendre polynomials can be a first approximation of the solution. The even-order polynomials do not meet the approximate boundary conditions.

In an unpublished work, Jesus Pelaez and Manuel Ruiz obtained an approximate solution by asymptotic expansion of the solution in powers of $\varepsilon = b / (1 - b) \approx 0.085$:

$$\left.\begin{array}{l} A = A_0 + \varepsilon A_1 + \cdots \\ \lambda = \lambda_0 + \varepsilon \lambda_1 + \cdots \end{array}\right\} \quad \text{with:} \quad \left.\begin{array}{l} A_0(x) = C_0 P_n^0(x) \\ 2\lambda_0 = n(n+1) \end{array}\right\} \quad \text{as first approximation, and:}$$

$$\lambda_1 = -2\frac{n(n+1)-2}{\pi n(n+1)}(1+2n)\frac{\Gamma\left(1+\dfrac{n}{2}\right)^2}{\Gamma\left(\dfrac{1}{2}+\dfrac{n}{2}\right)^2} \tag{27}$$

$$A_1 = C_1 P_n^0(x) + 4\frac{\lambda_0 - 1}{\pi\lambda_0}\frac{\Gamma\left(1+\dfrac{n}{2}\right)^2}{\Gamma\left(\dfrac{1}{2}+\dfrac{n}{2}\right)^2}Q_n^0(x) + 2\lambda_1\left(Q_n^0(x)\int_0^x Q_n^0(y)P_n^0(y)dy + P_n^0(x)\int_0^x P_n^0(y)^2 dy\right)$$

as the second. Γ is the Gamma function. The singularity at the free end due to $Q_n(x)$ is controlled because its coefficient tends to 0 as x approaches -1. The approximate eigenfunctions (A_0 only) are shown in Figure 2. Fortunately, there is no need to compute A_1 for our purposes. With λ_1 we can compute the time evolution of the different eigenmodes. The eigenvalues we will consider are:

n	1	2	3	4	5	6
λ	1.0000	5.3864	13.3127	24.7645	39.7405	58.2405

Table 1

Approximate Eigenfunctions
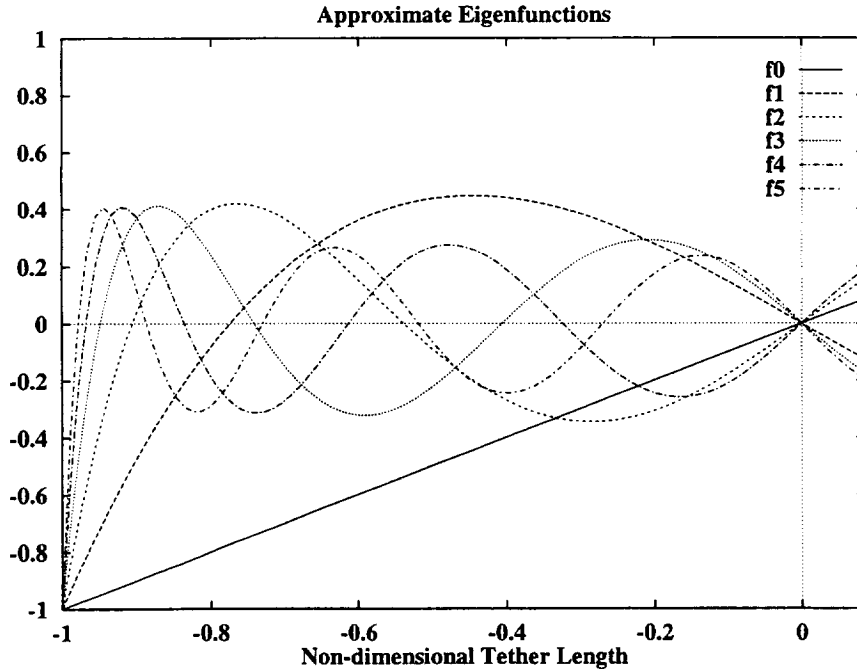
Figure 2: Six first approximate Eigenfunctions (A_0 only).

9

Numerical Computation of the Eigenmodes' Time Equations

Substituting these values of λ in the time equations (21), we obtain:

$$\ddot{Z} + \left(\lambda G(\tau) + \frac{\omega^2}{\kappa n^2}\right)Z = 0$$

$$\ddot{E} + (\lambda G(\tau) - H(\tau))E = 0 \tag{28}$$

Where H and G are functions of τ through v and θ. Dots mean derivation with regard to non-dimensional time τ. Since θ is only known as a function of time by integrating (5), there is no way to solve these equations analytically. A numerical integration has to be carried out, in parallel with the equations for θ, and this for each eigenvalue we want to explore.

For this, the system being linear, we will take two independent solutions and integrate them for a number of orbits to see their evolution. One will have initial deviation and zero initial speed, and the other initial speed and zero deviation. We will take the first six eigenvalues, corresponding to n=1,3,5,7,9,11.

To avoid the difficulty of solving Kepler's equation at each integration step, we will take v as the independent variable. This change implies:

$$\frac{dx}{d\tau} = \frac{dx}{dv}\frac{dv}{d\tau} = \dot{x}\frac{\omega}{n}; \quad \frac{d^2 x}{d\tau^2} = \frac{d}{d\tau}\left(\dot{x}\frac{\omega}{n}\right) = \ddot{x}\frac{\omega^2}{n^2} - \frac{2e\sin v \omega^2}{\kappa n^2}\dot{x} \tag{29}$$

which yields the system of equations:

$$\ddot{\theta} = \frac{2e\sin v}{\kappa}(\dot{\theta}+1) - \frac{3}{\kappa}\sin\theta\cos\theta$$

$$\ddot{E} = \frac{2e\sin v}{\kappa}\dot{E} - \left[(\lambda-1)G + \frac{3(\cos^2\theta - \sin^2\theta)}{\kappa}\right]E \tag{30}$$

$$\ddot{Z} = \frac{2e\sin v}{\kappa}\dot{Z} - \left[\lambda G + \frac{1}{\kappa}\right]Z$$

But now, G and H are functions of v:

$$G(v) = (\dot{\theta}+1)^2 + \frac{(3\cos^2\theta - 1)}{\kappa}$$

$$H(v) = (\dot{\theta}+1)^2 + \frac{(3\sin^2\theta - 1)}{\kappa} \tag{31}$$

And the initial conditions will be:

$$\theta(0) = 0 \quad E_1(0) = 0 \quad E_2(0) = 1 \quad Z_1(0) = 0 \quad Z_2(0) = 1$$

$$\dot{\theta}(0) = \Omega_0 \quad \dot{E}_1(0) = 1 \quad \dot{E}_2(0) = 0 \quad \dot{Z}_1(0) = 1 \quad \dot{Z}_2(0) = 0 \tag{32}$$

The initial libration angular speed is given by the gravity gradient pendulum speed at the crossing of the local vertical, obtained from the energy equation: $\dot{\theta}_0 = \omega_0\sqrt{3}\sin\theta_M$, where ω_0 is the circular orbit angular speed and θ_M the maximum libration amplitude before cutting. These angle and angular speed are referred to the circular orbit frame. After the cut, we use a frame tied to the elliptic orbit of the COM; therefore, speeds have to be adjusted. If system 1 is a fixed frame centered in the Earth, 2 the TS-bound frame, 0 the COM orbital frame, and 3 the circular orbit frame, the angular speed we seek is ω_{20}, and we can write:

$\dot{\theta}(0) = \omega_{20} = \omega_{23} + \omega_{31} - \omega_{01}$; where ω_{23} is $\dot{\theta}_0 = \omega_0\sqrt{3}\sin\theta_M$ above, ω_{31} is the circular angular speed ω_0, and ω_{01} is the angular speed of the elliptical orbit, which we take from [2]:

$$\omega_{01} = \dot{v}(v=0) = n\frac{(1+e\cos v)^2}{(1-e^2)^{3/2}} = \left(\frac{\omega_0}{1+3(1+u)\varepsilon+...}\right)\frac{(1+e)^{1/2}}{(1-e)^{3/2}} = \omega_0[1+(u-3)\varepsilon+...] \tag{33}$$

Adding the terms we obtain:

$$\omega_{20} = \frac{d\theta}{dt}(0) = \omega_0\sqrt{3}\sin\theta_M(1-2\varepsilon+...) \tag{34}$$

with respect to time, and:

$$\dot{\theta}(0) = \frac{d\theta}{dv}(0) = \frac{\omega_{20}}{\dot{v}_0} = \sqrt{3}\sin\theta_M\left[1 - 2\left(\sqrt{3}\sin\theta_M + 1\right)\varepsilon + ...\right] \qquad (35)$$

with respect to true anomaly, which is the one we will use in the numerical integration. This is done by the routine "TRVSA100.C", which computes the amplitudes of the oscillations for 100 periods of each independent solution and eigenvalue (not orbital periods) for values of the initial libration amplitude (θ_M) ranging from 0 to 60 degrees. The period of each oscillation is computed as well.

Remarkable points of the results are:

- Eigenvalue 0 diverges fast for both in-plane and out-of-plane oscillations. The greater θ_M, the faster it grows. This is not as troublesome as it looks, since the corresponding eigenmode, as shown in Figure 2, is a straight line. It only reflects the stability of the rigid body libration itself, which is bounded—at least while we are far from the libration to rotation transition. Linear stability is not the right tool for this mode: we should use orbital stability instead.

- Eigenvalue 1 diverges for in-plane oscillations for θ_M=54~55 deg., while remaining bounded for higher values of θ_M. Resonance rather than de-stabilizing low tension must be at work here. Initial conditions are important: initial deviation causes a faster divergence.

- Eigenvalues 2 and 3 diverge after a number of periods for in-plane oscillations and for the higher libration angles; Eigenvalues 4 and 5 remain bounded for the number of oscillations computed (100). Again, initial deviation is more critical than initial speed. The fact of being in phase or out of phase with the underlying librations seems to matter.

- All eigenmodes except 0 remain bounded for out-of-plane oscillations for the time computed.

We should look more closely at these points. The behavior of θ itself, the 0 eigenfunction, will be studied later on more in detail. For divergent eigenfunctions 1-3 in-plane, our problem is how long they will take to get out of control. We have computed the periods of the oscillations as well, but it is more convenient to display the oscillations vs. the true anomaly of the COM orbit, given in number of complete orbits. At the same time, we can give a wider variety of initial conditions to further explore the effect of having the oscillations in phase and out of phase. This is done by "TOVIC.C" and "TOVICNEG.C". The results show that the magnitude of the initial conditions does not matter at all, the equations being linear; the non-linearity and forcing terms, that could affect the nature of the solution, are limited to the libration equations and do not carry over to the linearized small deviation equations. For all eigenvalues losing stability, the critical case is initial deviation, except for eigenvalue 0, which de-stabilizes for initial speed—in phase with the libration. Sign does not affect significatively the results.

The resonance in Eigenvalue 1 for in-plane oscillations is investigated by sweeping more thoroughly the 51-61 degree zone. This is done in "TRVS100B.C", computing 100 oscillations for each eigenvalue and independent solution. Results plot oscillation amplitude versus true anomaly of COM orbit, measured in number of orbits. The results are shown in Figures 3-7. Figure 3 shows the amplitude of the libration computed with the full non-linear equations. E1 for Eigenvalue 0 in Figure 4 is the variation of the libration for initial speed perturbation, while E2 in Figure 5 is the initial deviation variation.

There is a resonance between 54 and 55 degrees. There is no resonance for out-of-plane oscillations. Curiously, there is no loss of stability for higher angles, and for 60 and 61 degrees oscillations remain bounded. For Eigenvalues 2 and 3, destabilization follows increasing libration angle, as was noted in "TRVSA100.C," "TOVIC.C," and "TOVICNEG.C."

This raises the point of whether there is another resonance at work with these eigenvalues for a higher libration angle. The case is not worth pursuing, though, since for these angles the tether goes slack and the equations used would no longer be valid. For null tension or even for very low tensions the model used would not be valid, and bending stiffness and coiling stresses would have to be considered. Tether points would start to move freely until they stray enough to make the tether taut again, causing a rebound. This is a scenario to be avoided at all costs.

Another point to study is the sensitivity of this resonance to variations in the eigenvalue. This will be considered after the Ritz-Galerkin method is used.

Th0 Pendular oscillation vs Theta Max

51 deg	——
52	------
53	········
54	············
55	—·—·—
56	—··—··
57	·········
58	·········
59	·········
60	——
61	------
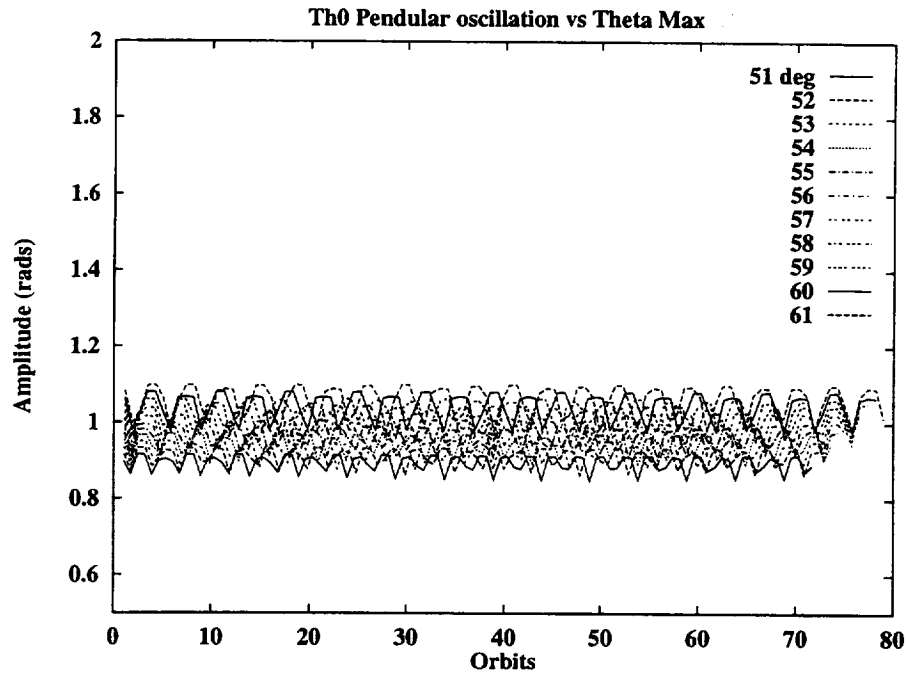
Figure 3 Libration amplitude (full non-linear equations) vs number of orbital periods, for different initial libration amplitudes (θ_{Max}).
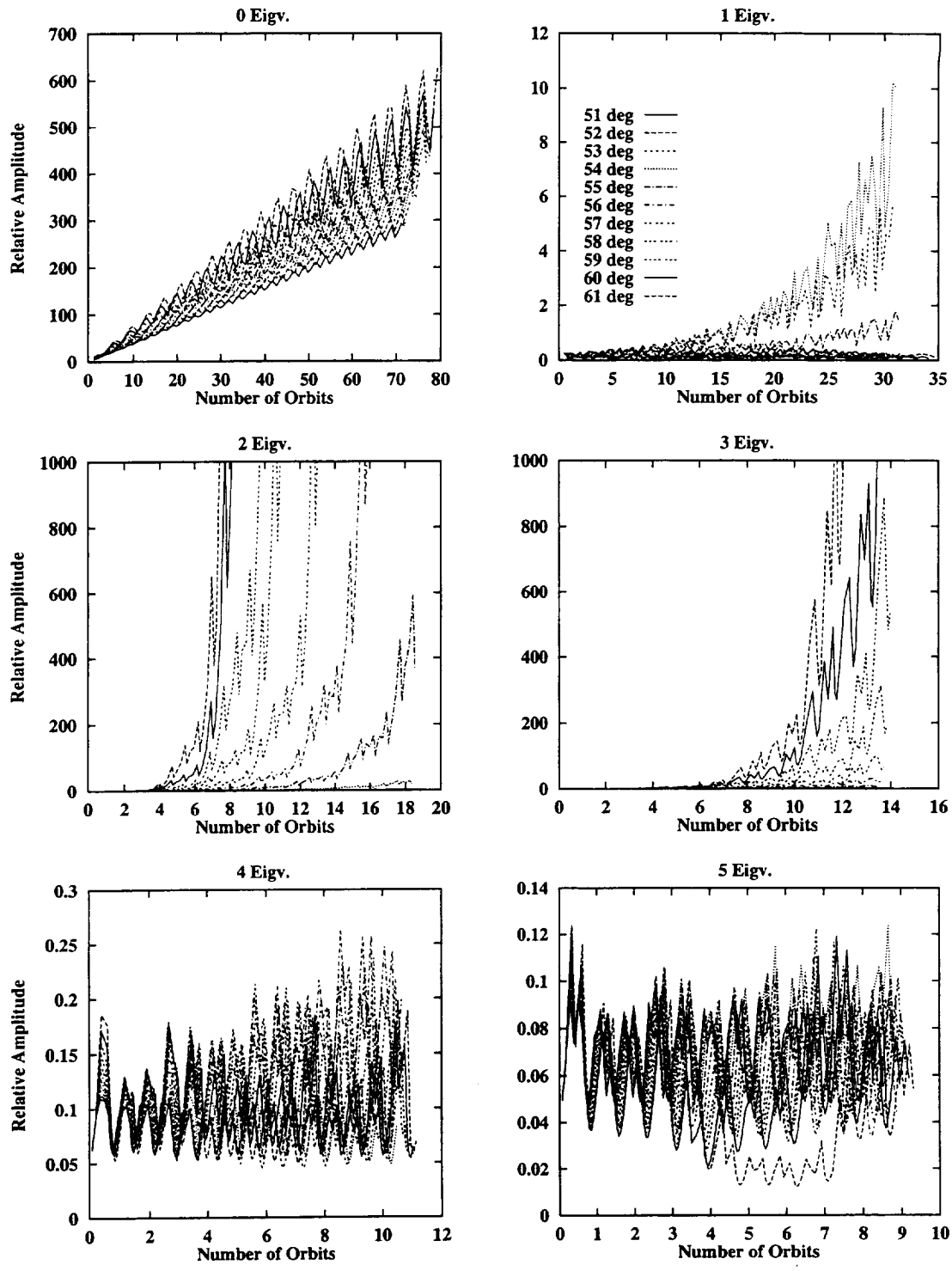
Figure 4 In-Plane Initial Speed, 100 Oscillations (E1): Amplitude vs number of orbits for different initial libration amplitude (θ_M) and for the first six eigenvalues.

13
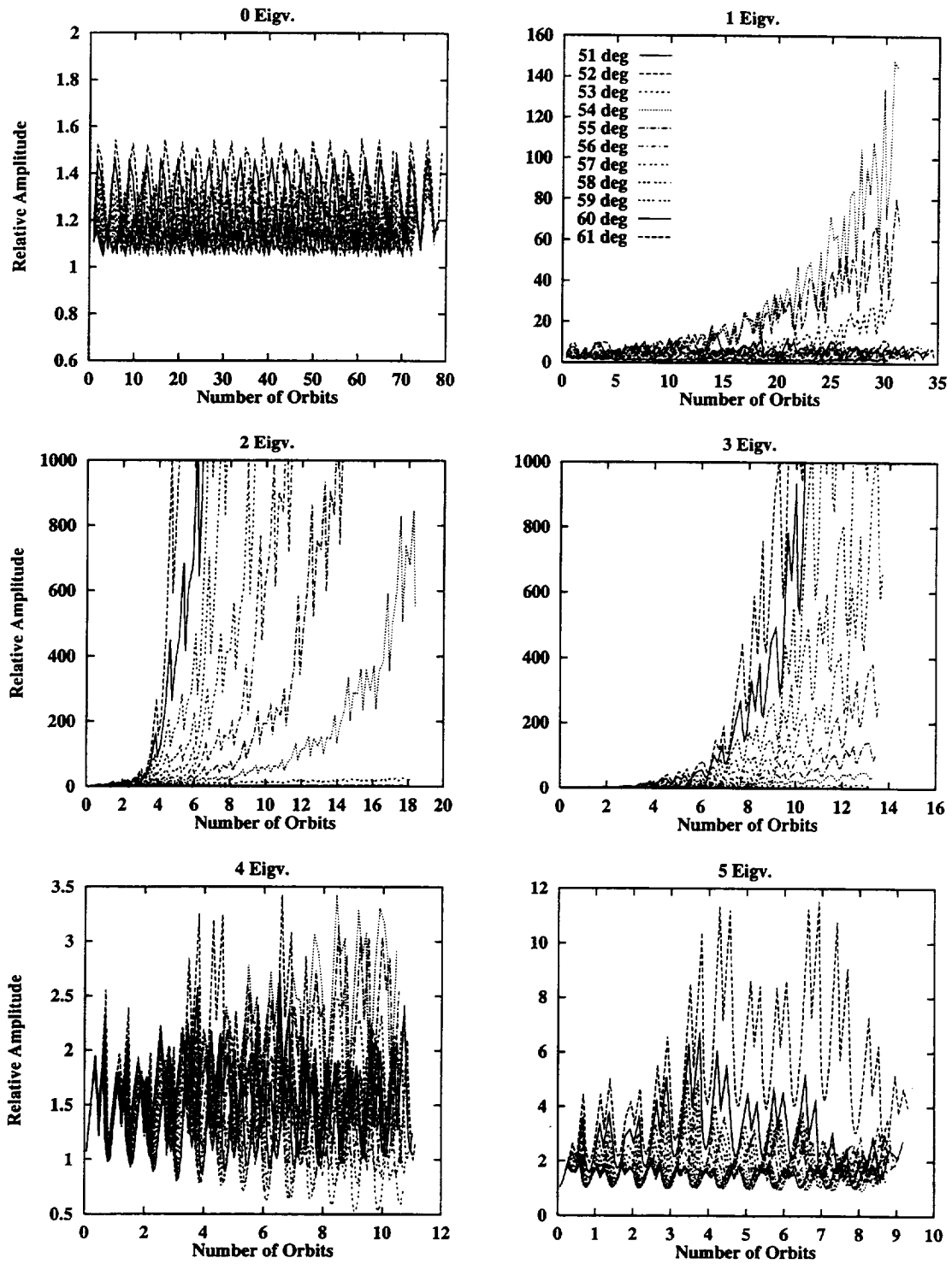
Figure 5 In-Plane Initial Deviation Oscillations (E2): Amplitude vs number of orbital periods for different initial libration amplitude (θ_M) and for the first six eigenvalues.

14
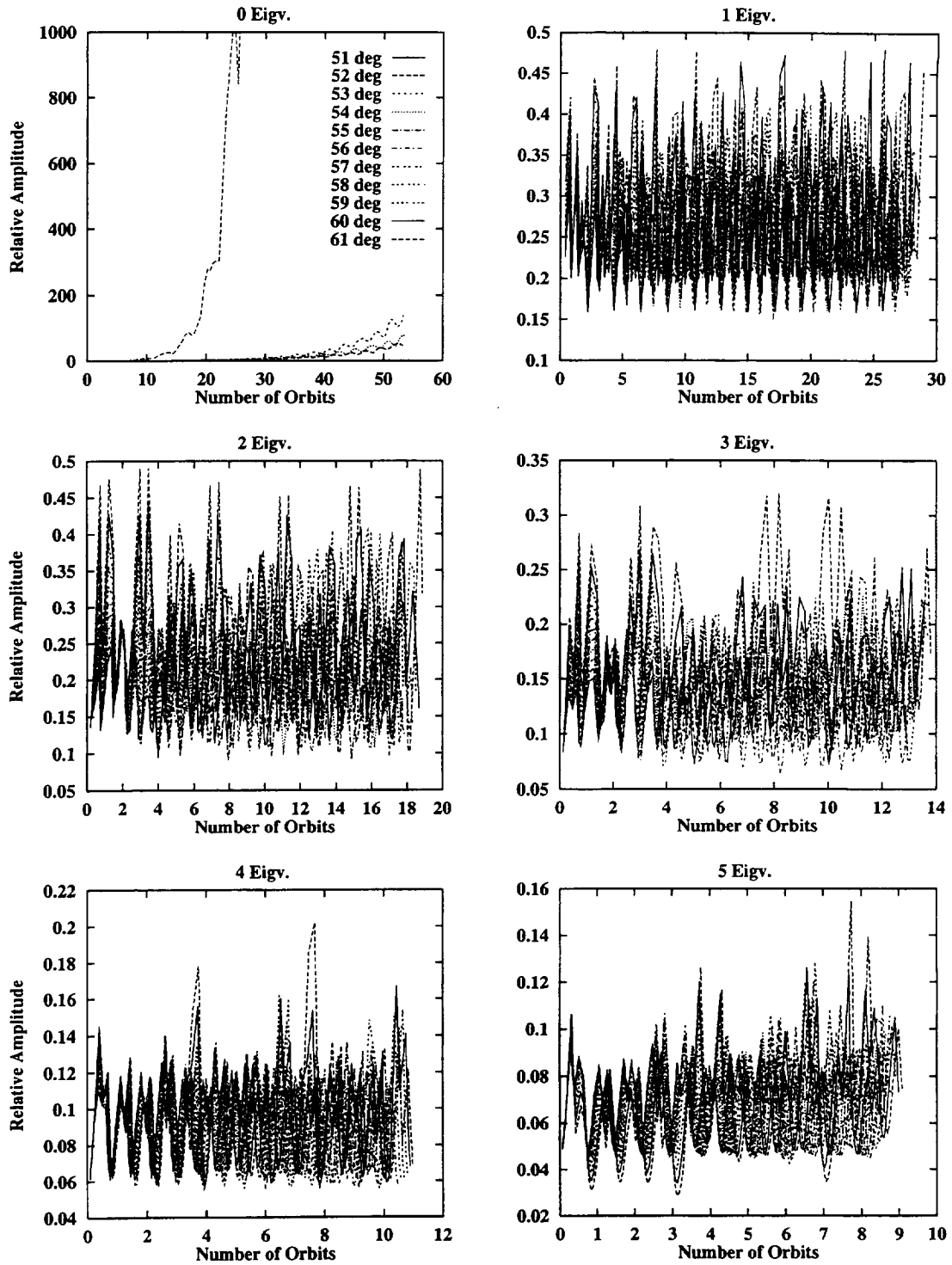
Figure 6 Out-of-Plane Initial Deviation Oscillations (Z1): Amplitude vs number of orbital periods for different initial libration amplitude (θ_M) and for the first six eigenvalues.

15
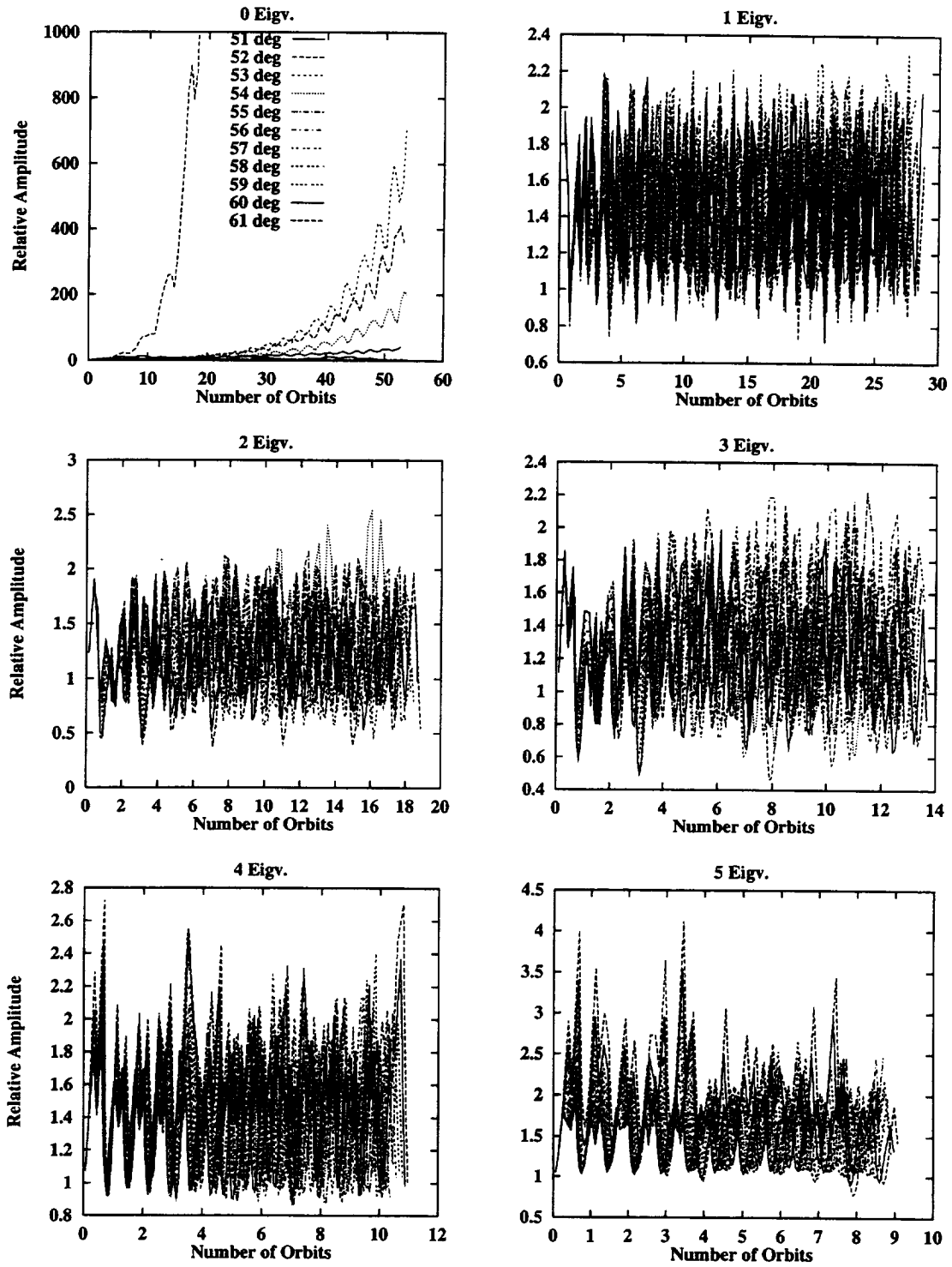
Figure 7 Out-of-Plane Initial Deviation Oscillations (Z2): Amplitude vs number of orbital periods for different initial libration amplitude (θ_M) and for the first six eigenvalues.

16

Ritz-Galerkin Method with Trigonometric Functions

We will Choose a set of simple orthogonal functions meeting the boundary conditions for the eigenvalue spatial problem, and try to minimize the residuals [9,12]:

$$\zeta_1(v,\tau) = \sum_{i=1}^{k} a_i(\tau)\phi_i(v) \qquad (36)$$

with a suitable number of terms k. As a first trial, we will choose trigonometric functions:

$$\phi_i = K_i \cos(2\pi i v) + \sin(2\pi i v) \qquad (37)$$

Where the constants K_i will be determined so that the boundary conditions (19) are met. Conditions (23) to (25) do not make sense here since we are not using separation of variables. These turned out to be the same for functions meeting the differential equation. Curiously, for functions (37), both boundary conditions are the same as well, but for different reasons: the integral in (19) will be zero for any periodic function integrated over a multiple of the period, and for trigonometric functions the second derivative has the same zeros as the function itself. Taking four terms for the trial solution, the constants are:

i	1	2	3	4
K	-0.5955	-1.8459	24.5599	1.5335

Table 2

Substituting the trial function in the differential equation, we obtain:

$$\ddot{\zeta}_1 - H(\tau)\zeta_1 - G(\tau)\left\{\left[(b-1)^2 - v^2\right]\zeta_1'\right\}' = 0 \qquad (38)$$

$$\sum_{i=1}^{k}\left(\ddot{a}_i\phi_i - Ha_i\phi_i - \frac{G}{2}\left\{\left[(b-1)^2 - v^2\right]a_i\phi_i'' - 2va_i\phi_i'\right\}\right) = R \approx 0 \qquad (39)$$

We will use Galerkin weighing to minimize the residual:

$$\int_{b-1}^{b}\phi_i R(a_j,\phi_j)dv = 0, \quad i,j = 1...4 \qquad (40)$$

For which we will have to compute the integrals: $\int \phi_i\phi_j$; $\int \phi_i v\phi_j'$; $\int \phi_i\left[(b-1)^2 - v^2\right]\phi_i''$; which we can put in matrix form:

C	ϕ_1	ϕ_2	ϕ_3	ϕ_4
ϕ_1	0.6773	0	0	0
ϕ_2	0	0.3395	0	0
ϕ_3	0	0	-0.5570	0
ϕ_4	0	0	0	0.2232

Table 3

CP	$v\phi_1$'	$v\phi_2$'	$v\phi_3$'	$v\phi_4$'
ϕ_1	-0.3387	1.6290	-10.7285	0.5682
ϕ_2	-1.6290	-1.1019	-61.9249	-2.5623
ϕ_3	10.7285	61.9249	-151.0478	77.1426
ϕ_4	-0.5682	2.5623	-77.1426	-0.83789

Table 4

CS	[...]φ₁"	[...]φ₂"	[...]φ₃"	[...]φ₄"
ϕ_1	**-15.8799**	**8.6882**	**-48.2787**	**-2.4244**
ϕ_2	**2.1720**	**-203.3531**	**-445.8599**	**.13.6656**
ϕ_3	**-5.3643**	**-198.1599**	**-62532.1924**	**705.3039**
ϕ_4	**-0.1515**	**-3.4164**	**396.7334**	**-616.0203**

Table 5

Defining the vector: $\mathbf{a} = \lfloor a_1 \quad a_2 \quad a_3 \quad a_4 \rfloor^T$, we can write the matrix equation:

$$C(\ddot{a} - Ha) - \frac{G}{2}(CS - 2CP)a = 0 \tag{41}$$

$$\ddot{a} = \left[HI + GC^{-1}(CS - 2CP)/2\right]a = (HI + GA)a \tag{42}$$

Where **I** is the unit matrix and **A** is:

-11.2219	4.0083	-19.7986	-0.9507
1.2320	-45.6377	-73.0591	-1.9378
-0.0444	-0.5329	-102.9973	9.9119
-0.3843	-2.5484	164.4063	-186.3008

Table 6

Elements in the main diagonal are big and negative, which is good. The trial functions are not eigenvalues, but ϕ_1 and ϕ_2 come close to eigenfunctions 3 and 5, as can be seen from the proximity of the diagonal terms. Now we have to integrate the time equations for **a**, but this has to be done numerically: G and H are functions of τ and θ, which can be obtained as a function of τ only through numerical integration. Again, in order to avoid integrating Kepler's equation at every step, we shift to true anomaly as variable. The equations will be:

$$\ddot{a} = \frac{2e\sin\nu}{\kappa}\dot{a} + \left[H(\nu)I + G(\nu)A\right]a \tag{43}$$

Where H and G are now those in (31). There is a great similarity with the separation of variables solution. If A were just diagonal with the eigenvalues as diagonal terms, the equations would be exactly the same. As in the previous case, the integration is made by taking two independent particular solutions and running them for a number of orbits. We will take only the two first functions, a_1 and a_2, and integrate a1a, a1b, a2a, a2b and θ for a number of orbits. A is the initial speed solution, and B the initial deviation solution. This is done by "RITZTRIG.C". The results are shown in Figure 8. All solutions show the behavior of the most unstable eigenmodes of the previous section. This is to be expected, since trigonometric functions are not eigenfunctions of the problem, and each one of them includes a mixture of all modes. The coefficient computations can be checked in the MapleV script in Appendix A.
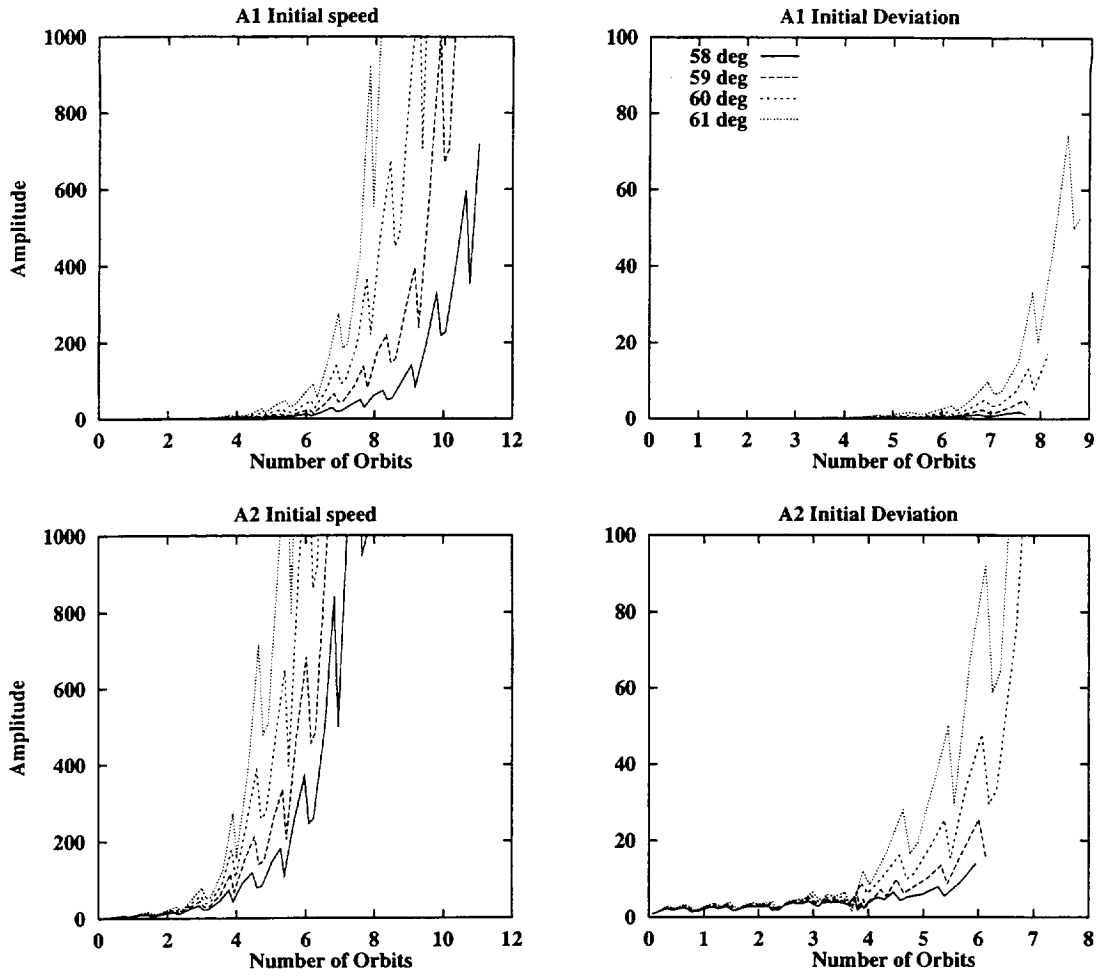
Figure 8 In-plane oscillations for Ritz method with trigonometic functions: A1 (first mode) and A2 (second mode); oscillation amplitude vs number of orbits.

Ritz-Galerkin Method with Legendre Polynomials

The results of the previous section do not show much detail, since the trial functions are not eigenfunctions and therefore each one includes a mixture of all modes. If we want a more detailed output, the trial functions should be as close as possible to the real eigenfunctions. This is easily done using the approximate analytical solution introduced in (27). Rearranging it and reducing the number of repeated arbitrary constants, we obtain:

$$A(x) = C_0 \left\{ P_n(x) \left[1 + \varepsilon K + 2\lambda_1 \varepsilon \int_0^x P_n(u) Q_n(u) du \right] + Q_n(x) \varepsilon \left[\frac{4(\lambda_0 - 1)\Gamma\left(1 + \frac{n}{2}\right)^2}{\pi \lambda_0 \Gamma\left(\frac{1+n}{2}\right)^2} - 2\lambda_1 \int_0^x P_n(u)^2 du \right] \right\}$$

(44)

Where we had made the change v=x(1-b). Since this solution is an approximation, it will fulfill the differential equation and boundary conditions (26) only up to $O(\varepsilon)$. The value of the constant K cannot be determined from the $O(1)$ and $O(\varepsilon)$ problems, we would need to go up to $O(\varepsilon^2)$, which is already unmanageable. But this is not a problem when we use Ritz method: we are not dealing with the Sturm-Liouville equations (22), but with the general problem (17) with boundary conditions (19). We can then choose K so that the boundary conditions are met. Still, seeing how close our trial solutions come to meeting equation (26) tells us how close we are to the real eigenfunctions. Going back to the variable v, our trial functions will be:

$$\zeta_1(v, \tau) = \sum_{i=1}^k c_i(\tau) A_i(v)$$

(45)

As in the previous section, only in-plane oscillations will be considered, since out-of-plane oscillations were all well behaved—except the fist eigenvalue, which is not a real problem and will be treated separately.

We will choose K_i so that the conditions (19) are met. This is done with a symbolic manipulator, MapleV. The results are collected in the MapleV script in Annex B, showing also how closely the spatial differential equation and the different boundary conditions are met. In the computation of $Q_0(x)$ we use a recurrence relation from [8, § 8.6.19]. The values of K selected to minimize conditions (19) are: $K_1=0$, $K_3=1.7418$, $K_5=0.6094$. Thus our trial functions are:

$$\zeta_1(\tau, v) = \sum_{i=1} c_i(\tau) \phi_i(v) = \sum_{i=1} c_i(\tau) A_i\left(\frac{v}{1-b}\right), \qquad i = 1,3,5$$

(46)

Substituting this in (18), we obtain:

$$\sum_i \left\{ \ddot{c}_i A_i - H(\tau) c_i A_i - \frac{G(\tau)}{2} \left[(b^2 - 1) - v^2 \right] \frac{c_i}{(1-b)^2} A_i'' + \frac{G(\tau) v c_i}{1-b} A_i' \right\} = R(c_i, A_i, v) \approx 0$$

(47)

As we did above, we will minimize the Galerkin-weighed residuals:

$$\int_{b-1}^b A_i R(c_j, A_j, v) dv = 0$$

(48)

For this we will have to compute 27 integrals. It will be simpler to return to the variable x:

$$(1-b)\int_{-1}^\varepsilon A_i A_j dx; \quad (1-b)^2 \int_{-1}^\varepsilon x A_i' A_j dx; \quad (1-b)^3 \int_{-1}^\varepsilon (1-x^2) A_i'' A_j dx; \quad i, j = 1,3,5$$

(49)

This can be put in matrix form defining the vector c and the matrixes **A**, **AP**, and **AS** for the time functions, the integrals of function products, the integrals of functions times first derivatives, and the integrals of functions times second derivatives, respectively. The integrals are computed with MapleV, as shown in Appendix C, and their values are:

20

A	ϕ_1	ϕ_2	ϕ_3
ϕ_1	0.3336	0.01171	-0.005983
ϕ_2		0.2226	-0.0006923
ϕ_3			0.1260

Table 7

AP	$x\phi_1$'	$x\phi_2$'	$x\phi_3$'
ϕ_1	0.3336	1.163	1.097
ϕ_2	0.01171	0.5938	1.280
ϕ_3	-0.005983	0.008283	0.5253

Table 8

AS	$[1-x^2]\phi_1$''	$[1-x^2]\phi_2$''	$[1-x^2]\phi_3$''
$\phi 1$	0	2.186	2.375
$\phi 2$	0	-1.267	2.540
$\phi 3$	0	0.04185	-2.381

Table 9

$$A\left(\ddot{c}-Hc\right)-\frac{G}{2}ASc+GAPc=0 \tag{50}$$

$$\ddot{c}=\left[HI+GA^{-1}\left(\frac{AS}{2}-AP\right)\right]c=(HI+GB)c \tag{51}$$

Where I is the unit matrix and the value of B, again from MapleV, is:

-1	-0.1663	-.0305
0	-5.5120	-0.0829
0	-0.0693	-13.6147

Table 10

Since the function we used was an approximation, and the boundary conditions were approximately met too, there is no point in keeping too many digits in B. We can see that the matrix is decoupled to nearly order $O(\varepsilon)$, and the terms in the main diagonal are very close to the analytical eigenvalues in Table 1.

If the boundary condition for the first derivative had been taken into account in the optimization of K_i, the diagonal terms would be closer to the eigenvalues and the modes would be more neatly separated; but the basic assumption of Ritz method—that trial functions meet boundary conditions—would not be as accurately met and the results would be less reliable.

For the numerical integration we turn again to true anomaly instead of non-dimensional time. The equations to be run are:

$$\ddot{\theta}=\frac{2e\sin v}{\kappa}\left(\dot{\theta}+1\right)-\frac{3\cos\theta\sin\theta}{\kappa}$$

$$\ddot{c}=\frac{2e\sin v}{\kappa}\dot{c}+(HI+GB)c \tag{52}$$

With initial condition (35) for θ, and a pair of independent solutions for c, which is a linear system: initial unit speed and zero deviation (a), and initial unit deviation and zero speed (b). This means integrating a total of 14 first-order equations. Solutions will be c1a, c1b, c3a, c3b, c5a, and c5b. The code for this is in "RITZLEG.C." c1 corresponds to the eigenvalue we earlier called 0, which is the rectilinear shape; c3 corresponds to eigenvalue 1 of previous figures, and c5 to eigenvalue 2.

The results are shown in Figure 9. All solutions grow exponentially after a number of orbits. This is similar to the previous case, in which trigonometric functions encompass all eigenmodes and diverge quickly, while for the approximate eigenfunctions there were clearly stable and unstable ones. In this case the onset of instability

can be traced to the coupling terms in matrix **B**. Although small—say of order ε—their effect would be felt after a time of order $1/\varepsilon$. Thus c1 will feel the influence of c3 after $1/0.16$, or about two orbits. This is not noticeable because the second eigenvalue takes about 30 orbits to diverge. It would feel the influence of c5 after $1/0.03$, or about 10 orbits, and so it diverges at that time. The initial deviation solution diverges earlier because the corresponding c5b does so as well. Finally, c3 should diverge after $1/0.08$, or 6 orbits, and indeed it does so.

Thus the off-diagonal terms of matrix B couple the modes and mask each one's proper behavior. Short of an exact eigenmode, we can simply omit these terms and keep the main diagonal, or the approximate eigenmodes. This is done in "RITZLEG2.C." The results are shown in Figure 10. Each mode recovers its own personality, and we notice even the decay of the initial deviation c1b solution (eigenvalue 0 previously) for 42 degrees, that was present in the "TRVSA100.C" results (not shown in Fig. 5 because the "TRVSB100.C" results scan only 51-61 degrees). Of the θ_M values computed, this is the closest to 45 degrees, where the maximum of the restoring term $3\sin\theta\cos\theta$ is experienced.
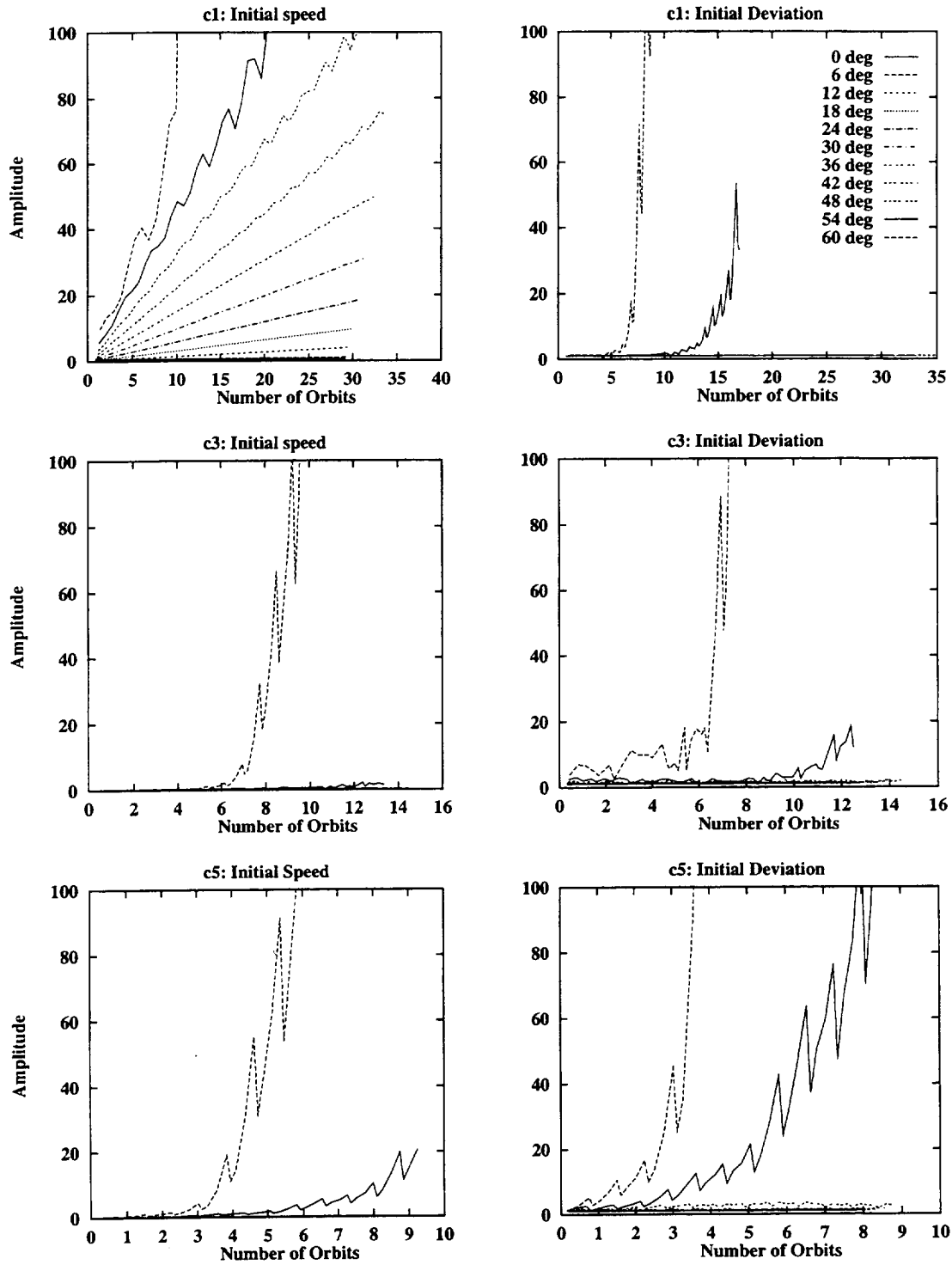
Figure 9 In-plane oscillations for Ritz method with Legendre functions: 3 first modes; oscillation amplitude vs number of orbits.
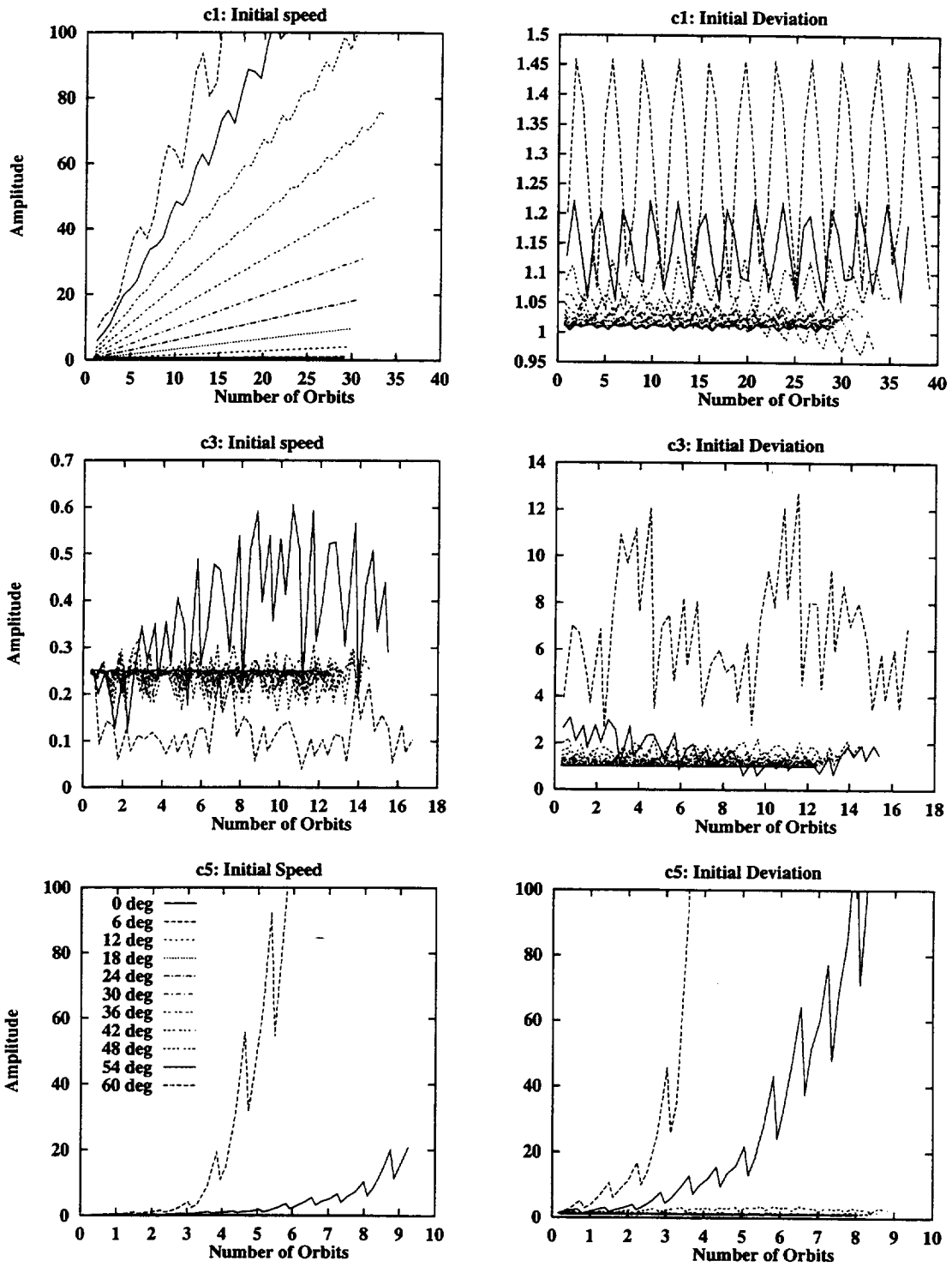
Figure 10 In-plane oscillations for Ritz method with decoupled Legendre functions: 3 first modes; oscillation amplitude vs number of orbits.

Numerical Determination of Eigenvalues

The approximate solution (27) to the Sturm-Liouville problem (22) cannot go beyond the $O(\varepsilon)$ expansion, since the equations become too complex. There is always the possibility of numerically solving the differential equation. A tabulated solution is not easy to handle, but what we need for the time equations is only the eigenvalue. We set then to solve equation (22) with boundary conditions (23), (24), or (25) which, as we saw before, are exactly the same. (23) or (25) are easy to impose, while (24) can only be used after the integration to check the accuracy of the solution.

The only boundary condition at the free end is that the tension be zero, which causes the coefficient of A" to be zero. A"(b-1) is thus an indetermination of type 0/0, and cannot be used to start a run. What we know is that it cannot be infinite, since it is related to the curvature of the tether. Therefore, the rest of the differential equation must be zero as well, which provides a boundary condition to check proximity to the real eigenvalue. We can thus start integrating at v=b with boundary condition (22) and an arbitrary value for A(b). Since eigenfunctions are defined except for a multiplicative constant, we may normalize the value of A so that, for the linear solution, A(b-1)=1, and thus A(b)=b/(1-b).

At the free end we will require that A" be finite, that is,

$$-(1-b)A'(1-b) + \lambda A(1-b) = 0 \tag{53}$$

which is the same condition imposed on the end mass, (25). The functions to integrate are:

i	y[i]	dy[i]	Init. Cond.
1	$\int Adv$	y[2]	0
2	A	y[3]	b/(1-b)
3	A'	$(2vy[3] - 2\lambda y[2])/\left[(b-1)^2 - v^2\right]$	$\lambda/(1-b)$
4	λ	0	k(k+1)/2 (1,3,5...)

Table 11

With this we start a shooting method integrating routine in order to determine λ. The residual of (53) is taken as a function of λ whose roots we try to find with a combined shooting method/Newton-Raphson algorithm [6, pp. 756ff]. This is done calculating the Jacobian (which in this case is just the derivative, since we have only one variable):

$$\left.\begin{array}{ccc} \lambda_1 & \to & R(\lambda_1) \\ \lambda_1 + \Delta\lambda & \to & R(\lambda_1 + \Delta\lambda) \end{array}\right\} \quad J = \frac{R(\lambda_1 + \Delta\lambda) - R(\lambda_1)}{\Delta\lambda} \to \lambda_2 = \lambda_1 - \frac{R(\lambda_1)}{J} \tag{54}$$

We use as seed value the approximate eigenvalues found by asymptotic expansion, (27). y[1], which is condition (24), can be used as a further check of our approximation.

Still another simplification can be made by a change in variables: x=-v, which avoids integrating backwards and checking all integration routines for the sign of h. The form of the differential equation does not change at all:

$$\left[(b-1)^2 - x^2\right]A'' - 2xA' + 2\lambda A = 0 \tag{55}$$

And the boundary conditions remain unchanged, except that they are imposed at -b; the integrating interval becomes [-b:1-b]. The functions to be integrated now are:

i	y[i]	dy[i]	Init. Cond.
1	$\int Adv$	y[2]	0
2	A	y[3]	-b/(1-b)
3	A'	$(2xy[3] - 2\lambda y[2])/\left[(b-1)^2 - x^2\right]$	$\lambda/(1-b)$
4	λ	0	k(k+1)/2 (1,3,5...)

Table 12

There is an additional problem: the equation is singular in x=1-b, the free end. We cannot integrate all the way to the end, because A" will be unbounded in all iterations short of the exact eigenvalue. To sidestep this singularity, we will stop within a distance δ of the end. δ is chosen as $\sim 10^{-8}$ so that it is much smaller than the approximation we seek (about ε^3, with $\varepsilon \sim 0.085$), while still big enough that division by δ^2 will not cause overflow for double precision arithmetic. Otherwise, the error in each integration step goes out of hand as we approach the end.

This is done by "EIGVAL.C," using routines taken from [6] like `fdjac.c`, `fmin.c`, `lnsrch.c`, while others have been modified to fit this problem, like `newt.c`, `odeint.c`, and `shoot.c`. The first six eigenvalues are computed with this program.

λ	Numerical	Analytical	Ritz-Legendre[1]	Ritz-Legendre[2]
$\lambda 0$	1.000000	1.000	1.000	1.000
$\lambda 1$	5.439627	5.386	5.512	5.477
$\lambda 2$	13.453447	13.312	13.614	13.558
$\lambda 3$	25.031209	24.764	-	-
$\lambda 4$	40.172217	39.740	-	-
$\lambda 5$	58.875815	58.240	-	-

Table 13

The approximate analytical values come short of the numerical values, while the diagonal terms of matrix B in the Ritz method with Legendre polynomials outstrip them. The difference is greater when only the Ritz method-specific boundary conditions (19) are used to optimize the free parameter K (column 1). If condition (25) is included in the optimization (column 2), the diagonal values are closer to the numerical eigenvalues, but the Ritz method results are not as reliable.

These numerical eigenvalues are used to compute again the transversal oscillations. This is done by "TRVC100.C."

The reason for repeating the same computations every time we find some small change in the eigenvalues is that the stability of the modes may depend sensitively on the eigenvalues. For a circular orbit, the equations of the transversal oscillations become Mathieu equations [3, p. 386], whose stability areas are well known. The unstable areas increase for larger libration angles, so that a change in the eigenvalue may, depending on where we stay, push a mode in or out of the unstable area for a certain libration angle, or could raise or lower the libration angle at which a mode loses stability.

When we are in an elliptical orbit, more terms enter the equations and we have the additional resonance with the orbital frequency; but for small eccentricities we expect some similarity with the Mathieu pattern. A new run is thus well justified. The results are collected in Figures 11-14. Again, remarkable points are:

- The initial speed E1 solution shows that de-stabilization of eigenvalue 1 is pushed up to near 55 degrees., while in Fig. 4 it was closer to 54 degrees. Other eigenvalues keep the same behavior, with small variations in amplitude indicating that we are getting closer or farther from the unstable areas.
- The initial deviation E2 shows the same shift towards 55 degree de-stabilization as E1. Eigenvalue 5 takes longer to diverge.
- Initial speed out-of-plane Z1 shows no change with respect to Fig. 6, apart from eigenvalue 3 that shows a beginning of de-stabilization which was not present in any of the out-of-plane eigenvalues except 0.
- Initial deviation Z2 shows two unstability zones for eigenvalue 0, for 60 degrees and larger, and for 53 degrees; the latter just started to show in Z1. It seems that, as θ_M grows, we enter an unstable Mathieu zone, go out of it as it twists left, and finally enter the second unstable zone for 60 degrees and larger.

26
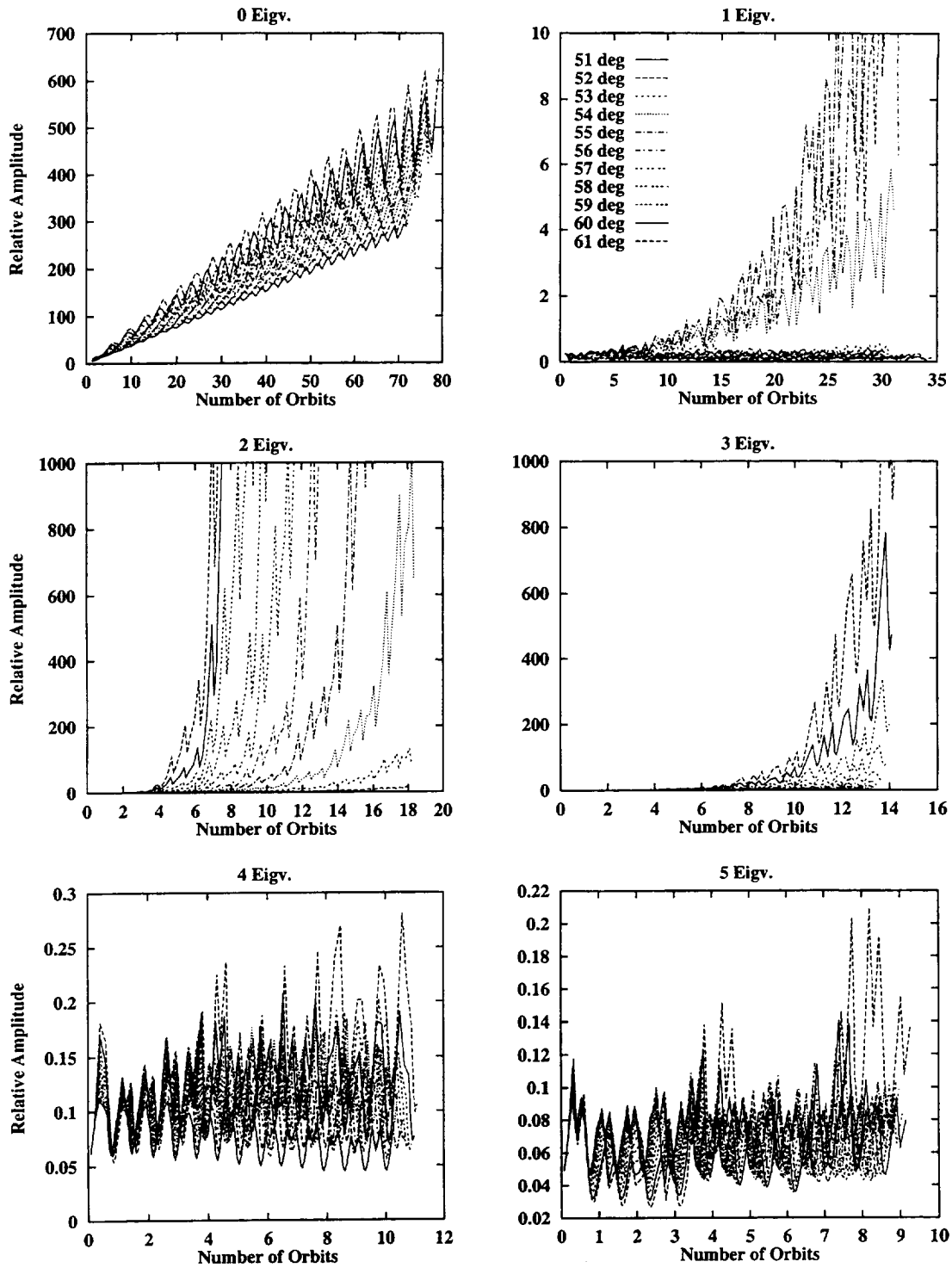
Figure 11 Numerical eigenvalues, in-plane initial speed (E1), 100 Oscillations: Amplitude vs number of orbits for different θ_M and for the first six eigenvalues.
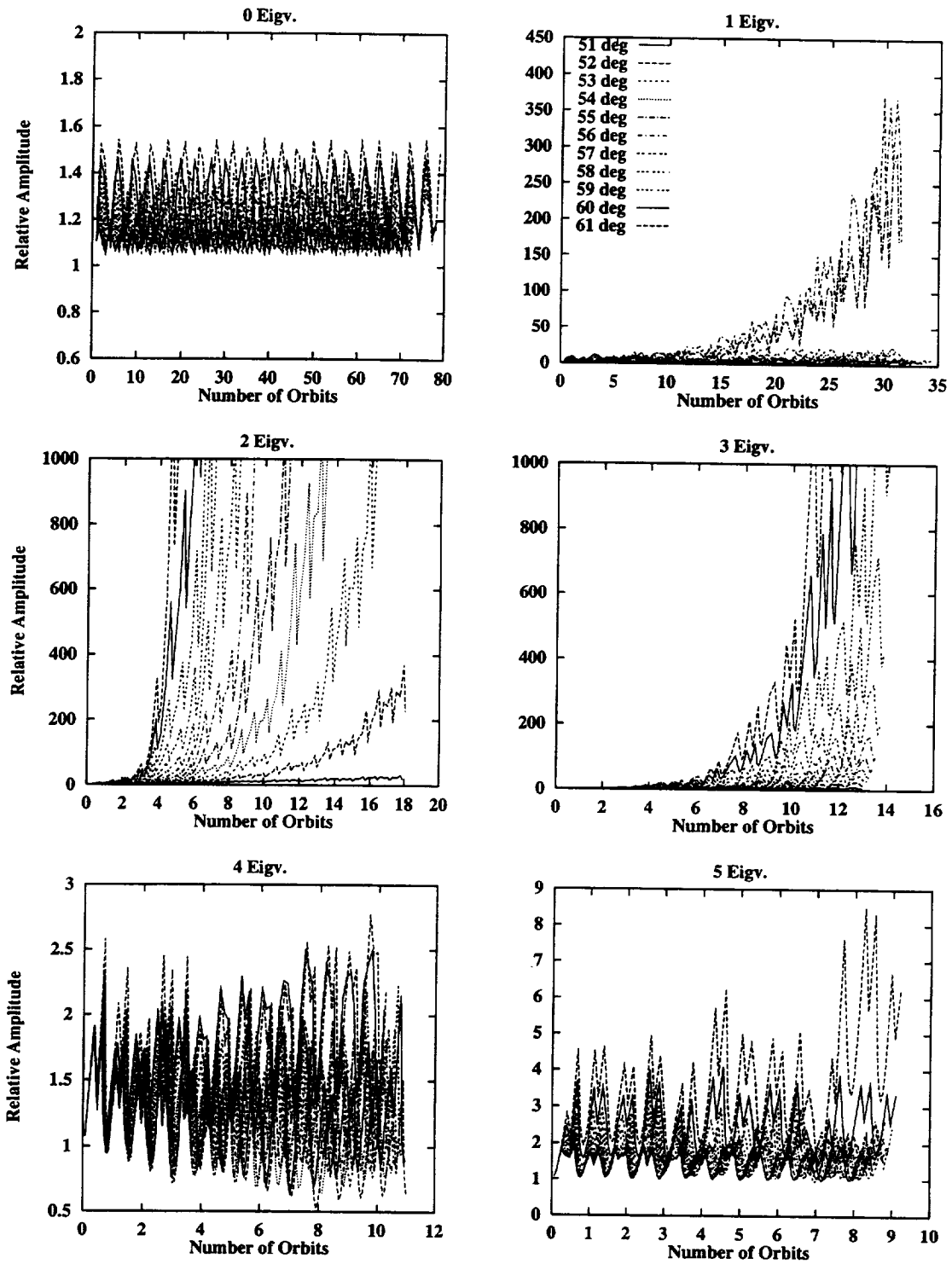
Figure 12 Numerical eigenvalues, in-plane initial deviation (E2), 100 Oscillations: Amplitude vs number of orbits for different θ_M and for the first six eigenvalues.
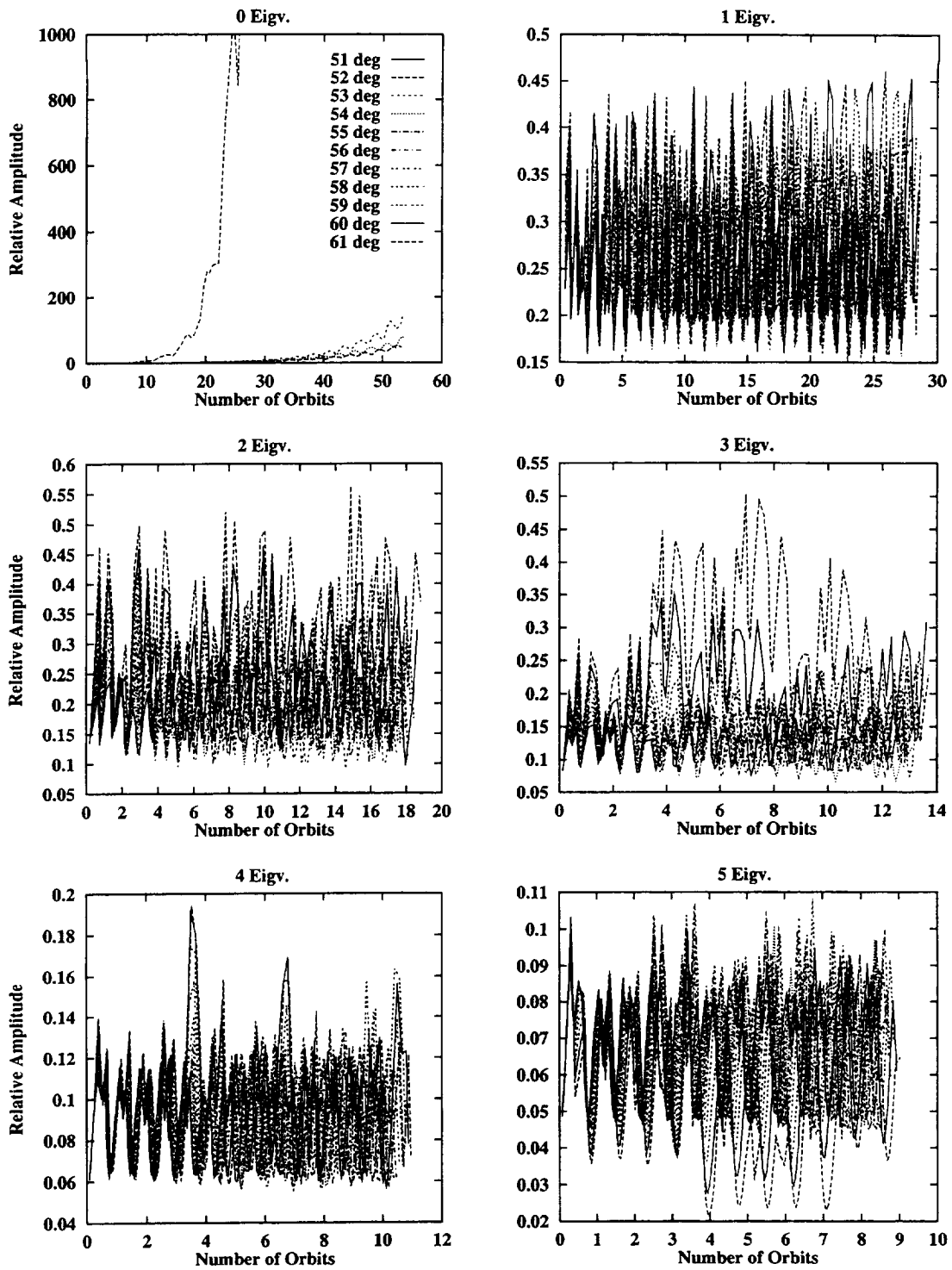
Figure 13 Numerical eigenvalues, out-of-plane initial speed (Z1), 100 Oscillations: Amplitude vs number of orbits for different θ_M and for the first six eigenvalues.
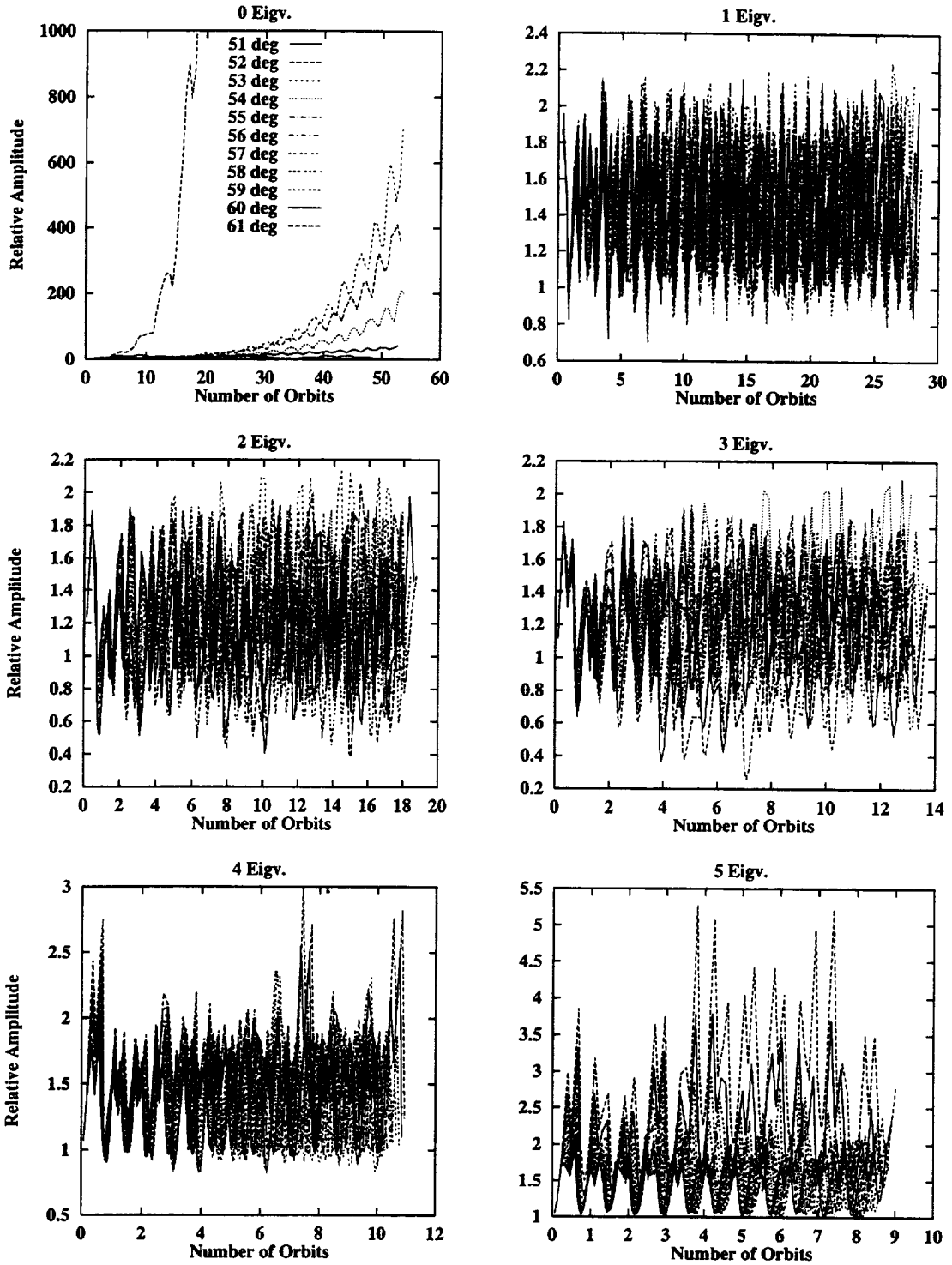
Figure 14 Numerical eigenvalues, out-of-plane initial deviation (Z2), 100 Oscillations: Amplitude vs number of orbits for different θ_M and for the first six eigenvalues.

30

Unstable Modes

The previous analysis of transverse oscillations has singled out some unstable modes and de-stabilizing factors that need further study. At the same time we should check the limits of our assumptions, like the decoupling of transverse oscillations. Points to be studied are:

- Relation of tension and stability
- Zero mode divergence
- Out-of-plane oscillation coupling
- Libration to rotation transition

Tension and Stability

For transverse oscillations, tension is the main stabilization factor, providing the restoring force for the oscillations. As tension becomes smaller, oscillations tend to increase in amplitude. Pendular libration and tension are governed by equations (6):

$$\ddot{\theta} - \frac{2e\sin v}{\kappa}(\dot{\theta}+1) + \frac{3}{\kappa}\sin\theta\cos\theta = 0$$

$$F = \frac{\omega^2}{2n^2}\left[(\dot{\theta}+1)^2 - \frac{1}{\kappa}(1-3\cos^2\theta)\right]\left[(b-1)^2 - v^2\right] = \frac{\omega^2}{2n^2}G(v)P(v)$$
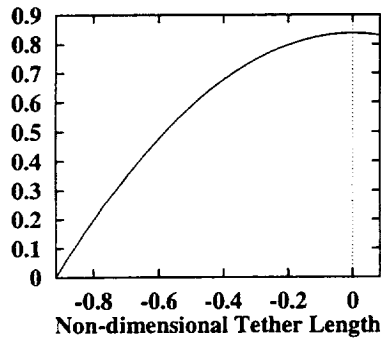
Figure 15 Tension distribution

P(v) reaches its maximum at the COM, and is zero at the free end. The tension distribution keeps its shape at all times, its magnitude governed by G(v). When G becomes zero, the tether goes slack at all points at the same time, and from that moment on the equations used are no longer valid. The tension time dependence, G, appears in the restoring term of transverse oscillation equations (28):

$$\ddot{Z} + \left(\lambda G(\tau) + \frac{\omega^2}{\kappa n^2}\right)Z = 0$$

$$\ddot{E} + \left(\lambda G(\tau) - H(\tau)\right)E = 0$$

It is thus interesting to see when the tension and the restoring terms go to zero. This is done in "THETA20.C," computing θ, G, and H for a number of orbits. the results are shown in Figures 16 and 17.

Theta remains bounded, and the tension is positive up to $\theta_M=63$ degrees. G goes to zero between 63 and 64 degrees. There is a zone where H is bigger than G, so that the restoring force is negative for low eigenvalues, specifically for $\lambda=1$ (eigenvalue 0). Since λ increases fast, for eigenvalues 1 and above, the value of H is not a problem except when G is very close to zero, that is, for large libration amplitudes. For angles above 63 degrees, G has negative zones, so that larger values of λ mean broader negative restoring force zones.

Out-of-plane oscillations are more stable because of the positive ω^2 term. This is just part of the picture. Resonance with libration and orbital frequency has to be taken into account as well. We will look into these in the following.
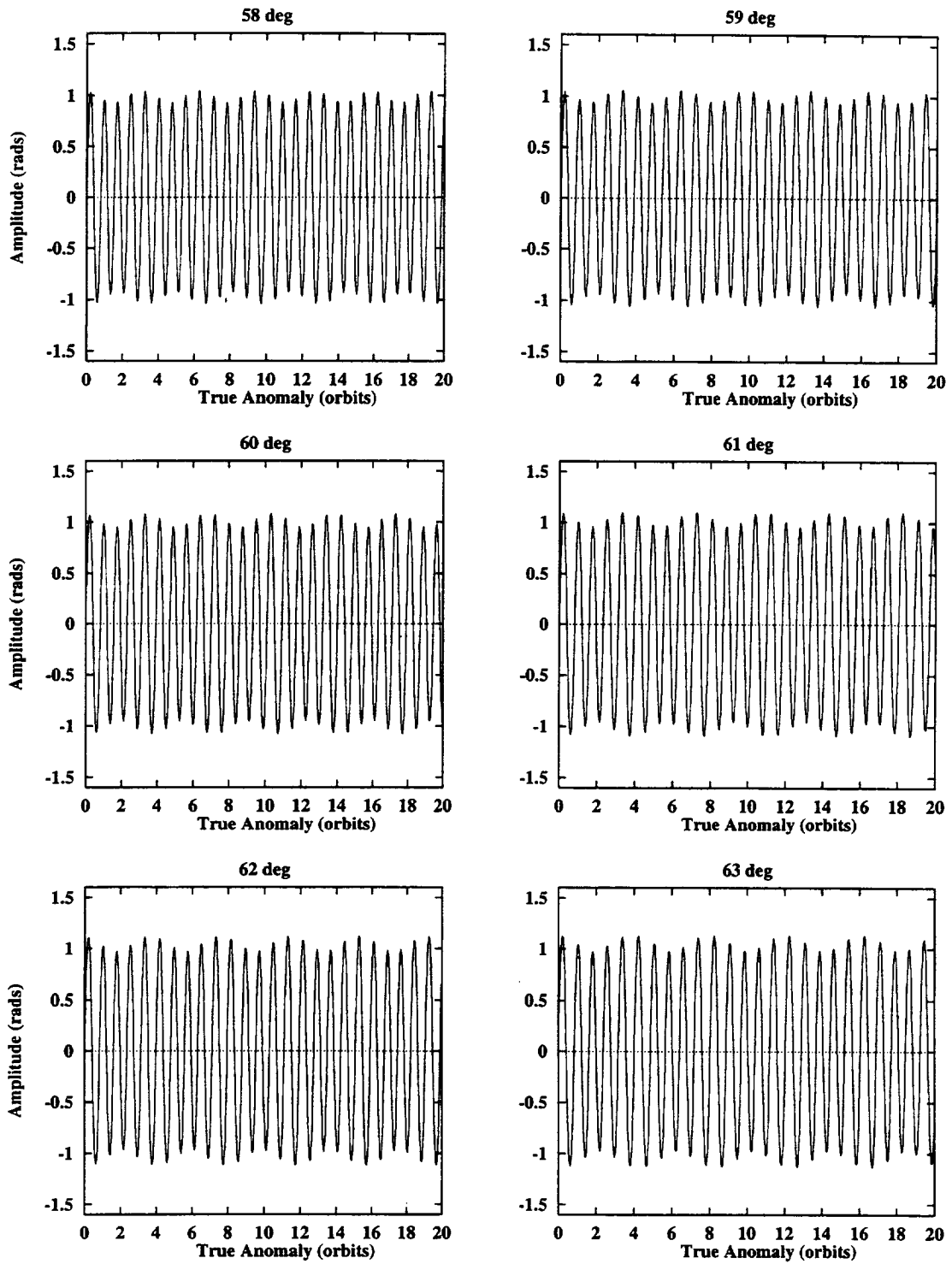
Figure 16 Libration angle for different initial libration amplitudes.
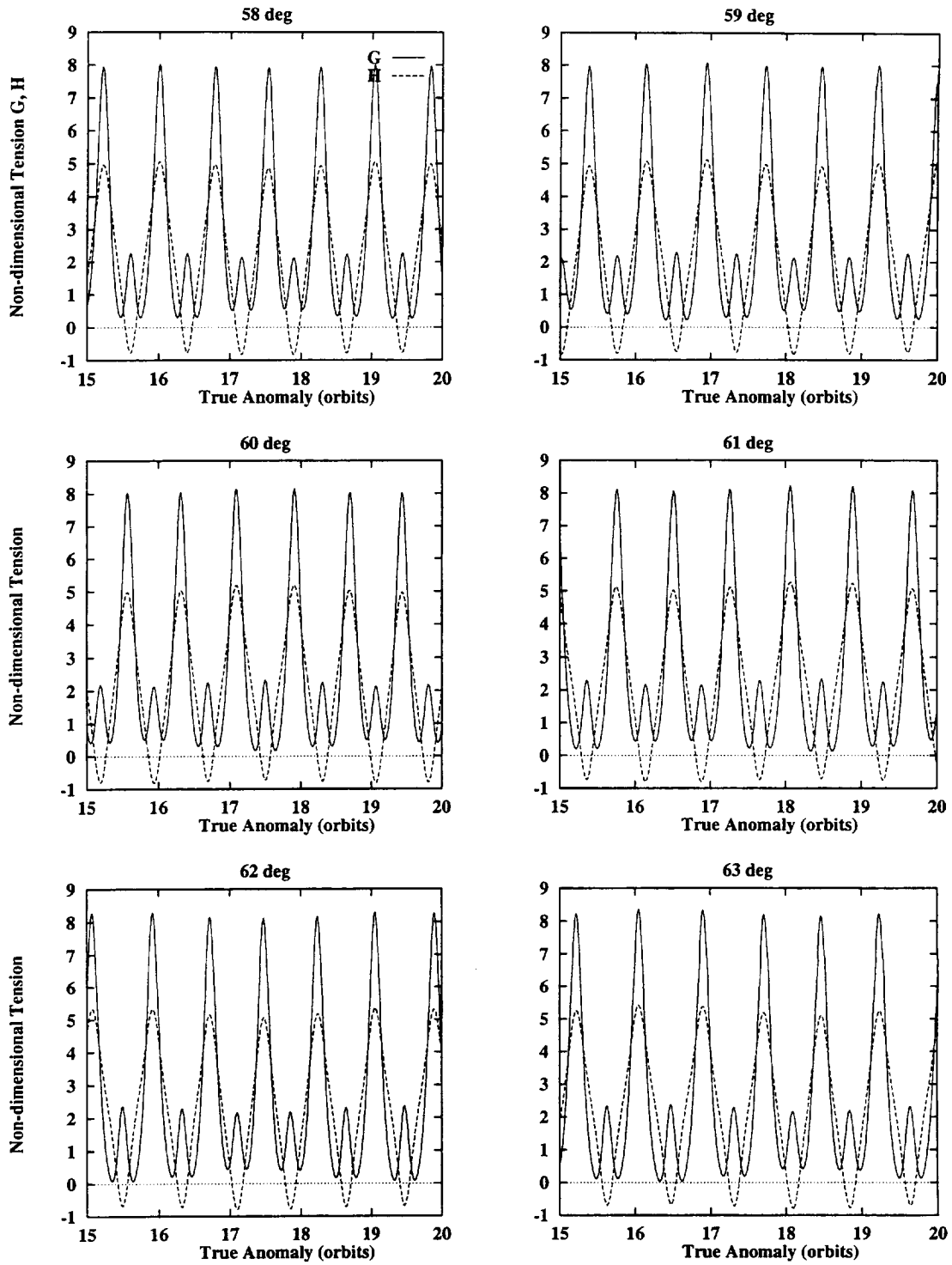
Figure 17 Time-dependent factor of tether tension, G(ν), and H(ν) for different initial libration amplitudes.

Instability of Eigenvalue 0

Eigenvalue 0 is unstable for initial speed in-plane and for all out-of-plane transverse oscillations. Initial deviation in-plane oscillations remain bounded (at least for the number of orbits computed), and even shows a decrease for 42 degrees (cf. Fig. 10).

Eigenvalue 0 is a rectilinear shape, and corresponds to a variation in the initial conditions of the pendular motion. From the equations of pendular motion (3), introducing non-dimensional time τ, we obtain:

$$\ddot{\theta} - \frac{2e\sin v\omega^2}{\kappa n^2} - 2\dot{\varphi}\tan\varphi\left(\dot{\theta} + \frac{\omega}{n}\right) + \frac{3\omega^2}{\kappa n^2}\cos\theta\sin\theta = 0$$

$$\ddot{\varphi} + \left[\left(\dot{\theta} + \frac{\omega}{n}\right)^2 + \frac{3\omega^2}{\kappa n^2}\cos^2\theta\right]\sin\varphi\cos\varphi = 0 \tag{56}$$

For libration in the orbital plane, φ is 0, so that we can consider only θ. Giving an infinitesimal variation to θ we get:

$$\ddot{\theta} + \delta\ddot{\theta} - \frac{2e\sin v\omega^2}{\kappa n^2} + \frac{3\omega^2}{\kappa n^2}\cos(\theta + \delta\theta)\sin(\theta + \delta\theta) = 0 \tag{57}$$

Considering (56) and dropping higher order terms, we get:

$$\delta\ddot{\theta} + \frac{3\omega^2}{\kappa n^2}\left[\cos^2\theta - \sin^2\theta\right]\delta\theta = 0 \tag{59}$$

Which is precisely equation (28) for in-plane transverse oscillations E and $\lambda=1$. In the same way, if we substitute an infinitesimal deviation $\delta\varphi$ for the $\varphi=0$ out-of-plane libration solution, we get:

$$\delta\ddot{\varphi} + \left[\left(\dot{\theta} + \frac{\omega}{n}\right)^2 + \frac{3\omega^2}{\kappa n^2}\cos^2\theta\right]\delta\varphi = 0 \tag{60}$$

Which is precisely equation (28) for Z and $\lambda=1$. Therefore the increase in Eigenvalue 0 amplitudes is not worrisome. There is a monotonous linear increase in E1 with subharmonic modulation, as shown in Figures 4, 10 and 11. Z1 and Z2 show an exponential growth. This corresponds to orbital stability. The evolutions of θ and φ are non-linear oscillations, with the period depending on the amplitude (plus the forcing term due to the elliptical orbit, which is small). A change in initial conditions means a change in period, so that the small initial deviation will increase continuously, but not go beyond the amplitude of the new oscillation, which remains bounded as long as we are far from the potential crest. We will consider later on at what initial conditions inertial orbital period forcing moves the libration into rotation.
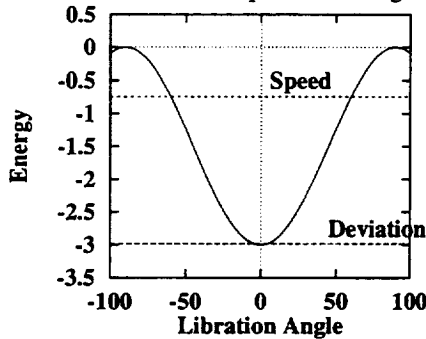
Figure 18 Gravity gradient pendulum potential

Z1 and Z2 are deviations from a zero amplitude non-linear oscillation, in which case the linearization is quite accurate; however, the restoring term varies with time, which may cause resonance. This accounts for the exponential amplitude growth of Z1 and Z2.

E1 and E2 behave differently, the latter remaining bounded for the time interval computed (50-100 orbits). The libration movement is essentially a gravity gradient pendulum (soft spring) with a small forcing term due to ellipticity of the orbit. The small forcing term will have an accumulated effect when there is resonance, but for a short span can be left out. This leaves a conservative force field with a potential function, as shown in Figure 18. An infinitesimal deviation when the pendulum crosses the vertical means moving along a nearly horizontal potential curve (deviation line in Fig. 18). This will add to the total energy an amount one order of magnitude smaller. For libration amplitudes of about 60 degrees a speed differential means moving up a potential curve with a high slope (speed line in Fig. 18). This will add to the total energy something of its own order, thus affecting the amplitude and the period.

Initial Speed

0.5
0.4
0.3 T2-T1
0.2 dT
0.1
0
-0.1
-0.2
-0.3
-0.4
-0.5
-0.6

Amplitude (rads)

0 1 2 3 4 5
True Anomaly (orbits)

Initial Deviation

0.03
0.025
0.02 T2-T1
0.015 dT
0.01
0.005
0
-0.005
-0.01
-0.015
-0.02
-0.025

0 1 2 3 4 5
True Anomaly (orbits)
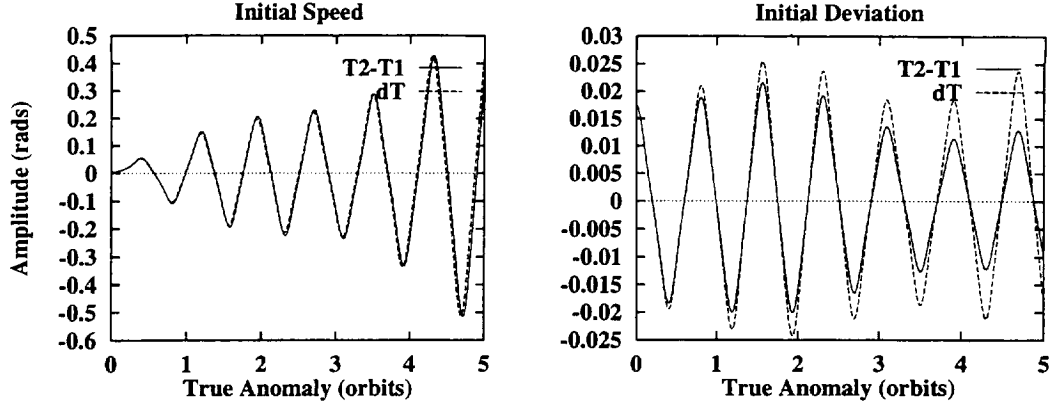
Figure 19 Eigenvalue 0 and the difference between two librations.

This can be checked by comparing the Eigenvalue 0 deviation for 60 degrees libration with the difference between the basic libration (60 degrees) and the new libration obtained by adding the initial conditions of the Eigenvalue 0. We will use for initial speed the speed difference at zero crossing between a 60 degree libration and a 61 degree libration, while for initial deviation we will just push the 60 degree libration one degree away. Figure 19 shows the agreement between the libration increment and the differential.

The initial conditions for initial speed and deviation are:

$$\theta_1(0) = 0 \quad \dot{\theta}_1(0) = \sqrt{3}\sin 60 \qquad \theta_1(0) = 0 \quad \dot{\theta}_1(0) = \sqrt{3}\sin 60$$

$$\theta_2(0) = 0 \quad \dot{\theta}_2(0) = \sqrt{3}\sin 61 \qquad \theta_2(0) = 1 \quad \dot{\theta}_2(0) = \sqrt{3}\sin 60$$

$$\delta\theta(0) = 0 \quad \delta\dot{\theta}(0) = \dot{\theta}_2(0) - \dot{\theta}_1(0) \qquad \delta\theta(0) = 1 \quad \delta\dot{\theta}(0) = 0$$

As shown in Fig. 19, the agreement is quite good, given the fact that eccentricity has been assumed to remain constant, while in fact it depends on the initial libration conditions. The difference, however, will be of a smaller order. Thus the divergence in Eigenvalue 0 is not a problem.

Out-of-Plane Oscillations and Coupling

We will now consider the out-of-plane libration. Z1 and Z2 lose stability faster than E1 for Eigenvalue 0, which is the linearized libration. We will compare these solutions with the full non-linear libration for small amplitudes. Changing variables in equations (56) and (60) from τ to true anomaly ν we obtain:

$$\ddot{\theta} = \frac{2e\sin\nu}{\kappa}(\dot{\theta}+1) + 2\dot{\phi}\tan\phi(\dot{\theta}+1) - \frac{3}{\kappa}\cos\theta\sin\theta$$

$$\ddot{\phi} = \frac{2e\sin\nu}{\kappa}\dot{\phi} - \left[(\dot{\theta}+1)^2 + \frac{3}{\kappa}\cos^2\theta\right]\sin\phi\cos\phi \qquad (61)$$

$$\delta\ddot{\phi} = \frac{2e\sin\nu}{\kappa}\delta\dot{\phi} - \left[(\dot{\theta}+1)^2 + \frac{3}{\kappa}\cos^2\theta\right]\delta\phi$$

Still, in order to make the initial conditions comparable, we have to relate the initial speed and deviation. For this we assume a small oscillation whose simplified equation would be: $\ddot{\phi} + \omega^2\phi = 0$. An initial deviation solution of amplitude A would have a speed Aω when crossing the orbital plane. We compute ω from the value of the $\delta\phi$ coefficient for $\theta=0$ and $\theta_M=60$ degrees:

$$\omega = \sqrt{(\dot{\theta}(0)+1)^2 + \frac{3}{1+e}} \qquad (62)$$

We will consider that ϕ is small, so that the ϕ term in θ equation will be small as well. For the coupling term to be smaller than the velocity term (order ε), ϕ should be: $\dot{\phi}\tan\phi \approx \varepsilon \quad \Rightarrow \quad \begin{cases} \dot{\phi} \approx \sqrt{\varepsilon} \\ \tan\phi \equiv \phi \approx \sqrt{\varepsilon} \end{cases}$.

35

As we can see in Figure 20, the linearized and the non-linear oscillations agree quite well while the amplitude remains small, but as oscillations grow bigger the linearized Z1 and Z2 solutions diverge, while the real non-linear oscillation remains bounded. In short, the oscillations out of the orbital plane will not cause trouble.
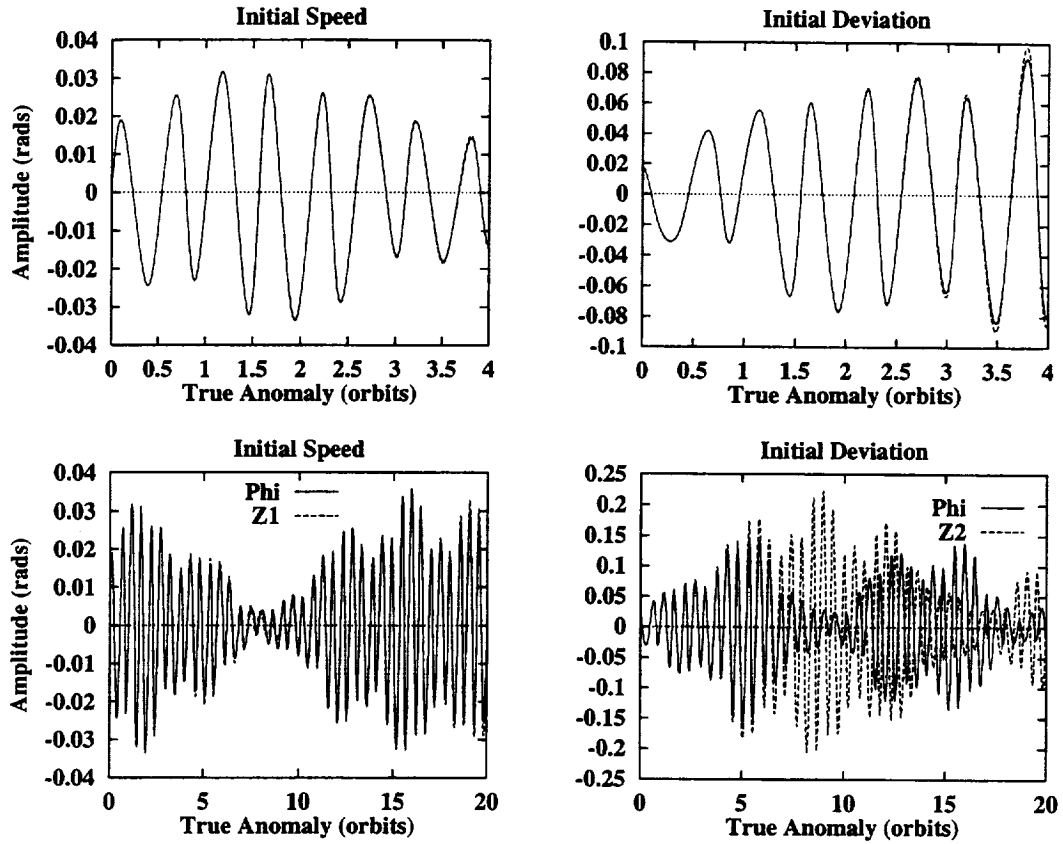
Figure 20 Non-linear out-of-plane oscillation φ and linearized oscillations Z1 and Z2, for 4 and for 20 orbits.

Still to be considered is the extent of the coupling influence in the libration itself. We have assumed its effect to be small compared with the speed term. We will see how small.
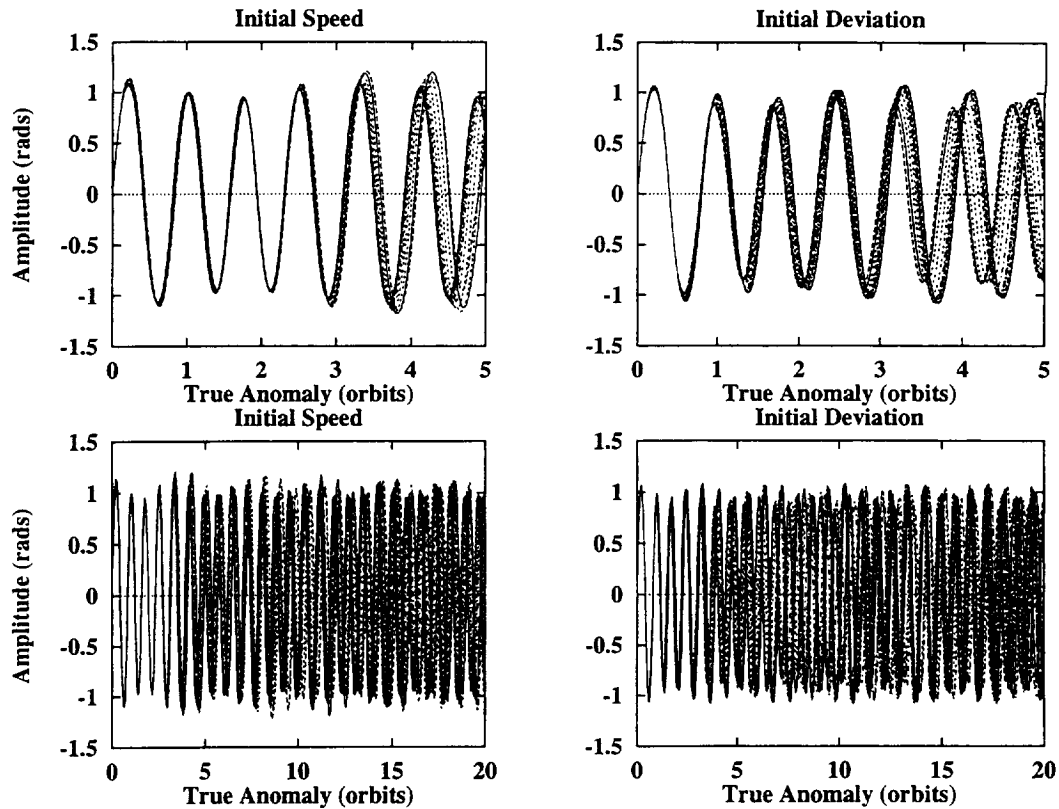
Figure 21 Influence of φ on the orbital plane libration for θ_M=60 deg.

We will integrate the full libration equations for 60 degree in-plane libration, and out of plane oscillations ranging from 0 to 10 degree amplitude. The initial deviation will correspond to full amplitude, and initial speed to the plane crossing speed for that amplitude according to (62).

The results are shown in Figure 21. In both cases, there is an effect over the amplitude and the period of the libration, which becomes smaller as φ increases. For the time—20 orbits—and the out-of-plane oscillations computed—0 to 9 degrees—the effect is not enough to push the libration into rotation. It is enough, however, to disrupt significatively the libration, so that the computations made to maximize the momentum transfer to the satellite would no longer be valid.

Consequently, out-of-plane oscillations should not be allowed to increase beyond a few degrees of amplitude.

Libration to Rotation Transition

In what we have been studying, the assumption was made that the tether librates without going into a rotation. However, the gravity gradient pendulum is a sort of soft spring, so that at large amplitudes we must be wary of going over the potential crest. The inertial term acts as a periodic forcing, which may force the libration into rotation when we are close to the limit, or have a cumulative effect through resonance. We will see what are the libration angles and speeds leading to rotation. Even though it may happen at angles that will never be reached—tension becomes zero between 63 and 64 degrees—it is good to know how safe we are at 60 degrees.
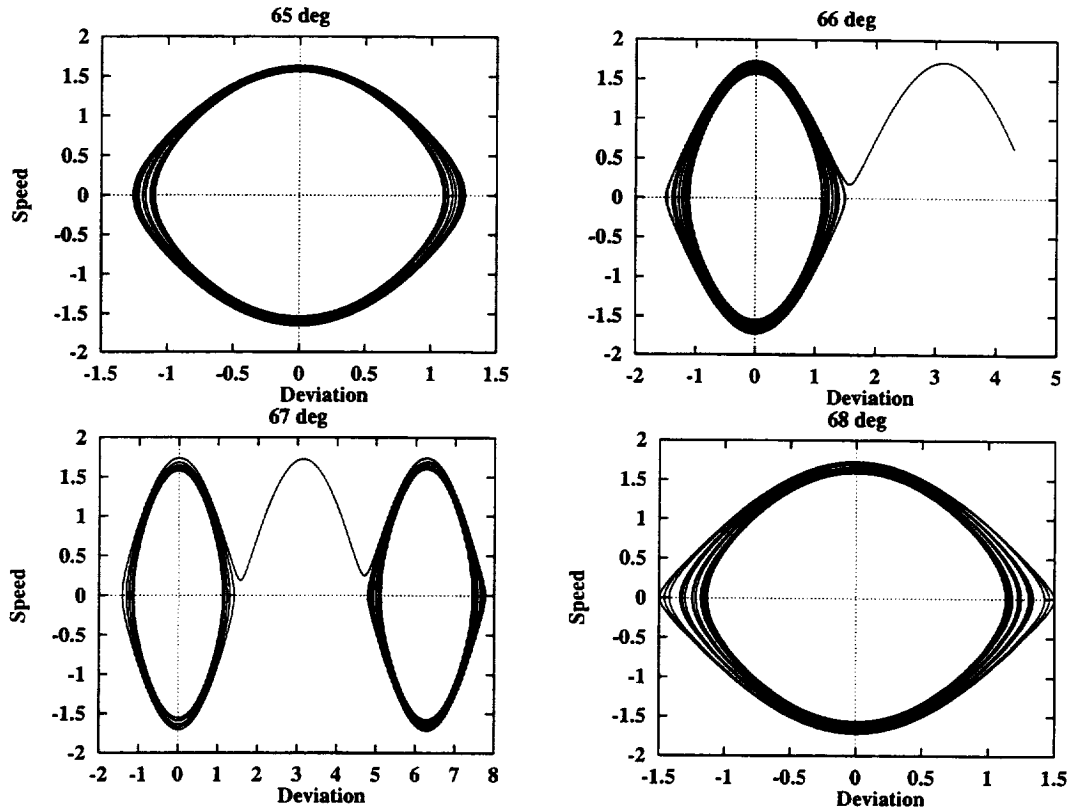
Figure 22 Libration phase maps for initial deviation. 20 orbits.

Resonance is an important factor. Initial deviation means cutting the tether at extreme amplitude and no speed. This sends the TS into a low orbit with a smaller eccentricity. Still, there is a transition to rotation for 66 and 67 degrees, while for lower and higher angles there is no transition, as shown in Figure 22. This is an effect of resonance with the forcing term, which increases the energy of the libration. The initial deviation condition is far from our case, since we will be cutting the tether at vertical crossing, which is a pure initial speed condition.

The case we are most interested in is the initial speed libration. Here, the transition is more regular. As shown in Figure 23, amplitude keeps growing, but there is no transition to rotation within the interesting libration angles.

38
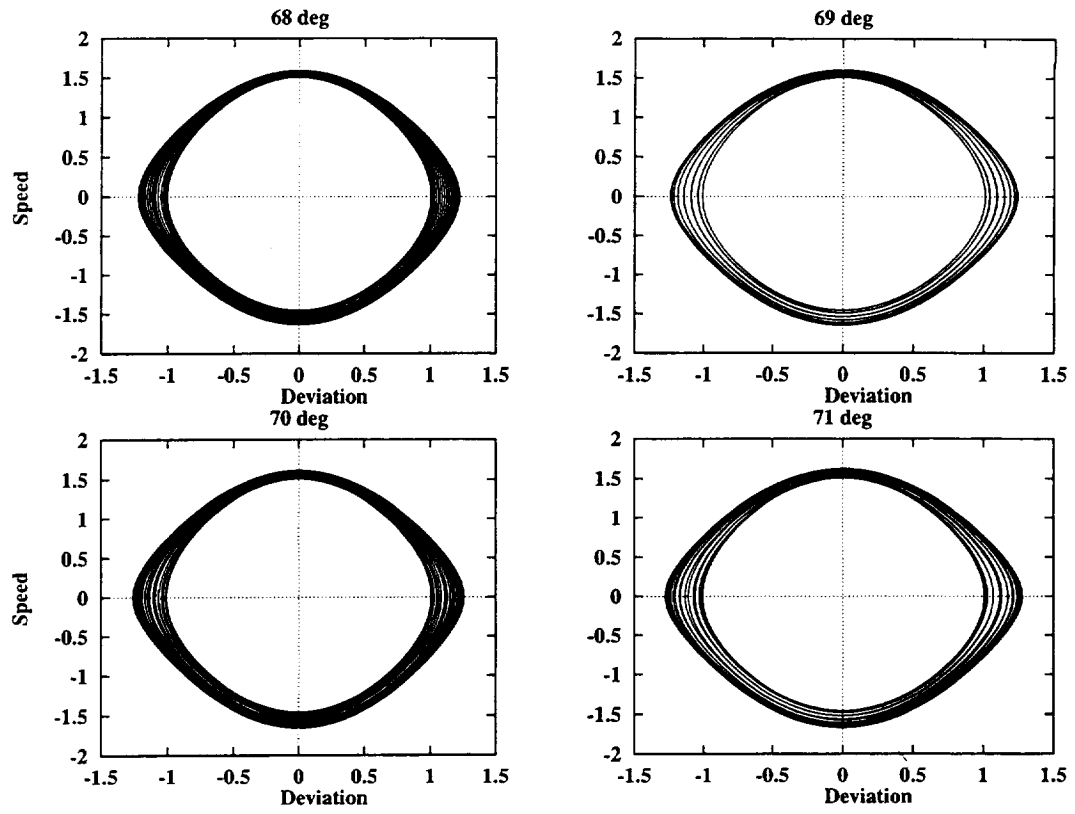
Figure 23 Libration phase maps for initial speed, 50 orbits.

DECAY MINIMIZATION

The purpose of the swinging tether, double cut procedure is to maximize the useful life of the satellite. We seek the combination of parameters that will yield the maximum orbital lifetime. For this, we will seek to minimize the initial orbital decay rate as a function of the deployment free parameters.

Assuming that the Shuttle is in a circular orbit, the deployment strategy leaves three free parameters:

- Libration amplitude, which depends on the tether deployment strategy.
- First cut timing, or gravity gradient pendulum libration angle at cut time.
- Second cut timing, or libration angle of the TS in the elliptical orbit frame.

The Shuttle will be in a circular orbit at an altitude of 297 Km, with 57 degrees inclination. The tether is 20 Km long, with a linear density of $3.3\,10^{-4}$ Kg/m, and the end mass is $m_A=32$ Kg. We assume the earth to be spherical, its radius equal to the equatorial radius. This is a conservative assumption, since the orbital altitude will be greater than the equatorial altitude for most of the period, with a correspondingly lower air density and lower decay rate. Thus the circular orbit radius will be $R_0=6675.16$ Km, and its angular rate will be ω_0.

After deployment, the TS librates as a gravity gradient pendulum governed by equation (5). Since e is zero, the equation admits an energy integral:

$$\dot{\theta}^2 + 3\omega_0^2 \sin^2 \theta = 3\omega_0^2 \sin^2 \theta_M \tag{63}$$

Where θ_M is the maximum amplitude of the gravity gradient pendulum libration. We keep the same reference frame we have adopted previously, with Ox as the local vertical and Oz in the orbital speed direction. δ will be the libration angle at cut time. L_f will be the final deployed length of the tether; ξ_F will be the distance from the TS center of mass to the free end, that is: $\xi_F=\alpha L_F$, with $\alpha=1-b$ as defined in (4).

We will compute the parameters of the different stages of the TS motion as a function of the deployment free parameters.

Elliptical Orbit of the COM

When the tether is cut at the orbiter end, its center of mass, which we will call G, enters an elliptical orbit [2] with the initial conditions:

$$\mathbf{R}_0^G = \begin{Bmatrix} R_0 + \xi_F \cos\delta \\ 0 \\ \xi_F \sin\delta \end{Bmatrix} \qquad \mathbf{v}_0^G = \begin{Bmatrix} -(\omega_0 + \dot{\theta}_0)\xi_F \sin\delta \\ 0 \\ \omega_0 R_0 + (\omega_0 + \dot{\theta}_0)\xi_F \cos\delta \end{Bmatrix} \tag{64}$$

The initial libration angular speed can be obtained from the energy equation (63): $\dot{\theta}_0 = \omega_0 u$, with:

$$u = \sqrt{3}\sqrt{\sin^2 \theta_M - \sin^2 \delta} \tag{65}$$

which is different from the parameter u used in [2]. Since the tether is much shorter than the orbital radius, we can use an expansion in powers of a small parameter $\dfrac{\xi_F}{R_0} = \varepsilon \ll 1$, leading to:

$$\mathbf{R}_0^G = R_0 \begin{Bmatrix} 1 + \varepsilon\cos\delta \\ 0 \\ \varepsilon\sin\delta \end{Bmatrix} \qquad \mathbf{v}_0^G = \omega_0 R_0 \begin{Bmatrix} -(1+u)\varepsilon\sin\delta \\ 0 \\ 1 + (1+u)\varepsilon\cos\delta \end{Bmatrix} \tag{66}$$

The orbital parameters can thus be expressed as follows:

$$e = \sqrt{3\cos^2 \delta(u+1)(u+3)+u^2}\,\varepsilon + \cos\delta \frac{\left(\cos^2 \delta + 1\right)\left(9 + 18u + 12u^2 + 2u^3\right)}{2\sqrt{3\cos^2 \delta(u+1)(u+3)+u^2}}\varepsilon^2 + \dots \tag{67}$$

$$a = R_0\left\{1 + 2\cos\delta(u+2)\varepsilon + \left[\cos^2 \delta\left(13 + 16u + 4u^2\right) + 2 + 2u + u^2\right]\varepsilon^2 + \dots\right\} \tag{68}$$

$$n = \sqrt{\frac{\mu}{a^3}} = \omega_0\left\{1 - 3\cos\delta(2+u)\varepsilon - \frac{3}{2}\left[\left(u^2 + 2u + 2\right) - \cos^2 \delta\left(u^2 + 4u + 7\right)\right]\varepsilon^2 + \dots\right\} \tag{69}$$

$$\Delta h_p = a(1-e) - R_0 = R_0\left[-\sqrt{3\cos^2\delta(u+1)(u+3)+u^2} + 2\cos\delta(u+2)\right]\varepsilon+\ldots$$

$$\Delta h_a = a(1+e) - R_0 = R_0\left[\sqrt{3\cos^2\delta(u+1)(u+3)+u^2} + 2\cos\delta(u+2)\right]\varepsilon+\ldots$$

(70)

For small δ, these expressions reduce to the equations derived in [1, p. 4-5] and [2, pp. 5-6]. Since we are precisely trying to study the influence of δ in decay rate, we cannot assume at the beginning that it is small. We still need the argument of the perigee, which can be obtained from: $\sin v_i = \dfrac{r \wedge e}{|r| \cdot |e|} \bullet j$, which gives:

$$v_i = -\arcsin\left(\frac{u\sin\delta}{v}\right) - u\sin\delta\,\frac{\cos^2\delta(2u^2+6u+3)-(4u+3)}{2v^2}\varepsilon+\ldots$$

(71)

where:
$$v = \sqrt{3\cos^2\delta(u+3)(u+1)+u}$$

(72)

With the expressions above, the orbit of the COM is perfectly determined. The details of the mathematical derivations and simplifications are in Appendix E.

Libration of the Tethered System in an Elliptical Orbit
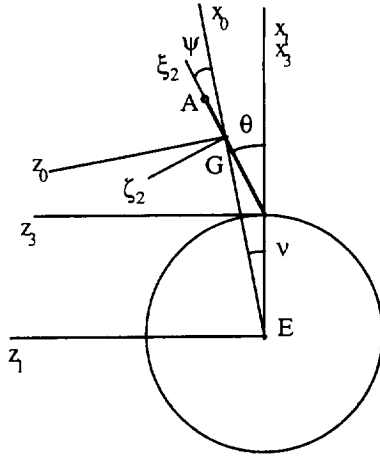
Figure 24 Reference frames for the first cut.

After the first cut, the TS continues its libration given by eqs. (5) while its COM follows an elliptical orbit. A new reference frame is erected, Gxyz, with G at the TS COM, Gx along the local vertical towards zenith, Gz in the orbital plane and Gy normal to the other two. This is the same reference frame defined in page 3. As we saw before, equations (5)—or equations (6) when we take true anomaly as variable—have to be integrated numerically. For this, the initial conditions must be determined.

Referring the index 1 to an earth-centered fixed frame, 2 to the TS, 0 to the COM orbital frame, and 3 to the circular orbit frame, we seek $\omega_{20}=\omega_{23}+\omega_{31}-\omega_{01}$ (cf. page 9).

Besides, we will temporarily distinguish between:

- θ= angle between the rigid tether and the local vertical at the Orbiter.

- ψ= angle between the rigid tether and the local vertical at the COM.

Later on both will be called θ, but initially we have to distinguish between them. At cut time we have therefore:

$$\psi_0 = \theta_0 - v_0 = \delta - \arctan\frac{\xi_F\sin\delta}{R_0 + \xi_F\cos\delta} = \delta - \arctan\frac{\varepsilon\sin\delta}{1+\varepsilon\cos\delta} \approx \delta - \varepsilon\sin\delta + \varepsilon^2\cos\delta\sin\delta$$

(73)

For the initial angular speed, we use (33)-(35), taking into account that the parameters u and ε from [2] used there are different from what we are using here. With the new u and ε, and substituting (67) and (69), we obtain:

$$\dot{v} = n\frac{(1+e\cos v)^2}{(1-e^2)^{3/2}} = \omega_0\left\{1+\left[c_0 + c_1\cos v + c_2\cos^2 v\right]\varepsilon+\ldots\right\}$$

(74)

with:

$$\begin{cases} c_0 = -3\cos\delta(u+2)+\varepsilon\left[6\cos^2\delta(2+u)^2 - 3(u+1)\right] \\ c_1 = 2v - \varepsilon\cos\delta\left[(2u+1)(2u^2-9)+(16u^3+96u^2+180u+99)\cos^2\delta\right]/v \\ c_2 = \varepsilon v^2 \end{cases}$$

(75)

41

In order to obtain the initial angular rate ω_{01}, we only have to substitute the true anomaly at cut time from (71) in the angular rate expression (74):

$$\omega_{01} = \dot{v}(v_i) = \omega \frac{(1 + e \cos v_i)^2}{(1 - e^2)^{3/2}} = \omega_0 \left[1 + u \cos \delta\varepsilon - u(2\cos^2 \delta - 1)\varepsilon^2 + ...\right] \qquad (76)$$

From (63) we obtain: $\omega_{23} = \dot{\theta}_0 = \omega_0 u$; $\omega_{31} = \omega_0 = \sqrt{\frac{\mu}{R_0^3}}$. Adding all the terms, we obtain the initial conditions:

$$\left(\frac{d\psi}{dt}\right)_0 = \omega_{20} = \omega_0 u \left[1 - \cos \delta\varepsilon + \left(2\cos^2 \delta - 1\right)\varepsilon^2 + ...\right]$$

$$\left(\frac{d\psi}{dv}\right)_0 = \frac{\omega_{20}}{\omega_{01}} = u \left\{1 - \cos \delta(1 + u)\varepsilon + \left[\cos^2 \delta(u + 2) - 1\right](u + 1)\varepsilon^2 + ...\right\} \qquad (77)$$

We can now integrate the libration equation. We return to using θ for the libration angle, once the circular orbit frame has disappeared and there is no possibility of confusion. As usual, we adopt v as the integration variable. In order to obtain the TS angular speed needed in the momentum transfer computations, we will have to multiply times the orbital angular speed. We integrate numerically equation (6) with initial conditions (73) and (77), up to the true anomaly at the second cut.

Final Orbit of the Satellite

The computation process we are following is:

- Circular Shuttle orbit: R_0, ω_0.
- Elliptical orbit of the COM after the first cut: $a(\delta, \theta_M)$, $e(\delta, \theta_M)$, $v_i(\delta, \theta_M)$, $\omega(\delta, \theta_M)$, $\theta(v)$, $\theta'(v)$.
- Elliptical orbit of the satellite after the second cut: $a_s(\delta, \theta_M, v_c)$, $e_s(\delta, \theta_M, v_c)$, $v_{is}(\delta, \theta_M, v_c)$.

Where v_c is the true anomaly of the COM orbit at the time of the second cut. In order to determine the final orbit parameters, we will obtain first the position and speed of the end mass (A) as a function of v and the COM orbital parameters.

$$r^A = r^G + GA = \lfloor R + GA \cos \theta, 0, GA \sin \theta \rfloor \qquad (78)$$

Were: $R = \frac{a(1 - e^2)}{1 + e \cos \kappa}$, and $GA = L_F - \xi_F = \frac{(1 - \alpha)}{\alpha} \xi_F = \beta \varepsilon R_0$; with $\beta = 0.0934937$. If we compare terms:

$$\varepsilon = 0.0028 \qquad \beta = 0.0934$$
$$\varepsilon^2 = 0.0000822 \qquad \beta^2 = 0.00874 \sim \varepsilon$$

Consequently, we only need to keep terms in ε, β, β^2, and $\varepsilon\beta$, if we are disregarding terms of order $O(\varepsilon^2)$. Actually, there should not be any need for analytical computations at this stage: once the libration has to be computed numerically, we can simply compute speeds and positions at each requested point and apply standard formulas to obtain the orbital parameters. However, the problem is stiff due to the magnitude difference between a, R_0, and a-R_0. We will perfect the algebra in order to compute only the increments, which yield reasonable results without resorting to double precision. From the previous section we have:

$$a = R_0(1 + a_1\varepsilon) \qquad \omega = \omega_0(1 + \omega_1\varepsilon) \qquad e = e_1\varepsilon \qquad \dot{v} = \omega_0\left[1 + \left(c_0 + c_1 \cos v + c_2 \cos^2 v\right)\right]$$

where the perturbations are known and computed. If we desire greater precision, the ε^2 terms can be included. The absolute speed of the end mass is:

$$v_{21}^A = v_{20}^A + v_{01}^A = v_{20}^A + v_{01}^G + \bar{\omega}_{01} \wedge GA = \left(\dot{\theta} + 1\right)\dot{v}\beta\varepsilon R_0 \begin{bmatrix} -\sin\theta \\ 0 \\ \cos\theta \end{bmatrix} + \frac{a\omega}{\sqrt{1 - e^2}} \begin{Bmatrix} e\sin v \\ 0 \\ 1 + e\cos v \end{Bmatrix} \qquad (79)$$

Developing in powers of the small parameters:

$$\mathbf{r}^A = R_0 \left\{ \begin{array}{c} 1 + \varepsilon(\beta\cos\theta + a_1 - e_1\cos\nu) + O(\varepsilon^2) \\ 0 \\ \beta\varepsilon\sin\theta \end{array} \right\} = R_0 \left\{ \begin{array}{c} 1 + \varepsilon r_{1x} \\ 0 \\ \varepsilon r_{1z} \end{array} \right\}$$

$$\mathbf{v}_{21}^A = R_0\omega_0 \left\{ \begin{array}{c} \varepsilon\left[e_1\sin\nu - \beta(\dot\theta+1)\sin\theta\right] + \cdots \\ 0 \\ 1 + \varepsilon\left[e_1\cos\nu + a_1 + \omega_1 + \beta(\dot\vartheta+1)\cos\theta\right] + \cdots \end{array} \right\} = R_0\omega_0 \left\{ \begin{array}{c} \varepsilon v_{1x} \\ 0 \\ 1 + \varepsilon v_{1z} \end{array} \right\}$$

(80)

The details of the simplification can be checked in Appendix F. Keeping only the perturbations of $\mathbf{r}^A$ and $\mathbf{v}^A$, we compute the parameters of the final orbit:

$$a_s = R_0(1 + a_{s1}\varepsilon)$$
with:
$$e_s = e_{s1}\varepsilon$$

$$a_{s1} = 2(v_{1z} + r_{1x}) + \varepsilon(5v_{1z}^2 + v_{1x}^2 + r_{1z}^2 + 2r_{1x}^2 + 8r_{1x}v_{1z})$$

$$e_{s1} = A - \frac{\varepsilon\left[-4v_{1z}^3 - 10r_{1x}v_{1z}^2 - 2v_{1z}r_{1z}^2 + 2v_{1z}r_{1z}v_{1z} - 4v_{1z}r_{1x}^2 + 2v_{1x}r_{1x}r_{1z} + r_{1x}r_{1z}^2 - 2v_{1z}v_{1x}^2 - 2r_{1x}v_{1x}^2\right]}{2A}$$ (81)

$$A = \sqrt{4v_{1z}^2 + 4r_{1x}v_{1z} + r_{1x}^2 + r_{1z}^2 + 2r_{1z}v_{1x} + v_{1x}^2}$$

Again, the details of operations and simplifications are in Appendix F. The expressions above provide the parameters of the final orbit of the satellite, as a function of δ, θ_M, and v_c. We can then compute the orbital decay rate.

Orbital Decay Rate

Speed Determination

In order to find the height loss due to air drag, we will assume:
- Spherical earth and atmosphere.
- Atmosphere rotating at the earth angular speed
- Exponential density model.

The diurnal bulge will not be considered at this stage. Night/day changes will not be considered either, nor solar activity changes: we are seeking a simple analytical model for a first estimate.

We introduce an earth centered "fixed" frame (system 1); the orbital frame (system 0), which is actually the frame of the polar coordinates in the orbital plane; and the satellite itself (system 2).

Air drag can be estimated [1, 7, 11] as:

$$\mathbf{D} = -\frac{1}{2}\rho v_{20}^2 A C_D \frac{\mathbf{v}_{20}}{|\mathbf{v}_{20}|}$$ (82)

Where ρ is the air density, A the average cross section of the satellite, and C_D the drag coefficient [1, p. 6-8]. In order to compute the relative speed we need the orbital speed of the satellite and the rotational speed of the atmosphere, projected onto the orbital frame, $\mathbf{u_r}, \mathbf{u_v}, \mathbf{u_z}$:

$$\mathbf{v}_{21}^s = \frac{a\omega}{\sqrt{1-e^2}}\lfloor e\sin\nu, 1 + e\cos\nu, 0 \rfloor = \frac{\mu}{h}\lfloor e\sin\nu, 1 + e\cos\nu, 0 \rfloor$$

$$\mathbf{v}_{01}^s = \bar\Omega_E \wedge \mathbf{r}^s \text{ with: } \begin{cases} \mathbf{r} = r\mathbf{u}_r = \dfrac{a(1-e^2)}{1+e\cos\nu}\mathbf{u}_r \\ \bar\Omega_E = \Omega_E\lfloor \sin i\sin(\omega_p + \nu), \sin i\cos(\omega_p + \nu), \cos i \rfloor \end{cases}$$

$$\mathbf{v}_{20}^s = \left\{ \begin{array}{c} \dfrac{a\omega e \sin v}{\sqrt{1-e^2}} \\[2ex] \dfrac{a\omega(1+e\cos v)}{\sqrt{1-e^2}} - \dfrac{\Omega_E a(1-e^2)\cos i}{1+e\cos v} \\[2ex] \dfrac{\Omega_E a(1-e^2)\sin i\cos(\omega_p + v)}{1+e\cos v} \end{array} \right\} \tag{83}$$

where ω_p is the argument of perigee from the line of nodes, and Ω_E the earth's rotational speed. The drag expression includes the square of the speed. The air speed is small with regard to the satellite orbital speed, and eccentricity is small as well. We will try a Taylor expansion, but we must check the orders of magnitude of the quantities involved:

- $\Omega_E = 7.292\,10^{-5}$ rad/sec [7, p. 350].
- $\Omega_E/\omega \sim 0.05$
- $e \sim 0.02$

Consequently, we can drop terms of order e^2, Ω_E^2, and $e\Omega_E$. The squared speed will be:

$$v_{20}^2 = \left(\frac{\mu}{h}\right)(1+2e\cos v)\left[1 - 2\frac{\Omega_E}{\Omega}\cos i(1-e\cos v)\right] \tag{84}$$

where we have used the approximate orbital rate, $\Omega = \dfrac{v}{r} = \dfrac{\mu^2}{h^3}(1+2e\cos v) \approx n(1+2e\cos v)$. The last term in (84) can also be dropped, since it is of order $e\Omega_E$. This leaves the same expression as in [7].

Energy Loss

The variation of mechanical energy can be obtained from the drag power: $\dfrac{dE}{dt} = \mathbf{D}\cdot\mathbf{v}$, with $\mathbf{D}$ and $\mathbf{v}$ as shown above. The dot product can be approximated by: $\dfrac{\mathbf{v}_{20}^s}{\left|\mathbf{v}_{20}^s\right|}\cdot\mathbf{v}_{21}^s \approx \left|\mathbf{v}_{21}^s\right|$, since the difference is of order e^2.

This leaves just the product of scalar values:

$$\frac{dE}{dt} = D\left|\mathbf{v}_{21}^s\right| \tag{85}$$

Orbital Decay Rate

Semiaxis and eccentricity variations can be obtained from the equations for variations of elements [7, p. 210]. The semiaxis variation can be obtained directly from the energy equation:

$$E = -\frac{m\mu}{2a} \quad\Rightarrow\quad \frac{da}{dt} = \frac{2a^2}{m\mu}\frac{dE}{dt} = \frac{2a^2}{m\mu}Dv$$

Substituting the value of v, expanding, and dropping terms of order e^2, we obtain:

$$\frac{da}{dt} = \frac{2D}{m\Omega}(1+3e\cos v) = \frac{2D}{mn}(1+e\cos v) \tag{86}$$

The second form is obviously easier for integration.

Semiaxis Decay in One Orbit

It is possible to integrate (86) for one orbit, and obtain the decrement of the semiaxis. By minimizing this expression, we will maximize the life expectancy of the satellite. For the analytical integration, it is simpler to shift to eccentric anomaly, E:

$$\Delta a = \int_0^T da = \int_0^{2\pi} \frac{da}{dt}\frac{dt}{dE}dE \tag{87}$$

44

We need to relate v and t with E:

$$\left.\begin{array}{l} nt = E - e\sin E \\ ndt = dE(1 - e\cos E) \end{array}\right\} \quad dt = \frac{1 - e\cos E}{n}dE \quad \Rightarrow \quad da = \frac{2D(1 + e\cos v)}{mn^2}(1 - e\cos E)dE$$

$$\cos v = \frac{\cos E - e}{1 - e\cos E} \quad ; \quad 1 + e\cos v \approx \frac{1}{1 - e\cos E} \quad \Rightarrow \quad da = \frac{2D}{mn^2 dE}$$

The air drag must be expressed in terms of E as well:

$$D = -\frac{1}{2}\rho AC_D \frac{\mu^2}{h^2}\left(1 + 2e\frac{\cos E - e}{1 - e\cos E}\right)\left[1 - 2\frac{\Omega_E}{n}(1 - 3e\cos v)\cos i\right] \approx$$

$$\approx -\frac{1}{2}\rho AC_D \frac{\mu^2}{h^2}(1 + 2e\cos E)\left[1 - 2\frac{\Omega_E}{n}\cos i\right] \tag{88}$$

For the air density, we will use the well known exponential model: $\rho = \rho_0 e^{\frac{h_0 - h}{H}}$, where H is the scale height which varies with the reference height h_0. We only have to give h as a function of E and orbital parameters:

$$\frac{h_0 - h}{H} = \frac{h_0 - [a(1 - e\cos E) - R_E]}{H} = \frac{h_0 + R_E - a + ae\cos E}{H}$$

Substituting these expressions into the integral, we obtain:

$$\Delta a = -\frac{\rho_0 AC_D \mu}{mn^2 h^2}e^{\frac{h_0 + R_E - a}{H}}\left(1 + 2\frac{\Omega_E}{n}\cos i\right)\int_0^{2\pi} e^{-\frac{ae}{H}\cos E}(1 + 2e\cos E)dE \tag{89}$$

Where we have considered that Δa and Δe will be much smaller than a and e, which, in turn, can be assumed constant for one orbit. Thus the integral admits an analytic solution in terms of Bessel functions [7, p. 212]:

$$\Delta a_{2\pi} = -\left(2\pi\frac{AC_D \rho_0}{m}\right)\left(\frac{\mu^2}{n^2 h^2}\right)\left(e^{\frac{h_0 + R_E - a}{H}}\right)\left(1 - 2\frac{\Omega_E}{n}\cos i\right)\left[I_0\left(\frac{ae}{H}\right) + 2eI_1\left(\frac{ae}{H}\right)\right] \tag{90}$$

The values of the constants used are:

- $\dfrac{AC_D}{m} = \dfrac{1}{\beta} = \dfrac{1}{118}\dfrac{m^2}{Kg} = \dfrac{1}{118}10^{-6}\dfrac{Km^2}{\cdot Kg}$, from [1, p. 8].

- $\rho_0 = \rho(300Km) = 3.3 \cdot 10^{-14}\dfrac{g}{cm^3} = 3.3 \cdot 10^{-2}\dfrac{Kg}{Km^3}$, from [12].

- $H(300Km) = 55.77Km$, from [12].

Consequently, the value of the first parenthesis is: $K=0.1757 \cdot 10^{-8} \ Km^{-2}$.

- $\dfrac{\mu^2}{n^2 h^2} \approx a^2$

- $e^{\frac{h_0 + R_E - a}{H}} = e^{\frac{6678.16 - a}{55.77}}$

- $1 - 2\Omega_E\sqrt{\dfrac{a^3}{\mu}}\cos i = 1 - 0.125 \cdot 10^{-6}\sqrt{a^3}$

where we have used $\Omega_E = 7.29 \cdot 10^{-5} rad/sec$ and $\mu = 398618 Km^3/sec^{-1}$, from [5, pp. 350-51]; and $i = 57$ deg from the latest unpublished flight data.

If we finally introduce the orbit parameters in the main term plus the small-perturbation form obtained in (81), we have:

$$\Delta a = 0.17(0.415 + 0.0021a_{sl} + 0.0000023a_{sl}^2)e^{0.05 - 0.306a_{sl}}[I_0(z) + 0.0054I_1(z)] \tag{91}$$

Where: $z = 0.45 \cdot 10^{-2}(66.75 + 0.18a_{sl})e_{sl}$.

Again, the computational details are shown in Appendix H.

Computation Results

We expect that the maximum perigee height, which is the main concern for orbital decay, will be attained if the tether is cut at apogee, with zero libration and positive libration speed, so that additional momentum is transferred to the satellite. We thus compute the orbital decay rate as a function of three parameters: libration amplitude before the first cut, θ_M; libration angle at the first cut, δ; and COM orbit true anomaly at the second cut, v_c (the second cut time would be an equivalent variable, as they are related by the Kepler's equation). Integrating for a range of values, we obtain:

- Minimum decay rate always for $\delta=0$, but with small sensitivity for values δ of up to $\theta_M/2$.
- Minimum decay rate when the tether is cut at apogee, with the second apogee passage yielding a lower rate than the first; small sensitivity to true anomaly as well.
- Minimum decay rate for $\theta_M\sim 60$ degrees.

The lowest value in the range explored is for:

Δa:	0.014541	Km/orbit
θ_M:	60.000000	deg
δ:	0.000000	deg
v_c:	559.529114	deg
$\theta(v_c)$:	-6.386499	deg
$\theta'(v_c)$:	82.325592	deg/rad v

The results can be seen in Figs. 25-31. For low libration angles, the cut at the first apogee passage produces a minimum decay rate, as seen in Fig. 25. As the libration angle increases, the boost from the tether increases as the libration speed tunes its phase with the orbital anomaly, so that the absolute minimum is reached for 60 degrees (Fig. 27). The libration speed is then positive and maximum (Fig. 28). The apogee and perigee heights obtained are shown in Figs. 29-31 for different θ_M.

Orbital Decay Rate for Theta Max = 24 deg

decay rate

da/dt	——
0.0277	⋯⋯
0.0268	⋯⋯
0.0259	–⋅–
0.025	–⋅⋅–
0.0241	⋯⋯
0.0232	⋯⋯
0.0223	⋯⋯
0.0214	——
0.0205	––––
0.0196	⋯⋯

0.029
0.028
0.027
0.026
0.025
0.024
0.023
0.022
0.021
0.02
0.019
0.018

-20 -15 -10 -5 0 5 10 15 20
delta (deg)

100 200 300 400 500 600 700
anomaly (deg)

Orbital Decay Rate for Theta Max = 48 deg

decay rate
0.04

da/dt	——
0.0343	⋯⋯
0.0324	⋯⋯
0.0305	–⋅–
0.0287	–⋅⋅–
0.0268	⋯⋯
0.0249	⋯⋯
0.0231	⋯⋯
0.0212	——
0.0193	––––
0.0175	⋯⋯

0.035
0.03
0.025
0.02
0.015

-40 -30 -20 -10 0 10 20 30 40
delta (deg)
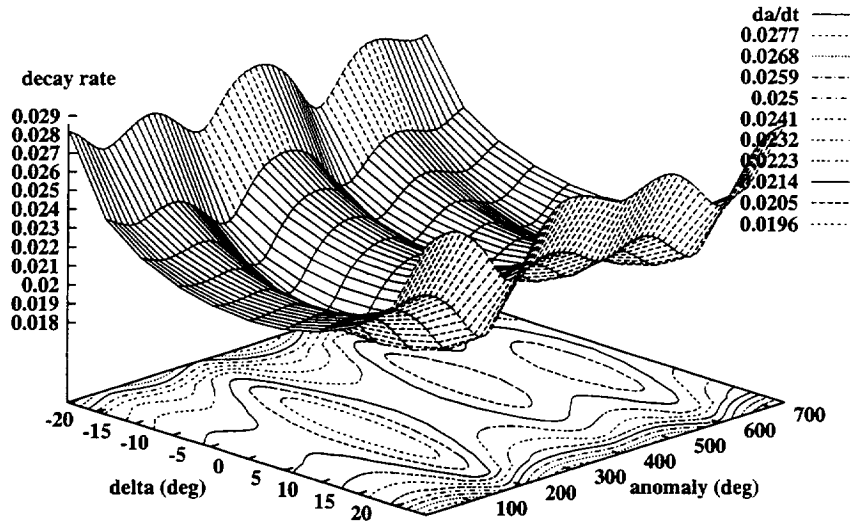
100 200 300 400 500 600 700
anomaly (deg)
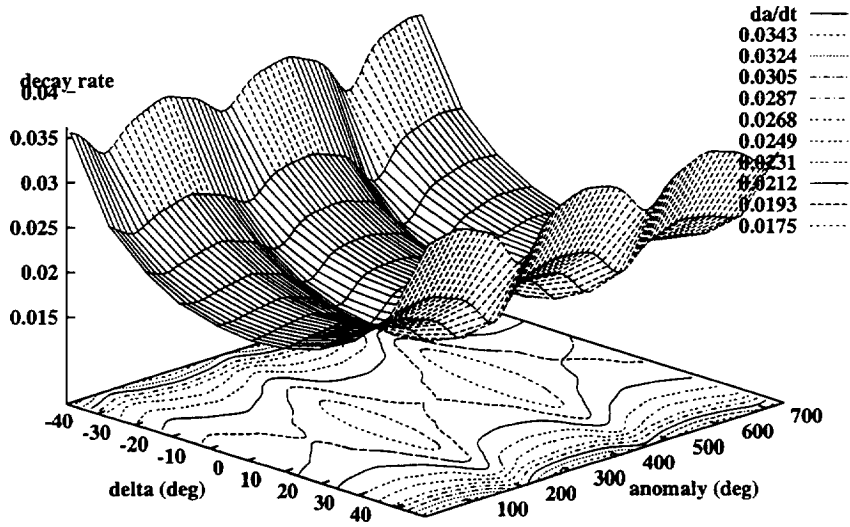
Figure 25 Decay rate (Km/orbit) for lower libration angles.

47

Orbital Decay Rate for Theta Max = 58 deg

decay rate

0.023
0.022
0.021
0.02
0.019
0.018
0.017
0.016
0.015
0.014

-20
-10
0
10
20
delta (deg)

100 200 300 400 500 600 700
anomaly (deg)

da/dt ——
0.0217 ·······
0.021 ········
0.0203 —·—·
0.0196 —·· ·
0.0188 ········
0.0181 ········
0.0174 ········
0.0167 ——
0.016 -----
0.0153 ·······

Orbital Decay Rate for Theta Max = 59 deg

decay rate

0.023
0.022
0.021
0.02
0.019
0.018
0.017
0.016
0.015
0.014

-20
-10
0
10
20
delta (deg)

100 200 300 400 500 600 700
anomaly (deg)

da/dt ——
0.0218 ·······
0.0211 ········
0.0204 —·—·
0.0196 —·· ·
0.0189 ········
0.0182 ········
0.0175 ········
0.0168 ——
0.016 -----
0.0153 ·······
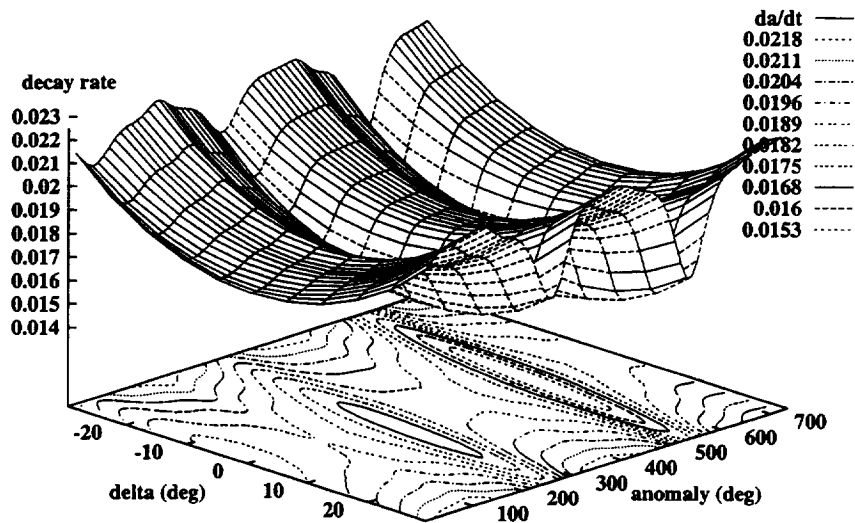
Figure 26 Decay rate (Km/orbit) for libration angles closer to the minimum (60 deg).

48

Orbital Decay Rate for Theta Max = 60 deg

da/dt	——
0.0219	······
0.0211	·········
0.0204	─ ──
0.0197	── ·
0.0189	·····
0.0182	·········
0.0175	········
0.0167	——
0.016	─────
0.0153	······

Orbital Decay Rate for Theta Max = 61 deg

da/dt	——
0.0219	······
0.0212	·········
0.0205	─ ──
0.0197	── ·
0.019	·····
0.0183	·········
0.0175	········
0.0168	——
0.016	─────
0.0153	······
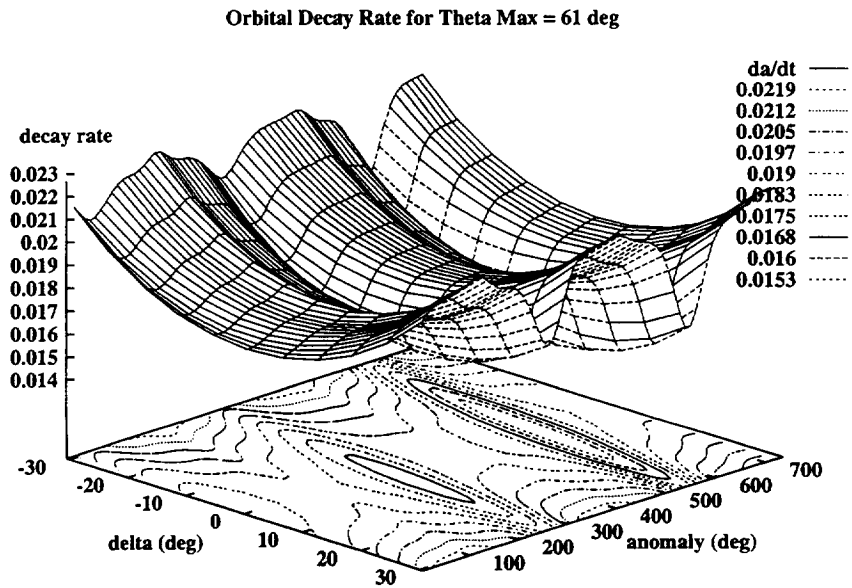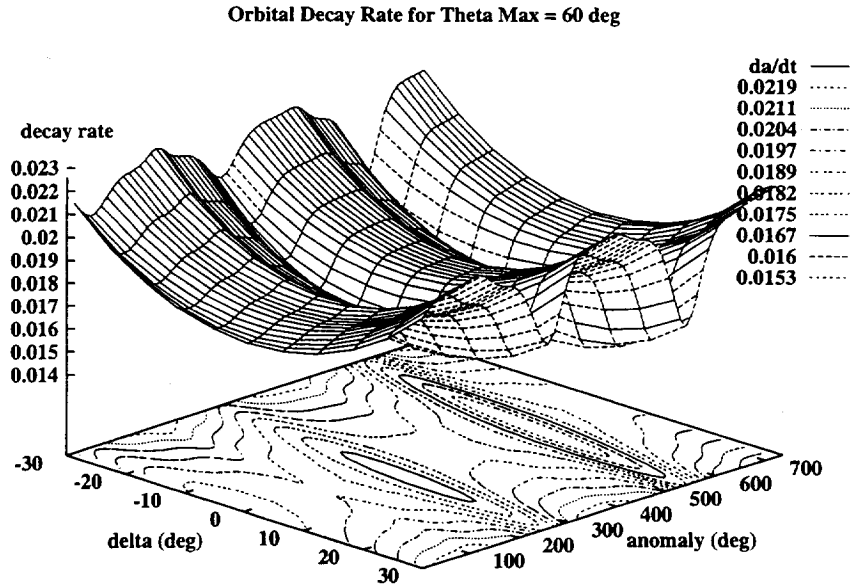
Figure 27 Decay rate (Km/orbit) for libration angles about the minimum (60 deg).

49

Libration Angle for Theta Max = 61 deg

Theta
0.901
0.701
0.5
0.3
0.0992
-0.101
-0.302
-0.503
-0.703
-0.904

rad
1.5
1
0.5
0
-0.5
-1
-1.5

delta (deg)
-30 -20 -10 0 10 20 30

anomaly (deg)
100 200 300 400 500 600 700
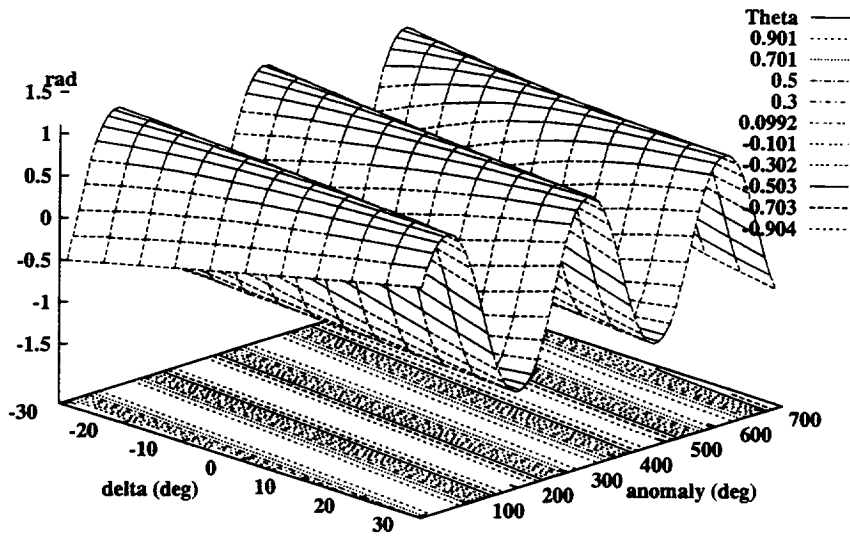
Libration Angular Speed for Theta Max = 60 deg

dTheta/dnu
1.22
0.945
0.67
0.394
0.118
-0.158
-0.434
-0.71
-0.986
-1.26

rad/anomaly rad
1.5
1
0.5
0
-0.5
-1
-1.5
-2

delta (deg)
-30 -20 -10 0 10 20 30

anomaly (deg)
100 200 300 400 500 600 700
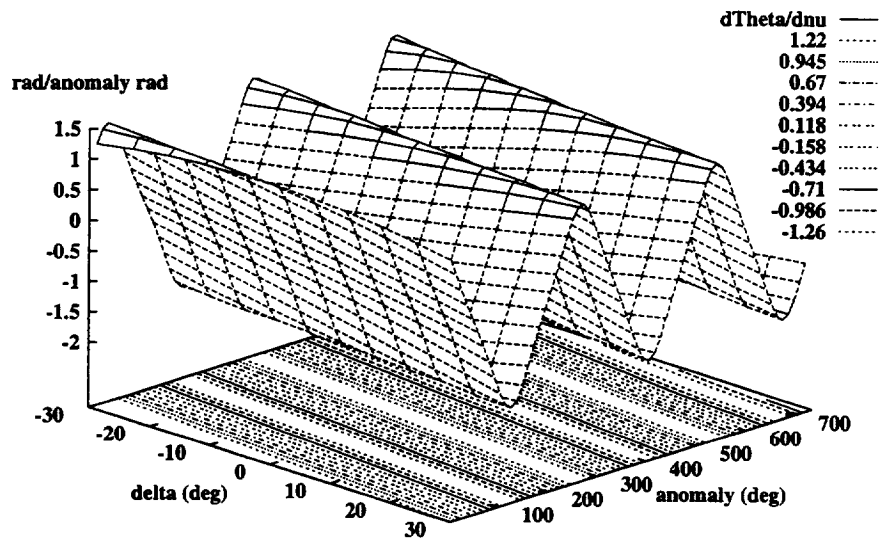
Figure 28 TS Libration angle and libration speed after the fitst cut for the minimum decay rate libration (60 degrees).

Apogee Height for Theta Max = 58 deg

Perigee Height for Theta Max = 59 deg
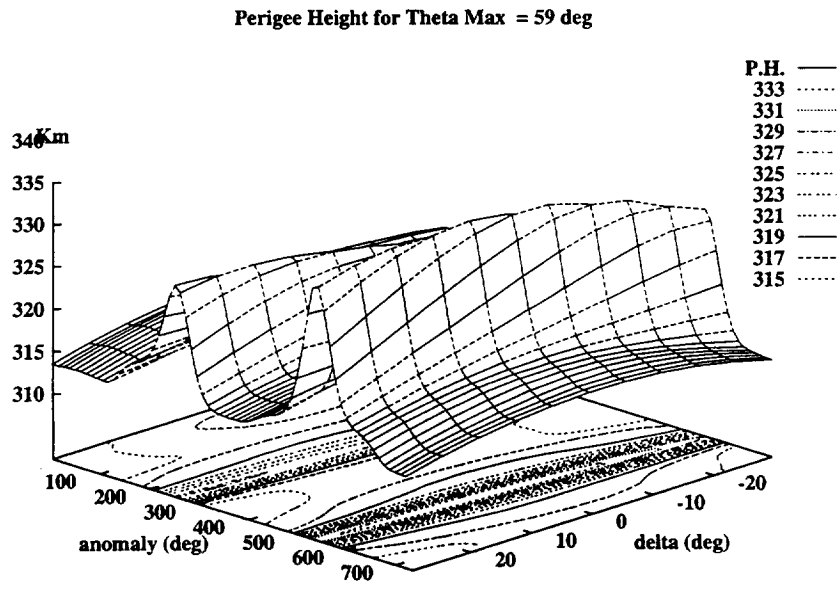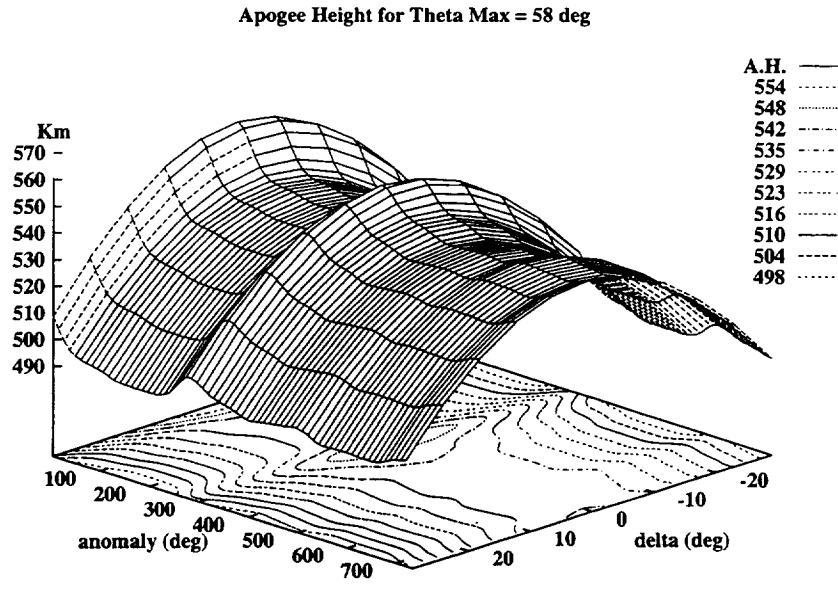
Figure 29 Satellite apogee and perigee height vs true anomaly at the second cut and libration angle at the first cut, for $\theta_M=59$ deg.

Apogee Height for Theta Max = 60 deg
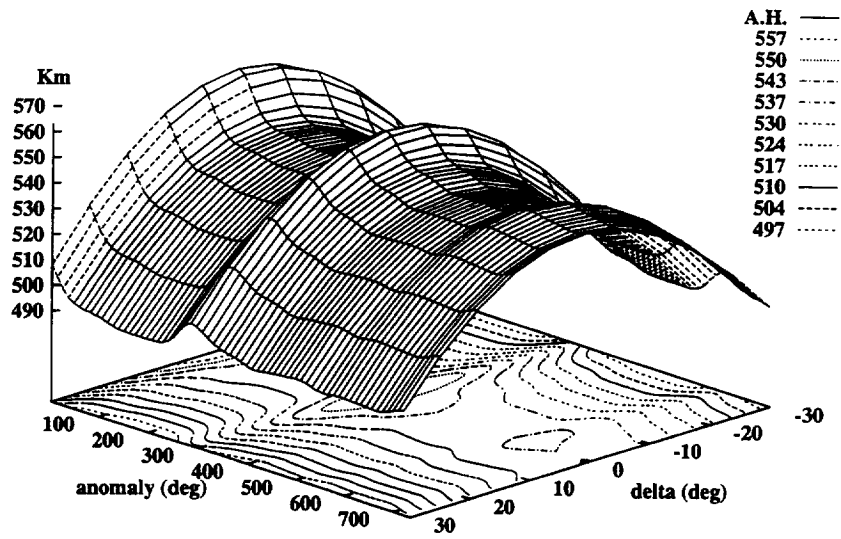
Perigee Height for Theta Max = 60 deg
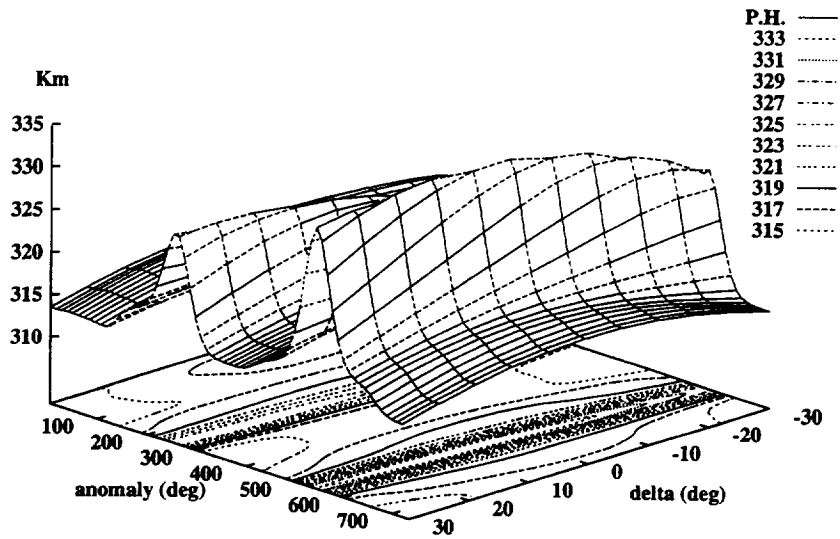
Figure 30 Satellite apogee and perigee height vs true anomaly at the second cut and libration angle at the first cut, for $\theta_M=60$ deg.

Apogee Height for Theta Max = 61 deg
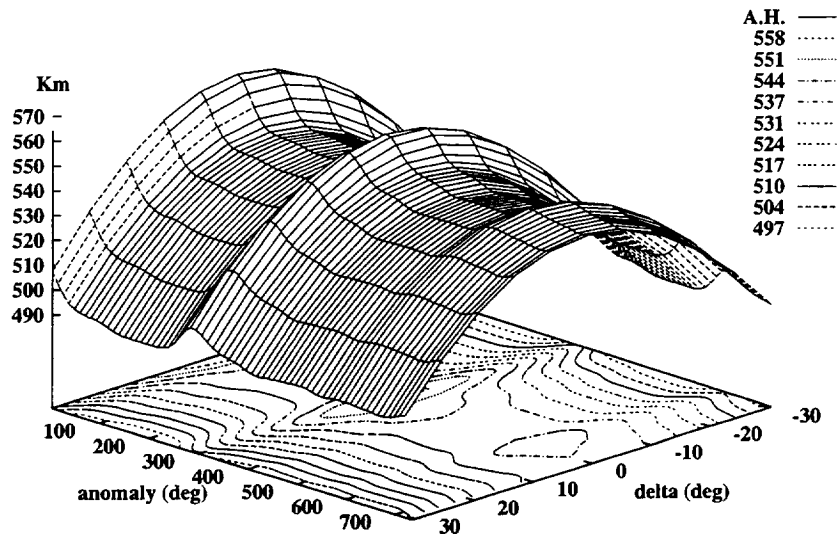
Perigee Height for Theta Max = 61 deg
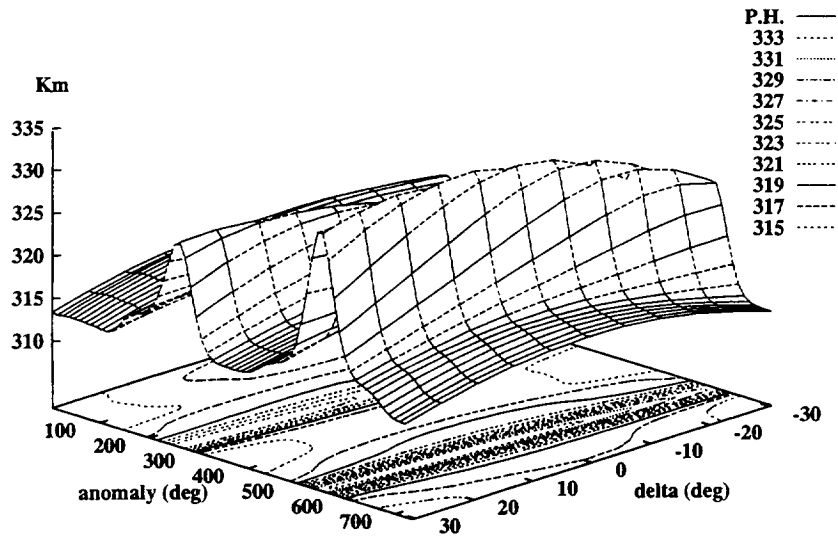
Figure 31 Satellite apogee and perigee height vs true anomaly at the second cut and libration angle at the first cut, for $\theta_M=61$ deg.

REFERENCES

1. Lorenzini, E., Gullahorn, G., and Cosmo, M., *Tethered Systems Dynamics and Flight Data Analysis*, Final Report to NASA for Grant NAG8-1046, May 1995.

2. Pelaez Alvarez, J. and Lorenzini, E., "Sensitivity Analysis of SEDSAT Orbital Injection." Proceedings of the *Fourth International Conference on Tethers In Space*, 10-14 April 1995, Smithsonian Institution, Washington, DC; Vol. I, pp. 563-576.

3. Beletski, V.V. 1993, *Dynamics of Space Tethered* Systems (San Diego, CA: American Astronautical Society; Russian original: Moscow: Nauka, 1990).

4. Singh, R.B. and Demin, V.G., "About the Motion of a Heavy Flexible String Attached to the Satellite in the Central Field of Attraction." *Celestial Mechanics*, 6 (1972), 268-277.

5. Hagedorn, P., "Some Remarks on the String Problem Treated by Singh and Demin." *Celestial Mechanics*, 11 (1975), 59-73.

6. Press, W.H. et al. 1992, *Numerical Recipes in C*, 2nd Edition (Cambridge, MA: Cambridge university Press).

7. Deutsch, R. 1963, *Orbital Dynamics of Space Vehicles* (Englewood Cliffs, NJ: Prentice-Hall).

8. Abramowith, M. and Stegun, I. 1972, *Handbook of Mathematical Functions* (New York: Dover).

9. Meirovitch, L. 1990, *Dynamics and control of Structures* (New York: Wiley Interscience).

10. Timoshenko, S., Young, D.H., Weaver, W. 1974, *Vibration Problems in Engineering*, 4th Edition (New York: Wiley).

11. King-Hele, D. 1964, *Theory of Satellite Orbits in an Atmosphere*, (London: Butterworths).

12. Johnson, F.S., ed. 1965, *Satellite Environment Handbook*, (Stanford, CA: Stanford University Press), p. 16.

DYNAMICS AND CONTROL OF SEDSAT

Introductory Remarks

The satellite SEDSAT, built by a team of students of the University of Alabama at Huntsville, will be injected into a higher orbit from the Space Shuttle in July 1997 by using a 20-km-long librating tether acting as a sling shot. Since the satellite is required to have a lifetime of about 3 years, without reboosting, the height and eccentricity of the final orbit are a primary concern. The injection velocity (ΔV) at the satellite release must be maximized in order to maximize the apogee height of the final orbit and consequently the satellite lifetime. Moreover, the final orbit must be as insensitive as possible to variations of the deployer's friction parameters in order to provide an accurate orbital transfer of the satellite. Consequently, the magnitude, direction, and timing of the ΔV at satellite release (i.e., when the tether crosses the local vertical and the tether is cut from the Shuttle) must be accurate and as insensitive as possible to variations of the model parameters. A non-linear control law (feedforward-feedback) for driving the satellite to the desired state at the end of deployment was developed during the 1994-1995 research activity on this grant [1]. The control law is based on predefined reference profiles which are dependent upon the conditions at satellite ejection from the Shuttle. These conditions at satellite ejection have changed since the control law that was delivered to NASA in December 1994 due to Shuttle safety considerations. Consequently, new reference profiles had to be generated and some of the control parameters modified in order to cope with the new initial conditions.

New Reference Profiles and Control Parameters

Before describing the changes to the SEDSAT deployment control law, we will recall the basics of the SEDS deployer tension model and the control law. The reader should read Refs. [1-2] for a more detailed treatment of the subject.

SEDS Deployer's Tension Model

The tension model for the SEDS deployer is as follows:

$$T = \left[T_0 + I\rho \dot{L}^2 A_{rel}^{-E} \right] \cdot e^B \cdot e^{f \cdot |\theta_0 - \theta|} \tag{92}$$

where $A_{rel} = 1 - A\, L/L_{end}$, L_{end} = final tether length = 20 km, A = tether annulus solidity = 0.9424, E = area exponent = 0.6, B = brake parameter = $2\pi f\, n$, n = number of brake turns, f = friction coefficient = 0.18 (best estimate), T_0 = static (or minimum) tension, I = inertia multiplier = 4.1, ρ = linear density of tether = 3.3 kg/km, θ_0 = null exit angle, and θ = tether's exit angle (for a deployer aligned along the Nadir, θ coincides with the in-plane libration angle). In summary, this approximate tension model consists of a static tension term T_0, an hydraulic tension term proportional to $\dot{L}^2$, an exponential brake multiplier, and an exponential exit-angle multiplier. Parameters of the tension model are uncertain as they depend on environmental conditions and many other uncontrollable, or poorly controllable, factors. The most influential, from the deployment dynamics standpoint, and also less certain parameter of the tension model is T_0. A likely estimate of the value of T_0 from the flights of SEDS-I and II is about 20 mN with an expected variability of ± 10 mN.

<u>Basics of Deployment Control Law</u>

SEDSAT is ejected from the Shuttle with initial conditions (i.e., ejection angle and magnitude of ejection velocity) such that the amplitude of the final tether libration in the orbital plane is insensitive to variations of the static tension of the deployer's tension model. During this time (free-deployment phase), the brake is not engaged. At a tether length greater than about 15 km, the brake is engaged to slow down the tether exit velocity. The brake utilizes a feedback-feedforward, non-linear control law [2-4] to lead the system to the desired state vector at the end of deployment. The control law is based on precomputed length and length rate profiles (i.e., the non-linear portion of the control law) and on a linear feedback which keeps the system state along the desired state trajectory.

The timing of the crossing of the local vertical is dependent upon the final libration amplitude. This amplitude is affected by the errors of the conditions at ejection with respect to the desired ejection conditions. A change of the magnitude of the ejection velocity require the computation of new reference profiles and also the evaluation of the new ejection angle that provides insensitivity to the static tension during the free-deployment phase.

The ejection velocity of SEDSAT has been changed several time from the original $V_0 = 1.47$ m/s to the latest $V_0 = 2.5$ m/s as a consequence of Shuttle's safety considerations. A number of reference profiles (from SEDSAT_Ref39 to SEDSAT_Ref53) have been derived to accommodate these changes. As a result, the ejection angle must be changed from $\theta_0 = -31°$ (upward and forward) consistent with $V_0 = 1.47$ m/s to $\theta_0 = -21°$ consistent with $V_0 = 2.5$ m/s.

In this report we present only the results of the latest reference profile and the associated control parameters, namely, SEDSAT_Ref53_1Sep95 (the numbering is sequential from the beginning of the SEDSAT control law analysis). At the time of the delivery of the control law to NASA/MSFC, on 1 September 1995, the system and tension nominal parameters were as follows:

Tension model parameters

T_0 = minimum tension = 20 mN
I   = inertia multiplier = 4.1
A   = annulus solidity = 0.9424
E   = area exponent = 0.6
f   = friction coefficient = 0.18

System parameters

Satellite mass = 36.3 kg
Tether linear density = 0.33 kg/km
Shuttle orbit = 297 km circular
Orbital inclination = 57°
Tether length = 20 km
Tether diameter = 0.8 mm
Tether material = Spectra 1000

Table 14. Control and system parameters for SEDSAT_Ref39 and SEDSAT_Ref53

-------- CONTROL PARAMETERS ---

No.	PARAMETER	TYPE	Units	REF39	REF53 (new)
1.	c	Filter Coefficient	(none)	0.125	0.125
2.	K1	TurnCount Gain	(1/Turn)	0.002	0.002
3.	DZTC	TurnCount Deadzone	(Turn)	5	5
4.	TCELIM	Maximum Turn Count Error	(Turn)	5000	6500
5.	K2	Turn Count Rate Gain	(s/Turn)	0.2	0.2
6.	DZTCR	TurnCountRate Deadzone	(Turn/s)	0.5	0.5
7.	TCRELIM	Maximum Turn CountRate Error	(Turn/s)	10	25
8.	WAILP	Wrap Increment Upper Limit	(none)	2	2
9.	TBD s	Time after which bias is applied	(s)	65535	65535
10.	BIAS	Brake post Bias	(Turn)	0	0
11.	WACLP	WrapAdjustment Upper Limit	(Turn)	7	7
12.*	TCBS	TurnCount BrakeStop	(Turn)	46000	46000
13.*	A1	Coeff_1 in Variable Gains	(none)	0.6980403	0.6980403
14.*	A2	Coeff_2 in Variable Gain	(none)	5.738031e-6	5.738031e-6
15.	STOPDEPLOY	Time from eject. for Brake Ramping up	(s)	5000	4600

--------- INITIAL CONDITIONS AT EJECTION --

| | V_0 | Ejection velocity | (m/s) | 1.47 | 2.5 |
| | θ_0 | Ejection angle (up and forward) | (deg) | -31 | -21 |

----
* These parameters are very likely to change for the SEDSAT flight tether

Table 14 shows the control law parameters for SEDSAT_Ref53. The logical names of the control variables in the first column of Table 14 are in accordance with the document *SEDS Deployer Flight Software Requirement Specification (DMO6)* [7]. Table 14 not only shows the values of the control and system parameters for the latest control law SEDAT_Ref53_1Sep95 (V_0 = 2.5 m/s) but also shows the corresponding values of the previously released control law SEDSAT_Ref39_6Dec94 (V_0 = 1.47 m/s).

As indicated in Table 14, some of the control parameters will likely need to be changed as the characteristics of the flight tether for SEDSAT will become known after the deployment tests are conducted.

The reference profiles, which are expressed in terms of number of deployed turns and turn rate, will also have to be modified as a consequence of a change in the relationship between tether length and tether turns. The maximum number of tether turns on the spool used to derive SEDSAT_Ref53 is 46200. The reference tables for SEDSAT_Ref53 are shown in Appendix I. The reference length, rate and brake profiles are shown in Fig. 31. Note that the in-plane libration angle and angular rate, depicted in Fig. 31, are not reference variables. They are shown here only for the sake of completeness.

The dynamics of SEDSAT deployment according to the new reference profiles, for reference conditions, is shown in Fig. 32. Under reference conditions, the satellite will take 4480 s to reach the final tether length of about 20 km and 4780 s to cross the local vertical (LV).
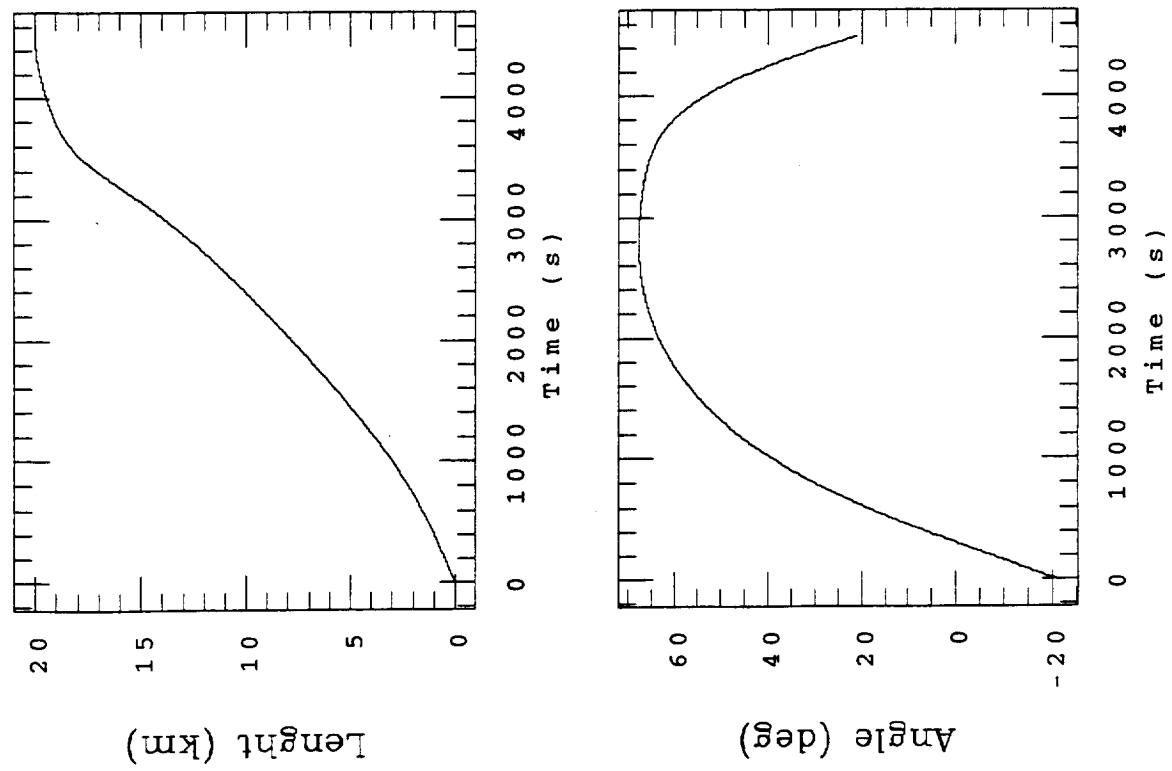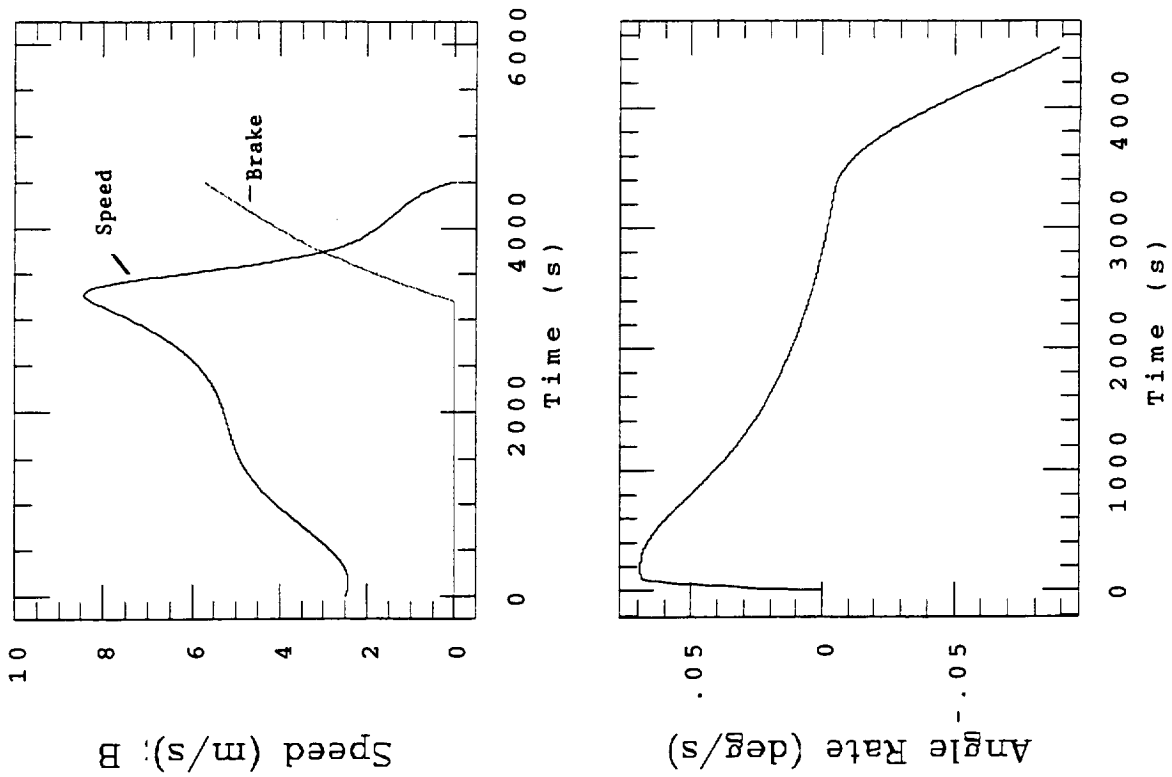
Fig. 31. Reference profiles for SEDSAT_Ref53.
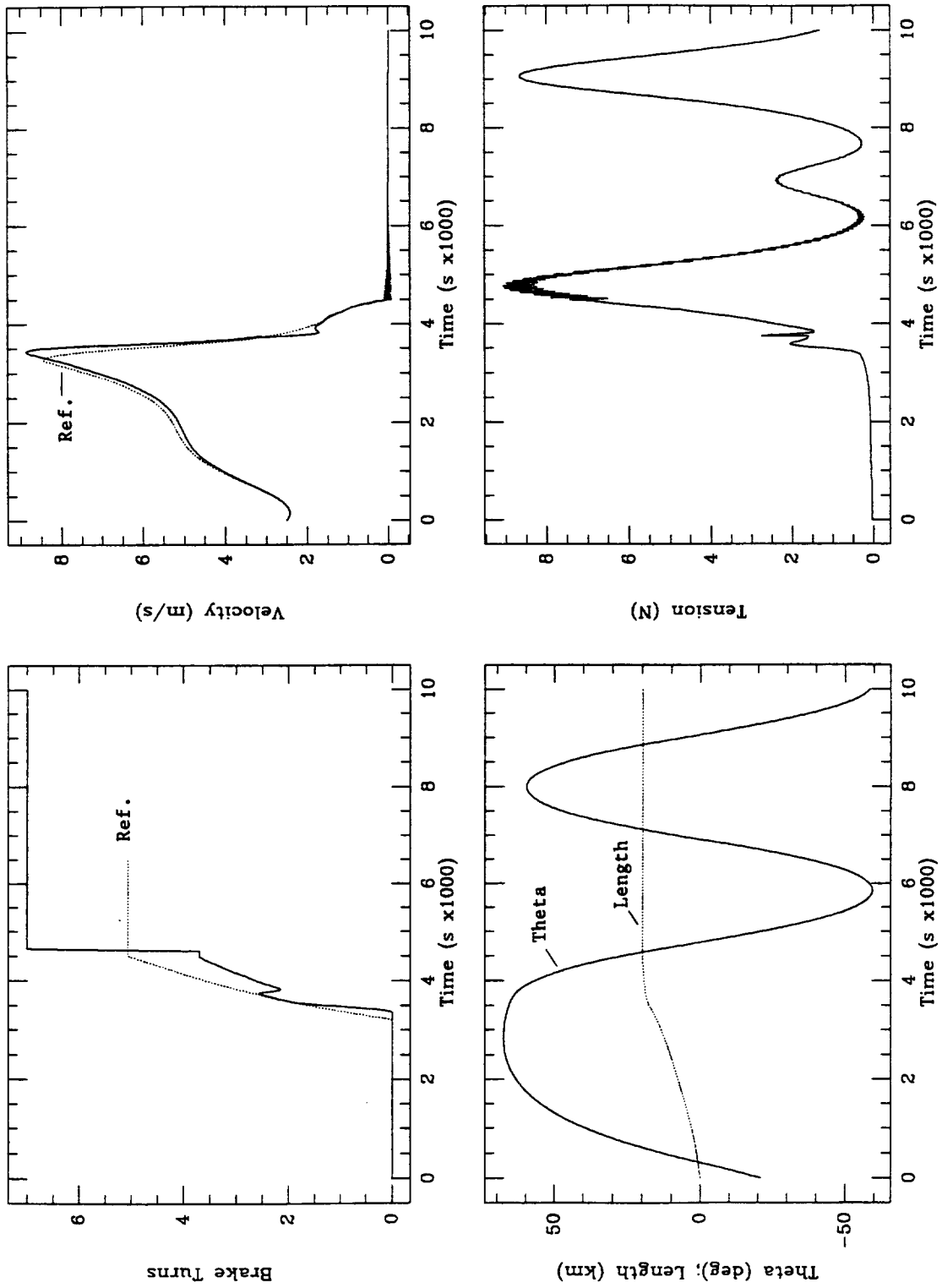
Fig. 32. Deployment dynamics for SEDSAT_Ref53 (reference conditions)

Sensitivity of New Deployment Control Law to Errors

We rewrite here below the reference conditions which were adopted for deriving SEDSAT_Ref53:

Tension model parameters

T_0 = minimum tension = 20 mN
I   = inertia multiplier = 4.1
A   = annulus solidity = 0.9424
E   = area exponent = 0.6
f   = friction coefficient = 0.18

Initial conditions

V_0 = ejection velocity = 2.5 m/s
θ_0 = ejection angle = -21° (up and forward)

Table 2 shows the timing errors Δt at the crossing of LV with respect to the nominal value for errors affecting the minimum tension T_0, the Inertia Multiplier I, the ejection angle θ_0 and the ejection velocity V_0.

Table 2. Δt (s) errors at the crossing of LV for SEDSAT_Ref53

Lead cases	Δt error at LV	Δt error at LV	Lag cases
Ref conditions but T_0 = 10 mN (-50%)	-8 s	+8 s	Ref conditions but T_0 = 30 mN (+50%)
Ref conditions but I = 5.1 (+25%)	-40 s	+60 s	Ref conditions but I = 3.1 (-25%)
Ref conditions but θ_0 = -23° (+10%)	-54 s	+60 s	Ref conditions but θ_0 = -19° (-10%)
Ref conditions but V_0 = 2.63 m/s (+5%)	-90 s	+94 s	Ref conditions but V_0 = 2.38 m/s (-5%)

Timing errors due to initial conditions are proportional to initial condition errors as follows:

18 s per 1% of ejection velocity (magnitude) error
28 s per 1° (or 5%) ejection angle error

Timing errors at LV crossing (and release) of less than ±100 s have negligible effect (≤ 100 m altitude variations) on the perigee height after release. The effect on the apogee altitude is less than ±1% of the apogee height after release. Timing errors of ±100 s correspond to maximum tether angle deviations with respect to LV of about ±10°.

In Figs. 33(a)-33(h) the dynamics of SEDSAT for off-nominal values of the parameters above is compared to the nominal deployment dynamics.

61
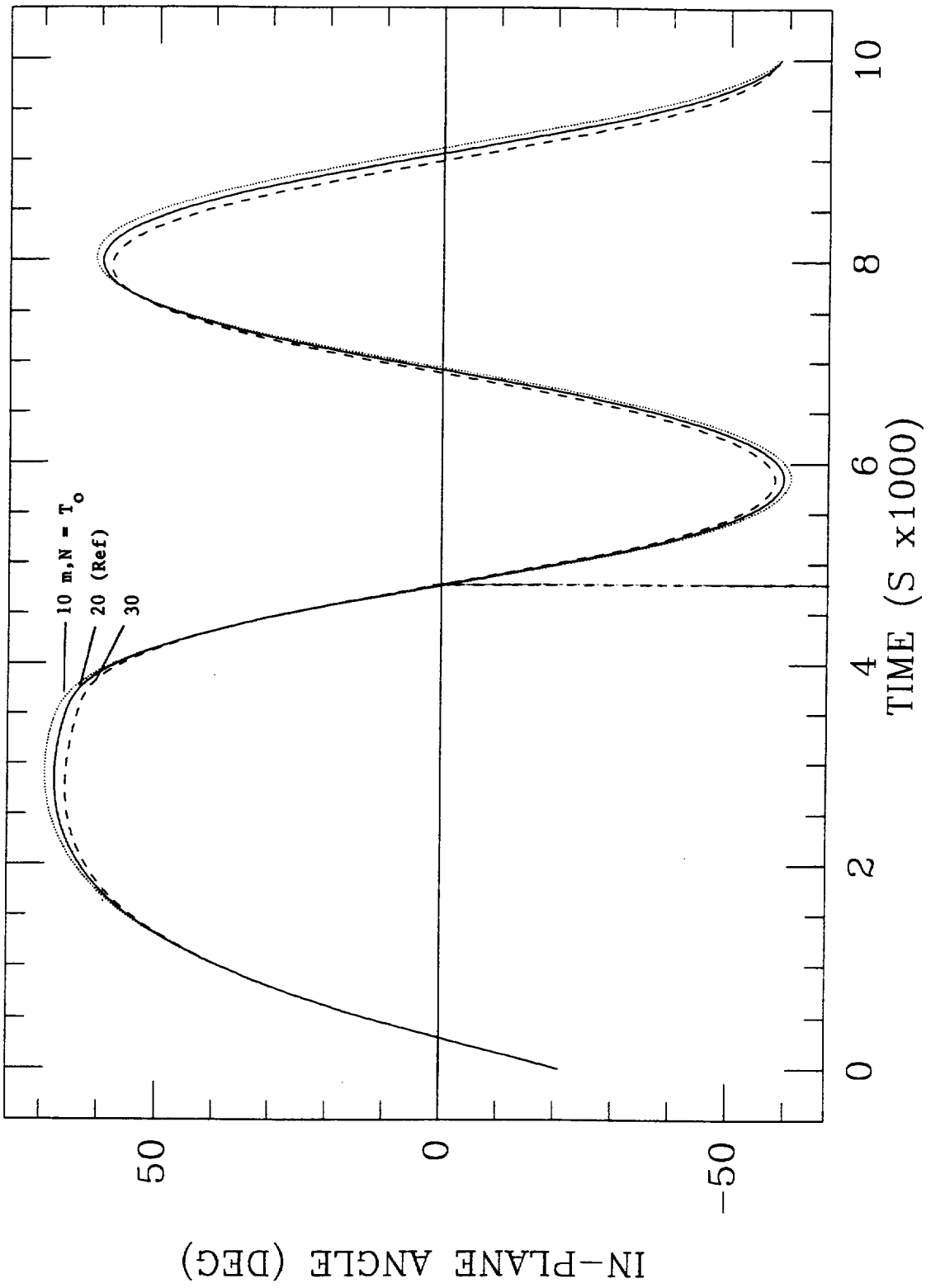
Fig. 33(a). Sensitivity of deployment to Minimum Tension
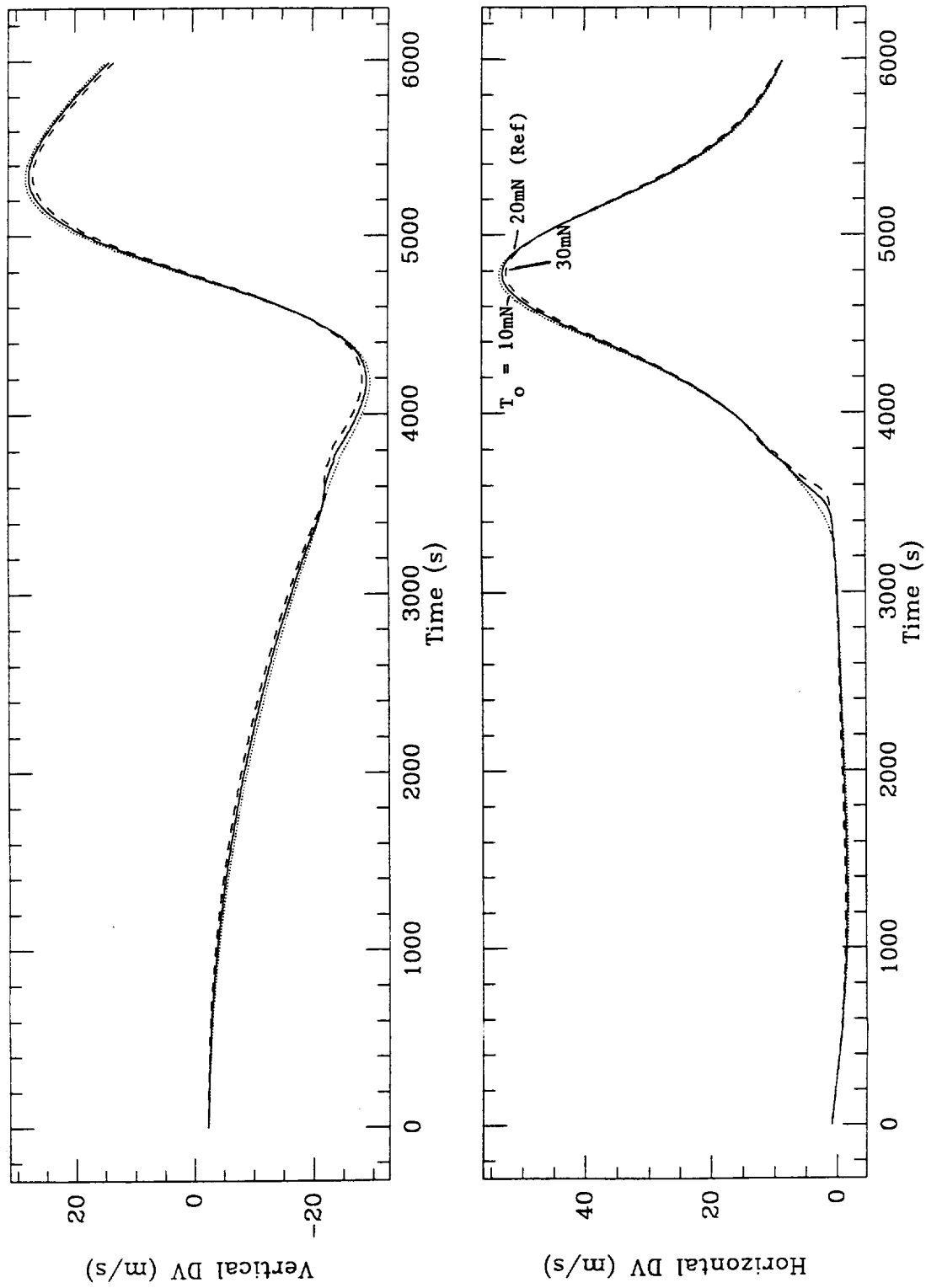
Fig. 33(b). Sensitivity of deployment to Minimum Tension (total ΔV)
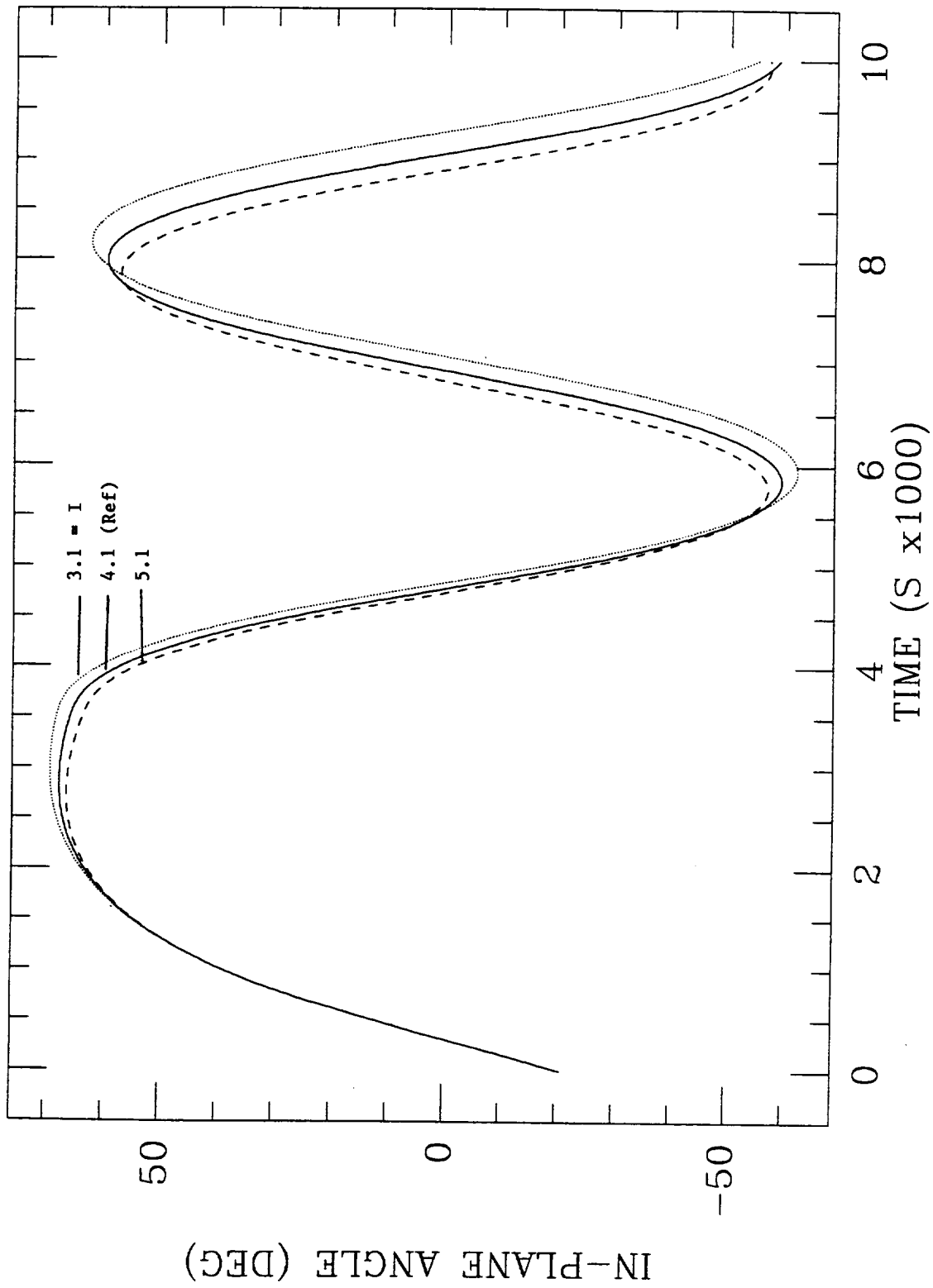
Fig. 33(c). Sensitivity of deployment to Inertia Multiplier

64
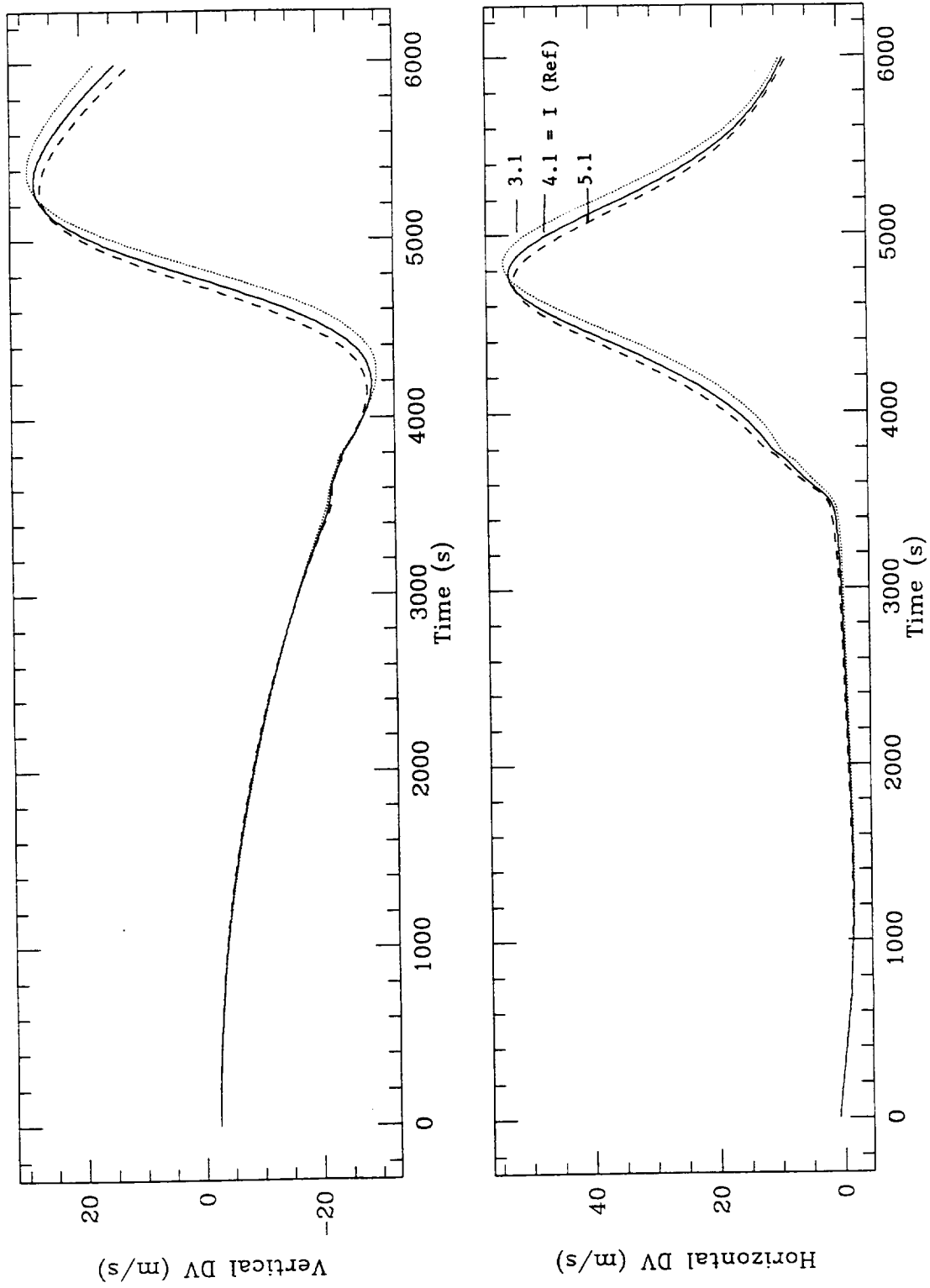
Fig. 33(d). Sensitivity of deployment to Inertia Multiplier (total ΔV)

65
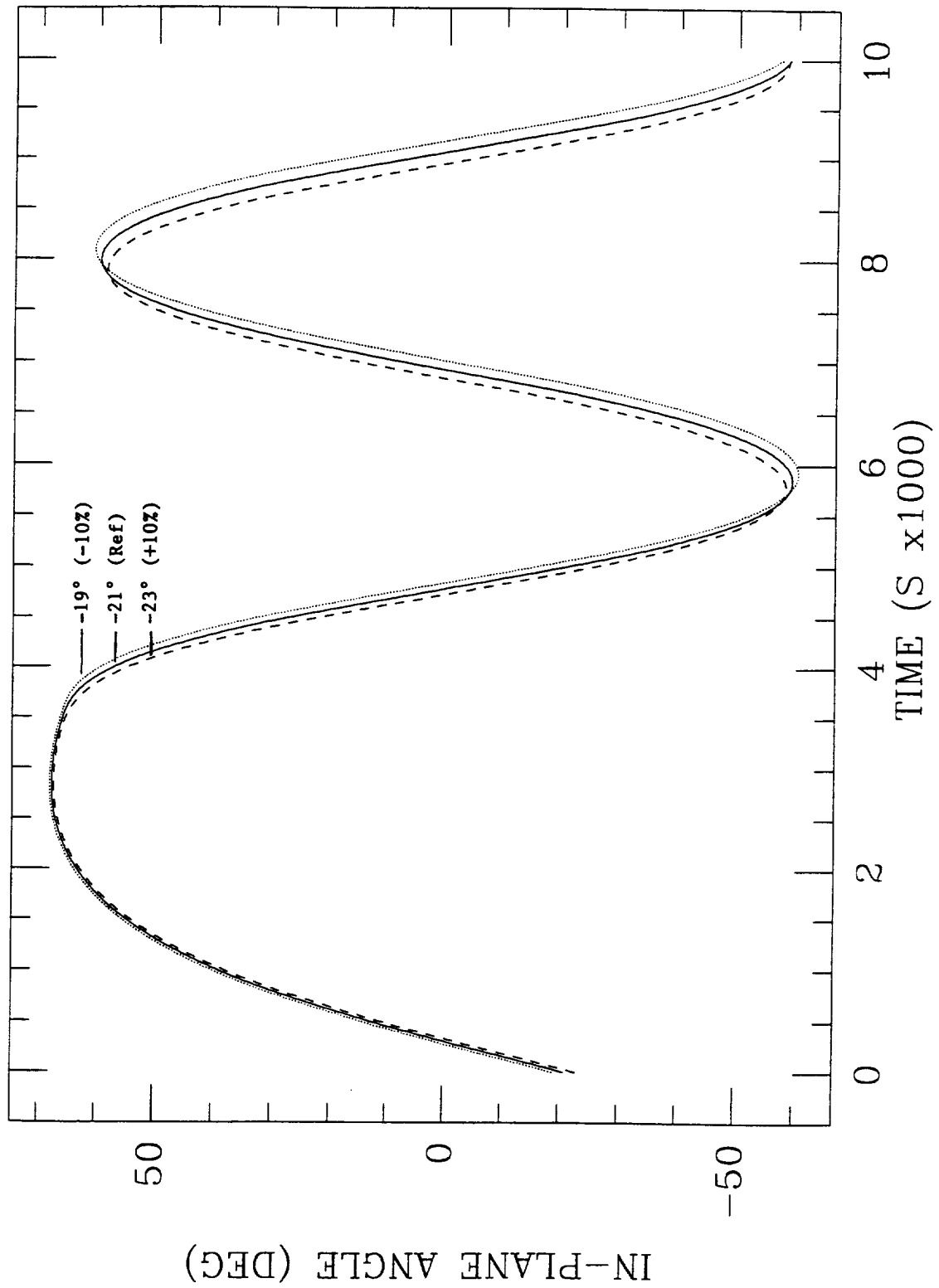
Fig. 33(e). Sensitivity of deployment to Ejection Angle

66
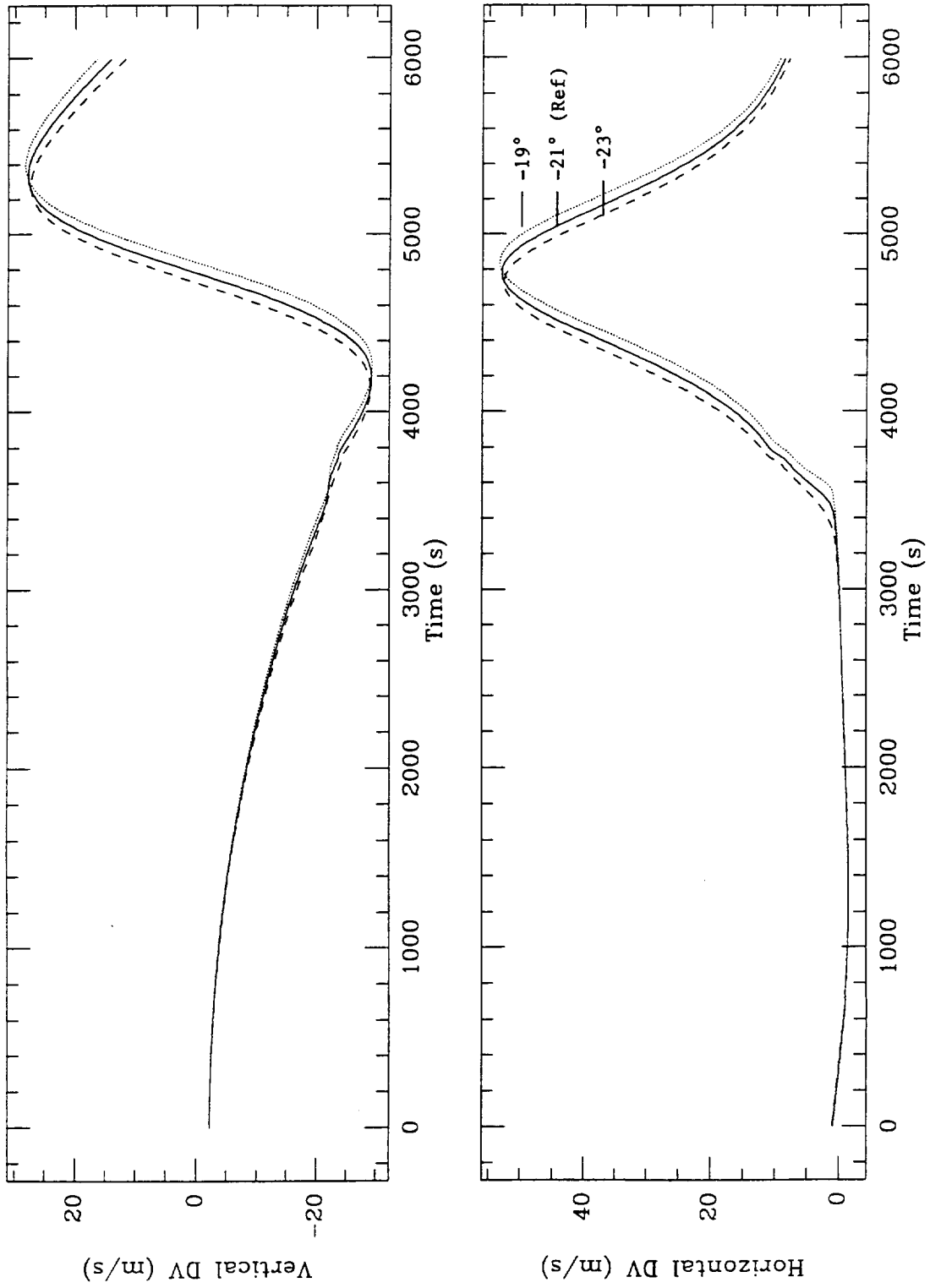
Fig. 33(f). Sensitivity of deployment to Ejection Angle (total ΔV)

67
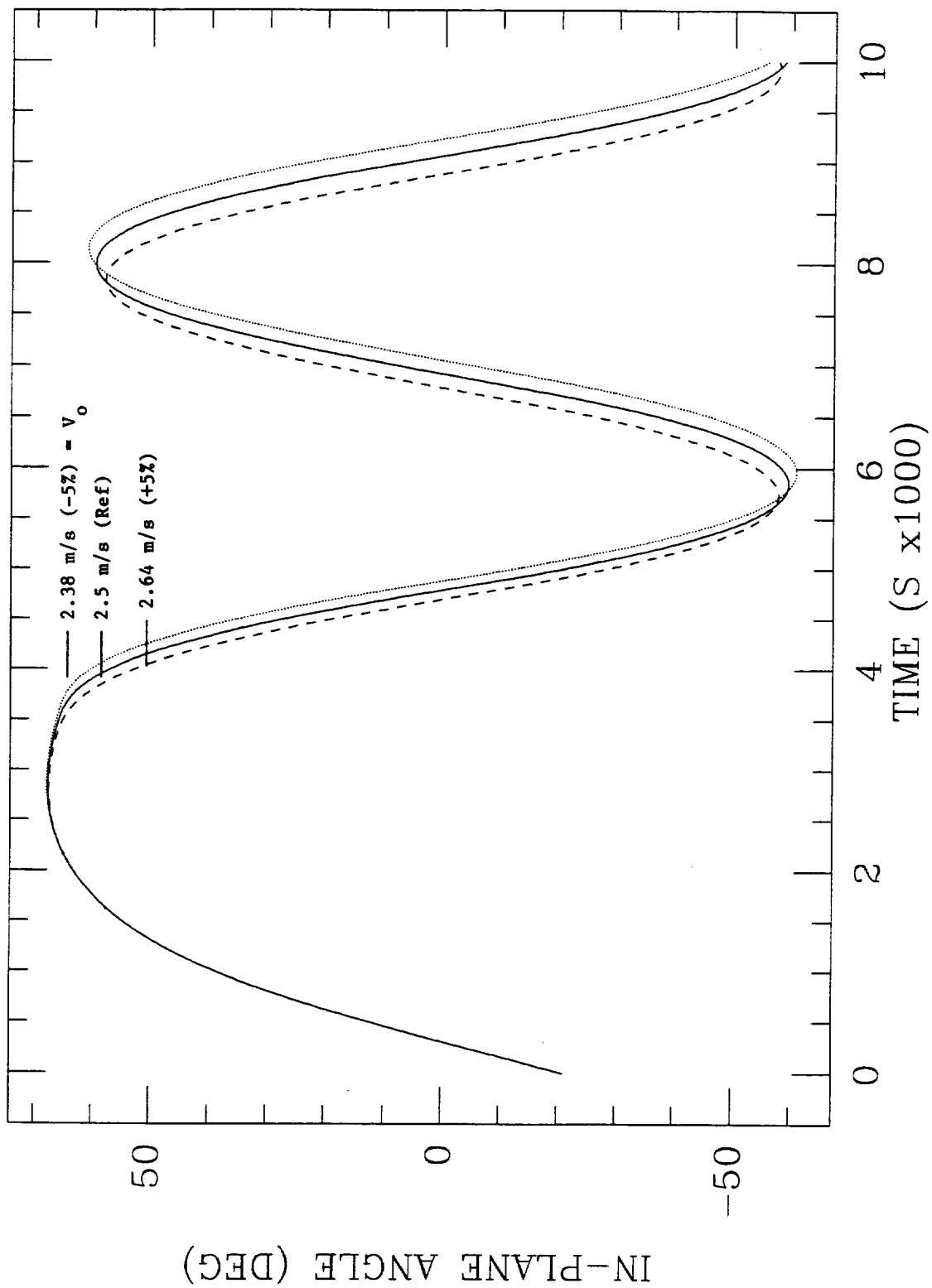
Fig. 33(g). Sensitivity of deployment to Ejection Velocity
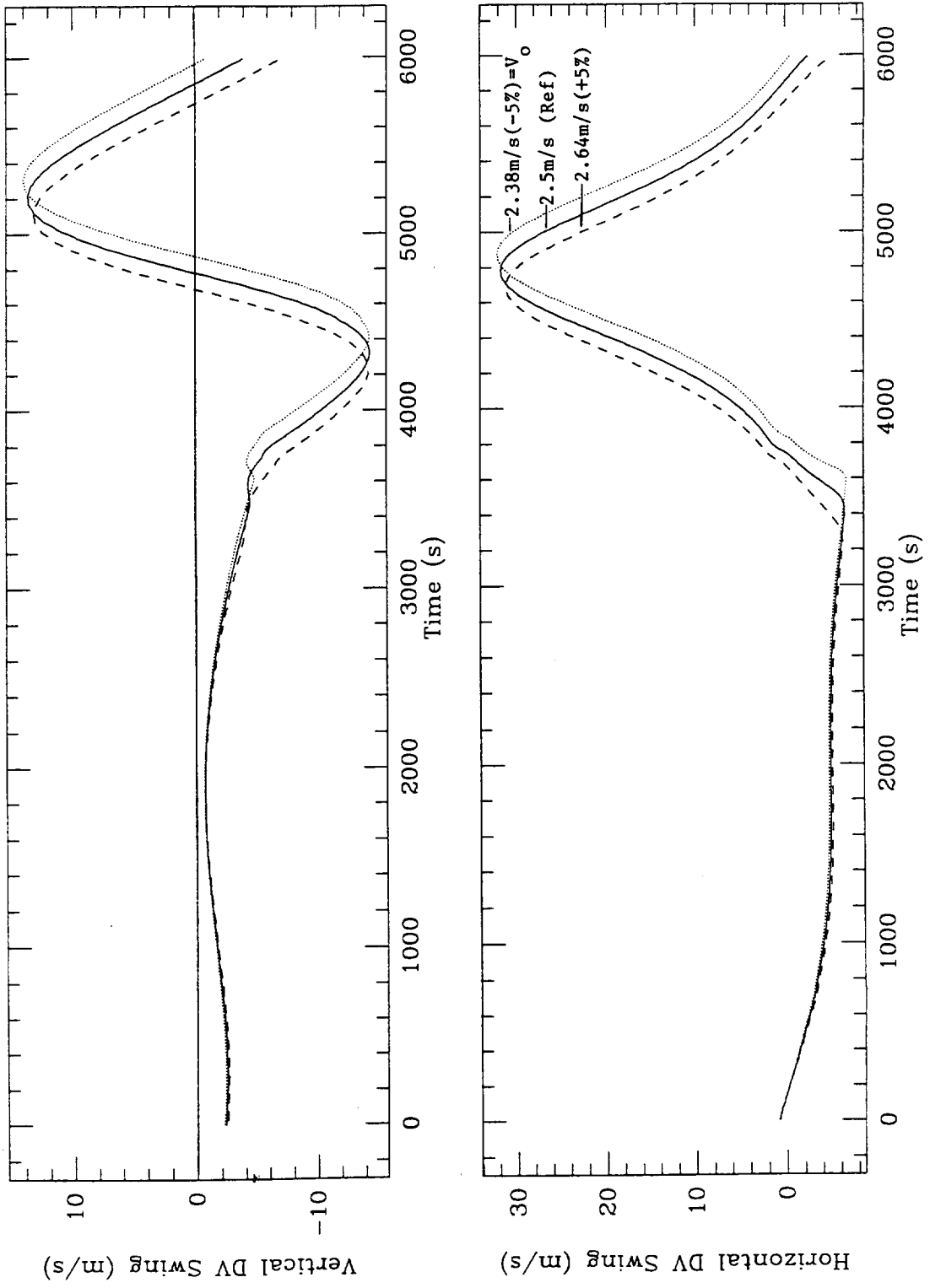
Fig. 33(h). Sensitivity of deployment to Ejection Velocity (total ΔV)

69
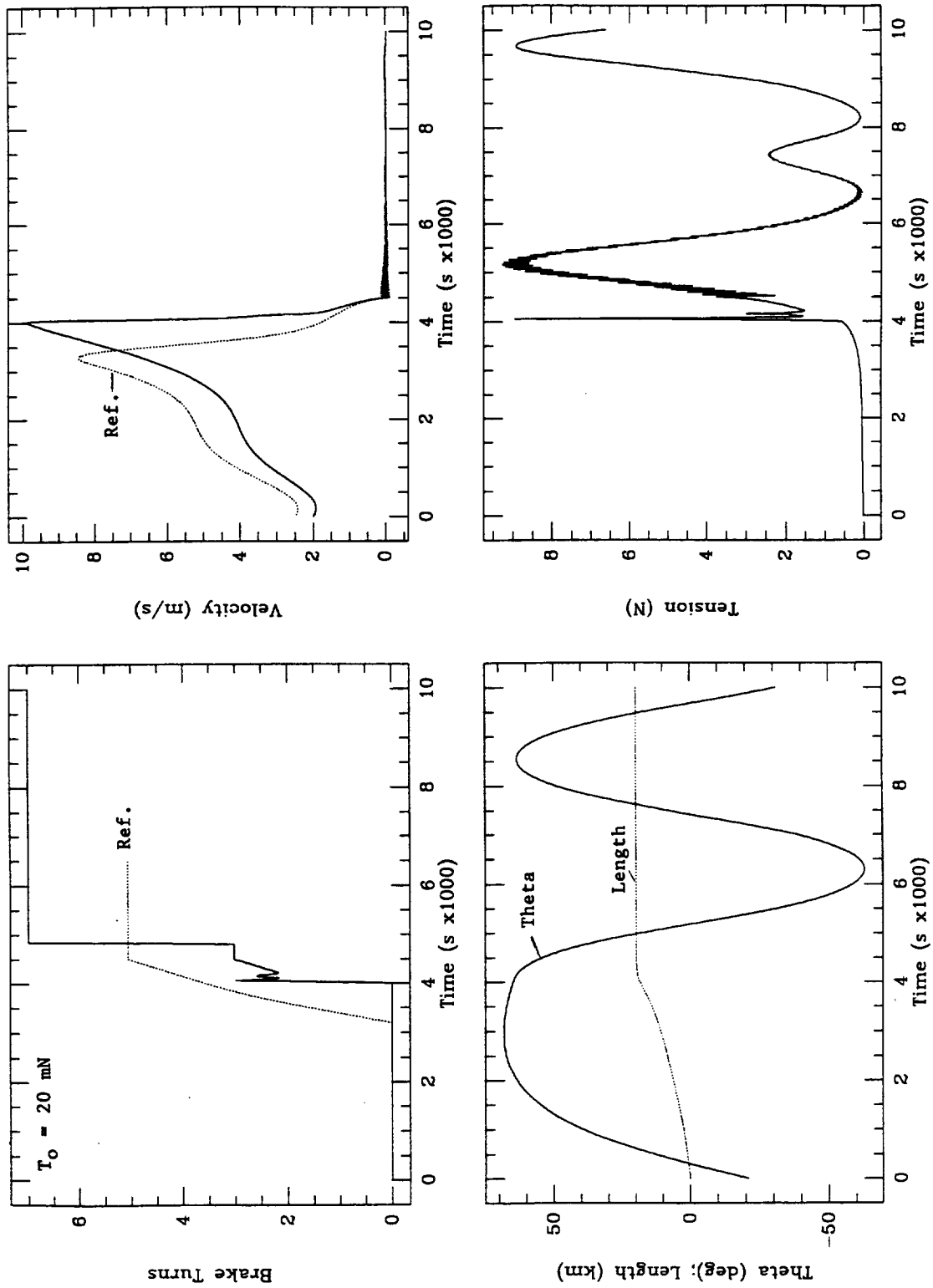
Fig. 34. SEDSAT deployment for $V_0 = 2$ m/s (ejection mechanism malfunction).

70
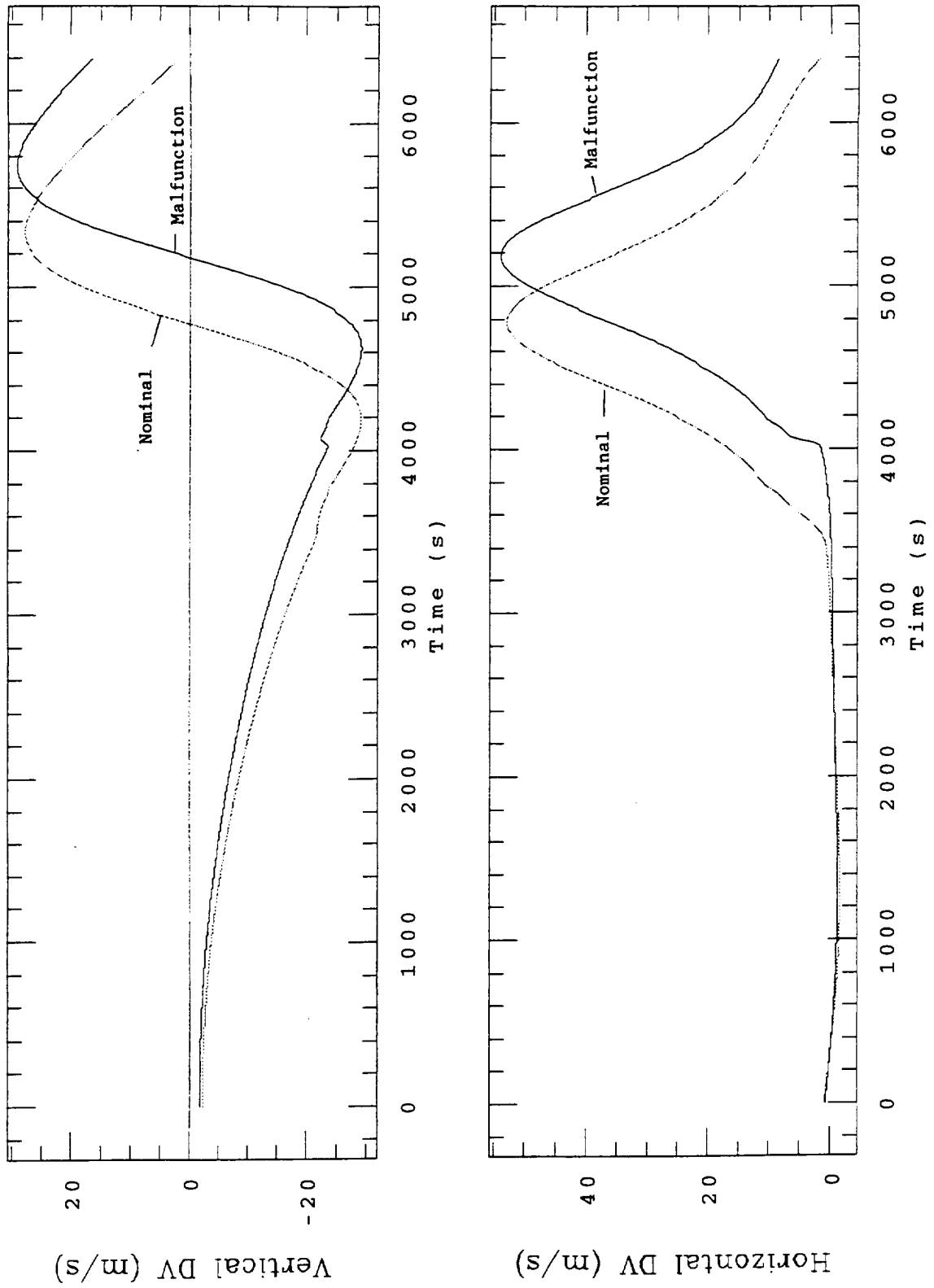
Fig. 34(b). SEDSAT deployment for $V_0 = 2$ m/s (malfunction; total ΔV).

71

Finally, a malfunction of the ejection mechanism was analyzed. In this scenario, the ejection velocity is reduced from $V_0 = 2.5$ m/s to $V_0 = 2$ m/s due to an assumed breakage of one ejection spring. The dynamics of SEDSAT for this malfunction is shown in Figs. 34(a)-34(b). The satellite deployment still reaches a length of about 20 km (19.8 km to be specific) in 4488 s (only 8 s longer than the nominal case) but the tether will cross LV at t = 5182 s (i.e., 402 s longer than the nominal case). The orbital injection of the satellite would still be acceptable if the satellite is released at the time the tether actually crosses LV.

The ΔV imparted to the center of mass of the tether-satellite system consists of a hanging component (that depends on tether length) and a swinging component that is due to the motion of the tether-satellite system with respect to the LH-LV reference frame. The hanging component is less affected by the timing errors than the swinging component. The (nominal) hanging component ΔV_H is equal to 21 m/s at release while the (nominal) swinging component ΔV_S is equal to 32 m/s. The nominal (i.e., reference conditions) post-release orbit of the satellite-tether system is about 317 km X 560 km, with respect to a spherical Earth of equatorial radius, after the first tether cut at the Shuttle end.

The absolute time of the first cut (or equivalently the orbital anomaly) is not critical for SEDSAT because there is no specific requirement on the phase of the final orbit for this mission. However, the sensitivity of the release time to variations of the deployer's model parameters can be more or less important depending on the level of crew and on-board equipment involvement in estimating the tether LV crossing. In the simplest scenario, the LV crossing could be based solely on the deployment start time and, consequently, the insensitivity of the maneuver duration to different deployer's parameters is important for obtaining an accurate ΔV at release.

For example the timing errors associated with the expected variations of the static tension is only ±10 s. The hydraulic component (proportional to L^2) in the deployer's tension model also has an effect on the deployment dynamics and, hence, on the timing and magnitude of ΔV at the crossing of LV. Unfortunately, the ejection angle that cancels the effect of the hydraulic tension term has the opposite sign of the ejection angle that cancels the effect of the minimum tension. It can be inferred from Fig. 33(c), which show the libration angle for different values of the hydraulic tension term, that a variation of the inertia multiplier I of ±25%, with respect to the reference value of 4.1, implies a variation of the timing to cross LV of about ±60 s.

The variation of the horizontal component of the total ΔV at release due to timing errors of ±100 s is less than ±1 m/s at the nominal time of LV crossing. The variation of the vertical component of the total ΔV is less than ±7 m/s at the nominal time of LV crossing. However, a vertical ΔV produces an increase (or decrease) of the orbital height which is about 1/4 of the effect produced by an horizontal ΔV.

In summary, if the tether cut is done at the nominal time of LV crossing from the start of deployment, the dispersion of the horizontal ΔV component is minimized. If the same tether cut is done at the actual crossing of LV, the dispersion of the vertical ΔV component is minimized. The latter case requires more crew and on-board equipment involvement. The two cases produce comparable dispersion in terms of the height of the

final orbit. The former case can produce a slightly different phasing of the initial and final orbit which, however, is not an issue for SEDSAT at present.

The time accuracy at release is definitely important for future missions which are expected to use a SEDS-type deployer for the atmospheric reentry of capsules. In this case the dispersion of the absolute time at release determines to a large extent the dispersion of the reentry capsule footprint. For instance, a timing error of the reentry ΔV in LEO of ±20 s implies, approximately, a ±148 km (±80 nmi) error in the length of the footprint. It is worth remembering that the length of the footprint of the *Gemini* capsule was typically ±185 km (±100 nmi) [7].

Concluding Remarks

In 1997, SEDSAT will the deployed on a 20-km-long tether from the Shuttle orbiting on a 297-km circular orbit and released into a higher orbit. The final tether length of 20 km is reached in 1 hr 14 min 40 s according to the new control law SEDSAT_Ref53 described in this report. Upon crossing the local vertical at t = 1 hr 19 min 40 s (i.e., 5 min after reaching the final deployed length), the tether is cut at the Shuttle and, consequently, the satellite with the attached tether is injected into an higher orbit thanks to the librating tether acting as a sling shot. After the first tether cut (at the Shuttle end) the orbit of the satellite-tether system will be about 317 km X 560 km, with respect to a spherical Earth.

The expected timing errors at LV crossing (and release) of less than ±100 s have negligible effect (≤ 100 m altitude variations) on the perigee height after release. The effect on the apogee altitude is approximately ±1% of the apogee height after release (i.e., about 6 km). Timing errors of ±100 s correspond to maximum tether angle deviations with respect to LV of ±11°.

References

1. Carroll, J. A., " Users Guide to SEDS, The Small Expendable-Tether Deployment System," Tether Applications, La Jolla, CA, April 1990.

2. E.C. Lorenzini, M.L. Cosmo and G.G. Gullahorn, "Tethered Systems Dynamics and Flight Data Analysis." Final Report on First Year Activity, NASA Grant NAG8-1046, May 1995.

3. Bortolami, S.B., E.C. Lorenzini, C.C. Rupp, and F. Angrilli, "Control Law for the Deployment of SEDS-II" <u>Advances in the Astronautical Sciences</u>, *Astrodynamics 1993*, Vol. 85, 733-748, AAS 1993.

4. E.C. Lorenzini, D.K. Mowery, and C.C. Rupp, "Dynamics and Control of SEDSAT Deployment." Proceedings of the *Fourth International Conference on Tethers in Space*, 10-14 April 1995, Smithsonian Institution, Washington, DC.

5. E.C. Lorenzini, S. Bortolami, C.C. Rupp and F. Angrilli, "Design and Flight Performance of the SEDS-II Tethered Satellite Deployment Control Law." <u>Journal of Guidance, Control and Dynamics</u>, 1996 (in press).

6. Carroll, A.J., "SEDS Deployer Design and Flight Performance," Proceedings of the AIAA Space Programs and Technology Conference Exhibit, 21-23 September 1993, Huntsville, Alabama, AIAA paper 93-4764.

7. Griffin, M.D., and J.R. French, "Space Vehicle Design." p. 252, AIAA Education Series, 1991.

8. Pelaez, J., "On the Dynamics of the Deployment of a Tether from an Orbiter." Proceedings of the *International Round Table on Tethers in Space*, 28-30 September 1994, ESA/ESTEC, Noordwijk, The Netherlands.

RITZTRIG.MS
RITZ METHOD WITH TRIGONOMETRIC FUNCTIONS
> b:=1/(1+32/(3.3E-4*20E3))/2;
> with(linalg):

$$b := .08549222800$$

Warning: new definition for norm
Warning: new definition for trace

> F:=v->K*cos(2*n*Pi*v)+sin(2*n*Pi*v);

$$F := v \rightarrow K \cos(2\,n\,\pi\,v) + \sin(2\,n\,\pi\,v)$$

> R2:=int(F(v),v=b-1..b)+(1/2/b-1)*F(b):
> Kn2:=solve(R2=0,K) $ n=1..4;

$$Kn2 := -.5955804727, -1.845948652, 24.55995647, 1.533481529$$

> DF2:=diff(diff(F(v),v),v):
> R1:=subs(v=b,DF2);
> Kn1:=solve(R1=0,K) $ n=1..4;

$$R1 := -4\,K\cos(.1709844560\,n\,\pi)\,n^2\,\pi^2 - 4\sin(.1709844560\,n\,\pi)\,n^2\,\pi^2$$

$$Kn1 := -.5955804728, -1.845948652, 24.55995647, 1.533481529$$

> evalf(subs({K=Kn1[1],n=1},R1));
> evalf(subs({K=Kn1[1],n=1},R2));
> evalf(subs({K=Kn2[1],n=1},R1));
> evalf(subs({K=Kn2[1],n=1},R2));

$$0$$

$$0$$

$$0$$

$$0$$

> evalf(subs({K=Kn1[2],n=2},R1));
> evalf(subs({K=Kn1[2],n=2},R2));
> evalf(subs({K=Kn2[2],n=2},R1));
> evalf(subs({K=Kn2[2],n=2},R2));

$$0$$

$$-.1 \ 10^{-8}$$

$$0$$

$$-.1 \ 10^{-8}$$

> evalf(subs({K=Kn1[3],n=3},R1));
> evalf(subs({K=Kn1[3],n=3},R2));
> evalf(subs({K=Kn2[3],n=3},R1));
> evalf(subs({K=Kn2[3],n=3},R2));

$$0$$

$$.1 \ 10^{-8}$$

$$0$$

$$.1 \ 10^{-8}$$

```
> evalf(subs({K=Kn1[4],n=4},R1));
> evalf(subs({K=Kn1[4],n=4},R2));
> evalf(subs({K=Kn2[4],n=4},R1));
> evalf(subs({K=Kn2[4],n=4},R2));
```

$$.1 \ 10^{-6}$$

$$-.1 \ 10^{-8}$$

$$.1 \ 10^{-6}$$

$$-.1 \ 10^{-8}$$

```
> F1:=subs({K=Kn1[1],n=1},F(v));
```

$$F1 := -.5955804728 \cos(2 \, \pi \, v) + \sin(2 \, \pi \, v)$$

```
> F2:=subs({K=Kn1[2],n=2},F(v));
```

$$F2 := -1.845948652 \cos(4 \, \pi \, v) + \sin(4 \, \pi \, v)$$

```
> F3:=subs({K=Kn1[3],n=3},F(v));
```

$$F3 := 24.55995647 \cos(6 \, \pi \, v) + \sin(6 \, \pi \, v)$$

```
> F4:=subs({K=Kn1[4],n=4},F(v));
```

$$F4 := 1.533481529 \cos(8 \, \pi \, v) + \sin(8 \, \pi \, v)$$

```
> plot({F1,F2,F3,F4},v=b-1..b);
```
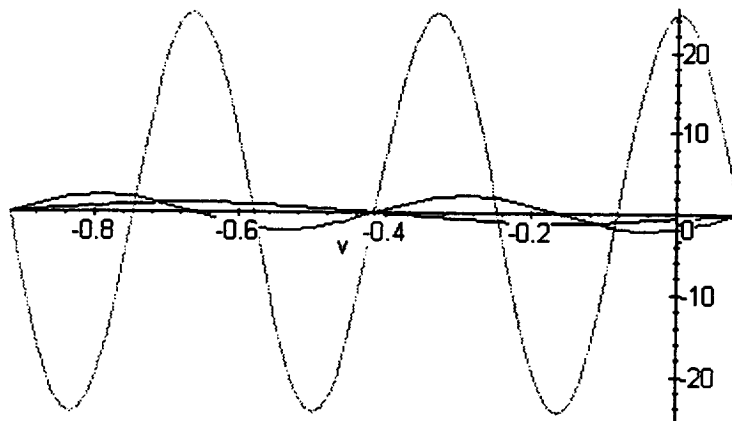


```
> c:=array(1..4,1..4);
```

$$c := \text{array}(1 .. 4, 1 .. 4, [\ ])$$

```
> c[1,1]:=int(F1*F1,v=b-1..b);
> c[1,2]:=int(F1*F2,v=b-1..b);c[1,2]:=0;
> c[1,3]:=int(F1*F3,v=b-1..b);c[1,3]:=0;
> c[1,4]:=int(F1*F4,v=b-1..b);c[1,4]:=0;
```

$$c_{1,\,1} := .6773580491$$

$$c_{1,\,2} := .3395305451 \ 10^{-9}$$

$$c_{1,\,2} := 0$$

$$c_{1,3} := -.5570423009 \ 10^{-8}$$

$$c_{1,3} := 0$$

$$c_{1,4} := .2232413334 \ 10^{-9}$$

$$c_{1,4} := 0$$

```
> c[2,1]:=int(F2*F1,v=b-1..b);c[2,1]:=0;
> c[2,2]:=int(F2*F2,v=b-1..b);
> c[2,3]:=int(F2*F3,v=b-1..b);c[2,3]:=0;
> c[2,4]:=int(F2*F4,v=b-1..b);c[2,4]:=0;
```

$$c_{2,1} := .3395305451 \ 10^{-9}$$

$$c_{2,1} := 0$$

$$c_{2,2} := 2.203763211$$

$$c_{2,3} := 0$$

$$c_{2,3} := 0$$

$$c_{2,4} := -.5305164769 \ 10^{-9}$$

$$c_{2,4} := 0$$

```
> c[3,1]:=int(F3*F1,v=b-1..b);c[3,1]:=0;
> c[3,2]:=int(F3*F2,v=b-1..b);c[3,2]:=0;
> c[3,3]:=int(F3*F3,v=b-1..b);
> c[3,4]:=int(F3*F4,v=b-1..b);c[3,4]:=0;
```

$$c_{3,1} := -.5570423009 \ 10^{-8}$$

$$c_{3,1} := 0$$

$$c_{3,2} := 0$$

$$c_{3,2} := 0$$

$$c_{3,3} := 302.0957310$$

$$c_{3,4} := -.1136821022 \ 10^{-8}$$

$$c_{3,4} := 0$$

```
> c[4,1]:=int(F4*F1,v=b-1..b);c[4,1]:=0;
> c[4,2]:=int(F4*F2,v=b-1..b);c[4,2]:=0;
```

```
> c[4,3]:=int(F4*F3,v=b-1..b);c[4,3]:=0;
> c[4,4]:=int(F4*F4,v=b-1..b);
```

$$c_{4,\,1} := .2232413334 \ 10^{-9}$$

$$c_{4,\,1} := 0$$

$$c_{4,\,2} := -.5305164769 \ 10^{-9}$$

$$c_{4,\,2} := 0$$

$$c_{4,\,3} := -.1136821022 \ 10^{-8}$$

$$c_{4,\,3} := 0$$

$$c_{4,\,4} := 1.675782800$$

```
> cp:=array(1..4,1..4);
```

$$cp := array(\ 1 .. 4,\ 1 .. 4,\ [\ \ ])$$

```
> cp[1,1]:=int(F1*diff(F1,v)*v,v=b-1..b);
> cp[1,2]:=int(F1*diff(F2,v)*v,v=b-1..b);
> cp[1,3]:=int(F1*diff(F3,v)*v,v=b-1..b);
> cp[1,4]:=int(F1*diff(F4,v)*v,v=b-1..b);
```

$$cp_{1,\,1} := -.3386790252$$

$$cp_{1,\,2} := 1.629034753$$

$$cp_{1,\,3} := -10.72859139$$

$$cp_{1,\,4} := -.5682202935$$

```
> cp[2,1]:=int(F2*diff(F1,v)*v,v=b-1..b);
> cp[2,2]:=int(F2*diff(F2,v)*v,v=b-1..b);
> cp[2,3]:=int(F2*diff(F3,v)*v,v=b-1..b);
> cp[2,4]:=int(F2*diff(F4,v)*v,v=b-1..b);
```

$$cp_{2,\,1} := -1.629034753$$

$$cp_{2,\,2} := -1.101881606$$

$$cp_{2,\,3} := -61.92499786$$

$$cp_{2,\,4} := -2.562300523$$

```
> cp[3,1]:=int(F3*diff(F1,v)*v,v=b-1..b);
> cp[3,2]:=int(F3*diff(F2,v)*v,v=b-1..b);
> cp[3,3]:=int(F3*diff(F3,v)*v,v=b-1..b);
> cp[3,4]:=int(F3*diff(F4,v)*v,v=b-1..b);
```

$$cp_{3,1} := 10.72859140$$

$$cp_{3,2} := 61.92499789$$

$$cp_{3,3} := -151.0478655$$

$$cp_{3,4} := 77.14261558$$

```
> cp[4,1]:=int(F4*diff(F1,v)*v,v=b-1..b);
> cp[4,2]:=int(F4*diff(F2,v)*v,v=b-1..b);
> cp[4,3]:=int(F4*diff(F3,v)*v,v=b-1..b);
> cp[4,4]:=int(F4*diff(F4,v)*v,v=b-1..b);
```

$$cp_{4,1} := .5682202936$$

$$cp_{4,2} := 2.562300523$$

$$cp_{4,3} := -77.14261558$$

$$cp_{4,4} := -.8378914009$$

```
> cs:=array(1..4,1..4):
```

```
> cs[1,1]:=int(F1*diff(diff(F1,v),v)*((b-1)**2-v**2),v=b-1..b);
> cs[1,2]:=int(F1*diff(diff(F2,v),v)*((b-1)**2-v**2),v=b-1..b);
> cs[1,3]:=int(F1*diff(diff(F3,v),v)*((b-1)**2-v**2),v=b-1..b);
> cs[1,4]:=int(F1*diff(diff(F4,v),v)*((b-1)**2-v**2),v=b-1..b);
```

$$cs_{1,1} := -15.87987864$$

$$cs_{1,2} := 8.688185347$$

$$cs_{1,3} := -48.27866129$$

$$cs_{1,4} := -2.424406593$$

```
> cs[2,1]:=int(F2*diff(diff(F1,v),v)*((b-1)**2-v**2),v=b-1..b);
> cs[2,2]:=int(F2*diff(diff(F2,v),v)*((b-1)**2-v**2),v=b-1..b);
> cs[2,3]:=int(F2*diff(diff(F3,v),v)*((b-1)**2-v**2),v=b-1..b);
> cs[2,4]:=int(F2*diff(diff(F4,v),v)*((b-1)**2-v**2),v=b-1..b);
```

$$cs_{2,1} := 2.172046338$$

$$cs_{2,2} := -203.3531074$$

$$cs_{2,3} := -445.8599847$$

$$cs_{2,4} := -13.66560282$$

```
> cs[3,1]:=int(F3*diff(diff(F1,v),v)*((b-1)**2-v**2),v=b-1..b);
> cs[3,2]:=int(F3*diff(diff(F2,v),v)*((b-1)**2-v**2),v=b-1..b);
> cs[3,3]:=int(F3*diff(diff(F3,v),v)*((b-1)**2-v**2),v=b-1..b);
```

```
> cs[3,4]:=int(F3*diff(diff(F4,v),v)*((b-1)**2-v**2),v=b-1..b);
```

$$cs_{3,\ 1} := -5.364295710$$

$$cs_{3,\ 2} := -198.1599933$$

$$cs_{3,\ 3} := -62532.19241$$

$$cs_{3,\ 4} := 705.3039141$$

```
> cs[4,1]:=int(F4*diff(diff(F1,v),v)*((b-1)**2-v**2),v=b-1..b);
> cs[4,2]:=int(F4*diff(diff(F2,v),v)*((b-1)**2-v**2),v=b-1..b);
> cs[4,3]:=int(F4*diff(diff(F3,v),v)*((b-1)**2-v**2),v=b-1..b);
> cs[4,4]:=int(F4*diff(diff(F4,v),v)*((b-1)**2-v**2),v=b-1..b);
```

$$cs_{4,\ 1} := -.1515254114$$

$$cs_{4,\ 2} := -3.416400702$$

$$cs_{4,\ 3} := 396.7334516$$

$$cs_{4,\ 4} := -616.0203632$$

```
> ai:=array([a1,a2,a3,a4]);
```

$$ai := [a1 \quad a2 \quad a3 \quad a4]$$

```
> ais:=array([a1s,a2s,a3s,a4s]);
```

$$ais := [a1s \quad a2s \quad a3s \quad a4s]$$

```
> A:=evalm(inverse(c)&*(cs/2-cp));
```

$$A := \begin{bmatrix} -11.22192363 & 4.008305393 & -19.79859733 & -.9507276165 \\ 1.232009822 & -45.63769444 & -73.05911707 & -1.937822023 \\ -.04439234943 & -.5329601775 & -102.9973122 & .9119934944 \\ -.3842878678 & -2.548361800 & 164.4063546 & -183.3007775 \end{bmatrix}$$

RITZLEG0.MS
Detemination of the Constants Ki in trial solution not have Legendre
> b:=1/(1+32/(3.3E-4*20E3))/2;
> epsilon:=b/(1-b);

$$b := .08549222800$$

$$\varepsilon := .09348441929$$

> with(orthopoly):
Maple does not have Legendre functions of the second kind, but they can be given in terms of Pn(x) through the formula (cf. Abramowitz, 8.6.19):

> WW:=(n,x)->sum(P(i-1,x)*P(n+1-i,x)/i,i=1..n+1);

$$WW := (n, x) \rightarrow \sum_{i=1}^{n+1} \frac{P(i-1, x)\, P(n+1-i, x)}{i}$$

> Q:=(n,x)->P(n,x)*ln((x+1)/(1-x))/2-WW(n-1,x);

$$Q := (n, x) \rightarrow \frac{1}{2} P(n, x) \ln\left(\frac{x+1}{1-x}\right) - WW(n-1, x)$$

> lambda0:=n->n*(n+1)/2;

$$\lambda 0 := n \rightarrow \frac{1}{2} n\,(n+1)$$

> lambda1:=n->4*(1-lambda0(n))*(n+1/2)*GAMMA(1+n/2)**2/GAMMA((1+n)/2)**2/Pi/lambda0(n);

$$\lambda 1 := n \rightarrow 4 \frac{(1 - \lambda 0(n))\left(n + \frac{1}{2}\right)\Gamma\left(1 + \frac{1}{2} n\right)^2}{\Gamma\left(\frac{1}{2} n + \frac{1}{2}\right)^2 \pi\, \lambda 0(n)}$$

The solution of the Diff.Eq. in space is:
> F0:=(n,x)->P(n,x);
> F1:=(n,x)->P(n,x)*(K+2*lambda1(n)*int(P(n,u)*Q(n,u),u=0..x))+
> Q(n,x)*((lambda0(n)-1)*4*GAMMA(1+n/2)**2/lambda0(n)/Pi/GAMMA((1+n)/2)**2
> -2*lambda1(n)*int(P(n,u)**2,u=0..x));
> F:=F0+epsilon*F1;

$$F0 := P$$

$$F1 := (n, x) \rightarrow P(n, x)\left(K + 2\,\lambda 1(n) \int_0^x P(n, u)\, Q(n, u)\, du\right)$$

$$+ Q(n, x)\left(4 \frac{(\lambda 0(n) - 1)\,\Gamma\left(1 + \frac{1}{2} n\right)^2}{\lambda 0(n)\,\pi\,\Gamma\left(\frac{1}{2} n + \frac{1}{2}\right)^2} - 2\,\lambda 1(n) \int_0^x P(n, u)^2\, du\right)$$

$$F := P + .09348441929\, F1$$

Where the constant K is not determinedby the B.C.; probably we would have to go to the
e*e approximation to have it determined. We will try later to choose a value that minimizes
deviation from the approximate B.C.

> lambda:=n->lambda0(n)+epsilon*lambda1(n);

$$\lambda := n \rightarrow \lambda 0(n) + \varepsilon \, \lambda 1(n)$$

The Diff.Equation is:

> ED:=(n,x)->(1-x**2)*diff(diff(F(n,x),x),x)-2*x*diff(F(n,x),x)+2*lambda(n)*F(n,x);

$$ED :=$$

$$(n, x) \rightarrow \left(1 - x^2\right) \text{diff}(\text{diff}(F(n, x), x), x) - 2\,x\,\text{diff}(F(n, x), x) + 2\,\lambda(n)\,F(n, x)$$

We will see how close the asymptotic development solution meets the equation; since K
is not determined, we will give several values:

> plot({subs(K=0,ED(5,x)),subs(K=0.5,ED(5,x)),subs(K=1,ED(5,x))},x=-1..epsilon,title=`Residue for n=5`)
> ;

Residue for n=5
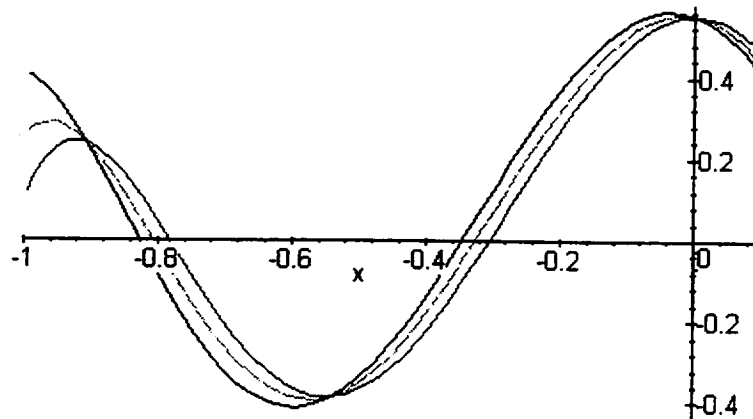
> plot({subs(K=0,ED(3,x)),subs(K=0.5,ED(3,x)),subs(K=1,ED(3,x))},x=-1..epsilon,title=`Residue for n=3`)
> ;

Residue for n=3
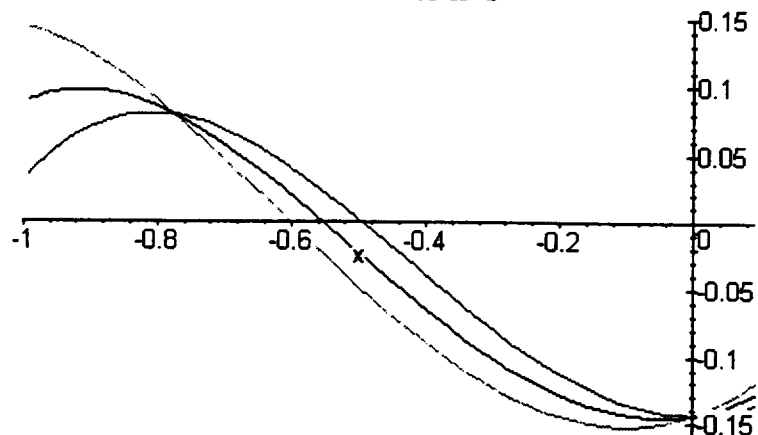
> plot({subs(K=0,ED(1,x)),subs(K=0.5,ED(1,x)),subs(K=1,ED(1,x))},x=-1..epsilon,title=`Residue for n=1`)
> ;

Residue for n=1
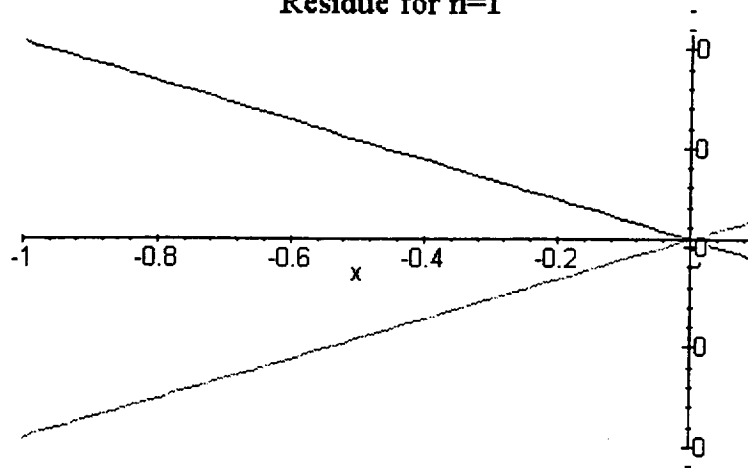
We will check that the solutions F0 and F1 are of the same order:

```
> plot({F0(5,x),subs(K=0,F1(5,x)),subs(K=0.5,F1(5,x)),subs(K=1,F1(5,x))},x=-1..epsilon,title=`Functions f
> or n=5 and different K`);
```

Functions for n=5 and different K
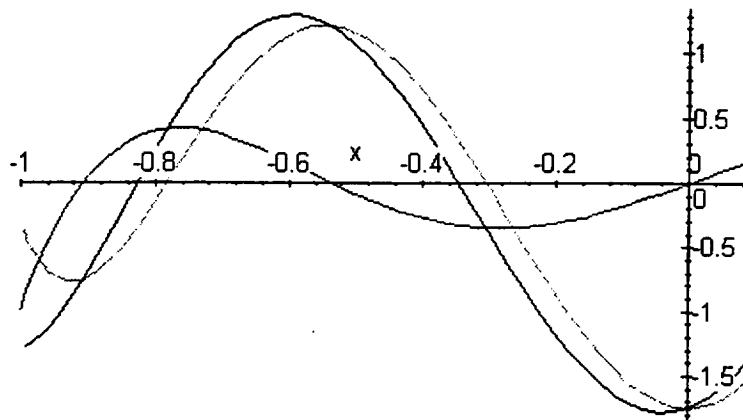
```
> plot({F0(3,x),subs(K=0,F1(3,x)),subs(K=0.5,F1(3,x)),subs(K=1,F1(3,x))},x=-1..epsilon,title=`Functions f
> or n=3 and different K`);
```

Functions for n=3 and different K
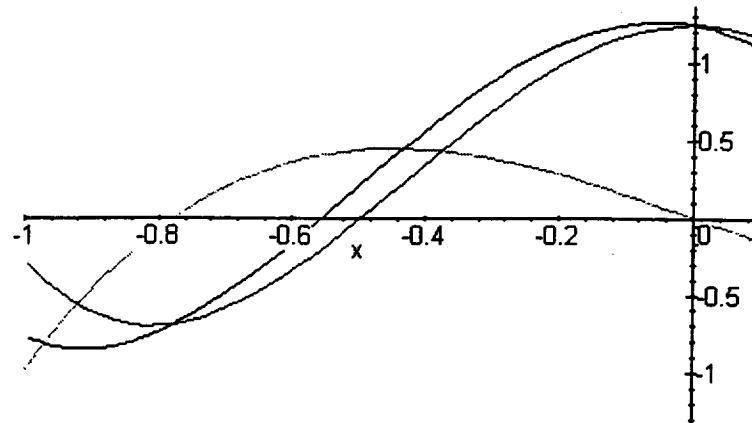

```
> plot({F0(1,x),subs(K=0,F1(1,x)),subs(K=0.5,F1(1,x)),subs(K=1,F1(1,x))},x=-1..epsilon,title=`Functions for n=
> 1 and different K`);
```

Functions for n=1 and different K
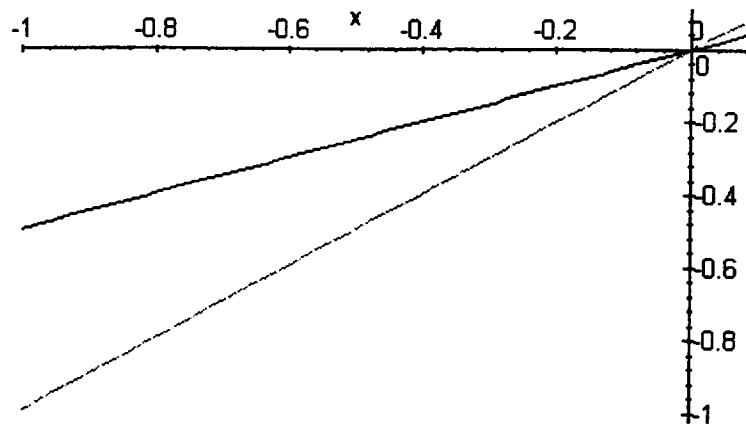
The three B.C. (second derivative zero at b/(1-b), first derivative=lambda*function/b, and Center of Mass integral) are the same when the Diff.Eq. is fulfilled; since this solution is approximate, the three B.C. will also be approximately met. We will try to choose the value of K so as to bring them closer.

```
> phi1:=eval(F(1,x));
```

$$\phi1 := x + .09348441929\, x\, K$$

```
> phi3:=eval(F(3,x)):
```

```
> phi5:=eval(F(5,x)):
```

```
> phi1s:=diff(diff(phi1,x),x);
```

$$phi1s := 0$$

```
> phi3s:=diff(diff(phi3,x),x):
> phi5s:=diff(diff(phi5,x),x):
> phi1p:=diff(phi1,x);
```

$$philp := 1 + .09348441929\ K$$

```
> phi3p:=diff(phi3,x):
```

```
> phi5p:=diff(phi5,x):
```

Residuals for the different B.C.:
```
> R1s:=subs(x=epsilon,phi1s);
> R3s:=evalf(subs(x=epsilon,phi3s));
> R5s:=evalf(subs(x=epsilon,phi5s));
```

$$R1s := 0$$

$$R3s := -.1325489892 + .1310900497\ K$$

$$R5s := .1697377198 - .4467859534\ K$$

```
> R1p:=evalf(subs(x=epsilon, phi1p*epsilon-(lambda(1))*phi1));
> R3p:=evalf(subs(x=epsilon, phi3p*epsilon-(lambda(3))*phi3));
> R5p:=evalf(subs(x=epsilon, phi5p*epsilon-(lambda(5))*phi5));
```

$$R1p := 0$$

$$R3p := .00209883271 + .05704708175\ K$$

$$R5p := -.1549035234 - .1949139959\ K$$

```
> R1i:=evalf((1-b)*int(F(1,x),x=-1..epsilon)+(1/2/b-1)*F(1,epsilon));
> R3i:=evalf((1-b)*int(F(3,x),x=-1..epsilon)+(1/2/b-1)*F(3,epsilon));
> R5i:=evalf((1-b)*int(F(5,x),x=-1..epsilon)+(1/2/b-1)*F(5,epsilon));
```

$$R1i := -.2\ 10^{-9} - .2\ 10^{-10}\ K$$

$$R3i := -.00433781797 - .1097409326\ 10^{-10}\ I - .05250279174\ K$$

$$R5i := .0589231983 + .2194818653\ 10^{-10}\ I + .07157678227\ K$$

The first eigenfunction is linear; the value of K does not affect the B.C. at all: make it zero.
```
> Kp[1]:=solve(R1p,K);
> Ks[1]:=solve(R1s,K);
> Ki[1]:=fsolve(Re(R1i),K);
```

$$Kp_1 := K$$

$$Ks_1 := K$$

$$Ki_1 := -10.00000000$$

```
> plot(subs(K=0,phi1),x=-1..epsilon, title='First Eigenfunction for K=0');
```

First Eigenfunction for K=0
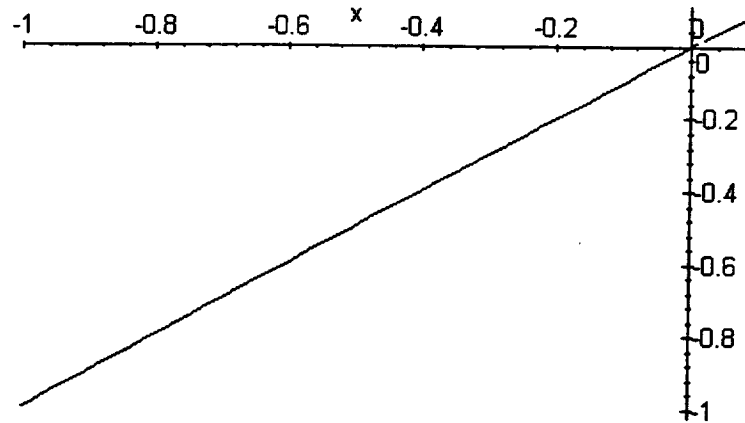

```
> Kp[3]:=solve(R3p,K);
> Ks[3]:=solve(R3s,K);
> Ki[3]:=fsolve(Re(R3i),K);
> plot({R3p,R3s,Re(R3i)},K=-10..10,title=`B.C. Residuals for different K`);
```

B.C. Residuals for different K
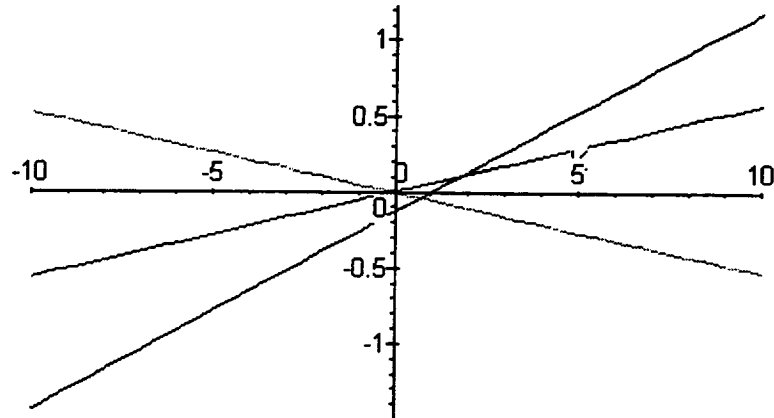
$$Kp_3 := -.03679123709$$

$$Ks_3 := 1.011129292$$

$$Ki_3 := -.08262071075$$

We will choose the one minimizing the residual of the two B.C. which apply to the general problem, the integral and second derivative ones:

```
> Kav[3]:=fsolve(R3s+Re(R3i),K);
```

$$Kav_3 := 1.741844807$$

```
> plot({subs(K=0,phi3),subs(K=Kav[3],phi3),subs(K=Kp[3],phi3),subs(K=Ks[3],phi3),subs(K=Ki[3],phi3)},
> x=-1..epsilon,title=`Second eigenfunction for different K`);
```

B 6

Second eigenfunction for different K
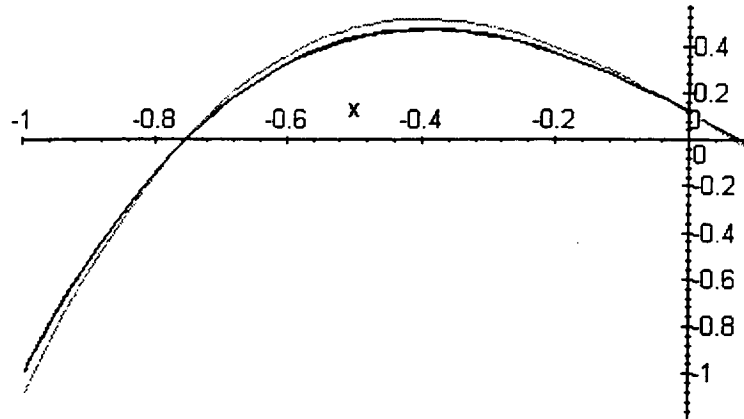

```
> Kp[5]:=solve(R5p,K);
> Ks[5]:=solve(R5s,K);
> Ki[5]:=fsolve(Re(R5i),K);
> plot({R5p,R5s,Re(R5i)},K=-10..10,title=`B.C. Residuals for different K`);
```

B.C. Residuals for different K
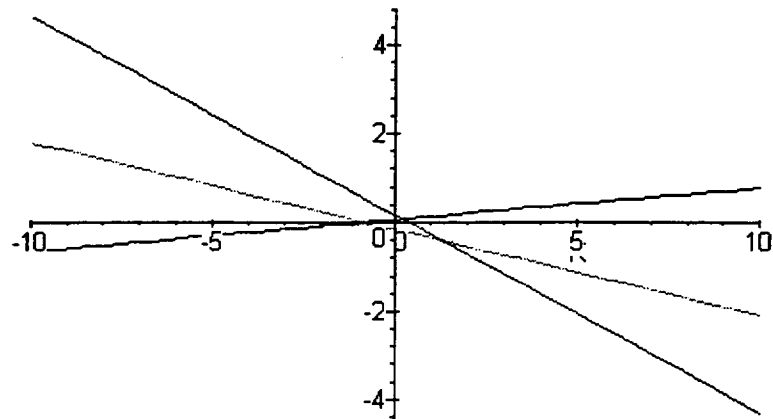
$$Kp_5 := -.7947275550$$

$$Ks_5 := .3799083622$$

$$Ki_5 := -.8232166414$$

```
> Kav[5]:=fsolve(R5s+Re(R5i),K);
```

$$Kav_5 := .6094225187$$

```
> plot({subs(K=0,phi5),subs(K=Kav[5],phi5),subs(K=Kp[5],phi5),subs(K=Ks[5],phi5),subs(K=Ki[5],phi5)},
> x=-1..epsilon,title=`Third Eigenfunction for different K`);
```

Third Eigenfunction for different K
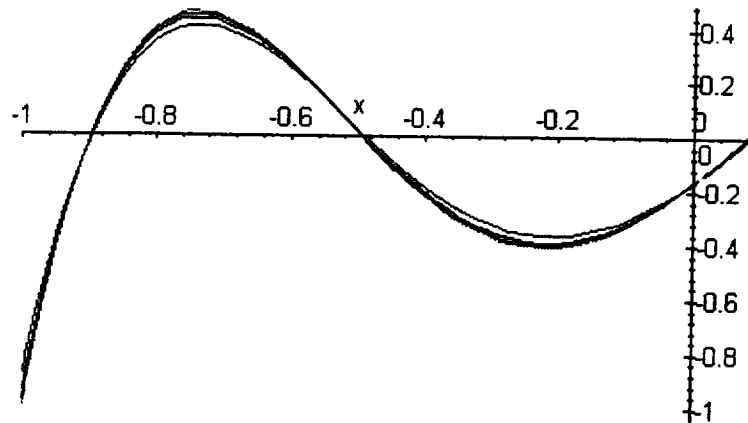
The value of K does not affect much the shape of the 3rd and 5th Eigenfunctions; the value of the B.C. residuals is small, except for the 5th function. So we will choose K=0 for the 1st Eigenfunction, and K=Kav for the 3rd and 5th, which minimizes the sum of the two ideally identical B.C. If we try to minimize the first derivative B.C., the function will be closer to the eigenfunctions, but the B.C. Ritz trial functions must fulfill would be less accurately met; so we choose K to minimize only Ri and Rs.

```
> plot({subs(K=0,phi1),subs(K=Kav[3],phi3),subs(K=Kav[5],phi5)},x=-1..epsilon,title=`Functions for K min
> imizing B.C. residuals`);
```

Functions for K minimizing B.C. residuals
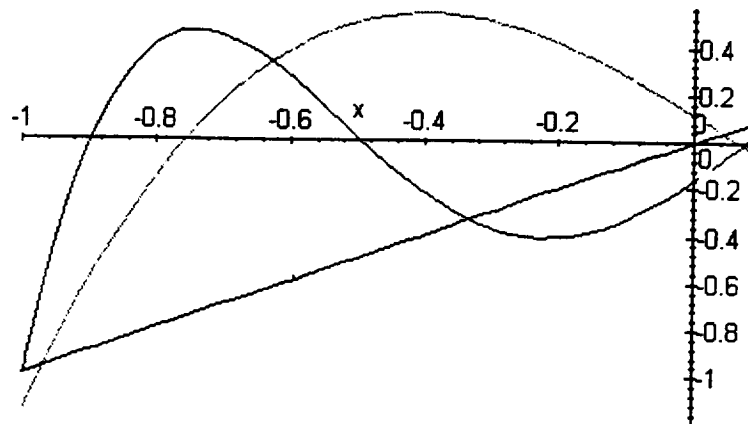
```
> phi1:=subs(K=0,phi1);
```

$$\phi 1 := x$$

```
> phi3:=subs(K=Kav[3], phi3);
```

$$\phi 3 := \frac{5}{2}x^3 - \frac{3}{2}x + .09348441929 \left(\frac{5}{2}x^3 - \frac{3}{2}x \right) \left(1.741844807 - \frac{15}{16} \ln\left(-\frac{1+x}{-1+x} \right) - \frac{505}{32}x^4 \right.$$

$$- \frac{315}{64} \ln\left(-\frac{1+x}{-1+x} \right) x^3 + \frac{375}{32}x^6 - \frac{375}{64} \ln\left(-\frac{1+x}{-1+x} \right) x^7 + \frac{15}{8} \ln\left(-2\frac{1}{-1+x} \right)$$

$$\left. + \frac{315}{32} \ln\left(-\frac{1+x}{-1+x} \right) x^5 + \frac{45}{8}x^2 - \frac{15}{8} \ln(2) \right) + .09348441929$$

B 8

$$\phi3 := \frac{5}{2}x^3 - \frac{3}{2}x + .09348441929\left(\frac{5}{2}x^3 - \frac{3}{2}x\right)\left(1.741844807 - \frac{15}{16}\ln\left(-\frac{1+x}{-1+x}\right) - \frac{505}{32}x^4\right.$$

$$- \frac{315}{64}\ln\left(-\frac{1+x}{-1+x}\right)x^3 + \frac{375}{32}x^6 - \frac{375}{64}\ln\left(-\frac{1+x}{-1+x}\right)x^7 + \frac{15}{8}\ln\left(-2\frac{1}{-1+x}\right)$$

$$\left.+ \frac{315}{32}\ln\left(-\frac{1+x}{-1+x}\right)x^5 + \frac{45}{8}x^2 - \frac{15}{8}\ln(2)\right)$$

$$+ .09348441929\left(\frac{1}{2}\left(\frac{5}{2}x^3 - \frac{3}{2}x\right)\ln\left(\frac{1+x}{1-x}\right) - \frac{5}{2}x^2 + \frac{2}{3}\right)\left(\frac{15}{8} + \frac{375}{32}x^7 + \frac{315}{32}x^3 - \frac{315}{16}x^5\right)$$

> phi5:=subs(K=Kav[5],phi5);

$$\phi5 := \frac{63}{8}x^5 - \frac{35}{4}x^3 + \frac{15}{8}x + .09348441929\left(\frac{63}{8}x^5 - \frac{35}{4}x^3 + \frac{15}{8}x\right)\left(.6094225187\right.$$

$$+ \frac{105}{32}\ln\left(-2\frac{1}{-1+x}\right) - \frac{992985}{2048}x^8 - \frac{86625}{4096}\ln\left(-\frac{1+x}{-1+x}\right)x^3 - \frac{278495}{2048}x^4$$

$$- \frac{416745}{4096}\ln\left(-\frac{1+x}{-1+x}\right)x^{11} - \frac{105}{64}\ln\left(-\frac{1+x}{-1+x}\right) + \frac{282975}{1024}\ln\left(-\frac{1+x}{-1+x}\right)x^9$$

$$+ \frac{121275}{1024}\ln\left(-\frac{1+x}{-1+x}\right)x^5 - \frac{560175}{2048}\ln\left(-\frac{1+x}{-1+x}\right)x^7 + \frac{525}{32}x^2 + \frac{416745}{2048}x^{10} + \frac{826399}{2048}x^6$$

$$\left.- \frac{105}{32}\ln(2)\right) + .09348441929\left(\frac{1}{2}\left(\frac{63}{8}x^5 - \frac{35}{4}x^3 + \frac{15}{8}x\right)\ln\left(\frac{1+x}{1-x}\right) - \frac{21}{4}x^4 + \frac{9}{2}x^2 - \frac{9}{20}\right.$$

$$\left.- \frac{3}{4}x\left(\frac{5}{2}x^3 - \frac{3}{2}x\right) - \frac{1}{3}\left(\frac{3}{2}x^2 - \frac{1}{2}\right)^2\right)$$

$$\left(\frac{105}{32} - \frac{121275}{512}x^5 + \frac{86625}{2048}x^3 + \frac{560175}{1024}x^7 - \frac{282975}{512}x^9 + \frac{416745}{2048}x^{11}\right)$$

RITZLEG1.MS: Ritz matrix coefficients

```
> assume(x,real)
> assume(x,real);
> b:=1/(1+32/(3.3E-4*20E3))/2:
> epsilon:=b/(1-b):
> with(orthopoly):
> WW:=(n,x)->sum(P(i-1,x)*P(n+1-i,x)/i,i=1..n+1):
> Q:=(n,x)->P(n,x)*ln((x+1)/(1-x))/2-WW(n-1,x):
> lambda0:=n->n*(n+1)/2:
> lambda1:=n->4*(1-lambda0(n))*(n+1/2)*GAMMA(1+n/2)**2/GAMMA((1+n)/2)**2/Pi/lambda0(n):
> F0:=(n,x)->P(n,x):
> F1:=(n,x)->P(n,x)*(K+2*lambda1(n)*int(P(n,u)*Q(n,u),u=0..x))+
> Q(n,x)*((lambda0(n)-1)*4*GAMMA(1+n/2)**2/lambda0(n)/Pi/GAMMA((1+n)/2)**2
> -2*lambda1(n)*int(P(n,u)**2,u=0..x)):
> F:=F0+epsilon*F1:
> lambda:=n->lambda0(n)+epsilon*lambda1(n):
> Phi1:=F(1,x):
> Phi3:=F(3,x):
> Phi5:=F(5,x):
> phi1:=subs(K=0,Phi1):
> phi3:=simplify((subs(K=1.741844807,Phi3))):
> phi5:=simplify(eval((subs(K=0.6094225187,F(5,x))))):
> phi1p:=simplify(diff(phi1,x)):
> phi3p:=simplify(diff(phi3,x)):
> phi5p:=simplify(diff(phi5,x)):
> phi1s:=simplify(diff(phi1p,x));
> phi3s:=simplify(diff(phi3p,x)):
> phi5s:=simplify(diff(phi5p,x)):
> with(linalg):
> A:=matrix(3,3);
> A[1,1]:=Re(int(phi1*phi1,x=-1..epsilon));
> A[1,2]:=Re(int(phi1*phi3,x=-1..epsilon));
> A[1,3]:=Re(int(phi1*phi5,x=-1..epsilon));
> A[2,1]:=Re(int(phi3*phi1,x=-1..epsilon));
> A[2,2]:=Re(int(phi3*phi3,x=-1..epsilon));
> A[2,3]:=Re(int(phi3*phi5,x=-1..epsilon));
> A[3,1]:=Re(int(phi5*phi1,x=-1..epsilon));
> A[3,2]:=Re(int(phi5*phi3,x=-1..epsilon));
> A[3,3]:=Re(int(phi5*phi5,x=-1..epsilon));
```

$$A := \text{array}(1 .. 3, 1 .. 3, [\ ])$$

$$A_{1,\,1} := .3336056639$$

$$A_{1,\,2} := .01171152560$$

$$A_{1,\,3} := -.005983207937$$

$$A_{2,\,1} := .01171152560$$

$$A_{2,\,2} := .2226242651$$

$$A_{2,3} := -.0006923039365$$

$$A_{3,1} := -.005983207937$$

$$A_{3,2} := -.0006923039365$$

$$A_{3,3} := .1260037526$$

```
> Ap:=matrix(3,3);
> Ap[1,1]:=evalf(int(Re(x*phi1*phi1p),x=-1..epsilon));
> Ap[1,2]:=evalf(int(Re(x*phi1*phi3p),x=-1..epsilon));
> Ap[1,3]:=evalf(int(Re(x*phi1*phi5p),x=-1..epsilon));
> Ap[2,1]:=evalf(int(Re(x*phi3*phi1p),x=-1..epsilon));
> Ap[2,2]:=evalf(int(Re(x*phi3*phi3p),x=-1..epsilon));
> Ap[2,3]:=evalf(int(Re(x*phi3*phi5p),x=-1..epsilon));
> Ap[3,1]:=evalf(int(Re(x*phi5*phi1p),x=-1..epsilon));
> Ap[3,2]:=evalf(int(Re(x*phi5*phi3p),x=-1..epsilon));
> Ap[3,3]:=evalf(int(Re(x*phi5*phi5p),x=-1..epsilon));
```

$$Ap := \text{array}(1 .. 3, 1 .. 3, [\ ])$$

$$Ap_{1,1} := .3336056639$$

$$Ap_{1,2} := 1.163546054$$

$$Ap_{1,3} := 1.096924487$$

$$Ap_{2,1} := .01171152560$$

$$Ap_{2,2} := .5937740239$$

$$Ap_{2,3} := 1.280153230$$

$$Ap_{3,1} := -.005983207929$$

$$Ap_{3,2} := .008282910645$$

$$Ap_{3,3} := .5252840045$$

```
> As:=matrix(3,3);
> As[1,1]:=evalf(int(Re((1-x*x)*phi1*phi1s),x=-1..epsilon));
> As[1,2]:=evalf(int(Re((1-x*x)*phi1*phi3s),x=-1..epsilon));
> As[1,3]:=evalf(int(Re((1-x*x)*phi1*phi5s),x=-1..epsilon));
> As[2,1]:=evalf(int(Re((1-x*x)*phi3*phi1s),x=-1..epsilon));
> As[2,2]:=evalf(int(Re((1-x*x)*phi3*phi3s),x=-1..epsilon));
> As[2,3]:=evalf(int(Re((1-x*x)*phi3*phi5s),x=-1..epsilon));
> As[3,1]:=evalf(int(Re((1-x*x)*phi5*phi1s),x=-1..epsilon));
> As[3,2]:=evalf(int(Re((1-x*x)*phi5*phi3s),x=-1..epsilon));
> As[3,3]:=evalf(int(Re((1-x*x)*phi5*phi5s),x=-1..epsilon));
```

$$As := \text{array}(\,1\,..\,3,\,1\,..\,3,\,[\;]\,)$$

$$As_{1,\,1} := 0$$

$$As_{1,\,2} := 2.186056968$$

$$As_{1,\,3} := 2.375025574$$

$$As_{2,\,1} := 0$$

$$As_{2,\,2} := -1.267162894$$

$$As_{2,\,3} := 2.540174068$$

$$As_{3,\,1} := 0$$

$$As_{3,\,2} := .04185944138$$

$$As_{3,\,3} := -2.380685865$$

> B:=evalm(inverse(A)&*(As/2-Ap));

$$B := \begin{vmatrix} -1.000000000 & -.01663231022 & .0304933737 \\ -.81\ 10^{-11} & -5.512034854 & -.08915850384 \\ -.6\ 10^{-10} & .06929390492 & -13.61472320 \end{vmatrix}$$

>

1STCUT.MS
SEMIAXIS AND EXCENTRICITY PERTURBATIONS: DEPENDENCE ON THETA AND DELTA
> with(plots):

DELTA CANNOT BE GREATER THAN THETA
> delta:=alpha*theta;

$$\delta := \alpha\,\theta$$

> u:=sqrt(3*(sin(theta)^2-sin(delta)^2));

$$u := \sqrt{3\,\sin(\theta)^2 - 3\,\sin(\alpha\,\theta)^2}$$

PERTURBATION OF SEMIAXIS
> da:=2*cos(delta)*(u+2);

$$da := 2\,\cos(\alpha\,\theta)\left|\sqrt{3\,\sin(\theta)^2 - 3\,\sin(\alpha\,\theta)^2} + 2\right|$$

> plot3d(da,alpha=-1..1,theta=-Pi/3..Pi/3);
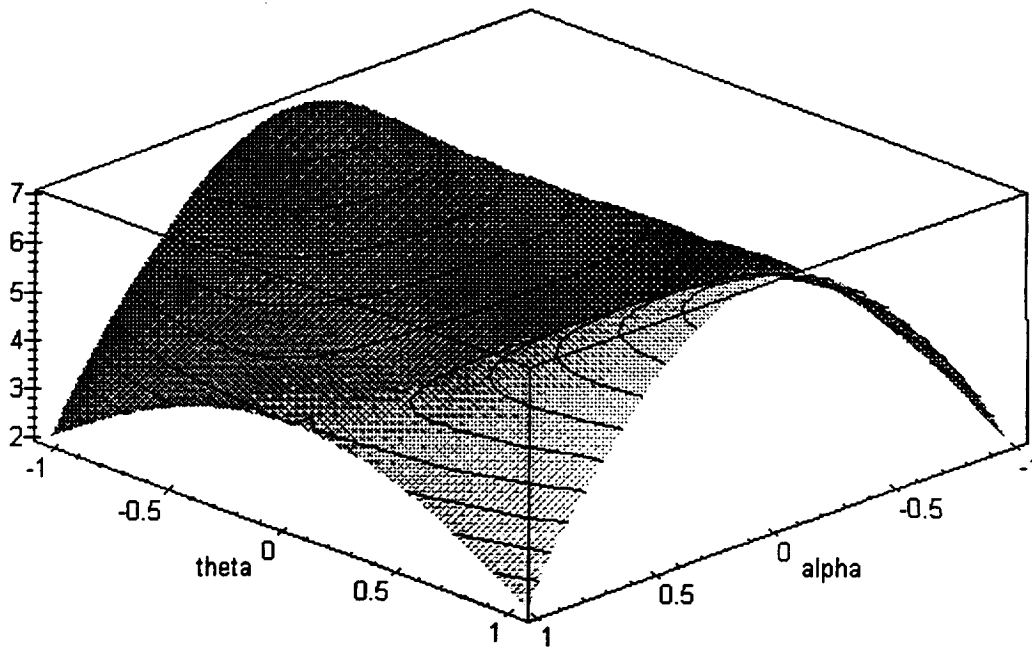
EXCENTRICITY:
> e:=sqrt(3*cos(delta)^2*(u+1)*(u+3)+u*u):
> plot3d(e,alpha=-1..1,theta=-Pi/3..Pi/3);
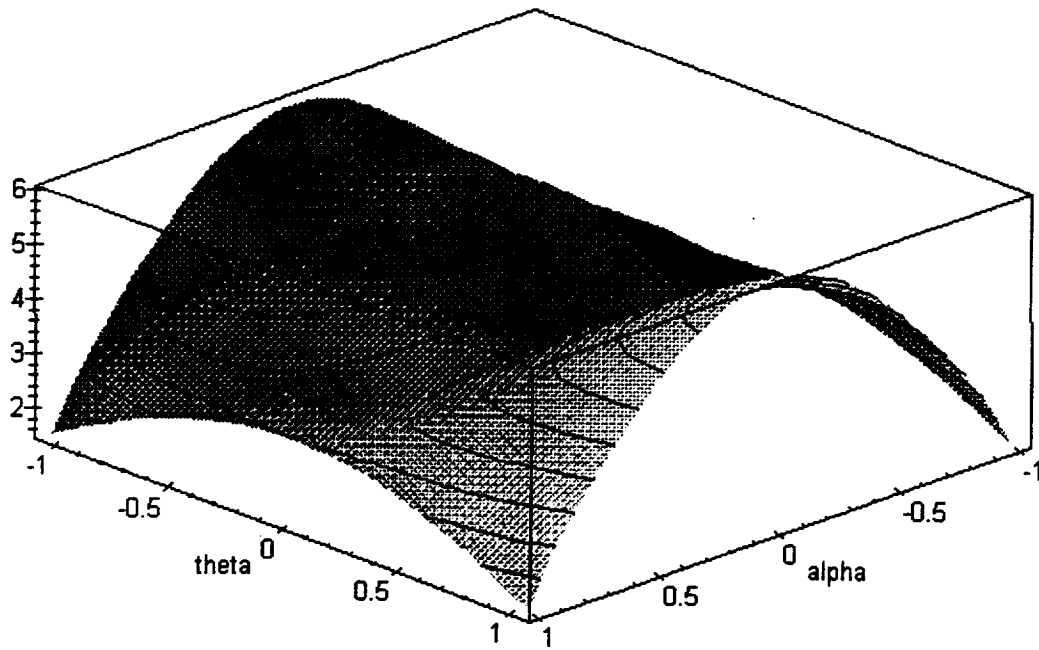
SO BIG THETA AND SMALL DELTA MAXIMIZE APOGEE HEIGHT, BUT ALSO
MAXIMIZES EXCENTRICITY. LET US SEE THE EFFECT ON PERIGEE HEIGHT:
```
> ph:=da-e:
> plot3d(ph,alpha=-1..1,theta=-Pi/3..Pi/3,view=0.95..1,contours=20);
```
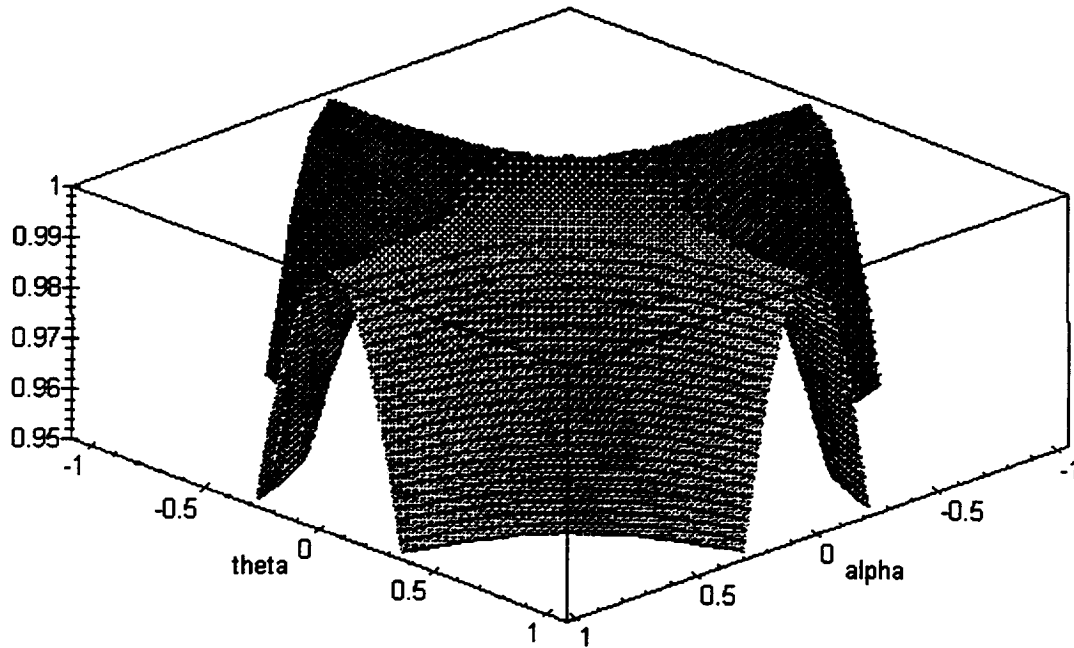
AS EXPECTED, THE MAXIMUM PERIGEE DEPENDS ON VERTICAL DISTANCE, AND IS NOT AFFECTED BY SPEED. IT IS HIGH AS LONG AS DELTA IS CLOSE TO ZERO. APOGEE HEIGHT, HOWEVER, DOES DEPEND ON SPEED:

```
> ah=da+e:
> plot3d(da+e,alpha=-1..1,theta=-Pi/3..Pi/3,contours=20);
```
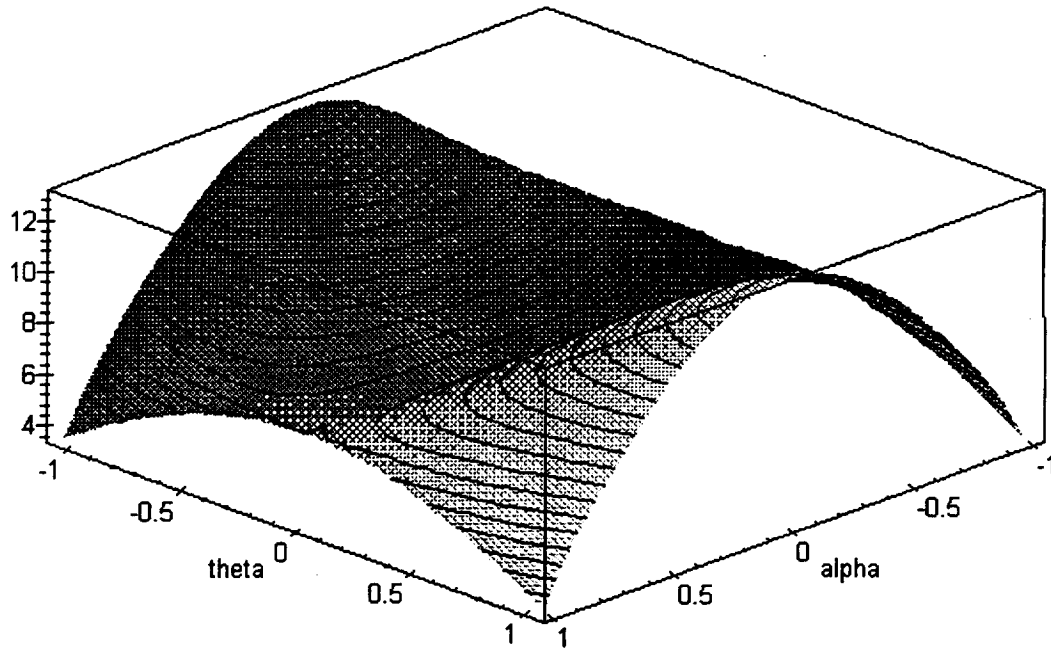

THE SWEET SPOT IS THUS MAX THETA AND ZERO DELTA

```
>
```

DECAY1.MS
DECAY MINIMIZATION
SHUTTLE IN CIRCULAR ORBIT
ELLIPTIC ORBIT OF THE CENTER OF MASS

> with(linalg):

> assume(r0,real, delta,real);

> additionally(r0>0);additionally(delta<Pi/2);additionally(delta>-Pi/2);

INITIAL POSITION OF CENTER OF MASS AT FIRST CUT:
(epsilon: C.O.M. length/circular orbit radius)

> r:=array([taylor(r0*(1+epsilon*cos(delta)),epsilon),0,taylor(r0*epsilon*sin(delta),epsilon)]);

$$r := [\, r0\!\sim +\, r0\!\sim \cos(\delta\!\sim)\,\varepsilon \quad 0 \quad r0\!\sim \sin(\delta\!\sim)\,\varepsilon\,]$$

INITIAL C.O.M. SPEED AT CUT TIME

> v:=array([taylor(-omega0*r0*epsilon*(1+u)*sin(delta),epsilon),0,
> taylor(omega0*r0*(1+epsilon*(1+u)*cos(delta)),epsilon)]);

$$v := [\, -\omega0\, r0\!\sim (1+u)\sin(\delta\!\sim)\,\varepsilon \quad 0 \quad \omega0\, r0\!\sim +\, \omega0\, r0\!\sim (1+u)\cos(\delta\!\sim)\,\varepsilon\,]$$

ANGULAR MOMENTUM PER UNIT MASS:

> h:=crossprod(r,v);

$$h := [\, 0 \quad (r0\!\sim \sin(\delta\!\sim)\,\varepsilon)\,(-\omega0\, r0\!\sim (1+u)\sin(\delta\!\sim)\,\varepsilon)$$
$$-\,(r0\!\sim +\, r0\!\sim \cos(\delta\!\sim)\,\varepsilon)\,(\omega0\, r0\!\sim +\, \omega0\, r0\!\sim (1+u)\cos(\delta\!\sim)\,\varepsilon) \quad 0\,]$$

> he:=simplify(taylor(h[2],epsilon));

$$he :=$$
$$-\omega0\, r0\!\sim^2 +\left|-2\, r0\!\sim^2 \cos(\delta\!\sim)\,\omega0 - r0\!\sim^2 \cos(\delta\!\sim)\,\omega0\, u\right|\varepsilon +\left|-\omega0\, r0\!\sim^2 - r0\!\sim^2 \omega0\, u\right|\varepsilon^2$$

> r2:=simplify(taylor(sqrt(dotprod(r,r,'orthogonal')),epsilon),trig);

$$r2 := r0\!\sim +\, r0\!\sim \cos(\delta\!\sim)\,\varepsilon +\left|\frac{1}{2}r0\!\sim -\frac{1}{2}r0\!\sim \cos(\delta\!\sim)^2\right|\varepsilon^2 +$$

$$\left|-\frac{1}{2}r0\!\sim \cos(\delta\!\sim) +\frac{1}{2}r0\!\sim \cos(\delta\!\sim)^3\right|\varepsilon^3 +\left|\frac{3}{4}r0\!\sim \cos(\delta\!\sim)^2 -\frac{5}{8}r0\!\sim \cos(\delta\!\sim)^4 -\frac{1}{8}r0\!\sim\right|\varepsilon^4 +$$

$$\left|-\frac{5}{4}r0\!\sim \cos(\delta\!\sim)^3 +\frac{7}{8}r0\!\sim \cos(\delta\!\sim)^5 +\frac{3}{8}r0\!\sim \cos(\delta\!\sim)\right|\varepsilon^5 + O\!\left|\varepsilon^6\right|$$

> omega0:=sqrt(mu/r0/r0/r0);

$$\omega0 := \frac{\sqrt{\dfrac{\mu}{r0\!\sim}}}{r0\!\sim}$$

EXCENTRICITY VECTOR

> e:=(evalm(-(r/r2)-(crossprod(h,v)/mu))):

> e1:=simplify(taylor(e[1],epsilon,4));

$$e1 := (3\cos(\delta\!\sim) + 2\cos(\delta\!\sim)\,u)\,\varepsilon +\left|\frac{3}{2}\cos(\delta\!\sim)^2 + 3\,u\cos(\delta\!\sim)^2 +\cos(\delta\!\sim)^2\,u^2 +\frac{3}{2}+u\right|\varepsilon^2$$

$$+\left|\cos(\delta\!\sim)^3 + 2\cos(\delta\!\sim)\,u +\cos(\delta\!\sim)\,u^2\right|\varepsilon^3 + O\!\left|\varepsilon^4\right|$$

> e2:=taylor(e[2],epsilon,3);

$$e2 := 0$$

> e3:=simplify(taylor(e[3],epsilon,4));

$$e3 := \sin(\delta\sim)\, u\, \varepsilon + \left| 3\cos(\delta\sim)\sin(\delta\sim) + 3\cos(\delta\sim)\sin(\delta\sim)\, u + \cos(\delta\sim)\sin(\delta\sim)\, u^2 \right| \varepsilon^2 + \left| \frac{3}{2}\sin(\delta\sim) - \frac{3}{2}\sin(\delta\sim)\cos(\delta\sim)^2 + 2\sin(\delta\sim)\, u + u^2\sin(\delta\sim) \right| \varepsilon^3 + O\!\left| \varepsilon^4 \right|$$

EXCENTRICITY

> ee:=simplify(taylor(sqrt(dotprod(e,e,'orthogonal')),epsilon,5));

$$ee := \sqrt{\%1}\,\varepsilon + \frac{1}{2}\cos(\delta\sim) \Big|$$

$$9\cos(\delta\sim)^2 + 18\, u\cos(\delta\sim)^2 + 9 + 18\, u + 12\cos(\delta\sim)^2 u^2 + 2\, u^3\cos(\delta\sim)^2 + 10\, u^2 + 2\, u^3$$

$$\left| \Big/ \sqrt{\%1}\,\varepsilon^2 - \frac{1}{8}\sqrt{\%1}\, \right| {-}528\cos(\delta\sim)^4 u^4 - 8\, u^5 - 20\, u^4 - 4\cos(\delta\sim)^4 u^6 - 24\, u^5\cos(\delta\sim)^2$$

$$- 80\, u^5\cos(\delta\sim)^4 - 120\cos(\delta\sim)^2 u^4 - 324\cos(\delta\sim)^4 + 108\cos(\delta\sim)^6 + 4\cos(\delta\sim)^6 u^6$$

$$- 2067\, u^2\cos(\delta\sim)^4 + 636\cos(\delta\sim)^6 u^3 + 48\cos(\delta\sim)^6 u^5 - 1552\, u^3\cos(\delta\sim)^4$$

$$+ 252\cos(\delta\sim)^6 u^4 + 753\cos(\delta\sim)^6 u^2 + 432\cos(\delta\sim)^6 u - 1296\, u\cos(\delta\sim)^4$$

$$- 45\cos(\delta\sim)^2 u^2 - 24\, u^3 - 9\, u^2 - 132\, u^3\cos(\delta\sim)^2 \left| \Big/ \right| 81\cos(\delta\sim)^4 + 216\, u\cos(\delta\sim)^4$$

$$+ 198\, u^2\cos(\delta\sim)^4 + 18\cos(\delta\sim)^2 u^2 + 72\, u^3\cos(\delta\sim)^4 + 24\, u^3\cos(\delta\sim)^2$$

$$+ 9\cos(\delta\sim)^4 u^4 + 6\cos(\delta\sim)^2 u^4 + u^4 \left| \varepsilon^3 + O\!\left| \varepsilon^4 \right|\right.$$

$$\%1 := 9\cos(\delta\sim)^2 + 12\, u\cos(\delta\sim)^2 + 3\cos(\delta\sim)^2 u^2 + u^2$$

> ee1:=simplify(coeff(ee,epsilon,1),trig);

$$ee1 := \sqrt{9\cos(\delta\sim)^2 + 12\, u\cos(\delta\sim)^2 + 3\cos(\delta\sim)^2 u^2 + u^2}$$

> ee2:=simplify(eval(coeff(ee,epsilon,2)));

$$ee2 := \frac{1}{2}\cos(\delta\sim) \Big|$$

$$9\cos(\delta\sim)^2 + 18\, u\cos(\delta\sim)^2 + 9 + 18\, u + 12\cos(\delta\sim)^2 u^2 + 2\, u^3\cos(\delta\sim)^2 + 10\, u^2 + 2\, u^3$$

$$\left| \Big/ \sqrt{9\cos(\delta\sim)^2 + 12\, u\cos(\delta\sim)^2 + 3\cos(\delta\sim)^2 u^2 + u^2} \right.$$

ENERGY CONSTANT

> EN:=simplify(taylor(dotprod(v,v,'orthogonal')/2-mu/r2,epsilon,4));

$$EN := -\frac{1}{2}\frac{\mu}{r0\sim} + \frac{\mu\cos(\delta\sim)(2+u)}{r0\sim}\varepsilon + \frac{1}{2}\frac{\mu\left|{-}3\cos(\delta\sim)^2 + 2 + 2\, u + u^2\right|}{r0\sim}\varepsilon^2 + \frac{1}{2}\frac{\mu\cos(\delta\sim)\left|{-}3 + 5\cos(\delta\sim)^2\right|}{r0\sim}\varepsilon^3 + O\!\left|\varepsilon^4\right|$$

SEMIMAJOR AXIS

> a:=simplify(taylor(-mu/EN/2,epsilon,4));

$$a := r0\sim + (4\ r0\sim \cos(\delta\sim) + 2\ r0\sim \cos(\delta\sim)\ u)\ \varepsilon +$$

$$\left| 13\ r0\sim \cos(\delta\sim)^2 + 2\ r0\sim + 2\ r0\sim\ u + r0\sim\ u^2 + 16\ r0\sim \cos(\delta\sim)^2\ u + 4\ r0\sim \cos(\delta\sim)^2\ u^2 \right|$$

$$\varepsilon^2 + \left| 13\ r0\sim \cos(\delta\sim) + 45\ r0\sim \cos(\delta\sim)^3 + 24\ r0\sim \cos(\delta\sim)\ u + 16\ r0\sim \cos(\delta\sim)\ u^2 \right.$$

$$\left. + 84\ r0\sim \cos(\delta\sim)^3\ u + 4\ r0\sim \cos(\delta\sim)\ u^3 + 48\ r0\sim \cos(\delta\sim)^3\ u^2 + 8\ r0\sim \cos(\delta\sim)^3\ u^3 \right| \varepsilon^3$$

$$+ O\left| \varepsilon^4 \right|$$

> simplify(coeff(a,epsilon,2)/r0);

$$13\ \cos(\delta\sim)^2 + 2 + 2\ u + u^2 + 16\ u\ \cos(\delta\sim)^2 + 4\ \cos(\delta\sim)^2\ u^2$$

MEAN ANGULAR RATE (TIMES CIRCULAR RATE)

> n:=simplify(taylor(sqrt(r0*r0*r0/a/a/a),epsilon,4));

$$n := 1 + (-6\ \cos(\delta\sim) - 3\ \cos(\delta\sim)\ u)\ \varepsilon +$$

$$\left| \frac{21}{2} \cos(\delta\sim)^2 - 3 - 3\ u - \frac{3}{2} u^2 + 6\ u\ \cos(\delta\sim)^2 + \frac{3}{2} \cos(\delta\sim)^2\ u^2 \right| \varepsilon^2 + \left| 6\ \cos(\delta\sim)\ u^2 \right.$$

$$+ 3\ \cos(\delta\sim)^3\ u^2 + \frac{3}{2} \cos(\delta\sim)^3\ u + 9\ \cos(\delta\sim)\ u - \frac{25}{2} \cos(\delta\sim)^3 + \frac{3}{2} \cos(\delta\sim)\ u^3$$

$$\left. + \frac{1}{2} u^3\ \cos(\delta\sim)^3 + \frac{21}{2} \cos(\delta\sim) \right| \varepsilon^3 + O\left| \varepsilon^4 \right|$$

ORBITAL PERIOD (TIMES 2Pi/CIRCULAR RATE)

> t:=simplify(taylor((a/r0)**(3/2),epsilon,3));

$$t := 1 + (6\ \cos(\delta\sim) + 3\ \cos(\delta\sim)\ u)\ \varepsilon +$$

$$\left| \frac{51}{2} \cos(\delta\sim)^2 + 3 + 3\ u + \frac{3}{2} u^2 + 30\ u\ \cos(\delta\sim)^2 + \frac{15}{2} \cos(\delta\sim)^2\ u^2 \right| \varepsilon^2 + O\left| \varepsilon^3 \right|$$

INCREASE IN PERIGEE HEIGHT OVER CIRCULAR ORBIT

> dhp:=simplify(taylor(a*(1-ee)-r0,epsilon,3));

$$dhp := \left| -r0\sim \sqrt{\%1} + 4\ r0\sim \cos(\delta\sim) + 2\ r0\sim \cos(\delta\sim)\ u \right| \varepsilon - \frac{1}{2} r0\sim \left| 81\ \cos(\delta\sim)^3 \right.$$

$$+ 150\ \cos(\delta\sim)^3\ u + 9\ \cos(\delta\sim) + 18\ \cos(\delta\sim)\ u + 84\ \cos(\delta\sim)^3\ u^2 + 14\ u^3\ \cos(\delta\sim)^3$$

$$+ 18\ \cos(\delta\sim)\ u^2 + 6\ \cos(\delta\sim)\ u^3 - 26\ \cos(\delta\sim)^2 \sqrt{\%1} - 4\ \sqrt{\%1} - 4\ u\ \sqrt{\%1} - 2\ u^2\ \sqrt{\%1}$$

$$\left. - 32\ \cos(\delta\sim)^2\ u\ \sqrt{\%1} - 8\ \cos(\delta\sim)^2\ u^2\ \sqrt{\%1} \right| / \sqrt{\%1}\ \varepsilon^2 + O\left| \varepsilon^3 \right|$$

$$\%1 := 9\ \cos(\delta\sim)^2 + 12\ u\ \cos(\delta\sim)^2 + 3\ \cos(\delta\sim)^2\ u^2 + u^2$$

INCREASE IN APOGEE HEIGHT

> dha:=simplify(taylor(a*(1+ee)-r0,epsilon,3));

$$dha := \left| r0\sim \sqrt{\%1} + 4\ r0\sim \cos(\delta\sim) + 2\ r0\sim \cos(\delta\sim)\ u \right| \varepsilon + \frac{1}{2} r0\sim \left| 81\ \cos(\delta\sim)^3 \right.$$

$$+ 150\ \cos(\delta\sim)^3\ u + 9\ \cos(\delta\sim) + 18\ \cos(\delta\sim)\ u + 84\ \cos(\delta\sim)^3\ u^2 + 14\ u^3\ \cos(\delta\sim)^3$$

$$+ 18 \cos(\delta\!\sim) \, u^2 + 6 \cos(\delta\!\sim) \, u^3 + 26 \cos(\delta\!\sim)^2 \sqrt{\%1} + 4 \sqrt{\%1} + 4 \, u \sqrt{\%1} + 2 \, u^2 \sqrt{\%1}$$

$$+ 32 \cos(\delta\!\sim)^2 \, u \sqrt{\%1} + 8 \cos(\delta\!\sim)^2 \, u^2 \sqrt{\%1} \Big| / \sqrt{\%1} \ \varepsilon^2 + O\big|\varepsilon^3\big|$$

$$\%1 := 9 \cos(\delta\!\sim)^2 + 12 \, u \cos(\delta\!\sim)^2 + 3 \cos(\delta\!\sim)^2 \, u^2 + u^2$$

```
> dhpt:=convert(simplify(subs({u=sqrt(3*sin(theta*Pi/18)**2-3*sin(delta)**2),r0=6378.16},dhp)),polynom
> ):
```

```
> dhpts:=subs(epsilon=0.9145*20/6378.16,dhpt) $ theta=3..6:
```

DELTA INFLUENCE IN PERIGEE HEIGHT FOR THETAM=30-60 DEG (KM)

```
> plot({dhpts},delta=-Pi/6..Pi/6);
```
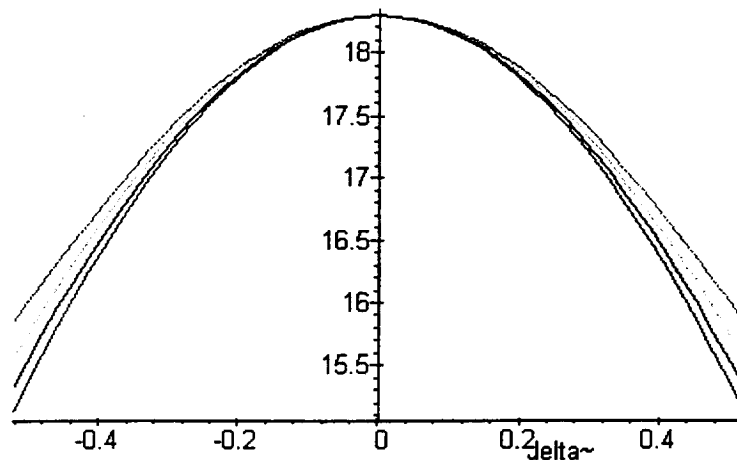


```
> dhat:=convert(simplify(subs({u=sqrt(3*sin(theta*Pi/18)**2-3*sin(delta)**2),r0=6378.16},dha)),polynom
> ):
```

```
> dhats:=subs(epsilon=0.9145*20/6378.16,dhat) $ theta=3..6:
```

DELTA INFLUENCE IN APOGEE HEIGHT FOR THETAM=30-60 DEG (KM)

```
> plot({dhats},delta=-Pi/6..Pi/6);
```
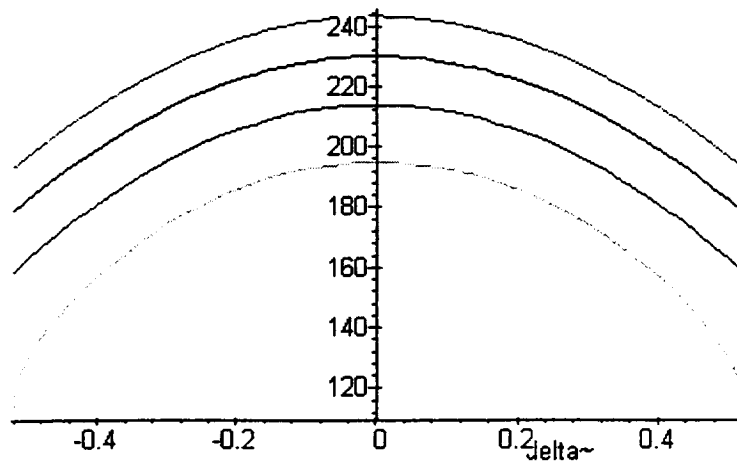
INITIAL TRUE ANOMALY

```
> sinnu0:=simplify(taylor(dotprod([0,1,0],crossprod(r,e),'orthogonal')/r2/ee,epsilon,5));
```

$$sinnu0 := -\frac{\sin(\delta\sim)\,u}{\sqrt{\%1}} - \frac{1}{2}\sin(\delta\sim)\,u\cos(\delta\sim)$$

$$\left|9\cos(\delta\sim)^2 + 24\,u\cos(\delta\sim)^2 + 18\cos(\delta\sim)^2 u^2 - 8\,u^2 + 4\,u^3\cos(\delta\sim)^2 - 9 - 18\,u\right|\Big/$$

$$\%1^{3/2}\,\varepsilon + \frac{1}{8}\sin(\delta\sim)\,u\Big|378\cos(\delta\sim)^6 - 792\,u^3\cos(\delta\sim)^2 + 1836\cos(\delta\sim)^6 u$$

$$+\, 3171\cos(\delta\sim)^6 u^2 - 999\cos(\delta\sim)^2 u^2 + 24\,u^3 + 16\,u^4 + 9\,u^2 + 176\,u^5\cos(\delta\sim)^4$$

$$-\, 324\cos(\delta\sim)^2 u^4 + 12\cos(\delta\sim)^6 u^6 - 21\,u^2\cos(\delta\sim)^4 + 468\cos(\delta\sim)^4 u^4$$

$$+\, 20\cos(\delta\sim)^4 u^6 - 48\,u^5\cos(\delta\sim)^2 + 1032\cos(\delta\sim)^6 u^4 - 108\,u\cos(\delta\sim)^4$$

$$-\, 162\cos(\delta\sim)^2 - 648\,u\cos(\delta\sim)^2 + 2568\cos(\delta\sim)^6 u^3 + 192\cos(\delta\sim)^6 u^5$$

$$+\, 400\,u^3\cos(\delta\sim)^4\Big|\Big/\%1^{5/2}\,\varepsilon^2 + O\!\left|\varepsilon^3\right|$$

$$\%1 := 9\cos(\delta\sim)^2 + 12\,u\cos(\delta\sim)^2 + 3\cos(\delta\sim)^2 u^2 + u^2$$

```
> nu0:=simplify(simplify(taylor(arcsin(sinnu0),epsilon,5),sqrt,assume=positive));
```

$$v0 := -\arcsin\!\left|\frac{\sin(\delta\sim)\,u}{\sqrt{\%1}}\right| - \frac{1}{2}\sin(\delta\sim)\,u$$

$$\left|9\cos(\delta\sim)^2 + 24\,u\cos(\delta\sim)^2 + 18\cos(\delta\sim)^2 u^2 - 8\,u^2 + 4\,u^3\cos(\delta\sim)^2 - 9 - 18\,u\right|$$

$$\mathrm{signum}(\cos(\delta\sim))\Big/\left|\%1^{3/2}\sqrt{\frac{(3+2\,u)^2}{\%1}}\right|\varepsilon + \frac{1}{4}\Big|8\cos(\delta\sim)^4 u^6 + 8\,u^6\cos(\delta\sim)^2$$

$$+\, 68\,u^5\cos(\delta\sim)^2 - 16\,u^5 + 108\,u^5\cos(\delta\sim)^4 - 124\,u^4 + 180\cos(\delta\sim)^2 u^4$$

$$+\, 540\cos(\delta\sim)^4 u^4 - 354\,u^3 + 152\,u^3\cos(\delta\sim)^2 + 1302\,u^3\cos(\delta\sim)^4 - 486\,u^2$$

$$-\, 24\cos(\delta\sim)^2 u^2 + 1590\,u^2\cos(\delta\sim)^4 + 918\,u\cos(\delta\sim)^4 - 324\,u - 54\,u\cos(\delta\sim)^2 - 81$$

$$+\, 189\cos(\delta\sim)^4\Big|\sin(\delta\sim)\,u\,\mathrm{signum}(\cos(\delta\sim))\cos(\delta\sim)\Big/\left|\%1^{5/2}\sqrt{\frac{(3+2\,u)^2}{\%1}}\right|\varepsilon^2 + O\!\left|\varepsilon^3\right|$$

$$\%1 := 9\cos(\delta\sim)^2 + 12\,u\cos(\delta\sim)^2 + 3\cos(\delta\sim)^2 u^2 + u^2$$

```
> simplify(coeff(nu0,epsilon,0));
```

$$-\arcsin\!\left|\frac{\sin(\delta\sim)\,u}{\sqrt{9\cos(\delta\sim)^2 + 12\,u\cos(\delta\sim)^2 + 3\cos(\delta\sim)^2 u^2 + u^2}}\right|$$

```
> simplify(simplify(coeff(nu0,epsilon,1),sqrt,assume=positive),pow);
```

$$-\frac{1}{2}\,\text{signum}(\cos(\delta\!\sim))\left|2\cos(\delta\!\sim)^2\,u^2 - 4\,u + 6\,u\cos(\delta\!\sim)^2 - 3 + 3\cos(\delta\!\sim)^2\right|u\sin(\delta\!\sim)\Big/$$

$$\sqrt{\dfrac{1}{9\cos(\delta\!\sim)^2 + 12\,u\cos(\delta\!\sim)^2 + 3\cos(\delta\!\sim)^2\,u^2 + u^2}}$$

$$\left|9\cos(\delta\!\sim)^2 + 12\,u\cos(\delta\!\sim)^2 + 3\cos(\delta\!\sim)^2\,u^2 + u^2\right|^{3/2}$$

```
> factor(4*u^3+18*u^2+24*u+9);
```

$$(3 + 2\,u)\left|2\,u^2 + 6\,u + 3\right|$$

```
> factor(8*u^2+18*u+9);
```

$$(3 + 2\,u)(4\,u + 3)$$

INITIAL ANGULAR SPEED OF ELLIPTIC ORBITAL FRAME
NOTE MAPLEV'S GLORIOUS STUPIDITY IN EASY SIMPLIFICATIONS,
WHILE HANDLING DIFFICULT ONES WELL.

```
> nup:=subs(signum(cos(delta))=1,simplify(taylor(n*(1+ee*cos(nu0))^2/(1-ee*ee)^(3/2),epsilon,3)));
```

$$nup := 1 + \left|2\,\sqrt{\%1}\,\cos(\delta\!\sim)\sqrt{\dfrac{(3+2\,u)^2}{\%1}} - 6\cos(\delta\!\sim) - 3\cos(\delta\!\sim)\,u\right|\varepsilon - \Big|{-270}\,u\cos(\delta\!\sim)^2$$

$$-\,216\cos(\delta\!\sim)^2\,u^2 - 9\,u^2 + 82\cos(\delta\!\sim)^2\,u^4 - 81\cos(\delta\!\sim)^2 + 20\,u^5\cos(\delta\!\sim)^2$$

$$+\,60\,u^5\cos(\delta\!\sim)^4 - 18\,u^3 + 30\,u^3\cos(\delta\!\sim)^2 + 558\cos(\delta\!\sim)^4\,u^4 - 8\,u^4$$

$$+\,1992\,u^3\cos(\delta\!\sim)^4 + 3411\,u^2\cos(\delta\!\sim)^4 + 2808\,u\cos(\delta\!\sim)^4 + 891\cos(\delta\!\sim)^4$$

$$+\,3\,u^3\sqrt{\%1}\sqrt{\dfrac{(3+2\,u)^2}{\%1}} + 3\,\sqrt{\%1}\sqrt{\dfrac{(3+2\,u)^2}{\%1}}\,u^2 - 297\cos(\delta\!\sim)^4\sqrt{\%1}\sqrt{\dfrac{(3+2\,u)^2}{\%1}}$$

$$+\,27\cos(\delta\!\sim)^2\sqrt{\%1}\sqrt{\dfrac{(3+2\,u)^2}{\%1}} - 30\,u^4\sqrt{\%1}\sqrt{\dfrac{(3+2\,u)^2}{\%1}}\cos(\delta\!\sim)^4$$

$$-\,10\,u^4\sqrt{\%1}\sqrt{\dfrac{(3+2\,u)^2}{\%1}}\cos(\delta\!\sim)^2 - 720\,u\sqrt{\%1}\sqrt{\dfrac{(3+2\,u)^2}{\%1}}\cos(\delta\!\sim)^4$$

$$+\,63\,u\sqrt{\%1}\sqrt{\dfrac{(3+2\,u)^2}{\%1}}\cos(\delta\!\sim)^2 + 12\,u^2\sqrt{\%1}\sqrt{\dfrac{(3+2\,u)^2}{\%1}}\cos(\delta\!\sim)^2$$

$$-\,27\,u^3\sqrt{\%1}\sqrt{\dfrac{(3+2\,u)^2}{\%1}}\cos(\delta\!\sim)^2 - 621\,u^2\sqrt{\%1}\sqrt{\dfrac{(3+2\,u)^2}{\%1}}\cos(\delta\!\sim)^4$$

$$-\,228\,u^3\sqrt{\%1}\sqrt{\dfrac{(3+2\,u)^2}{\%1}}\cos(\delta\!\sim)^4\Bigg/\left|\%1^{3/2}\sqrt{\dfrac{(3+2\,u)^2}{\%1}}\right|\varepsilon^2 + O\!\left|\varepsilon^3\right|$$

$$\%1 := 9\cos(\delta\sim)^2 + 12\,u\cos(\delta\sim)^2 + 3\cos(\delta\sim)^2\,u^2 + u^2$$

WITH A LITTLE COAXING, IT WILL DO IT:

```
> nup1:=simplify(subs(9*cos(delta)^2+12*cos(delta)^2*u+3*cos(delta)^2*u^2+u^2=c,coeff(nup,epsilon,
> 1)),sqrt,assume=positive);
```

$$nup1 := \cos(\delta\sim)\,u$$

```
> nup2:=coeff(nup,epsilon,2);
```

$$
nup2 := -\Bigg[-270\,u\cos(\delta\sim)^2 - 216\cos(\delta\sim)^2\,u^2 - 9\,u^2 + 82\cos(\delta\sim)^2\,u^4 - 81\cos(\delta\sim)^2
$$
$$
+ 20\,u^5\cos(\delta\sim)^2 + 60\,u^5\cos(\delta\sim)^4 - 18\,u^3 + 30\,u^3\cos(\delta\sim)^2 + 558\cos(\delta\sim)^4\,u^4 - 8\,u^4
$$
$$
+ 1992\,u^3\cos(\delta\sim)^4 + 3411\,u^2\cos(\delta\sim)^4 + 2808\,u\cos(\delta\sim)^4 + 891\cos(\delta\sim)^4
$$
$$
+ 3\,u^3\sqrt{\%1}\sqrt{\frac{(3+2\,u)^2}{\%1}} + 3\sqrt{\%1}\sqrt{\frac{(3+2\,u)^2}{\%1}}\,u^2 - 297\cos(\delta\sim)^4\sqrt{\%1}\sqrt{\frac{(3+2\,u)^2}{\%1}}
$$
$$
+ 27\cos(\delta\sim)^2\sqrt{\%1}\sqrt{\frac{(3+2\,u)^2}{\%1}} - 30\,u^4\sqrt{\%1}\sqrt{\frac{(3+2\,u)^2}{\%1}}\cos(\delta\sim)^4
$$
$$
- 10\,u^4\sqrt{\%1}\sqrt{\frac{(3+2\,u)^2}{\%1}}\cos(\delta\sim)^2 - 720\,u\sqrt{\%1}\sqrt{\frac{(3+2\,u)^2}{\%1}}\cos(\delta\sim)^4
$$
$$
+ 63\,u\sqrt{\%1}\sqrt{\frac{(3+2\,u)^2}{\%1}}\cos(\delta\sim)^2 + 12\,u^2\sqrt{\%1}\sqrt{\frac{(3+2\,u)^2}{\%1}}\cos(\delta\sim)^2
$$
$$
- 27\,u^3\sqrt{\%1}\sqrt{\frac{(3+2\,u)^2}{\%1}}\cos(\delta\sim)^2 - 621\,u^2\sqrt{\%1}\sqrt{\frac{(3+2\,u)^2}{\%1}}\cos(\delta\sim)^4
$$
$$
- 228\,u^3\sqrt{\%1}\sqrt{\frac{(3+2\,u)^2}{\%1}}\cos(\delta\sim)^4 \Bigg] \Bigg/ \Bigg[\%1^{3/2}\sqrt{\frac{(3+2\,u)^2}{\%1}} \Bigg]
$$

$$\%1 := 9\cos(\delta\sim)^2 + 12\,u\cos(\delta\sim)^2 + 3\cos(\delta\sim)^2\,u^2 + u^2$$

```
> nup2s:=subs({(9*cos(delta)^2+12*cos(delta)^2*u+3*cos(delta)^2*u^2+u^2)=c,sqrt((3+2*u)^2/(9*cos(d
> elta)^2+12*cos(delta)^2*u+3*cos(delta)^2*u^2+u^2))=(3+2*u)/sqrt(c)},nup2);
```

$$
nup2s := -\Bigg[-270\,u\cos(\delta\sim)^2 - 216\cos(\delta\sim)^2\,u^2 - 9\,u^2 - 621\,u^2\,(3+2\,u)\cos(\delta\sim)^4
$$
$$
- 228\,u^3\,(3+2\,u)\cos(\delta\sim)^4 - 27\,u^3\,(3+2\,u)\cos(\delta\sim)^2 - 30\,u^4\,(3+2\,u)\cos(\delta\sim)^4
$$
$$
- 10\,u^4\,(3+2\,u)\cos(\delta\sim)^2 + 27\cos(\delta\sim)^2\,(3+2\,u) - 720\,u\,(3+2\,u)\cos(\delta\sim)^4
$$
$$
+ 63\,u\,(3+2\,u)\cos(\delta\sim)^2 + 12\,u^2\,(3+2\,u)\cos(\delta\sim)^2 + 3\,u^3\,(3+2\,u) + 3\,(3+2\,u)\,u^2
$$
$$
- 297\cos(\delta\sim)^4\,(3+2\,u) + 82\cos(\delta\sim)^2\,u^4 - 81\cos(\delta\sim)^2 + 20\,u^5\cos(\delta\sim)^2
$$
$$
+ 60\,u^5\cos(\delta\sim)^4 - 18\,u^3 + 30\,u^3\cos(\delta\sim)^2 + 558\cos(\delta\sim)^4\,u^4 - 8\,u^4
$$

$$+ 1992 \, u^3 \cos(\delta\sim)^4 + 3411 \, u^2 \cos(\delta\sim)^4 + 2808 \, u \cos(\delta\sim)^4 + 891 \cos(\delta\sim)^4 \Bigg| \Bigg/ \left| c^{3/2} \right.$$

$$\sqrt{\left| \frac{(3 + 2 \, u)^2}{c} \right|}$$

> nup2ss:=simplify(simplify(nup2s,sqrt)*(c^(3/2)*sqrt((3+2*u)^2/c))/c/(3+2*u),radical);

$$nup2ss := - \Big| {-\cos(\delta\sim)^2 \, u^2 + 6 \, u^2 \cos(\delta\sim)^4 - u^2 - 12 \, u \cos(\delta\sim)^2 + 24 \, u \cos(\delta\sim)^4}$$
$$+ 18 \cos(\delta\sim)^4 - 9 \cos(\delta\sim)^2 \Big| u / c$$

> nup2sss:=subs(c=9*cos(delta)^2+12*cos(delta)^2*u+3*cos(delta)^2*u^2+u^2,nup2ss);

$$nup2sss := - \Big| {-\cos(\delta\sim)^2 \, u^2 + 6 \, u^2 \cos(\delta\sim)^4 - u^2 - 12 \, u \cos(\delta\sim)^2 + 24 \, u \cos(\delta\sim)^4}$$
$$+ 18 \cos(\delta\sim)^4 - 9 \cos(\delta\sim)^2 \Big| u \Big/ \Big| 9 \cos(\delta\sim)^2 + 12 \, u \cos(\delta\sim)^2 + 3 \cos(\delta\sim)^2 \, u^2 + u^2 \Big|$$

FINALLY:
> nup22:=simplify(nup2sss,radical);

$$nup22 := -u \Big| 2 \cos(\delta\sim)^2 - 1 \Big|$$

WE'LL CHECK FOR SIMPLIFICATION ERRORS: O.K.
> plot(subs(cos(delta)=0.5,nup2-nup2sss),u=-1.5..1.5);

> nudiff0:=1+nup1*epsilon+nup22*epsilon^2;

$$nudiff0 := 1 + \cos(\delta\sim) \, u \, \varepsilon - u \Big| 2 \cos(\delta\sim)^2 - 1 \Big| \varepsilon^2$$

> psi0:=simplify(taylor((u+1-nudiff0)/nudiff0,epsilon,3));

$$\psi0 := u + \Big| {-\cos(\delta\sim) \, u - \cos(\delta\sim) \, u^2} \Big| \varepsilon +$$
$$\Big| 2 \, u \cos(\delta\sim)^2 - u + 3 \cos(\delta\sim)^2 \, u^2 - u^2 + u^3 \cos(\delta\sim)^2 \Big| \varepsilon^2 + O \Big| \varepsilon^3 \Big|$$

> factor(coeff(psi0,epsilon,2));

$$u \, (1 + u) \Big| u \cos(\delta\sim)^2 + 2 \cos(\delta\sim)^2 - 1 \Big|$$

ANGULAR SPEED IN C.O.M. ELLIPTIC ORBIT
> nudiff:=subs(signum(cos(delta))=1,simplify(taylor(n*(1+ee*cos(nu))^2/(1-ee*ee)^(3/2),epsilon,4)));

$$nudiff := 1 + \Big| 2 \sqrt{\%1} \cos(v) - 6 \cos(\delta\sim) - 3 \cos(\delta\sim) \, u \Big| \varepsilon - \Big| 3 \, u \sqrt{\%1}$$
$$+ 99 \cos(\delta\sim)^3 \cos(v) - 24 \cos(\delta\sim)^2 \sqrt{\%1} + 3 \sqrt{\%1} - 24 \cos(\delta\sim)^2 \, u \sqrt{\%1}$$
$$- 6 \cos(\delta\sim)^2 \, u^2 \sqrt{\%1} - \cos(v)^2 \sqrt{\%1} \, u^2 - 12 \cos(v)^2 \sqrt{\%1} \, u \cos(\delta\sim)^2$$
$$- 3 \cos(v)^2 \sqrt{\%1} \cos(\delta\sim)^2 \, u^2 - 9 \cos(v)^2 \sqrt{\%1} \cos(\delta\sim)^2 + 2 \cos(\delta\sim) \cos(v) \, u^2$$
$$- 18 \cos(\delta\sim) \cos(v) \, u + 4 \cos(\delta\sim) \cos(v) \, u^3 + 96 \cos(\delta\sim)^3 \cos(v) \, u^2$$
$$+ 16 \cos(\delta\sim)^3 \cos(v) \, u^3 + 180 \cos(\delta\sim)^3 \cos(v) \, u - 9 \cos(\delta\sim) \cos(v) \Big| \Big/ \sqrt{\%1} \, \varepsilon^2 + \frac{1}{4} \Big|$$

$$72 \cos(\delta\sim) \cos(v)^2 \sqrt{\%1} \, u^3 + 36 \cos(\delta\sim) \cos(v)^2 \sqrt{\%1} \, u^2$$

$+ 1080 \cos(\delta\sim)^3 \cos(v)^2 \sqrt{\%1} \, u - 3564 \cos(v) \cos(\delta\sim)^4 - 1416 \cos(v) \, u^3 \cos(\delta\sim)^2$

$- 13284 \cos(v) \, u \cos(\delta\sim)^4 - 603 \cos(v) \cos(\delta\sim)^2 \, u^2 + 864 \cos(\delta\sim)^3 \sqrt{\%1}$

$+ 9 \cos(v) \, u^2 + 24 \cos(v) \, u^3 - 16 \cos(v) \, u^5 - 4 \cos(v) \, u^4 + 144 \cos(\delta\sim) \, u^3 \sqrt{\%1}$

$+ 96 \cos(\delta\sim) \, u^2 \sqrt{\%1} + 2448 \cos(\delta\sim)^3 \, u \sqrt{\%1} + 324 \cos(\delta\sim)^3 \cos(v)^2 \sqrt{\%1}$

$+ 52176 \cos(\delta\sim)^6 \cos(v) \, u^3 + 1104 \cos(\delta\sim)^4 \cos(v) \, u^4 + 20772 \cos(\delta\sim)^6 \cos(v) \, u^4$

$+ 24 \cos(\delta\sim)^2 \cos(v) \, u^6 + 356 \cos(\delta\sim)^6 \cos(v) \, u^6 + 196 \cos(\delta\sim)^4 \cos(v) \, u^6$

$+ 4272 \cos(\delta\sim)^6 \cos(v) \, u^5 + 1184 \cos(\delta\sim)^4 \cos(v) \, u^5 + 49140 \cos(\delta\sim)^6 \cos(v) \, u$

$- 120 \cos(\delta\sim)^5 \sqrt{\%1} \, u^5 - 840 \cos(v)^2 \cos(\delta\sim)^5 \sqrt{\%1} \, u^4 - 8880 \cos(\delta\sim)^5 \sqrt{\%1} \, u^2$

$- 96 \cos(\delta\sim)^3 \sqrt{\%1} \, u^4 + 48 \cos(\delta\sim) \sqrt{\%1} \, u^4 + 70959 \cos(\delta\sim)^6 \cos(v) \, u^2$

$+ 16 \cos(v)^2 \cos(\delta\sim) \sqrt{\%1} \, u^4 - 4 \cos(v)^2 \cos(\delta\sim) \sqrt{\%1} \, u^5$

$+ 48 \cos(v)^2 \cos(\delta\sim)^3 \sqrt{\%1} \, u^3 - 40 \cos(v)^2 \cos(\delta\sim)^3 \sqrt{\%1} \, u^5$

$- 84 \cos(v)^2 \cos(\delta\sim)^5 \sqrt{\%1} \, u^5 - 5940 \cos(v)^2 \cos(\delta\sim)^5 \sqrt{\%1} \, u^2$

$- 168 \cos(v)^2 \cos(\delta\sim)^3 \sqrt{\%1} \, u^4 + 13500 \cos(\delta\sim)^6 \cos(v)$

$- 3240 \cos(v)^2 \cos(\delta\sim)^5 \sqrt{\%1} \, u^3 - 5076 \cos(v)^2 \cos(\delta\sim)^5 \sqrt{\%1} \, u$

$- 4680 \cos(\delta\sim)^5 \sqrt{\%1} \, u^3 - 8160 \cos(\delta\sim)^5 \sqrt{\%1} \, u + 2128 \cos(\delta\sim)^3 \sqrt{\%1} \, u^2$

$- 40 \cos(\delta\sim)^3 \sqrt{\%1} \, u^5 + 936 \cos(v)^2 \cos(\delta\sim)^3 \sqrt{\%1} \, u^2 - 15861 \cos(\delta\sim)^4 \cos(v) \, u^2$

$- 6008 \cos(\delta\sim)^4 \cos(v) \, u^3 - 96 \cos(\delta\sim)^2 \cos(v) \, u^5 - 864 \cos(\delta\sim)^2 \cos(v) \, u^4$

$- 1620 \cos(v)^2 \cos(\delta\sim)^5 \sqrt{\%1} - 2880 \cos(\delta\sim)^5 \sqrt{\%1} + 528 \cos(\delta\sim)^3 \sqrt{\%1} \, u^3$

$- 1200 \cos(\delta\sim)^5 \sqrt{\%1} \, u^4 \Big/ \%1^{3/2} \, \varepsilon^3 + O\big| \varepsilon^4 \big|$

$\%1 := 9 \cos(\delta\sim)^2 + 12 \, u \cos(\delta\sim)^2 + 3 \cos(\delta\sim)^2 \, u^2 + u^2$

SINCE COEFFICENTS SEEM TO GROW, WE WILL CHECK THAT GREATER ORDER TERMS REMAIN SMALL, GIVING VALUES TO THETA AND DELTA FOR A COMPLETE ORBIT IN NU:

```
> nudiffs:=convert(nudiff,polynom);
```

$\textit{nudiffs} := 1 + \big| 2 \sqrt{\%1} \cos(v) - 6 \cos(\delta\sim) - 3 \cos(\delta\sim) \, u \big| \varepsilon - \big| 3 \, u \sqrt{\%1}$

$+ 99 \cos(\delta\sim)^3 \cos(v) - 24 \cos(\delta\sim)^2 \sqrt{\%1} + 3 \sqrt{\%1} - 24 \cos(\delta\sim)^2 \, u \sqrt{\%1}$

$- 6 \cos(\delta\sim)^2 \, u^2 \sqrt{\%1} - \cos(v)^2 \sqrt{\%1} \, u^2 - 12 \cos(v)^2 \sqrt{\%1} \, u \cos(\delta\sim)^2$

$- 3 \cos(v)^2 \sqrt{\%1} \cos(\delta\sim)^2 \, u^2 - 9 \cos(v)^2 \sqrt{\%1} \cos(\delta\sim)^2 + 2 \cos(\delta\sim) \cos(v) \, u^2$

$- 18 \cos(\delta\sim) \cos(v) \, u + 4 \cos(\delta\sim) \cos(v) \, u^3 + 96 \cos(\delta\sim)^3 \cos(v) \, u^2$

$$+ 16 \cos(\delta\!\sim)^3 \cos(v)\, u^3 + 180 \cos(\delta\!\sim)^3 \cos(v)\, u - 9 \cos(\delta\!\sim) \cos(v) \Big| \varepsilon^2 \Big/ \sqrt{\%1} + \frac{1}{4} \Big|$$

$$72 \cos(\delta\!\sim) \cos(v)^2 \sqrt{\%1}\, u^3 + 36 \cos(\delta\!\sim) \cos(v)^2 \sqrt{\%1}\, u^2$$

$$+ 1080 \cos(\delta\!\sim)^3 \cos(v)^2 \sqrt{\%1}\, u - 3564 \cos(v) \cos(\delta\!\sim)^4 - 1416 \cos(v)\, u^3 \cos(\delta\!\sim)^2$$

$$- 13284 \cos(v)\, u \cos(\delta\!\sim)^4 - 603 \cos(v) \cos(\delta\!\sim)^2 u^2 + 864 \cos(\delta\!\sim)^3 \sqrt{\%1}$$

$$+ 9 \cos(v)\, u^2 + 24 \cos(v)\, u^3 - 16 \cos(v)\, u^5 - 4 \cos(v)\, u^4 + 144 \cos(\delta\!\sim)\, u^3 \sqrt{\%1}$$

$$+ 96 \cos(\delta\!\sim)\, u^2 \sqrt{\%1} + 2448 \cos(\delta\!\sim)^3 u \sqrt{\%1} + 324 \cos(\delta\!\sim)^3 \cos(v)^2 \sqrt{\%1}$$

$$+ 52176 \cos(\delta\!\sim)^6 \cos(v)\, u^3 + 1104 \cos(\delta\!\sim)^4 \cos(v)\, u^4 + 20772 \cos(\delta\!\sim)^6 \cos(v)\, u^4$$

$$+ 24 \cos(\delta\!\sim)^2 \cos(v)\, u^6 + 356 \cos(\delta\!\sim)^6 \cos(v)\, u^6 + 196 \cos(\delta\!\sim)^4 \cos(v)\, u^6$$

$$+ 4272 \cos(\delta\!\sim)^6 \cos(v)\, u^5 + 1184 \cos(\delta\!\sim)^4 \cos(v)\, u^5 + 49140 \cos(\delta\!\sim)^6 \cos(v)\, u$$

$$- 120 \cos(\delta\!\sim)^5 \sqrt{\%1}\, u^5 - 840 \cos(v)^2 \cos(\delta\!\sim)^5 \sqrt{\%1}\, u^4 - 8880 \cos(\delta\!\sim)^5 \sqrt{\%1}\, u^2$$

$$- 96 \cos(\delta\!\sim)^3 \sqrt{\%1}\, u^4 + 48 \cos(\delta\!\sim) \sqrt{\%1}\, u^4 + 70959 \cos(\delta\!\sim)^6 \cos(v)\, u^2$$

$$+ 16 \cos(v)^2 \cos(\delta\!\sim) \sqrt{\%1}\, u^4 - 4 \cos(v)^2 \cos(\delta\!\sim) \sqrt{\%1}\, u^5$$

$$+ 48 \cos(v)^2 \cos(\delta\!\sim)^3 \sqrt{\%1}\, u^3 - 40 \cos(v)^2 \cos(\delta\!\sim)^3 \sqrt{\%1}\, u^5$$

$$- 84 \cos(v)^2 \cos(\delta\!\sim)^5 \sqrt{\%1}\, u^5 - 5940 \cos(v)^2 \cos(\delta\!\sim)^5 \sqrt{\%1}\, u^2$$

$$- 168 \cos(v)^2 \cos(\delta\!\sim)^3 \sqrt{\%1}\, u^4 + 13500 \cos(\delta\!\sim)^6 \cos(v)$$

$$- 3240 \cos(v)^2 \cos(\delta\!\sim)^5 \sqrt{\%1}\, u^3 - 5076 \cos(v)^2 \cos(\delta\!\sim)^5 \sqrt{\%1}\, u$$

$$- 4680 \cos(\delta\!\sim)^5 \sqrt{\%1}\, u^3 - 8160 \cos(\delta\!\sim)^5 \sqrt{\%1}\, u + 2128 \cos(\delta\!\sim)^3 \sqrt{\%1}\, u^2$$

$$- 40 \cos(\delta\!\sim)^3 \sqrt{\%1}\, u^5 + 936 \cos(v)^2 \cos(\delta\!\sim)^3 \sqrt{\%1}\, u^2 - 15861 \cos(\delta\!\sim)^4 \cos(v)\, u^2$$

$$- 6008 \cos(\delta\!\sim)^4 \cos(v)\, u^3 - 96 \cos(\delta\!\sim)^2 \cos(v)\, u^5 - 864 \cos(\delta\!\sim)^2 \cos(v)\, u^4$$

$$- 1620 \cos(v)^2 \cos(\delta\!\sim)^5 \sqrt{\%1} - 2880 \cos(\delta\!\sim)^5 \sqrt{\%1} + 528 \cos(\delta\!\sim)^3 \sqrt{\%1}\, u^3$$

$$- 1200 \cos(\delta\!\sim)^5 \sqrt{\%1}\, u^4 \Big| \varepsilon^3 \Big/ \%1^{3/2}$$

$$\%1 := 9 \cos(\delta\!\sim)^2 + 12\, u \cos(\delta\!\sim)^2 + 3 \cos(\delta\!\sim)^2 u^2 + u^2$$

TERM OF ORDER EPSILON (DELTA 0, THETA 1 RADIAN):

```
> nud1:=eval(subs({theta=1,delta=0},subs(u=sqrt(3*sin(theta)^2-3*sin(delta)^2),coeff(nudiffs,epsilon,1)
> )));
```

$$nud1 := 2 \sqrt{9 + 12 \sqrt{3} \sqrt{\sin(1)^2} + 12 \sin(1)^2 \cos(v) - 6 - 3 \sqrt{3} \sqrt{\sin(1)^2}}$$

EPSILON SQUARE:

```
> nud2:=eval(subs({theta=1,delta=0},subs(u=sqrt(3*sin(theta)^2-3*sin(delta)^2),coeff(nudiffs,epsilon,2)
> )));
```

$$nud2 := - \left| -21 \sqrt{3} \sqrt{\sin(1)^2} \sqrt{\%1} + 90 \cos(v) - 21 \sqrt{\%1} - 18 \sin(1)^2 \sqrt{\%1} \right.$$

$$- 12 \cos(v)^2 \sqrt{\%1} \sin(1)^2 - 12 \cos(v)^2 \sqrt{\%1} \sqrt{3} \sqrt{\sin(1)^2} - 9 \cos(v)^2 \sqrt{\%1}$$

$$\left. + 294 \cos(v) \sin(1)^2 + 162 \cos(v) \sqrt{3} \sqrt{\sin(1)^2} + 60 \cos(v) \sqrt{3} \left| \sin(1)^2 \right|^{3/2} \right| / \sqrt{\%1}$$

$$\%1 := 9 + 12 \sqrt{3} \sqrt{\sin(1)^2} + 12 \sin(1)^2$$

EPSILON CUBE:

```
> nud3:=eval(subs({theta=1,delta=0},subs(u=sqrt(3*sin(theta)^2-3*sin(delta)^2),coeff(nudiffs,epsilon,3)
> )));
```

$$nud3 := \frac{1}{4} \left| -19968 \sin(1)^2 \sqrt{\%1} + 163512 \cos(v) \sin(1)^2 \right.$$

$$- 9360 \cos(v)^2 \sqrt{\%1} \sqrt{3} \left| \sin(1)^2 \right|^{3/2} - 1152 \cos(v)^2 \sqrt{\%1} \sqrt{3} \left| \sin(1)^2 \right|^{5/2} - 2016 \sqrt{\%1}$$

$$+ 9936 \cos(v) - 3996 \cos(v)^2 \sqrt{\%1} \sqrt{3} \sqrt{\sin(1)^2} + 35856 \cos(v) \sqrt{3} \sqrt{\sin(1)^2}$$

$$- 1296 \cos(v)^2 \sqrt{\%1} - 5712 \sqrt{3} \sqrt{\sin(1)^2} \sqrt{\%1} - 14904 \cos(v)^2 \sqrt{\%1} \sin(1)^2$$

$$+ 134328 \cos(v) \sqrt{3} \left| \sin(1)^2 \right|^{3/2} + 48096 \cos(v) \sqrt{3} \left| \sin(1)^2 \right|^{5/2}$$

$$- 8928 \cos(v)^2 \sqrt{\%1} \sin(1)^4 - 12024 \sqrt{3} \left| \sin(1)^2 \right|^{3/2} \sqrt{\%1}$$

$$- 1440 \sqrt{\%1} \sqrt{3} \left| \sin(1)^2 \right|^{5/2} + 189072 \cos(v) \sin(1)^4 + 15552 \cos(v) \sin(1)^6$$

$$\left. - 11232 \sqrt{\%1} \sin(1)^4 \right| / \%1^{3/2}$$

$$\%1 := 9 + 12 \sqrt{3} \sqrt{\sin(1)^2} + 12 \sin(1)^2$$

EPSILON BY ANOTHER NAME, SO THAT IT WILL NOT DISTURB THE REST OF THE CALCULATIONS:

```
> sigma:=0.9145*20/6378.16;
```

$$\sigma := .002867598179$$

THE THIRD TERM GETS MUCH BIGGER THAN THE SECOND:

```
> plot({nud2,nud3},nu=0..2*Pi);
```
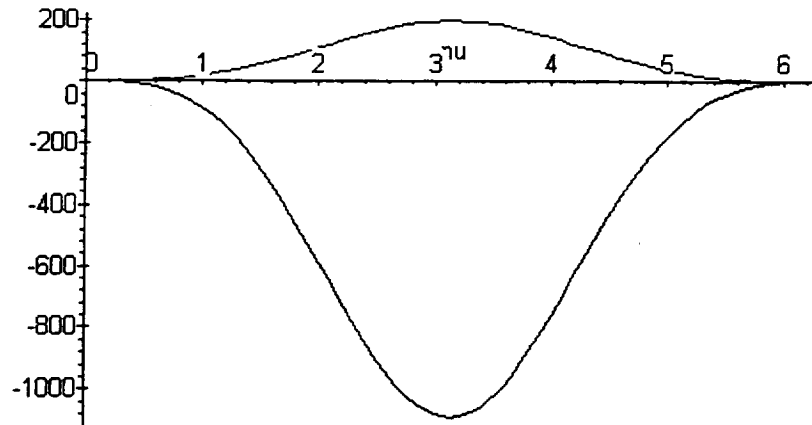
BUT EPSILON CUBE KEEPS IT SMALL:
```
> plot({sigma*nud2,sigma*sigma*nud3},nu=0..2*Pi);
```
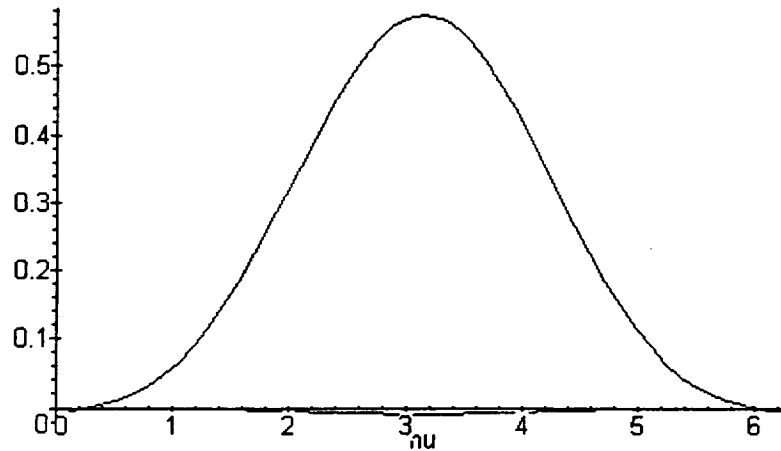

THE SECOND IS ALSO BIGGER THAN THE FIRST:
```
> plot({nud1,nud2},nu=0..2*Pi);
```
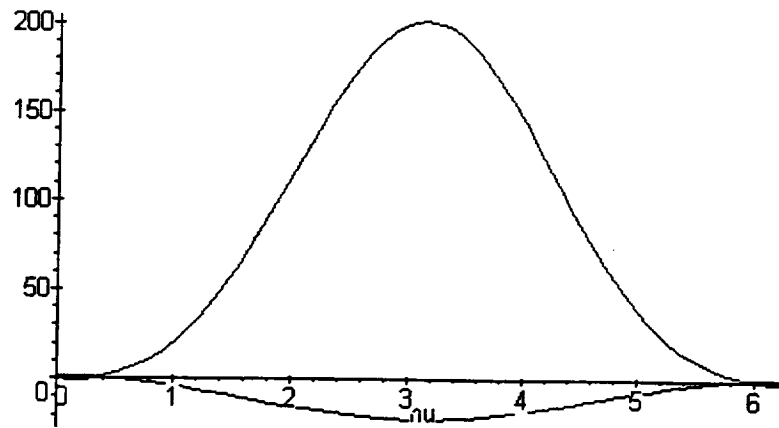
BUT EPSILON PUTS THINGS IN PERSPECTIVE: WE NEED ONLY KEEP TERMS TO ORDER EPSILON SQUARE.

```
> plot({nud1,sigma*nud2},nu=0..2*Pi);
```
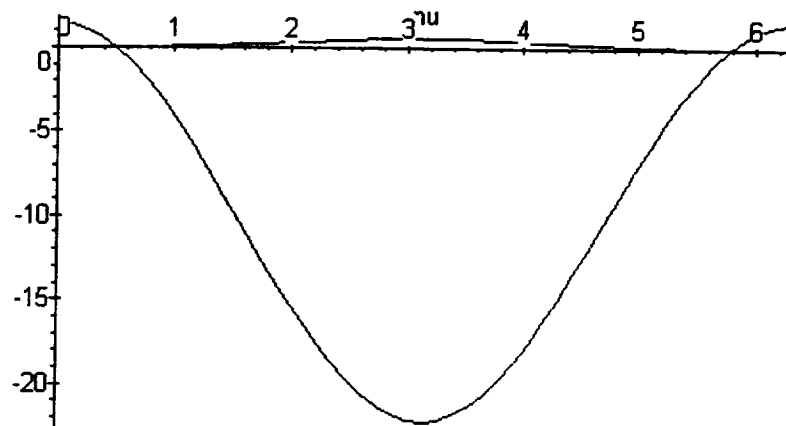

AND NOW THE WHOLE PICTURE:

```
> plot({1+sigma*nud1,sigma*sigma*nud2},nu=0..2*Pi);
```
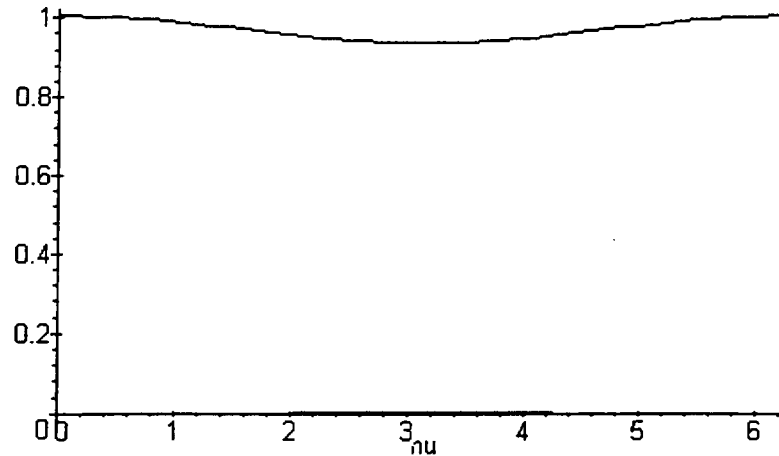
WE WILL CONTINUE SIMPLIFYING THE TERMS OF INSTANT ANGULAR SPEED

> nudiff1:=coeff(nudiff,epsilon,1);

$$nudiff1 :=$$

$$2\sqrt{9\cos(\delta\sim)^2 + 12\,u\cos(\delta\sim)^2 + 3\cos(\delta\sim)^2\,u^2 + u^2}\,\cos(\nu) - 6\cos(\delta\sim) - 3\cos(\delta\sim)\,u$$

> nudiff2:=coeff(nudiff,epsilon,2);

$$nudiff2 := -\Big|3\,u\,\sqrt{\%1} + 99\cos(\delta\sim)^3\cos(\nu) - 24\cos(\delta\sim)^2\sqrt{\%1} + 3\sqrt{\%1}$$

$$- 24\cos(\delta\sim)^2\,u\,\sqrt{\%1} - 6\cos(\delta\sim)^2\,u^2\,\sqrt{\%1} - \cos(\nu)^2\,\sqrt{\%1}\,u^2$$

$$- 12\cos(\nu)^2\,\sqrt{\%1}\,u\cos(\delta\sim)^2 - 3\cos(\nu)^2\,\sqrt{\%1}\,\cos(\delta\sim)^2\,u^2$$

$$- 9\cos(\nu)^2\,\sqrt{\%1}\,\cos(\delta\sim)^2 + 2\cos(\delta\sim)\cos(\nu)\,u^2 - 18\cos(\delta\sim)\cos(\nu)\,u$$

$$+ 4\cos(\delta\sim)\cos(\nu)\,u^3 + 96\cos(\delta\sim)^3\cos(\nu)\,u^2 + 16\cos(\delta\sim)^3\cos(\nu)\,u^3$$

$$+ 180\cos(\delta\sim)^3\cos(\nu)\,u - 9\cos(\delta\sim)\cos(\nu)\Big|\Big/\sqrt{\%1}$$

$$\%1 := 9\cos(\delta\sim)^2 + 12\,u\cos(\delta\sim)^2 + 3\cos(\delta\sim)^2\,u^2 + u^2$$

> nudiff2:=collect(simplify(nudiff2,radical,assume=positive),cos(nu));

$$nudiff2 :=$$

$$-\frac{\left|-9\cos(\delta\sim)^2\sqrt{\%1} - u^2\sqrt{\%1} - 12\cos(\delta\sim)^2\,u\,\sqrt{\%1} - 3\cos(\delta\sim)^2\,u^2\sqrt{\%1}\right|\cos(\nu)^2}{\sqrt{\%1}} -$$

$$99\cos(\delta\sim)^3 + 2\cos(\delta\sim)\,u^2 - 18\cos(\delta\sim)\,u + 4\cos(\delta\sim)\,u^3 + 96\cos(\delta\sim)^3\,u^2$$

$$+ 16\,u^3\cos(\delta\sim)^3 + 180\cos(\delta\sim)^3\,u - 9\cos(\delta\sim)\big|\cos(\nu)\big/\sqrt{\%1}$$

$$-\frac{3\,u\,\sqrt{\%1} - 6\cos(\delta\sim)^2\,u^2\sqrt{\%1} - 24\cos(\delta\sim)^2\sqrt{\%1} + 3\sqrt{\%1} - 24\cos(\delta\sim)^2\,u\,\sqrt{\%1}}{\sqrt{\%1}}$$

$$\%1 := 9 \cos(\delta\sim)^2 + 12\, u \cos(\delta\sim)^2 + 3 \cos(\delta\sim)^2 u^2 + u^2$$

```
> c0:=simplify(coeff(nudiff2,cos(nu),0),radical,assume=positive);
```

$$c0 := -3\, u + 6 \cos(\delta\sim)^2 u^2 + 24 \cos(\delta\sim)^2 - 3 + 24\, u \cos(\delta\sim)^2$$

```
> factor(coeff(c0,cos(delta)**2));
```

$$6\,(2 + u)^2$$

```
> factor(coeff(c0,cos(delta),0));
```

$$-3\, u - 3$$

```
> c1:=collect(coeff(nudiff2,cos(nu),1),cos(delta));
```

$$c1 := -\frac{\left|99 + 96\, u^2 + 16\, u^3 + 180\, u\right| \cos(\delta\sim)^3}{\sqrt{9 \cos(\delta\sim)^2 + 12\, u \cos(\delta\sim)^2 + 3 \cos(\delta\sim)^2 u^2 + u^2}}$$
$$-\frac{\left|2\, u^2 - 18\, u + 4\, u^3 - 9\right| \cos(\delta\sim)}{\sqrt{9 \cos(\delta\sim)^2 + 12\, u \cos(\delta\sim)^2 + 3 \cos(\delta\sim)^2 u^2 + u^2}}$$

```
> factor(16*u^3+99+180*u+96*u^2);
> factor(-9+4*u^3-18*u+2*u^2);
```

$$99 + 96\, u^2 + 16\, u^3 + 180\, u$$

$$(2\, u + 1)\left|2\, u^2 - 9\right|$$

```
> c2:=simplify(coeff(nudiff2,cos(nu),2),assume=positive);
```

$$c2 := 9 \cos(\delta\sim)^2 + 12\, u \cos(\delta\sim)^2 + 3 \cos(\delta\sim)^2 u^2 + u^2$$

```
> factor(coeff(c2,cos(delta)**2));
```

$$3\,(u + 3)\,(1 + u)$$

```
>
```

DECAY2.MS
DECAY MINIMIZATION: FINAL SATELLITE ORBIT

> r:=array([r0*(1+r1x*epsilon),0,r0*epsilon*r1z]);

$$r := [r0\,(1 + r1x\,\varepsilon) \quad 0 \quad r0\,\varepsilon\,r1z]$$

> v:=array([omega0*r0*epsilon*v1x,0,omega0*r0*(1+v1z*epsilon)]);

$$v := [\omega0\,r0\,\varepsilon\,v1x \quad 0 \quad \omega0\,r0\,(1 + v1z\,\varepsilon)]$$

> with(linalg):
> h:=crossprod(r,v);

$$h := \begin{vmatrix} 0 & r0^2\,\varepsilon^2\,r1z\,\omega0\,v1x - r0^2\,(1 + r1x\,\varepsilon)\,\omega0\,(1 + v1z\,\varepsilon) & 0 \end{vmatrix}$$

> h[2]:=collect(simplify(h[2]),epsilon);

$$h_2 := \left| r0^2\,r1z\,\omega0\,v1x - r0^2\,\omega0\,r1x\,v1z \right|\varepsilon^2 + \left| -r0^2\,\omega0\,v1z - r0^2\,\omega0\,r1x \right|\varepsilon - r0^2\,\omega0$$

> h2:=taylor(simplify(eval(h[2]*h[2])),epsilon);

$$h2 := r0^4\,\omega0^2 + r0^4\,\omega0^2\,(2\,v1z + 2\,r1x)\,\varepsilon +$$

$$r0^4\,\omega0^2\left| -2\,r1z\,v1x + 2\,r1x\,v1z + (v1z + r1x)^2 \right|\varepsilon^2 +$$

$$2\,r0^4\,\omega0^2\,(v1z + r1x)\,(-r1z\,v1x + r1x\,v1z)\,\varepsilon^3 + r0^4\,\omega0^2\,(-r1z\,v1x + r1x\,v1z)^2\,\varepsilon^4$$

> resc:=simplify(taylor(sqrt(dotprod(r,r,'orthogonal')),epsilon,4),sqrt,assume=positive);

$$resc := r0 + r0\,r1x\,\varepsilon + \frac{1}{2}\,r0\,r1z^2\,\varepsilon^2 - \frac{1}{2}\,r0\,r1x\,r1z^2\,\varepsilon^3 + O\left|\varepsilon^4\right|$$

> omega0:=sqrt(mu/r0/r0/r0);

$$\omega0 := \sqrt{\frac{\mu}{r0^3}}$$

> EN:=simplify(taylor(dotprod(v,v,'orthogonal')/2-mu/resc,epsilon,4),sqrt);

$$EN := -\frac{1}{2}\frac{\mu}{r0} + \frac{\mu\,(v1z + r1x)}{r0}\,\varepsilon + \frac{1}{2}\frac{\mu\left| v1z^2 + v1x^2 + r1z^2 - 2\,r1x^2 \right|}{r0}\,\varepsilon^2 +$$

$$\frac{1}{2}\frac{\mu\,r1x\left| -3\,r1z^2 + 2\,r1x^2 \right|}{r0}\,\varepsilon^3 + O\left|\varepsilon^4\right|$$

> as:=simplify(taylor(-mu/EN/2,epsilon,4));

$$as := r0 + 2\,(v1z + r1x)\,r0\,\varepsilon + \left| 5\,v1z^2 + v1x^2 + r1z^2 + 2\,r1x^2 + 8\,r1x\,v1z \right|r0\,\varepsilon^2 + \left| r1x\,r1z^2 \right.$$

$$+ 2\,r1x^3 + 12\,v1z^3 + 4\,v1z\,v1x^2 + 4\,v1z\,r1z^2 + 16\,v1z\,r1x^2 + 28\,r1x\,v1z^2 + 4\,r1x\,v1x^2 \left|\right.$$

$$r0\,\varepsilon^3 + O\left|\varepsilon^4\right|$$

> evs:=evalm(-r/resc-crossprod(h,v)/mu);

$$evs := \left| -\frac{r0\,(1 + r1x\,\varepsilon)}{r0 + r0\,r1x\,\varepsilon + \frac{1}{2}\,r0\,r1z^2\,\varepsilon^2 - \frac{1}{2}\,r0\,r1x\,r1z^2\,\varepsilon^3 + O\left|\varepsilon^4\right|} - \right|$$

$$\left| r0^2 \, rlz \sqrt{\frac{\mu}{r0^3}} \, vlx - r0^2 \sqrt{\frac{\mu}{r0^3}} \, rlx \, vlz \right| \varepsilon^2 + \left| -r0^2 \sqrt{\frac{\mu}{r0^3}} \, vlz - r0^2 \sqrt{\frac{\mu}{r0^3}} \, rlx \right| \varepsilon$$

$$- r0^2 \sqrt{\frac{\mu}{r0^3}} \left| \sqrt{\frac{\mu}{r0^3}} \, r0 \, (1 + vlz \, \varepsilon)/\mu \quad 0 \right.$$

$$-\frac{r0 \, \varepsilon \, rlz}{r0 + r0 \, rlx \, \varepsilon + \frac{1}{2} r0 \, rlz^2 \, \varepsilon^2 - \frac{1}{2} r0 \, rlx \, rlz^2 \, \varepsilon^3 + O\left|\varepsilon^4\right|} + \Bigg|$$

$$\left| r0^2 \, rlz \sqrt{\frac{\mu}{r0^3}} \, vlx - r0^2 \sqrt{\frac{\mu}{r0^3}} \, rlx \, vlz \right| \varepsilon^2 + \left| -r0^2 \sqrt{\frac{\mu}{r0^3}} \, vlz - r0^2 \sqrt{\frac{\mu}{r0^3}} \, rlx \right| \varepsilon$$

$$- r0^2 \sqrt{\frac{\mu}{r0^3}} \left| \sqrt{\frac{\mu}{r0^3}} \, r0 \, \varepsilon \, vlx / \mu \right|$$

```
> es:=simplify(taylor(sqrt(dotprod(evs,evs,'orthogonal')),epsilon,4),sqrt);
```

$$es := \sqrt{4 \, vlz^2 + 4 \, rlx \, vlz + rlx^2 + rlz^2 + 2 \, rlz \, vlx + vlx^2} \; \varepsilon + \frac{1}{2} \Big| 4 \, vlz^3 + 10 \, rlx \, vlz^2$$

$$+ 2 \, vlz \, rlz^2 - 2 \, vlz \, rlz \, vlx + 4 \, vlz \, rlx^2 - 2 \, vlx \, rlx \, rlz - rlx \, rlz^2 + 2 \, vlz \, vlx^2$$

$$+ 2 \, rlx \, vlx^2 \Big| \Big/ \sqrt{4 \, vlz^2 + 4 \, rlx \, vlz + rlx^2 + rlz^2 + 2 \, rlz \, vlx + vlx^2} \; \varepsilon^2 + O\left|\varepsilon^3\right|$$

ANOTHER WAY TO COMPUTE EXCENTRICITY:

```
> es2:=simplify(1+2*h2*EN/mu/mu);
```

$$es2 := \Big| 2 \, \big| r0 \, \mu + 2 \, r0 \, \mu \, (vlz + rlx) \, \varepsilon + r0 \, \mu \, \big| -2 \, rlz \, vlx + 4 \, rlx \, vlz + vlz^2 + rlx^2 \big| \varepsilon^2 +$$

$$2 \, r0 \, \mu \, (vlz + rlx)(-rlz \, vlx + rlx \, vlz) \, \varepsilon^3 + r0 \, \mu \, (-rlz \, vlx + rlx \, vlz)^2 \, \varepsilon^4 \big| \Big| - \frac{1}{2} \frac{\mu}{r0} +$$

$$\frac{\mu \, (vlz + rlx)}{r0} \, \varepsilon + \frac{1}{2} \frac{\mu \left| vlz^2 + vlx^2 + rlz^2 - 2 \, rlx^2 \right|}{r0} \, \varepsilon^2 + \frac{1}{2} \frac{\mu \, rlx \left| -3 \, rlz^2 + 2 \, rlx^2 \right|}{r0} \, \varepsilon^3 +$$

$$O\left|\varepsilon^4\right| \Big| + \mu^2 \Big| \Big/ \mu^2$$

```
> es2:=simplify(taylor(es2,epsilon));
```

$$es2 := \left| 4 \, vlz^2 + 4 \, rlx \, vlz + rlx^2 + rlz^2 + 2 \, rlz \, vlx + vlx^2 \right| \varepsilon^2 + \left| 4 \, vlz^3 + 10 \, rlx \, vlz^2 \right.$$

$$+ 2 \, vlz \, rlz^2 - 2 \, vlz \, rlz \, vlx + 4 \, vlz \, rlx^2 - 2 \, vlx \, rlx \, rlz - rlx \, rlz^2 + 2 \, vlz \, vlx^2$$

$$+ 2 \, rlx \, vlx^2 \Big| \varepsilon^3 + O\left|\varepsilon^4\right|$$

```
>
```

DECAY3.MS
ORBITAL DECAY RATE: DECREASE IN SEMIAXIS PER REVOLUTION.

```
> mu:=3.98618e5;
> cosi:=evalf(cos(57*Pi/180));
> h:=59.77;
> we:=7.292115e-5;
```

$$\mu := 398618.$$

$$cosi := .5446390348$$

$$h := 59.77$$

$$we := .00007292115$$

```
> K:=evalf(2*Pi/118*1e-6*3.3E-2);
```

$$K := .1757161993 \ 10^{-8}$$

```
> p:=K*a^2*exp((6678.16-a)/h)*(1-2*we*sqrt(a*a*a/mu)*cosi)*(BesselI(0,a*e/h)+2*e*BesselI(1,a*e/h
> ));
```

$$p := .1757161993 \ 10^{-8} \ a^2 \ e^{(111.7309687 - .01673080141 \ a)} \left| 1 - .1258096100 \ 10^{-6} \sqrt{a^3} \right|$$
$$(BesselI(0, .01673080141 \ a \ e) + 2 \ e \ BesselI(1, .01673080141 \ a \ e))$$

```
> with(plots):
> setoptions3d(axes=NORMAL,style=PATCHCONTOUR,contours=12,shading=Z):
> plot3d(p,a=6675..6878,e=0..0.03,title=`Semiaxis Decay`);
```

Semiaxis Decay
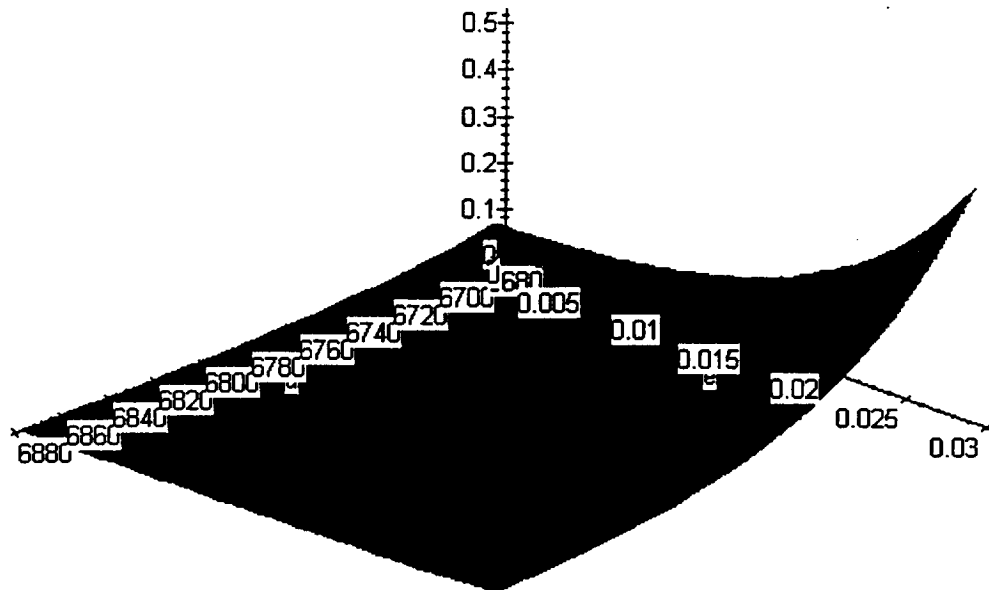
THE MINIMUM DECAY OCCURS FOR MAXIMUM a AND MINIMUM e:

```
> pe:=subs(e=ee/300,evalf(p));
```

$$pe := .1757161993 \ 10^{-8} \ a^2 \ e^{(111.6807763 \ - \ .01673080141 \ a)}$$

$$\left| 1. - .1258096100 \ 10^{-6} \ \sqrt{a^3} \right| (\text{BesselI}(0, .00005576933803 \ a \ ee)$$

$$+ .006666666666 \ ee \ \text{BesselI}(1, .00005576933803 \ a \ ee))$$

```
> pde:=evalf(pe) $ ee=0..6:
> plot({pde},a=6678..7000,title=`Decay Variation with Excentricity:  e=0-0.02`);
```

Decay Variation with Excentricity: e=0-0.02
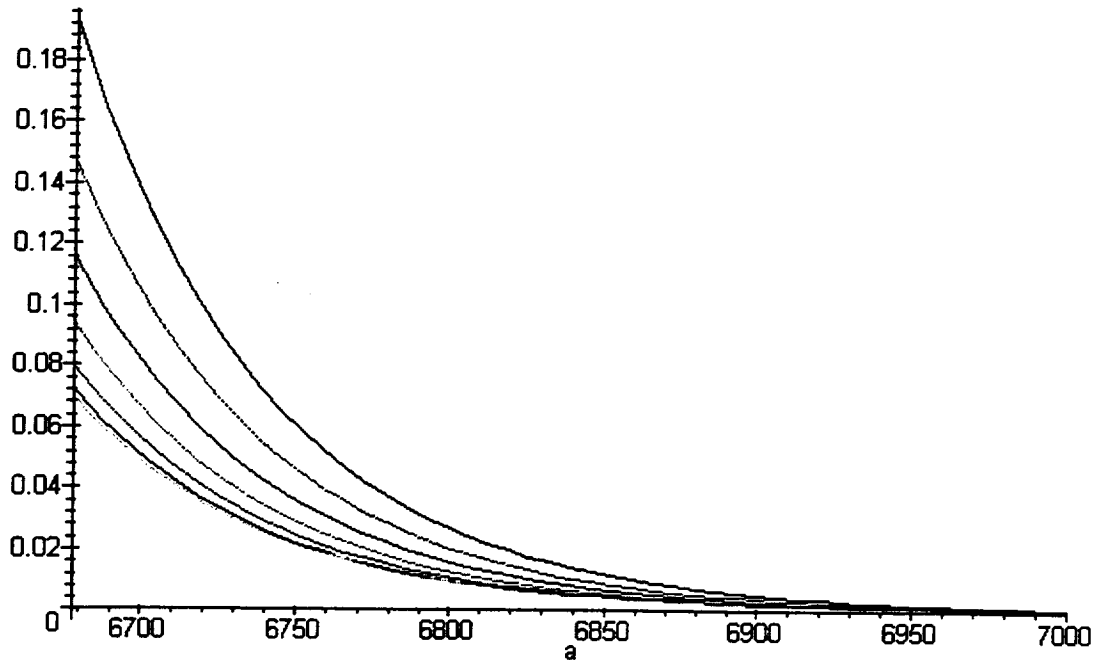

```
DECAY DECREASES WITH GROWING a AND WITH DIMINISHING e
> pa:=subs(a=6378+50*i,p):
> pda:=pa $ i=6..10:
> plot({pda},e=0..0.02,title=`Decay variation with excentricity, a=300-500 Km`);
```

Decay variation with excentricity, a=300-500 Km
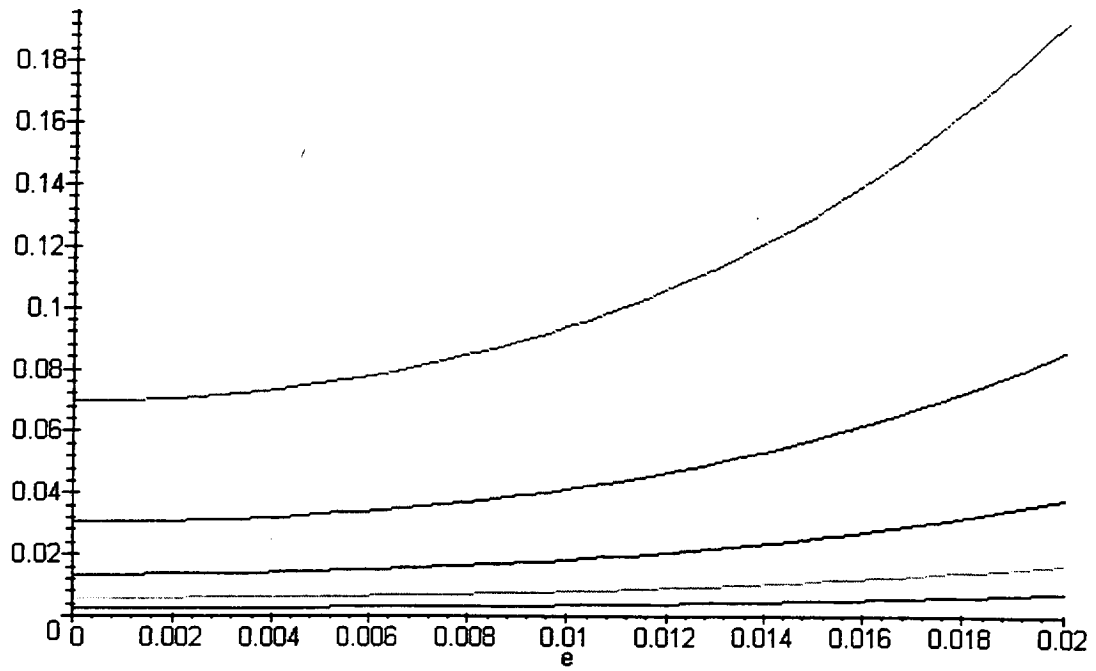
FOR ALL VALUES OF a, DECAY INCREASES WITH e

DECAY4.MS
DECAY RATE SIMPLIFIED EXPRESSION

> mu:=3.98618e5;
> cosi:=evalf(cos(57*Pi/180));
> h:=59.77;
> we:=7.292115e-5;

$$\mu := 398618.$$

$$cosi := .5446390348$$

$$h := 59.77$$

$$we := .00007292115$$

> K:=evalf(2*Pi/118*1e-6*3.3E-2);

$$K := .1757161993 \ 10^{-8}$$

> p1:=a^2*(1-2*we*sqrt(a*a*a/mu)*cosi);

$$p1 := a^2 \left(1 - .1258096100 \ 10^{-6} \sqrt{a^3} \right)$$

> p2:=(BesselI(0,u)+2*e*BesselI(1,u));

$$p2 := \text{BesselI}(0, u) + 2 \ e \ \text{BesselI}(1, u)$$

> pe:=exp((6678.16-a)/h);

$$pe := e^{(111.7309687 - .01673080141 \ a)}$$

> u:=evalf(simplify(a*e/h));

$$u := .01673080141 \ a \ e$$

> p:=K*p1*p2*pe;

$$p := .1757161993 \ 10^{-8} \ a^2 \left(1 - .1258096100 \ 10^{-6} \sqrt{a^3} \right)$$
$$(\text{BesselI}(0, .01673080141 \ a \ e) + 2 \ e \ \text{BesselI}(1, .01673080141 \ a \ e))$$
$$e^{(111.7309687 - .01673080141 \ a)}$$

> a:=r0*(1+as*epsilon);
> e:=epsilon*es;
> r0:=6675.16;

$$a := r0 \ (1 + as \ \varepsilon)$$

$$e := \varepsilon \ es$$

$$r0 := 6675.16$$

> p1t:=convert(taylor(p1,epsilon,3),polynom);

$$p1t := .4150051988 \ 10^8 + .7841517805 \ 10^8 \ as \ \varepsilon + .3118233101 \ 10^8 \ as^2 \ \varepsilon^2$$

> epsilon:=0.002740032;

$$\varepsilon := .002740032$$

> p1t;

$$.4150051988 \ 10^8 + 214860.0971 \ as + 234.1099365 \ as^2$$

> pe;

$$e^{(.0501924 - .3060089010\, as)}$$

> p2;

$$\text{BesselI}(0, .00004584293125\, (6675.16 + 18.29015201\, as)\, es)$$
$$+ .005480064\, es\, \text{BesselI}(1, .00004584293125\, (6675.16 + 18.29015201\, as)\, es)$$

> r0*epsilon/h;

$$.3060089010$$

>

Date: 1 September 1995
From: Enrico Lorenzini, Smithsonian Astrophysical Observatory

Reference profiles (last three columns of this file) for
SEDSAT control law REF53_1Sep95.

Initial conditions and satellite mass:
V0 = 2.5 m/s, Theta0 = 21 deg (up and fore), Satellite Mass = 36.3 kg

Reference profiles file:

Time (s)	Length (m)	Speed (m/s)	Turns	TurnRate (1/s)	BrakeTurns
0.00	0.500	2.500	3.	3.582	0.000
8.00	20.295	2.492	32.	3.572	0.000
16.00	40.070	2.485	60.	3.564	0.000
24.00	59.824	2.478	88.	3.556	0.000
32.00	79.559	2.472	117.	3.548	0.000
40.00	99.275	2.466	145.	3.542	0.000
48.00	118.970	2.461	173.	3.535	0.000
56.00	138.660	2.456	202.	3.530	0.000
64.00	158.320	2.451	230.	3.525	0.000
72.00	177.980	2.447	258.	3.520	0.000
80.00	197.610	2.443	286.	3.517	0.000
88.00	217.240	2.440	315.	3.513	0.000
96.00	236.850	2.437	343.	3.511	0.000
104.00	256.450	2.434	371.	3.508	0.000
112.00	276.040	2.432	399.	3.507	0.000
120.00	295.570	2.430	428.	3.506	0.000
128.00	315.060	2.429	456.	3.506	0.000
136.00	334.520	2.428	484.	3.506	0.000
144.00	353.950	2.427	512.	3.507	0.000
152.00	373.360	2.427	540.	3.508	0.000
160.00	392.750	2.428	568.	3.511	0.000
168.00	412.140	2.428	596.	3.513	0.000
176.00	431.540	2.430	624.	3.517	0.000
184.00	450.940	2.431	652.	3.521	0.000
192.00	470.360	2.434	680.	3.526	0.000
200.00	489.800	2.436	709.	3.531	0.000
208.00	509.270	2.439	737.	3.537	0.000
216.00	528.790	2.443	765.	3.544	0.000
224.00	548.360	2.447	793.	3.551	0.000
232.00	567.990	2.451	822.	3.559	0.000
240.00	587.670	2.455	851.	3.568	0.000
248.00	607.400	2.461	879.	3.577	0.000
256.00	627.170	2.466	908.	3.587	0.000
264.00	646.990	2.472	937.	3.597	0.000
272.00	666.840	2.479	966.	3.608	0.000
280.00	686.730	2.486	995.	3.620	0.000
288.00	706.660	2.493	1024.	3.633	0.000
296.00	726.610	2.501	1053.	3.646	0.000
304.00	746.580	2.509	1082.	3.660	0.000
312.00	766.580	2.518	1111.	3.674	0.000
320.00	786.590	2.527	1140.	3.689	0.000
328.00	806.680	2.537	1170.	3.705	0.000
336.00	826.930	2.547	1199.	3.722	0.000
344.00	847.320	2.557	1229.	3.739	0.000
352.00	867.830	2.568	1259.	3.756	0.000
360.00	888.470	2.578	1289.	3.774	0.000
368.00	909.220	2.590	1320.	3.792	0.000
376.00	930.080	2.601	1350.	3.811	0.000
384.00	951.030	2.613	1381.	3.831	0.000
392.00	972.060	2.626	1412.	3.851	0.000
400.00	993.170	2.639	1443.	3.872	0.000
408.00	1014.300	2.652	1474.	3.893	0.000

416.00	1035.600	2.666	1505.	3.916	0.000
424.00	1056.900	2.680	1536.	3.939	0.000
432.00	1078.200	2.694	1568.	3.962	0.000
440.00	1099.700	2.709	1599.	3.986	0.000
448.00	1121.400	2.724	1631.	4.010	0.000
456.00	1143.300	2.739	1663.	4.035	0.000
464.00	1165.300	2.755	1696.	4.060	0.000
472.00	1187.400	2.770	1728.	4.085	0.000
480.00	1209.700	2.786	1761.	4.111	0.000
488.00	1232.100	2.803	1794.	4.137	0.000
496.00	1254.700	2.819	1828.	4.164	0.000
504.00	1277.400	2.836	1861.	4.191	0.000
512.00	1300.200	2.853	1895.	4.219	0.000
520.00	1323.000	2.871	1929.	4.247	0.000
528.00	1346.000	2.888	1963.	4.276	0.000
536.00	1369.100	2.907	1997.	4.306	0.000
544.00	1392.400	2.925	2031.	4.336	0.000
552.00	1415.800	2.944	2066.	4.366	0.000
560.00	1439.400	2.962	2101.	4.396	0.000
568.00	1463.200	2.981	2136.	4.426	0.000
576.00	1487.100	3.000	2172.	4.457	0.000
584.00	1511.200	3.019	2208.	4.488	0.000
592.00	1535.500	3.038	2244.	4.519	0.000
600.00	1559.900	3.057	2280.	4.550	0.000
608.00	1584.500	3.077	2317.	4.582	0.000
616.00	1609.200	3.096	2354.	4.614	0.000
624.00	1634.100	3.116	2391.	4.647	0.000
632.00	1659.100	3.137	2428.	4.680	0.000
640.00	1684.200	3.157	2465.	4.714	0.000
648.00	1709.500	3.178	2503.	4.748	0.000
656.00	1735.000	3.198	2541.	4.782	0.000
664.00	1760.600	3.219	2580.	4.816	0.000
672.00	1786.400	3.240	2618.	4.850	0.000
680.00	1812.400	3.261	2657.	4.885	0.000
688.00	1838.600	3.282	2696.	4.919	0.000
696.00	1865.000	3.302	2736.	4.954	0.000
704.00	1891.500	3.323	2776.	4.988	0.000
712.00	1918.200	3.344	2816.	5.023	0.000
720.00	1945.000	3.365	2856.	5.058	0.000
728.00	1972.000	3.386	2897.	5.093	0.000
736.00	1999.200	3.407	2938.	5.128	0.000
744.00	2026.500	3.428	2979.	5.163	0.000
752.00	2054.000	3.449	3020.	5.199	0.000
760.00	2081.700	3.470	3062.	5.234	0.000
768.00	2109.500	3.491	3104.	5.270	0.000
776.00	2137.500	3.512	3146.	5.306	0.000
784.00	2165.700	3.533	3189.	5.341	0.000
792.00	2194.000	3.554	3232.	5.377	0.000
800.00	2222.600	3.575	3275.	5.414	0.000
808.00	2251.300	3.596	3318.	5.450	0.000
816.00	2280.100	3.618	3362.	5.486	0.000
824.00	2309.100	3.639	3406.	5.522	0.000
832.00	2338.400	3.660	3451.	5.558	0.000
840.00	2367.700	3.681	3495.	5.595	0.000
848.00	2397.300	3.702	3540.	5.631	0.000
856.00	2427.000	3.723	3585.	5.667	0.000
864.00	2456.900	3.744	3631.	5.704	0.000
872.00	2486.900	3.764	3677.	5.740	0.000
880.00	2517.100	3.785	3723.	5.776	0.000
888.00	2547.500	3.806	3769.	5.812	0.000
896.00	2578.000	3.826	3816.	5.848	0.000
904.00	2608.600	3.846	3862.	5.883	0.000
912.00	2639.500	3.866	3910.	5.919	0.000
920.00	2670.500	3.886	3957.	5.955	0.000
928.00	2701.600	3.906	4005.	5.991	0.000
936.00	2733.000	3.926	4053.	6.026	0.000

944.00	2764.500	3.946	4101.	6.062	0.000
952.00	2796.100	3.966	4150.	6.098	0.000
960.00	2828.000	3.986	4199.	6.133	0.000
968.00	2860.000	4.005	4248.	6.169	0.000
976.00	2892.100	4.025	4298.	6.205	0.000
984.00	2924.400	4.044	4348.	6.240	0.000
992.00	2956.800	4.063	4398.	6.275	0.000
1000.00	2989.400	4.082	4448.	6.309	0.000
1008.00	3022.100	4.101	4498.	6.344	0.000
1016.00	3054.900	4.119	4549.	6.378	0.000
1024.00	3087.900	4.138	4600.	6.413	0.000
1032.00	3121.100	4.156	4652.	6.447	0.000
1040.00	3154.400	4.174	4704.	6.481	0.000
1048.00	3187.900	4.192	4756.	6.515	0.000
1056.00	3221.500	4.210	4808.	6.549	0.000
1064.00	3255.300	4.228	4860.	6.583	0.000
1072.00	3289.300	4.246	4913.	6.617	0.000
1080.00	3323.300	4.263	4966.	6.650	0.000
1088.00	3357.500	4.280	5020.	6.683	0.000
1096.00	3391.800	4.297	5073.	6.717	0.000
1104.00	3426.200	4.314	5127.	6.750	0.000
1112.00	3460.800	4.331	5181.	6.782	0.000
1120.00	3495.500	4.347	5236.	6.815	0.000
1128.00	3530.300	4.364	5290.	6.847	0.000
1136.00	3565.200	4.380	5345.	6.879	0.000
1144.00	3600.300	4.396	5400.	6.911	0.000
1152.00	3635.500	4.412	5456.	6.943	0.000
1160.00	3670.900	4.427	5511.	6.974	0.000
1168.00	3706.400	4.443	5567.	7.006	0.000
1176.00	3742.100	4.458	5624.	7.037	0.000
1184.00	3777.900	4.473	5680.	7.068	0.000
1192.00	3813.700	4.488	5737.	7.099	0.000
1200.00	3849.700	4.503	5794.	7.130	0.000
1208.00	3885.800	4.517	5851.	7.160	0.000
1216.00	3921.900	4.532	5908.	7.191	0.000
1224.00	3958.200	4.546	5966.	7.221	0.000
1232.00	3994.600	4.560	6024.	7.251	0.000
1240.00	4031.100	4.574	6082.	7.280	0.000
1248.00	4067.700	4.587	6140.	7.310	0.000
1256.00	4104.400	4.601	6198.	7.339	0.000
1264.00	4141.300	4.614	6257.	7.368	0.000
1272.00	4178.300	4.627	6316.	7.397	0.000
1280.00	4215.400	4.640	6376.	7.426	0.000
1288.00	4252.700	4.653	6436.	7.454	0.000
1296.00	4290.000	4.665	6495.	7.482	0.000
1304.00	4327.400	4.677	6555.	7.510	0.000
1312.00	4364.800	4.690	6615.	7.538	0.000
1320.00	4402.300	4.702	6676.	7.566	0.000
1328.00	4440.000	4.714	6736.	7.594	0.000
1336.00	4477.700	4.725	6797.	7.621	0.000
1344.00	4515.500	4.737	6858.	7.648	0.000
1352.00	4553.400	4.748	6919.	7.675	0.000
1360.00	4591.400	4.759	6981.	7.702	0.000
1368.00	4629.500	4.770	7043.	7.728	0.000
1376.00	4667.700	4.781	7104.	7.754	0.000
1384.00	4706.100	4.791	7167.	7.781	0.000
1392.00	4744.500	4.802	7229.	7.806	0.000
1400.00	4783.000	4.812	7292.	7.832	0.000
1408.00	4821.600	4.822	7355.	7.858	0.000
1416.00	4860.200	4.832	7418.	7.883	0.000
1424.00	4898.900	4.842	7481.	7.909	0.000
1432.00	4937.600	4.851	7544.	7.934	0.000
1440.00	4976.400	4.861	7608.	7.959	0.000
1448.00	5015.300	4.870	7671.	7.984	0.000
1456.00	5054.300	4.879	7735.	8.008	0.000
1464.00	5093.300	4.888	7799.	8.033	0.000

1472.00	5132.400	4.897	7864.	8.057	0.000
1480.00	5171.700	4.906	7928.	8.081	0.000
1488.00	5211.000	4.914	7993.	8.105	0.000
1496.00	5250.400	4.922	8058.	8.129	0.000
1504.00	5289.800	4.931	8123.	8.152	0.000
1512.00	5329.300	4.939	8189.	8.176	0.000
1520.00	5368.900	4.947	8254.	8.199	0.000
1528.00	5408.500	4.955	8320.	8.222	0.000
1536.00	5448.100	4.962	8386.	8.246	0.000
1544.00	5487.800	4.970	8452.	8.269	0.000
1552.00	5527.600	4.977	8518.	8.292	0.000
1560.00	5567.400	4.985	8584.	8.315	0.000
1568.00	5607.300	4.992	8651.	8.337	0.000
1576.00	5647.200	4.999	8717.	8.360	0.000
1584.00	5687.300	5.006	8785.	8.382	0.000
1592.00	5727.400	5.013	8852.	8.404	0.000
1600.00	5767.500	5.019	8919.	8.426	0.000
1608.00	5807.700	5.026	8987.	8.448	0.000
1616.00	5848.000	5.032	9054.	8.470	0.000
1624.00	5888.300	5.039	9122.	8.492	0.000
1632.00	5928.600	5.045	9190.	8.514	0.000
1640.00	5969.000	5.051	9258.	8.536	0.000
1648.00	6009.400	5.057	9327.	8.557	0.000
1656.00	6049.900	5.064	9395.	8.579	0.000
1664.00	6090.400	5.070	9464.	8.601	0.000
1672.00	6131.000	5.076	9533.	8.623	0.000
1680.00	6171.600	5.082	9602.	8.644	0.000
1688.00	6212.200	5.087	9671.	8.666	0.000
1696.00	6253.000	5.093	9741.	8.687	0.000
1704.00	6293.700	5.098	9810.	8.708	0.000
1712.00	6334.600	5.103	9880.	8.729	0.000
1720.00	6375.400	5.109	9950.	8.750	0.000
1728.00	6416.400	5.114	10020.	8.771	0.000
1736.00	6457.300	5.119	10090.	8.792	0.000
1744.00	6498.300	5.124	10161.	8.814	0.000
1752.00	6539.300	5.130	10231.	8.835	0.000
1760.00	6580.300	5.135	10302.	8.856	0.000
1768.00	6621.400	5.140	10373.	8.877	0.000
1776.00	6662.600	5.145	10444.	8.899	0.000
1784.00	6703.700	5.150	10515.	8.920	0.000
1792.00	6745.000	5.155	10587.	8.942	0.000
1800.00	6786.200	5.160	10658.	8.963	0.000
1808.00	6827.500	5.165	10730.	8.985	0.000
1816.00	6868.900	5.170	10802.	9.006	0.000
1824.00	6910.300	5.175	10874.	9.028	0.000
1832.00	6951.700	5.180	10947.	9.050	0.000
1840.00	6993.100	5.185	11019.	9.071	0.000
1848.00	7034.700	5.190	11092.	9.093	0.000
1856.00	7076.200	5.195	11165.	9.115	0.000
1864.00	7117.800	5.200	11238.	9.137	0.000
1872.00	7159.400	5.204	11311.	9.159	0.000
1880.00	7201.000	5.209	11384.	9.181	0.000
1888.00	7242.700	5.214	11458.	9.203	0.000
1896.00	7284.500	5.219	11531.	9.225	0.000
1904.00	7326.200	5.224	11605.	9.248	0.000
1912.00	7368.000	5.229	11679.	9.270	0.000
1920.00	7409.900	5.234	11754.	9.293	0.000
1928.00	7451.700	5.239	11828.	9.316	0.000
1936.00	7493.700	5.244	11903.	9.339	0.000
1944.00	7535.600	5.249	11977.	9.363	0.000
1952.00	7577.700	5.254	12052.	9.386	0.000
1960.00	7619.700	5.259	12128.	9.410	0.000
1968.00	7661.800	5.264	12203.	9.434	0.000
1976.00	7703.900	5.269	12278.	9.458	0.000
1984.00	7746.100	5.274	12354.	9.482	0.000
1992.00	7788.300	5.280	12430.	9.506	0.000

2000.00	7830.600	5.285	12506.	9.531	0.000
2008.00	7872.900	5.290	12583.	9.556	0.000
2016.00	7915.200	5.296	12659.	9.581	0.000
2024.00	7957.600	5.301	12736.	9.606	0.000
2032.00	8000.000	5.306	12813.	9.631	0.000
2040.00	8042.500	5.312	12890.	9.656	0.000
2048.00	8085.000	5.318	12967.	9.682	0.000
2056.00	8127.600	5.324	13045.	9.709	0.000
2064.00	8170.200	5.330	13123.	9.736	0.000
2072.00	8212.900	5.336	13201.	9.763	0.000
2080.00	8255.600	5.342	13279.	9.790	0.000
2088.00	8298.400	5.348	13358.	9.818	0.000
2096.00	8341.200	5.355	13436.	9.846	0.000
2104.00	8384.100	5.361	13515.	9.874	0.000
2112.00	8427.000	5.368	13594.	9.903	0.000
2120.00	8469.900	5.374	13673.	9.932	0.000
2128.00	8512.900	5.381	13753.	9.961	0.000
2136.00	8556.000	5.388	13833.	9.990	0.000
2144.00	8599.100	5.394	13913.	10.020	0.000
2152.00	8642.200	5.402	13993.	10.050	0.000
2160.00	8685.500	5.409	14074.	10.081	0.000
2168.00	8728.800	5.416	14154.	10.112	0.000
2176.00	8772.200	5.424	14235.	10.144	0.000
2184.00	8815.600	5.431	14317.	10.176	0.000
2192.00	8859.100	5.439	14398.	10.209	0.000
2200.00	8902.700	5.447	14480.	10.242	0.000
2208.00	8946.300	5.455	14562.	10.275	0.000
2216.00	8990.000	5.464	14645.	10.309	0.000
2224.00	9033.800	5.472	14727.	10.343	0.000
2232.00	9077.500	5.481	14810.	10.378	0.000
2240.00	9121.400	5.489	14893.	10.413	0.000
2248.00	9165.200	5.498	14976.	10.449	0.000
2256.00	9209.200	5.507	15060.	10.485	0.000
2264.00	9253.300	5.516	15144.	10.521	0.000
2272.00	9297.500	5.525	15228.	10.559	0.000
2280.00	9341.800	5.535	15313.	10.597	0.000
2288.00	9386.100	5.545	15398.	10.635	0.000
2296.00	9430.600	5.555	15484.	10.675	0.000
2304.00	9475.100	5.565	15569.	10.714	0.000
2312.00	9519.700	5.575	15655.	10.755	0.000
2320.00	9564.300	5.585	15741.	10.795	0.000
2328.00	9609.100	5.596	15828.	10.837	0.000
2336.00	9653.800	5.607	15915.	10.879	0.000
2344.00	9698.700	5.618	16002.	10.921	0.000
2352.00	9743.600	5.629	16089.	10.964	0.000
2360.00	9788.600	5.640	16177.	11.008	0.000
2368.00	9833.800	5.652	16265.	11.052	0.000
2376.00	9879.000	5.664	16354.	11.098	0.000
2384.00	9924.400	5.676	16443.	11.144	0.000
2392.00	9969.900	5.688	16532.	11.190	0.000
2400.00	10016.000	5.701	16623.	11.238	0.000
2408.00	10061.000	5.714	16712.	11.286	0.000
2416.00	10107.000	5.727	16803.	11.335	0.000
2424.00	10153.000	5.740	16894.	11.385	0.000
2432.00	10199.000	5.753	16985.	11.435	0.000
2440.00	10245.000	5.767	17077.	11.486	0.000
2448.00	10291.000	5.781	17168.	11.538	0.000
2456.00	10337.000	5.795	17260.	11.590	0.000
2464.00	10384.000	5.809	17354.	11.644	0.000
2472.00	10430.000	5.824	17447.	11.698	0.000
2480.00	10477.000	5.838	17541.	11.753	0.000
2488.00	10524.000	5.853	17636.	11.809	0.000
2496.00	10571.000	5.869	17731.	11.867	0.000
2504.00	10618.000	5.884	17826.	11.924	0.000
2512.00	10665.000	5.900	17921.	11.983	0.000
2520.00	10712.000	5.916	18017.	12.042	0.000

2528.00	10760.000	5.932	18115.	12.103	0.000
2536.00	10807.000	5.949	18211.	12.165	0.000
2544.00	10855.000	5.966	18309.	12.227	0.000
2552.00	10902.000	5.983	18405.	12.290	0.000
2560.00	10950.000	6.000	18504.	12.354	0.000
2568.00	10998.000	6.018	18603.	12.419	0.000
2576.00	11046.000	6.035	18702.	12.485	0.000
2584.00	11095.000	6.054	18804.	12.553	0.000
2592.00	11143.000	6.072	18903.	12.621	0.000
2600.00	11192.000	6.091	19005.	12.690	0.000
2608.00	11241.000	6.109	19108.	12.761	0.000
2616.00	11290.000	6.129	19210.	12.833	0.000
2624.00	11339.000	6.148	19313.	12.905	0.000
2632.00	11388.000	6.168	19416.	12.979	0.000
2640.00	11438.000	6.188	19521.	13.054	0.000
2648.00	11487.000	6.208	19625.	13.130	0.000
2656.00	11537.000	6.229	19730.	13.207	0.000
2664.00	11587.000	6.249	19837.	13.286	0.000
2672.00	11637.000	6.271	19943.	13.365	0.000
2680.00	11687.000	6.292	20050.	13.446	0.000
2688.00	11737.000	6.313	20157.	13.527	0.000
2696.00	11788.000	6.335	20266.	13.611	0.000
2704.00	11839.000	6.358	20376.	13.696	0.000
2712.00	11890.000	6.380	20486.	13.782	0.000
2720.00	11941.000	6.403	20596.	13.869	0.000
2728.00	11992.000	6.426	20707.	13.957	0.000
2736.00	12044.000	6.449	20820.	14.047	0.000
2744.00	12096.000	6.473	20933.	14.139	0.000
2752.00	12148.000	6.497	21047.	14.232	0.000
2760.00	12200.000	6.521	21161.	14.326	0.000
2768.00	12252.000	6.545	21276.	14.421	0.000
2776.00	12304.000	6.570	21390.	14.518	0.000
2784.00	12357.000	6.595	21508.	14.616	0.000
2792.00	12410.000	6.621	21625.	14.717	0.000
2800.00	12463.000	6.646	21743.	14.818	0.000
2808.00	12516.000	6.672	21862.	14.921	0.000
2816.00	12570.000	6.698	21983.	15.026	0.000
2824.00	12623.000	6.725	22102.	15.132	0.000
2832.00	12677.000	6.751	22223.	15.239	0.000
2840.00	12731.000	6.778	22345.	15.349	0.000
2848.00	12786.000	6.805	22470.	15.461	0.000
2856.00	12840.000	6.833	22593.	15.573	0.000
2864.00	12895.000	6.861	22719.	15.688	0.000
2872.00	12950.000	6.889	22845.	15.805	0.000
2880.00	13005.000	6.917	22971.	15.923	0.000
2888.00	13061.000	6.946	23100.	16.044	0.000
2896.00	13116.000	6.975	23227.	16.165	0.000
2904.00	13172.000	7.004	23357.	16.289	0.000
2912.00	13228.000	7.034	23488.	16.415	0.000
2920.00	13285.000	7.063	23621.	16.543	0.000
2928.00	13341.000	7.093	23752.	16.672	0.000
2936.00	13398.000	7.123	23887.	16.804	0.000
2944.00	13455.000	7.154	24021.	16.937	0.000
2952.00	13513.000	7.185	24159.	17.074	0.000
2960.00	13571.000	7.215	24297.	17.212	0.000
2968.00	13628.000	7.247	24433.	17.352	0.000
2976.00	13686.000	7.278	24572.	17.494	0.000
2984.00	13745.000	7.310	24715.	17.640	0.000
2992.00	13803.000	7.343	24855.	17.787	0.000
3000.00	13862.000	7.375	24998.	17.937	0.000
3008.00	13921.000	7.407	25142.	18.088	0.000
3016.00	13980.000	7.440	25286.	18.242	0.000
3024.00	14040.000	7.473	25434.	18.398	0.000
3032.00	14099.000	7.506	25579.	18.556	0.000
3040.00	14159.000	7.539	25728.	18.717	0.000
3048.00	14220.000	7.573	25880.	18.882	0.000

3056.00	14281.000	7.606	26032.	19.050	0.000
3064.00	14342.000	7.641	26185.	19.219	0.000
3072.00	14403.000	7.675	26339.	19.392	0.000
3080.00	14465.000	7.710	26496.	19.569	0.000
3088.00	14527.000	7.745	26654.	19.749	0.000
3096.00	14590.000	7.780	26815.	19.933	0.000
3104.00	14652.000	7.816	26974.	20.119	0.000
3112.00	14715.000	7.852	27136.	20.309	0.000
3120.00	14778.000	7.888	27300.	20.502	0.000
3128.00	14842.000	7.924	27466.	20.699	0.000
3136.00	14905.000	7.960	27631.	20.897	0.000
3144.00	14969.000	7.997	27800.	21.099	0.000
3152.00	15033.000	8.033	27969.	21.305	0.000
3160.00	15097.000	8.069	28139.	21.512	0.000
3168.00	15161.000	8.106	28310.	21.723	0.000
3176.00	15226.000	8.142	28485.	21.938	0.000
3184.00	15291.000	8.178	28661.	22.156	0.000
3192.00	15357.000	8.214	28840.	22.378	0.000
3200.00	15423.000	8.250	29020.	22.603	0.000
3208.00	15489.000	8.285	29202.	22.830	0.046
3216.00	15555.000	8.318	29384.	23.053	0.091
3224.00	15622.000	8.347	29570.	23.272	0.136
3232.00	15689.000	8.373	29758.	23.484	0.181
3240.00	15756.000	8.395	29946.	23.689	0.226
3248.00	15823.000	8.413	30136.	23.886	0.271
3256.00	15890.000	8.426	30327.	24.074	0.316
3264.00	15958.000	8.436	30521.	24.256	0.360
3272.00	16025.000	8.440	30715.	24.425	0.404
3280.00	16093.000	8.440	30912.	24.586	0.448
3288.00	16160.000	8.435	31108.	24.733	0.492
3296.00	16228.000	8.425	31308.	24.871	0.535
3304.00	16295.000	8.409	31507.	24.993	0.578
3312.00	16362.000	8.388	31706.	25.101	0.622
3320.00	16429.000	8.362	31908.	25.196	0.664
3328.00	16496.000	8.329	32110.	25.275	0.707
3336.00	16563.000	8.291	32314.	25.339	0.750
3344.00	16629.000	8.247	32517.	25.384	0.792
3352.00	16695.000	8.197	32720.	25.413	0.834
3360.00	16760.000	8.141	32923.	25.422	0.876
3368.00	16825.000	8.078	33126.	25.413	0.918
3376.00	16889.000	8.010	33329.	25.384	0.960
3384.00	16953.000	7.936	33532.	25.337	1.001
3392.00	17016.000	7.857	33734.	25.270	1.042
3400.00	17079.000	7.771	33937.	25.184	1.083
3408.00	17141.000	7.680	34139.	25.078	1.124
3416.00	17202.000	7.584	34339.	24.951	1.165
3424.00	17262.000	7.483	34537.	24.803	1.205
3432.00	17321.000	7.377	34733.	24.636	1.245
3440.00	17380.000	7.266	34931.	24.452	1.286
3448.00	17438.000	7.152	35127.	24.250	1.325
3456.00	17494.000	7.033	35318.	24.026	1.365
3464.00	17550.000	6.911	35510.	23.789	1.405
3472.00	17605.000	6.786	35700.	23.535	1.444
3480.00	17659.000	6.659	35888.	23.267	1.483
3488.00	17711.000	6.529	36070.	22.980	1.522
3496.00	17763.000	6.397	36254.	22.685	1.561
3504.00	17814.000	6.264	36435.	22.377	1.599
3512.00	17863.000	6.129	36611.	22.056	1.637
3520.00	17912.000	5.994	36788.	21.729	1.676
3528.00	17959.000	5.859	36959.	21.391	1.713
3536.00	18006.000	5.724	37131.	21.050	1.751
3544.00	18051.000	5.589	37297.	20.700	1.789
3552.00	18095.000	5.456	37461.	20.347	1.826
3560.00	18138.000	5.323	37622.	19.991	1.863
3568.00	18180.000	5.192	37780.	19.633	1.900
3576.00	18221.000	5.063	37936.	19.275	1.937

3584.00	18261.000	4.936	38088.	18.917	1.974
3592.00	18300.000	4.812	38238.	18.562	2.010
3600.00	18338.000	4.689	38385.	18.208	2.046
3608.00	18375.000	4.570	38529.	17.859	2.082
3616.00	18411.000	4.453	38671.	17.514	2.118
3624.00	18446.000	4.339	38809.	17.173	2.154
3632.00	18481.000	4.228	38948.	16.841	2.189
3640.00	18514.000	4.121	39079.	16.513	2.224
3648.00	18547.000	4.016	39212.	16.193	2.260
3656.00	18578.000	3.915	39337.	15.877	2.294
3664.00	18609.000	3.818	39464.	15.572	2.329
3672.00	18639.000	3.723	39586.	15.274	2.364
3680.00	18669.000	3.632	39710.	14.987	2.398
3688.00	18698.000	3.544	39830.	14.707	2.432
3696.00	18726.000	3.459	39946.	14.434	2.466
3704.00	18753.000	3.377	40059.	14.169	2.500
3712.00	18780.000	3.298	40173.	13.914	2.533
3720.00	18806.000	3.222	40283.	13.667	2.566
3728.00	18831.000	3.149	40389.	13.427	2.600
3736.00	18856.000	3.079	40496.	13.196	2.633
3744.00	18880.000	3.011	40599.	12.973	2.665
3752.00	18904.000	2.946	40703.	12.758	2.698
3760.00	18928.000	2.884	40807.	12.553	2.730
3768.00	18950.000	2.824	40903.	12.351	2.762
3776.00	18973.000	2.766	41004.	12.161	2.793
3784.00	18995.000	2.711	41101.	11.976	2.825
3792.00	19016.000	2.658	41194.	11.797	2.856
3800.00	19037.000	2.607	41287.	11.626	2.886
3808.00	19058.000	2.558	41381.	11.463	2.917
3816.00	19078.000	2.511	41471.	11.304	2.947
3824.00	19098.000	2.466	41561.	11.153	2.977
3832.00	19118.000	2.422	41652.	11.008	3.007
3840.00	19137.000	2.380	41738.	10.867	3.036
3848.00	19156.000	2.340	41825.	10.731	3.066
3856.00	19174.000	2.301	41908.	10.600	3.095
3864.00	19193.000	2.264	41996.	10.476	3.123
3872.00	19210.000	2.228	42075.	10.352	3.152
3880.00	19228.000	2.193	42158.	10.235	3.180
3888.00	19246.000	2.159	42243.	10.124	3.208
3896.00	19263.000	2.126	42323.	10.013	3.236
3904.00	19280.000	2.095	42403.	9.908	3.264
3912.00	19296.000	2.064	42479.	9.803	3.291
3920.00	19313.000	2.034	42560.	9.704	3.318
3928.00	19329.000	2.005	42636.	9.606	3.346
3936.00	19345.000	1.977	42713.	9.511	3.372
3944.00	19360.000	1.950	42785.	9.417	3.399
3952.00	19376.000	1.923	42863.	9.328	3.426
3960.00	19391.000	1.897	42936.	9.239	3.452
3968.00	19406.000	1.872	43009.	9.153	3.478
3976.00	19421.000	1.847	43082.	9.069	3.504
3984.00	19436.000	1.822	43156.	8.986	3.530
3992.00	19450.000	1.798	43225.	8.904	3.556
4000.00	19465.000	1.775	43300.	8.825	3.581
4008.00	19479.000	1.752	43369.	8.746	3.607
4016.00	19493.000	1.730	43439.	8.668	3.632
4024.00	19506.000	1.707	43505.	8.589	3.657
4032.00	19520.000	1.686	43575.	8.515	3.682
4040.00	19533.000	1.664	43641.	8.438	3.707
4048.00	19547.000	1.643	43712.	8.365	3.732
4056.00	19560.000	1.622	43779.	8.291	3.756
4064.00	19573.000	1.601	43845.	8.217	3.781
4072.00	19585.000	1.581	43907.	8.142	3.805
4080.00	19598.000	1.561	43974.	8.070	3.830
4088.00	19610.000	1.541	44036.	7.995	3.854
4096.00	19622.000	1.521	44098.	7.921	3.878
4104.00	19635.000	1.501	44166.	7.851	3.902

4112.00	19646.000	1.481	44224.	7.774	3.926
4120.00	19658.000	1.462	44287.	7.701	3.950
4128.00	19670.000	1.442	44350.	7.628	3.974
4136.00	19681.000	1.423	44409.	7.551	3.998
4144.00	19693.000	1.403	44472.	7.477	4.021
4152.00	19704.000	1.384	44531.	7.401	4.045
4160.00	19715.000	1.365	44590.	7.323	4.069
4168.00	19726.000	1.345	44649.	7.246	4.092
4176.00	19736.000	1.326	44703.	7.165	4.116
4184.00	19747.000	1.306	44763.	7.085	4.139
4192.00	19757.000	1.286	44817.	7.003	4.162
4200.00	19767.000	1.267	44872.	6.918	4.186
4208.00	19777.000	1.247	44926.	6.833	4.209
4216.00	19787.000	1.227	44981.	6.747	4.233
4224.00	19797.000	1.207	45036.	6.659	4.256
4232.00	19807.000	1.186	45092.	6.569	4.279
4240.00	19816.000	1.166	45142.	6.475	4.303
4248.00	19825.000	1.145	45192.	6.380	4.326
4256.00	19834.000	1.123	45242.	6.282	4.349
4264.00	19843.000	1.102	45292.	6.181	4.373
4272.00	19852.000	1.080	45343.	6.079	4.396
4280.00	19861.000	1.058	45394.	5.973	4.420
4288.00	19869.000	1.035	45439.	5.862	4.443
4296.00	19877.000	1.012	45484.	5.748	4.467
4304.00	19885.000	0.988	45530.	5.628	4.491
4312.00	19893.000	0.963	45575.	5.503	4.515
4320.00	19901.000	0.938	45621.	5.373	4.539
4328.00	19908.000	0.911	45661.	5.235	4.564
4336.00	19915.000	0.884	45702.	5.092	4.588
4344.00	19922.000	0.856	45742.	4.942	4.613
4352.00	19929.000	0.826	45782.	4.787	4.637
4360.00	19935.000	0.796	45817.	4.624	4.662
4368.00	19942.000	0.765	45858.	4.456	4.686
4376.00	19948.000	0.734	45893.	4.280	4.711
4384.00	19953.000	0.701	45922.	4.096	4.735
4392.00	19959.000	0.666	45957.	3.905	4.760
4400.00	19964.000	0.631	45987.	3.706	4.784
4408.00	19969.000	0.594	46016.	3.497	4.808
4416.00	19973.000	0.556	46040.	3.278	4.832
4424.00	19978.000	0.516	46069.	3.049	4.856
4432.00	19982.000	0.474	46093.	2.806	4.880
4440.00	19985.000	0.430	46110.	2.548	4.903
4448.00	19989.000	0.383	46134.	2.273	4.927
4456.00	19991.000	0.333	46146.	1.976	4.950
4464.00	19994.000	0.278	46164.	1.653	4.972
4472.00	19996.000	0.218	46176.	1.297	4.995
4480.00	19997.000	0.150	46182.	0.891	5.017
4488.00	19998.000	0.068	46188.	0.407	5.038
4496.00	19998.000	-0.007	46188.	-0.044	5.059
4504.00	19998.000	0.000	46188.	0.000	5.059
4512.00	19998.000	0.000	46188.	0.000	5.059
4520.00	19998.000	0.000	46188.	0.000	5.059
4528.00	19998.000	0.000	46188.	0.000	5.059
4536.00	19998.000	0.000	46188.	0.000	5.059
4544.00	19998.000	0.000	46188.	0.000	5.059
4552.00	19998.000	0.000	46188.	0.000	5.059
4560.00	19998.000	0.000	46188.	0.000	5.059
4568.00	19998.000	0.000	46188.	0.000	5.059
4576.00	19998.000	0.000	46188.	0.000	5.059
4584.00	19998.000	0.000	46188.	0.000	5.059
4592.00	19998.000	0.000	46188.	0.000	5.059
4600.00	19998.000	0.000	46188.	0.000	5.059
4608.00	19998.000	0.000	46188.	0.000	5.059
4616.00	19998.000	0.000	46188.	0.000	5.059
4624.00	19998.000	0.000	46188.	0.000	5.059
4632.00	19998.000	0.000	46188.	0.000	5.059

4640.00	19998.000	0.000	46188.	0.000	5.059
4648.00	19998.000	0.000	46188.	0.000	5.059
4656.00	19998.000	0.000	46188.	0.000	5.059
4664.00	19998.000	0.000	46188.	0.000	5.059
4672.00	19998.000	0.000	46188.	0.000	5.059
4680.00	19998.000	0.000	46188.	0.000	5.059
4688.00	19998.000	0.000	46188.	0.000	5.059
4696.00	19998.000	0.000	46188.	0.000	5.059
4704.00	19998.000	0.000	46188.	0.000	5.059
4712.00	19998.000	0.000	46188.	0.000	5.059
4720.00	19998.000	0.000	46188.	0.000	5.059
4728.00	19998.000	0.000	46188.	0.000	5.059
4736.00	19998.000	0.000	46188.	0.000	5.059
4744.00	19998.000	0.000	46188.	0.000	5.059
4752.00	19998.000	0.000	46188.	0.000	5.059
4760.00	19998.000	0.000	46188.	0.000	5.059
4768.00	19998.000	0.000	46188.	0.000	5.059
4776.00	19998.000	0.000	46188.	0.000	5.059
4784.00	19998.000	0.000	46188.	0.000	5.059
4792.00	19998.000	0.000	46188.	0.000	5.059
4800.00	19998.000	0.000	46188.	0.000	5.059
4808.00	19998.000	0.000	46188.	0.000	5.059
4816.00	19998.000	0.000	46188.	0.000	5.059
4824.00	19998.000	0.000	46188.	0.000	5.059
4832.00	19998.000	0.000	46188.	0.000	5.059
4840.00	19998.000	0.000	46188.	0.000	5.059
4848.00	19998.000	0.000	46188.	0.000	5.059
4856.00	19998.000	0.000	46188.	0.000	5.059
4864.00	19998.000	0.000	46188.	0.000	5.059
4872.00	19998.000	0.000	46188.	0.000	5.059
4880.00	19998.000	0.000	46188.	0.000	5.059
4888.00	19998.000	0.000	46188.	0.000	5.059
4896.00	19998.000	0.000	46188.	0.000	5.059
4904.00	19998.000	0.000	46188.	0.000	5.059
4912.00	19998.000	0.000	46188.	0.000	5.059
4920.00	19998.000	0.000	46188.	0.000	5.059
4928.00	19998.000	0.000	46188.	0.000	5.059
4936.00	19998.000	0.000	46188.	0.000	5.059
4944.00	19998.000	0.000	46188.	0.000	5.059
4952.00	19998.000	0.000	46188.	0.000	5.059
4960.00	19998.000	0.000	46188.	0.000	5.059
4968.00	19998.000	0.000	46188.	0.000	5.059
4976.00	19998.000	0.000	46188.	0.000	5.059
4984.00	19998.000	0.000	46188.	0.000	5.059
4992.00	19998.000	0.000	46188.	0.000	5.059
5000.00	19998.000	0.000	46188.	0.000	5.059
5008.00	19998.000	0.000	46188.	0.000	5.059
5016.00	19998.000	0.000	46188.	0.000	5.059
5024.00	19998.000	0.000	46188.	0.000	5.059
5032.00	19998.000	0.000	46188.	0.000	5.059
5040.00	19998.000	0.000	46188.	0.000	5.059
5048.00	19998.000	0.000	46188.	0.000	5.059
5056.00	19998.000	0.000	46188.	0.000	5.059
5064.00	19998.000	0.000	46188.	0.000	5.059
5072.00	19998.000	0.000	46188.	0.000	5.059
5080.00	19998.000	0.000	46188.	0.000	5.059
5088.00	19998.000	0.000	46188.	0.000	5.059
5096.00	19998.000	0.000	46188.	0.000	5.059
5104.00	19998.000	0.000	46188.	0.000	5.059
5112.00	19998.000	0.000	46188.	0.000	5.059
5120.00	19998.000	0.000	46188.	0.000	5.059
5128.00	19998.000	0.000	46188.	0.000	5.059
5136.00	19998.000	0.000	46188.	0.000	5.059
5144.00	19998.000	0.000	46188.	0.000	5.059
5152.00	19998.000	0.000	46188.	0.000	5.059
5160.00	19998.000	0.000	46188.	0.000	5.059

5168.00	19998.000	0.000	46188.	0.000	5.059
5176.00	19998.000	0.000	46188.	0.000	5.059
5184.00	19998.000	0.000	46188.	0.000	5.059
5192.00	19998.000	0.000	46188.	0.000	5.059
5200.00	19998.000	0.000	46188.	0.000	5.059
5208.00	19998.000	0.000	46188.	0.000	5.059
5216.00	19998.000	0.000	46188.	0.000	5.059
5224.00	19998.000	0.000	46188.	0.000	5.059
5232.00	19998.000	0.000	46188.	0.000	5.059
5240.00	19998.000	0.000	46188.	0.000	5.059
5248.00	19998.000	0.000	46188.	0.000	5.059
5256.00	19998.000	0.000	46188.	0.000	5.059
5264.00	19998.000	0.000	46188.	0.000	5.059
5272.00	19998.000	0.000	46188.	0.000	5.059
5280.00	19998.000	0.000	46188.	0.000	5.059
5288.00	19998.000	0.000	46188.	0.000	5.059
5296.00	19998.000	0.000	46188.	0.000	5.059
5304.00	19998.000	0.000	46188.	0.000	5.059
5312.00	19998.000	0.000	46188.	0.000	5.059
5320.00	19998.000	0.000	46188.	0.000	5.059
5328.00	19998.000	0.000	46188.	0.000	5.059
5336.00	19998.000	0.000	46188.	0.000	5.059
5344.00	19998.000	0.000	46188.	0.000	5.059
5352.00	19998.000	0.000	46188.	0.000	5.059
5360.00	19998.000	0.000	46188.	0.000	5.059
5368.00	19998.000	0.000	46188.	0.000	5.059
5376.00	19998.000	0.000	46188.	0.000	5.059
5384.00	19998.000	0.000	46188.	0.000	5.059
5392.00	19998.000	0.000	46188.	0.000	5.059
5400.00	19998.000	0.000	46188.	0.000	5.059
5408.00	19998.000	0.000	46188.	0.000	5.059
5416.00	19998.000	0.000	46188.	0.000	5.059
5424.00	19998.000	0.000	46188.	0.000	5.059
5432.00	19998.000	0.000	46188.	0.000	5.059
5440.00	19998.000	0.000	46188.	0.000	5.059
5448.00	19998.000	0.000	46188.	0.000	5.059
5456.00	19998.000	0.000	46188.	0.000	5.059
5464.00	19998.000	0.000	46188.	0.000	5.059
5472.00	19998.000	0.000	46188.	0.000	5.059
5480.00	19998.000	0.000	46188.	0.000	5.059
5488.00	19998.000	0.000	46188.	0.000	5.059
5496.00	19998.000	0.000	46188.	0.000	5.059
5504.00	19998.000	0.000	46188.	0.000	5.059
5512.00	19998.000	0.000	46188.	0.000	5.059
5520.00	19998.000	0.000	46188.	0.000	5.059
5528.00	19998.000	0.000	46188.	0.000	5.059
5536.00	19998.000	0.000	46188.	0.000	5.059
5544.00	19998.000	0.000	46188.	0.000	5.059
5552.00	19998.000	0.000	46188.	0.000	5.059
5560.00	19998.000	0.000	46188.	0.000	5.059
5568.00	19998.000	0.000	46188.	0.000	5.059
5576.00	19998.000	0.000	46188.	0.000	5.059
5584.00	19998.000	0.000	46188.	0.000	5.059
5592.00	19998.000	0.000	46188.	0.000	5.059
5600.00	19998.000	0.000	46188.	0.000	5.059
5608.00	19998.000	0.000	46188.	0.000	5.059
5616.00	19998.000	0.000	46188.	0.000	5.059
5624.00	19998.000	0.000	46188.	0.000	5.059
5632.00	19998.000	0.000	46188.	0.000	5.059
5640.00	19998.000	0.000	46188.	0.000	5.059
5648.00	19998.000	0.000	46188.	0.000	5.059
5656.00	19998.000	0.000	46188.	0.000	5.059
5664.00	19998.000	0.000	46188.	0.000	5.059
5672.00	19998.000	0.000	46188.	0.000	5.059
5680.00	19998.000	0.000	46188.	0.000	5.059
5688.00	19998.000	0.000	46188.	0.000	5.059

5696.00	19998.000	0.000	46188.	0.000	5.059
5704.00	19998.000	0.000	46188.	0.000	5.059
5712.00	19998.000	0.000	46188.	0.000	5.059
5720.00	19998.000	0.000	46188.	0.000	5.059
5728.00	19998.000	0.000	46188.	0.000	5.059
5736.00	19998.000	0.000	46188.	0.000	5.059
5744.00	19998.000	0.000	46188.	0.000	5.059
5752.00	19998.000	0.000	46188.	0.000	5.059
5760.00	19998.000	0.000	46188.	0.000	5.059
5768.00	19998.000	0.000	46188.	0.000	5.059
5776.00	19998.000	0.000	46188.	0.000	5.059
5784.00	19998.000	0.000	46188.	0.000	5.059
5792.00	19998.000	0.000	46188.	0.000	5.059
5800.00	19998.000	0.000	46188.	0.000	5.059
5808.00	19998.000	0.000	46188.	0.000	5.059
5816.00	19998.000	0.000	46188.	0.000	5.059
5824.00	19998.000	0.000	46188.	0.000	5.059
5832.00	19998.000	0.000	46188.	0.000	5.059
5840.00	19998.000	0.000	46188.	0.000	5.059
5848.00	19998.000	0.000	46188.	0.000	5.059
5856.00	19998.000	0.000	46188.	0.000	5.059
5864.00	19998.000	0.000	46188.	0.000	5.059
5872.00	19998.000	0.000	46188.	0.000	5.059
5880.00	19998.000	0.000	46188.	0.000	5.059
5888.00	19998.000	0.000	46188.	0.000	5.059
5896.00	19998.000	0.000	46188.	0.000	5.059
5904.00	19998.000	0.000	46188.	0.000	5.059
5912.00	19998.000	0.000	46188.	0.000	5.059
5920.00	19998.000	0.000	46188.	0.000	5.059
5928.00	19998.000	0.000	46188.	0.000	5.059
5936.00	19998.000	0.000	46188.	0.000	5.059
5944.00	19998.000	0.000	46188.	0.000	5.059
5952.00	19998.000	0.000	46188.	0.000	5.059
5960.00	19998.000	0.000	46188.	0.000	5.059
5968.00	19998.000	0.000	46188.	0.000	5.059
5976.00	19998.000	0.000	46188.	0.000	5.059
5984.00	19998.000	0.000	46188.	0.000	5.059
5992.00	19998.000	0.000	46188.	0.000	5.059
6000.00	19998.000	0.000	46188.	0.000	5.059
6008.00	19998.000	0.000	46188.	0.000	5.059
6016.00	19998.000	0.000	46188.	0.000	5.059
6024.00	19998.000	0.000	46188.	0.000	5.059
6032.00	19998.000	0.000	46188.	0.000	5.059
6040.00	19998.000	0.000	46188.	0.000	5.059
6048.00	19998.000	0.000	46188.	0.000	5.059
6056.00	19998.000	0.000	46188.	0.000	5.059
6064.00	19998.000	0.000	46188.	0.000	5.059
6072.00	19998.000	0.000	46188.	0.000	5.059
6080.00	19998.000	0.000	46188.	0.000	5.059
6088.00	19998.000	0.000	46188.	0.000	5.059
6096.00	19998.000	0.000	46188.	0.000	5.059
6104.00	19998.000	0.000	46188.	0.000	5.059
6112.00	19998.000	0.000	46188.	0.000	5.059
6120.00	19998.000	0.000	46188.	0.000	5.059
6128.00	19998.000	0.000	46188.	0.000	5.059
6136.00	19998.000	0.000	46188.	0.000	5.059
6144.00	19998.000	0.000	46188.	0.000	5.059
6152.00	19998.000	0.000	46188.	0.000	5.059
6160.00	19998.000	0.000	46188.	0.000	5.059
6168.00	19998.000	0.000	46188.	0.000	5.059
6176.00	19998.000	0.000	46188.	0.000	5.059
6184.00	19998.000	0.000	46188.	0.000	5.059
6192.00	19998.000	0.000	46188.	0.000	5.059
6200.00	19998.000	0.000	46188.	0.000	5.059
6208.00	19998.000	0.000	46188.	0.000	5.059
6216.00	19998.000	0.000	46188.	0.000	5.059

6224.00	19998.000	0.000	46188.	0.000	5.059
6232.00	19998.000	0.000	46188.	0.000	5.059
6240.00	19998.000	0.000	46188.	0.000	5.059
6248.00	19998.000	0.000	46188.	0.000	5.059
6256.00	19998.000	0.000	46188.	0.000	5.059
6264.00	19998.000	0.000	46188.	0.000	5.059
6272.00	19998.000	0.000	46188.	0.000	5.059
6280.00	19998.000	0.000	46188.	0.000	5.059
6288.00	19998.000	0.000	46188.	0.000	5.059
6296.00	19998.000	0.000	46188.	0.000	5.059
6304.00	19998.000	0.000	46188.	0.000	5.059
6312.00	19998.000	0.000	46188.	0.000	5.059
6320.00	19998.000	0.000	46188.	0.000	5.059
6328.00	19998.000	0.000	46188.	0.000	5.059
6336.00	19998.000	0.000	46188.	0.000	5.059
6344.00	19998.000	0.000	46188.	0.000	5.059
6352.00	19998.000	0.000	46188.	0.000	5.059
6360.00	19998.000	0.000	46188.	0.000	5.059
6368.00	19998.000	0.000	46188.	0.000	5.059
6376.00	19998.000	0.000	46188.	0.000	5.059
6384.00	19998.000	0.000	46188.	0.000	5.059
6392.00	19998.000	0.000	46188.	0.000	5.059
6400.00	19998.000	0.000	46188.	0.000	5.059
6408.00	19998.000	0.000	46188.	0.000	5.059
6416.00	19998.000	0.000	46188.	0.000	5.059
6424.00	19998.000	0.000	46188.	0.000	5.059
6432.00	19998.000	0.000	46188.	0.000	5.059
6440.00	19998.000	0.000	46188.	0.000	5.059
6448.00	19998.000	0.000	46188.	0.000	5.059
6456.00	19998.000	0.000	46188.	0.000	5.059
6464.00	19998.000	0.000	46188.	0.000	5.059
6472.00	19998.000	0.000	46188.	0.000	5.059
6480.00	19998.000	0.000	46188.	0.000	5.059
6488.00	19998.000	0.000	46188.	0.000	5.059
6496.00	19998.000	0.000	46188.	0.000	5.059
6504.00	19998.000	0.000	46188.	0.000	5.059
6512.00	19998.000	0.000	46188.	0.000	5.059
6520.00	19998.000	0.000	46188.	0.000	5.059
6528.00	19998.000	0.000	46188.	0.000	5.059
6536.00	19998.000	0.000	46188.	0.000	5.059
6544.00	19998.000	0.000	46188.	0.000	5.059
6552.00	19998.000	0.000	46188.	0.000	5.059
6560.00	19998.000	0.000	46188.	0.000	5.059
6568.00	19998.000	0.000	46188.	0.000	5.059
6576.00	19998.000	0.000	46188.	0.000	5.059
6584.00	19998.000	0.000	46188.	0.000	5.059
6592.00	19998.000	0.000	46188.	0.000	5.059
6600.00	19998.000	0.000	46188.	0.000	5.059
6608.00	19998.000	0.000	46188.	0.000	5.059
6616.00	19998.000	0.000	46188.	0.000	5.059
6624.00	19998.000	0.000	46188.	0.000	5.059
6632.00	19998.000	0.000	46188.	0.000	5.059
6640.00	19998.000	0.000	46188.	0.000	5.059
6648.00	19998.000	0.000	46188.	0.000	5.059
6656.00	19998.000	0.000	46188.	0.000	5.059
6664.00	19998.000	0.000	46188.	0.000	5.059
6672.00	19998.000	0.000	46188.	0.000	5.059
6680.00	19998.000	0.000	46188.	0.000	5.059
6688.00	19998.000	0.000	46188.	0.000	5.059
6696.00	19998.000	0.000	46188.	0.000	5.059
6704.00	19998.000	0.000	46188.	0.000	5.059
6712.00	19998.000	0.000	46188.	0.000	5.059
6720.00	19998.000	0.000	46188.	0.000	5.059
6728.00	19998.000	0.000	46188.	0.000	5.059
6736.00	19998.000	0.000	46188.	0.000	5.059
6744.00	19998.000	0.000	46188.	0.000	5.059

6752.00	19998.000	0.000	46188.	0.000	5.059
6760.00	19998.000	0.000	46188.	0.000	5.059
6768.00	19998.000	0.000	46188.	0.000	5.059
6776.00	19998.000	0.000	46188.	0.000	5.059
6784.00	19998.000	0.000	46188.	0.000	5.059
6792.00	19998.000	0.000	46188.	0.000	5.059
6800.00	19998.000	0.000	46188.	0.000	5.059
6808.00	19998.000	0.000	46188.	0.000	5.059
6816.00	19998.000	0.000	46188.	0.000	5.059
6824.00	19998.000	0.000	46188.	0.000	5.059
6832.00	19998.000	0.000	46188.	0.000	5.059
6840.00	19998.000	0.000	46188.	0.000	5.059
6848.00	19998.000	0.000	46188.	0.000	5.059
6856.00	19998.000	0.000	46188.	0.000	5.059
6864.00	19998.000	0.000	46188.	0.000	5.059
6872.00	19998.000	0.000	46188.	0.000	5.059
6880.00	19998.000	0.000	46188.	0.000	5.059
6888.00	19998.000	0.000	46188.	0.000	5.059
6896.00	19998.000	0.000	46188.	0.000	5.059
6904.00	19998.000	0.000	46188.	0.000	5.059
6912.00	19998.000	0.000	46188.	0.000	5.059
6920.00	19998.000	0.000	46188.	0.000	5.059
6928.00	19998.000	0.000	46188.	0.000	5.059
6936.00	19998.000	0.000	46188.	0.000	5.059
6944.00	19998.000	0.000	46188.	0.000	5.059
6952.00	19998.000	0.000	46188.	0.000	5.059
6960.00	19998.000	0.000	46188.	0.000	5.059
6968.00	19998.000	0.000	46188.	0.000	5.059
6976.00	19998.000	0.000	46188.	0.000	5.059
6984.00	19998.000	0.000	46188.	0.000	5.059
6992.00	19998.000	0.000	46188.	0.000	5.059
7000.00	19998.000	0.000	46188.	0.000	5.059
7008.00	19998.000	0.000	46188.	0.000	5.059
7016.00	19998.000	0.000	46188.	0.000	5.059
7024.00	19998.000	0.000	46188.	0.000	5.059
7032.00	19998.000	0.000	46188.	0.000	5.059
7040.00	19998.000	0.000	46188.	0.000	5.059
7048.00	19998.000	0.000	46188.	0.000	5.059
7056.00	19998.000	0.000	46188.	0.000	5.059
7064.00	19998.000	0.000	46188.	0.000	5.059
7072.00	19998.000	0.000	46188.	0.000	5.059
7080.00	19998.000	0.000	46188.	0.000	5.059
7088.00	19998.000	0.000	46188.	0.000	5.059
7096.00	19998.000	0.000	46188.	0.000	5.059
7104.00	19998.000	0.000	46188.	0.000	5.059
7112.00	19998.000	0.000	46188.	0.000	5.059
7120.00	19998.000	0.000	46188.	0.000	5.059
7128.00	19998.000	0.000	46188.	0.000	5.059
7136.00	19998.000	0.000	46188.	0.000	5.059
7144.00	19998.000	0.000	46188.	0.000	5.059
7152.00	19998.000	0.000	46188.	0.000	5.059
7160.00	19998.000	0.000	46188.	0.000	5.059
7168.00	19998.000	0.000	46188.	0.000	5.059
7176.00	19998.000	0.000	46188.	0.000	5.059
7184.00	19998.000	0.000	46188.	0.000	5.059
7192.00	19998.000	0.000	46188.	0.000	5.059
7200.00	19998.000	0.000	46188.	0.000	5.059